

POSTFLIGHT EVALUATION OF ATLAS-CENTAUR AC-6

(Launched August 11, 1965)

By Staff of the Lewis Research Center

Lewis Research Center Cleveland, Ohio

GROUP 4
Downgraded at 3 year intervals;
declassified after 12 years

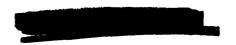
CLASSIFIED DOCUMENT-TITLE UNCLASSIFIED

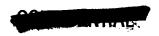
This material contains information affecting the national defense of the United States within the meaning of the espionage laws, Title 18, U.S.C., Secs. 793 and 794, the transmission or revelation of which in any manner to an unauthorized person is prohibited by law.

NOTICE

This document should not be returned after it has satisfied your requirements. It may be disposed of in accordance with your local security regulations or the appropriate provisions of the Industrial Security Manual for Safe-Guarding Classified Information.

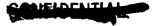
NATIONAL AERONAUTICS AND SPACE ADMINISTRATION





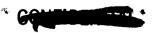
CONTENTS

	9	Page
I.	SUMMARY	1
II.	<u>INTRODUCTION</u>	3
III.		15
	SUMMARY	15
	ARRIVAL AND ERECTION	15
	PROPELLANT TANKING INTEGRATED TEST	15
	PARTIAL TANKING TEST	16
	FLIGHT ACCEPTANCE COMPOSITE TEST	16
	COMPOSITE READINESS TEST	16
	LAUNCH	17
	WEATHER	17
	LAUNCH ON TIME	17
	AC-6 PRELAUNCH HISTORY - 1965	18
		<u></u> .
IV.		19
	SUMMARY	19
	PROPELIANT-LOADING SYSTEM	19
	LH ₂ Systems	
	LO ₂ Systems	19
	LIQUID-HELIUM CHILLDOWN	
	PRESSURIZATION SYSTEM	
	UMBILICAL BOOMS	
	Upper Boom	
	Lower Boom	
	ENVIRONMENT CONTROL SYSTEM	
		2.1
٧.	TRAJECTORY	25
	SUMMARY	
	INTRODUCTION	
	Trajectory Definition	
	Rawinsonde Atmosphere Data	
	Telemetry and Other Measured Data	
	RESULTS	
	Atlas Parameters	
	Centaur Parameters	29
	Aerodynamic (Drag) Models	30
	Atlas Propellant Residuals	32
	AUTAS ITOPETTANO MESICUATS	JL
VI.	PROPULSION	51
	SUMMARY	51
	ATLAS	51
	CENTAUR	5 1
	MAIN ENGINES	52
	Boost Pumps	54
	Attitude Control and Hydrogen Peroxide Systems	55
	11001 date control and managemental contract parameters	JU



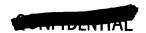
PARTIE S

	HYDRAULIC SISTEMS	57
	Atlas	
	Centaur	57
VII.	PROPELLANT SYSTEMS	79
, ,	SUMMARY	79
	CENTAUR PROPELLANT LOADING	79
	CENTAUR PROPELLANT UTILIZATION SYSTEM	80
	System Description	80
	System Performance	80
	System Accuracy	81
	PROPELIANT RESIDUALS AT MECO	81
	Liquid Residuals	81
	Gaseous Residuals	81
	CENTAUR PROPELLANT TANK PRESSURIZATION	81
	Powered-Flight Phase	81
	Propellant Tank Venting	82
		83
	Retromaneuver Blowdown	84
	DOUDTER FOLD DEFILETION DISTEM	04
VIII.		97
	SUMMARY	97
	EXTERNAL THERMAL ENVIRONMENT NOSE-FAIRING AND INSULATION PANELS	97
	INTERNAL TEMPERATURE CONTROL	98
	Payload Compartment	
	Interstage Adapter	
	INTERNAL THERMAL ENVIRONMENT CENTAUR ELECTRONICS COMPARTMENT	
	Centaur Thrust Section	99
IX.	VEHICLE STRUCTURES AND SEPARATION SYSTEMS	L13
	SUMMARY	
	FLIGHT LOADS	
	Longitudinal Loads	
	Vehicle Bending Moments	
	Gust Bending Moments	
	PAYLOAD ADAPTER LOADS	
	Insulation Panel Hoop Tension Loads	
	Interstage Adapter Differential Pressure Environment	
	Centaur Propellant Tank Pressures	
	Atlas Intermediate Bulkhead Differential Pressure	
	SEPARATION SYSTEMS	
	Insulation-Panel Separation	
	Nose-Fairing Separation	
	Atlas-Centaur Separation	
	Spacecraft Separation System	
	Separation latches	11
	Spacecraft separation	11
Y	VEHICLE DYNAMICS	12.
₹ ₹.•	SUMMARY	
	MODAL DYNAMICS	
	VIBRATIONS	
		(



COLUM

XI.	FLIGHT CONTROL	141
	SUMMARY	141
	ATLAS	141
	CENTAUR	142
	CENTAUR COAST PHASE	143
	CENTAUR RETROMANEUVER	144
XII.	GUIDANCE	147
		147
		148
		148
		149
		149
₹ ₹	A THE A CHARLES THE CHICK THAT AND A DATE TO THE CHICK A NEW AND	
YTTT.	ATLAS-CENTAUR INSTRUMENTATION, RADIO FREQUENCY, AND	707
		167
	• • • • • • • • • • • • • • • • • • • •	167
		167
		167
		16 8
		1 69
		170
	RANGE SAFETY SYSTEM	171
	TRACKING SYSTEMS	172
	C-Band	172
	Glotrac	174
	S-Band	174
	ELECTRICAL GSE	174
	APPENDIXES	
	A - SYMBOLS	1 85
	B - CAICULATIONS OF PROPELIANT RESIDUALS	189
	C - SYMBOLS AND DETAILED LISTING OF TRAJECTORY RECONSTRUCTION	T O 3
		191
	FOR AC-6 FLIGHT	TAT
	REFERENCES	233



I. SUMMARY

The sixth Atlas Centaur vehicle (AC-6) was successfully launched from the Eastern Test Range, Complex 36B, on August 11, 1965, at 0931:04.430 EST. A 2084-pound dynamic model of the Surveyor payload was placed in a simulated lunar transfer trajectory. Vehicle systems operated satisfactorily and all the flight objectives were accomplished.

Lift-off within 4 seconds of the window opening demonstrated the launch-on-time capability of the vehicle. Small deviations from the desired trajectory were accurately compensated for by the Centaur guidance system. Injection of the Surveyor model into a near-perfect lunar transfer trajectory would have resulted in an impact of the moon without a midcourse correction. To hit the precise target area on the lunar surface, the required correction would have been 4.25 meters per second, which is well within the spacecraft capability.

Normal thrust and impulse levels were obtained with both the Atlas and Centaur propulsion systems. However, a sizeable thrust overshoot on startup of the Centaur engines has not been resolved. A propellant-utilization system used for the first time on the Centaur, accurately controlled the fuel and oxidant consumption. The turnaround and retrothrust maneuver were performed without incident. Relatively high longitudinal modal excitations and lateral payload excitations were obtained at lift-off; these high perturbations are believed to be related to the launcher holddown arms.

Nominal temperatures were recorded for both the external vehicle skin and the payload compartment; however, abnormally low temperatures were measured in the forward equipment area, which may have resulted from leakage of cold helium purge gas. All vehicle electrical systems performed satisfactorily; the only difficulty with the RF systems was obtained with the C-band transponder. Most of the vehicle instrumentation yielded valid data.

The AC-6 vehicle was constructed with several new lightweight designs including the forward bulkhead, thrust barrel, interstage adapter and tank skin thickness reduction from 0.016 to 0.014 inch. No deficiencies were observed in any of these new structural elements.





II. <u>INTRODUCTION</u>

The AC-6 Atlas-Centaur vehicle, which was successfully launched from ETR Complex 36B on August 11, 1965 at 0931:04.430 EST, was the sixth in a series of development flights. (All symbols and abbreviations are defined in appendix A.) The AC-6 carried a 2084-pound dynamic model of the Surveyor payload that was successfully placed in a simulated lunar transfer trajectory. For a direct ascent and single-burn second stage, the space vehicle demonstrated a capability to launch on the proper azimuth for various times and days that the Earth and the moon were in the proper relation to each other. The launch windows for AC-6 were derived from the September-October launch opportunity dates to satisfy the requirements for the launch-on-time study as well as offering maximum launch opportunities and assuring a lunar miss. In order to have photographic coverage for use in potential failure analysis, the launch windows were biased by 6 hours to permit a daylight launch.

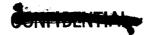
The AC-6 was the first vehicle flown wherein the Atlas sustainer stage operation was nominally terminated by a planned propellant depletion mode. A normal sustainer engine shutdown procedure consists of a "soft" shutdown phase and a "hard" shutdown phase.

From lift-off until booster engine cutoff, the Atlas is steered by a series of preprogramed pitch commands. At 8 seconds after booster engine cutoff, the Centaur guidance is admitted and is active throughout the remainder of the Atlas and Centaur portions of flight.

The following major changes to Centaur systems were incorporated on AC-6 to make it essentially an operational configuration:

- (1) Nominal tank skin thickness changed from 0.016 to 0.014 inch
- (2) Smaller LO₂ tank to eliminate slosh baffle and maintain vehicle stability
- (3) Revised station 219 tank ring (modified T-shape)
- (4) Station 408 ring modified to station 412 and revised (modified T-shape)
- (5) Lightweight thrust barrel
- (6) Lengthened insulation panels to accommodate longer LH₂ tank incurred by lowering the intermediate bulkhead
- (7) Lightweight forward bulkhead
- (8) Advanced propellant level indicating system





- (9) Separate and independent Range Safety Command battery pack
- (10) Lightweight dual range safety command receivers
- (11) Electrically functional Surveyor destruct subsystem (with inert pyrotechnics)
- (12) Redesigned lightweight interstage adapter
- (13) Single 100 ampere-hour battery for both telemetry and missile power Other Centaur changes that occurred between AC-5 and AC-6 were as follows:
 - (1) Revised location and alinement of attitude control engines
 - (2) Uprated hydraulic recirculation system
 - (3) Interstage-adapter shaped-charge area "finalized"
 - (4) New Atlas-Centaur separation guides
 - (5) Redesigned propellant ducts
 - (6) Minimum IO2 ullage standpipe
 - (7) Redesigned power changeover switch
 - (8) No separate telemetry changeover switch
 - (9) Fusing of nonessential systems on main missile battery

The flight test control criteria for AC-6 as stated in Section 8.6 of the Unified Test Plan (ref. 1) were as follows:

Basic Structure:

- (1) To demonstrate the structural integrity of the Atlas and Centaur vehicles during all powered phases of flight
- (2) To demonstrate the structural and thermal integrity of the Centaur nose-fairing and insulation panels

Separation and Jettison:

- (1) To demonstrate the satisfactory operation of the insulation-panel and nose-fairing-jettison systems
- (2) To demonstrate the satisfactory operation of the Atlas-Centaur separation system
- (3) To demonstrate the spacecraft separation system





Guidance:

- (1) To verify the integrity of the guidance system
- (2) To demonstrate the overall measuring accuracy of the guidance system
- (3) To verify that the guidance system provides proper discrete and steering signals to the Atlas and Centaur flight-control systems during closed-loop flight
- (4) To demonstrate that the guidance equations and associated trajectory parameters are satisfactory
- (5) To obtain data on accuracy of Atlas-Centaur lunar orbit injection by postinjection DSIF tracking of the Surveyor dynamic model S-band transponder

Centaur Propulsion:

- (1) To verify the ability of the Centaur propulsion system to start in the flight environment and then burn to guidance cutoff
- (2) To obtain data on the performance of the Centaur main-engine system
- (3) To obtain data on the performance of the $\rm H_2O_2$ attitude-control system Centaur Vehicle Systems:
- (1) To verify that the flight-control system supplies the proper signal for attitude control and dynamic stability of the Centaur vehicle
- (2) To obtain data on the capability of Centaur to perform the retromaneuver
- (3) To obtain data on the performance of the following systems:
 - (a) Hydraulic
 - (b) Pneumatic
 - (c) Electrical
 - (d) Radiofrequency: telemetry, Azusa, and C-band beacon
 - (e) Propellant utilization
 - (f) Propellant level indicating
- (4) To demonstrate the capability of the electromechanical timer for oneburn missions





Atlas Vehicle:

- (1) To obtain data on the performance of all the Atlas systems (including the propellant-depletion system)
- (2) To demonstrate the operation of the 165K-thrust MA-5 engine on the LV-3C vehicle

Launch Capability:

(1) To demonstrate the simulated lunar - launch-on-time (variable launch azimuth) capability of the Atlas-Centaur vehicle

Environment:

- (1) To obtain data on the flight environment including pressures, temperatures, and vibration levels
- (2) To obtain data on the spacecraft environment during the launch-tospacecraft separation phase of flight
- (3) To obtain data on the orbital environments, terminal behavior, and general postmission performance of vehicle systems until loss of all data links

The AC-6 sequence of flight events is presented in table II-I. Table II-II presents a weight summary for Atlas and Centaur. A schematic diagram of the flight is shown in figure II-1, and an illustration of the general arrangement of the Centaur stage is presented in figure II-2. Figure II-3 shows an illustration of the AC-6 dynamic model, SD-2.





TABLE II-I. - SEQUENCE OF FLIGHT EVENTS

Event	Time, sec			
	Programer	Nominal	Actual	
Lock LH ₂ vent valve Programer start; 2-in. rise Initiate roll program Initiate pitch program		T - 7.00 T + 0 T + 2 T + 15	T - 7.38 T + 0 T + 2.3 T + 15.3	
Open LH ₂ vent valve command Close LH ₂ vent valve command,	BECO + O	T + 69	T + 69.6 ⁺⁰ T + 141.6 ⁺⁰	
activate sustainer control, rate gyro gain to high Booster engine cutoff Jettison booster package	BECO + O BECO + 3.1		T + 141.79 T + 144.87	
Open LH ₂ vent valve command	BECO + 7	T + 149.7	T + 149.6+0	
Guidance admitted for steering control Jettison insulation panels Unlatch nose fairings Fire thruster bottles Start Centaur boost pumps	BECO + 8.0 BECO + 30 BECO + 54.5 BECO + 55 BECO + 62	T + 197.2	T + 171.62 T + 195.57±0.5 T + 196.47 T + 203.57±0.5	
Sustainer engine cutoff (due to LO ₂ depletion) Vernier engine cutoff	SECO + O	T + 234.8	T + 234.1 ⁺⁰	
Close LO_2 and LH_2 vent valves, pressurize LO_2 and LH_2 tanks	SECO + O	T + 234.8	T + 234.4+0	
Start Centaur programer	SECO + O	T + 234.8	T + 235.1 ⁺⁰	
Start hydraulic recirculating pump	SECO + 0.5		T + 235.6 ⁺⁰	
SECO discrete backup command from guidance	SECO + O	T + 234.8	T + 236.57	
Separate first and second stages	SECO + 1.9		T + 236.22	
Prestart, steering reference to Centaur	SECO + 3.5	T + 238.3	T + 238.6 ⁺⁰	
Start main engines, unnull main engine integrators, low rate gain, energize igniters		T + 243.3	T + 242.77	
Main engine cutoff, H ₂ O ₂ separate on, H ₂ O ₂ roll integrators unnulled, high rate gain, low displacement gain	MECO + O	T + 675.4	T + 679.07	
MECO backup, PU null	SECO + 453.5 (t)	T + 688.3	T + 688.6+0	
Safe Surveyor destruct	SECO + 454		T + 689.6 ⁺⁰	
Preseparation arming, extend landing gear, null main-engine integrators	t + 18	T + 706.3	T + 706.8 ⁺⁰	

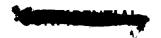


TABLE II-I. - Concluded. SEQUENCE OF FLIGHT EVENTS

Event	Time, sec			
	Programer	Nominal	Actual	
Unlock omni antenna	t + 28.5	T + 716.8	T + 717.1 ⁺⁰	
High power on, preseparation arming off	t + 49	T + 737.3	T + 736.57 ⁺¹	
Spacecraft electrical disconnect, switch guidance-spacecraft TLM channels	t + 54.5	T + 742.8	T + 742.57±0.5	
Separate spacecraft	t + 60		T + 747.57	
Start 180° turn, admit guidance for attitude control	t + 65	T + 753.3	T + 752.97	
End 180° turn, start retrothrust, prestart, start hydraulic recirculating pump	t + 185	Т + 873.3	T + 872.57	
Calibrate telemetry	t + 641	T + 1329.3	T + 1329.7+0	
Open LO ₂ and LH ₂ vent valves	t + 1165	T + 1853.3	T + 1853.3 ⁺⁰	
End retrothrust, power off	t + 1166	T + 1854.3	T + 1854.1 ⁺⁰	





TABLE II-II _ WEIGHT SUMMARY

Centaur stage	Weight,	Atlas stage	Weight,		
	1b		1b		
Basic hardware		Sustainer jettison weight			
Body group Propulsion group Guidance group Control group Pressurization group Electrical group	940 1 192 310 117 138 266	Sustainer dry weight Sustainer residuals Unburned expendables Interstage adapter Unburned lubrication oil	5 667 1 654 0 1 087 17		
Separation equipment Flight instrumentation	80 447	Total	8 425		
Miscellaneous equipment Spacecraft	153 2 084	Booster jettison weight			
Total	5 727	Booster dry weight Booster residuals Unburned lubrication oil	6 208 1 117 29		
Jettisonable hardwar		Total	7 354		
Nose fairing Insulation panels	2 006 1 218	Flight expendables			
Total	3 224	Main impulse RP-1	75 829		
Residuals		Main impulse O ₂ Helium panel purge	171 881		
LH2 trapped	72	Oxidizer vent loss Lubrication oil	15 173		
LO2 trapped Unburned ^a LH ₂ Unburned ^a LO ₂	68 91	Total	247 904		
Gaseous hydrogen	203 83	Ground ^c expendables			
Gaseous oxygen H2O2 Helium Ice	165 52 5 12	Fuel Oxidizer Lubrication oil	536 1 698 3		
Total	751	Exterior ice LN2 in helium shrouds Pre-ignition GO2 loss	50 140 450		
Expendables	1	Total	2 877		
Main impulse H ₂ Main impulse O ₂ Gas boiloff on ground bH ₂	4 966 25 153 27	Total tanked weight Minus ground run	266 560 -2 877		
Gas boiloff on ground b02 Inflight chill H2 Inflight chill 02 Boost-phase vent H2	26 11 13 83	Total Atlas weight at lift-off	263 683		
Boost-phase vent n2 Boost-phase vent 02 Sustainer-phase vent N2 Sustainer-phase vent 02 H2O2 Ice	20 46 38 49 50	Total Atlas-Centaur lift-off weight	303 814		
Total	30 482				
Total tanked weight Minus ground vent	40 184 -53				
Total Centaur weight at lift-off	40 131				

aIncludes flight performance reserve. bExpended prior to Atlas ignition. cGround run time, 2.05 sec.





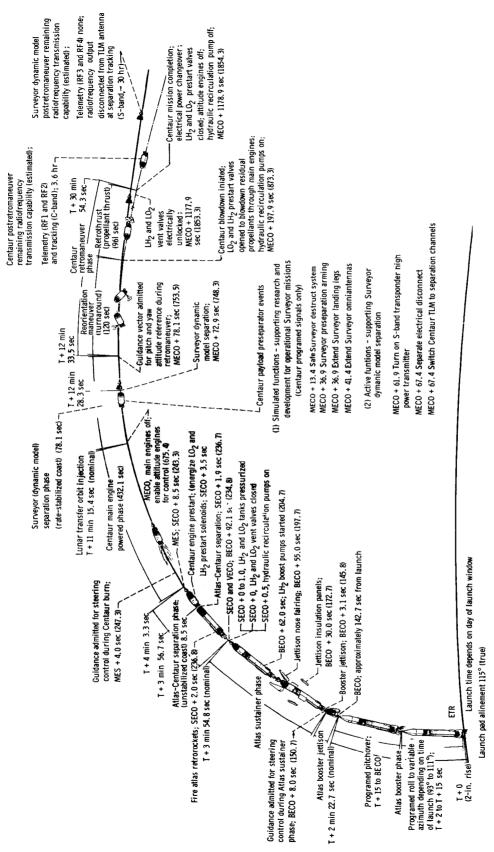


Figure II-1. - Atlas-Centaur-Surveyor dynamic model flight compendium. Times shown are preflight nominal. Actual times are given in table II-1.

CONFIDENTIAL.

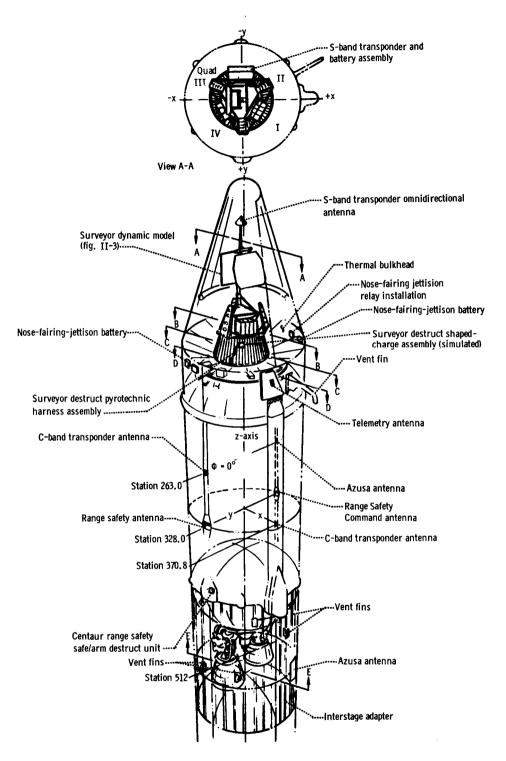
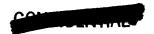
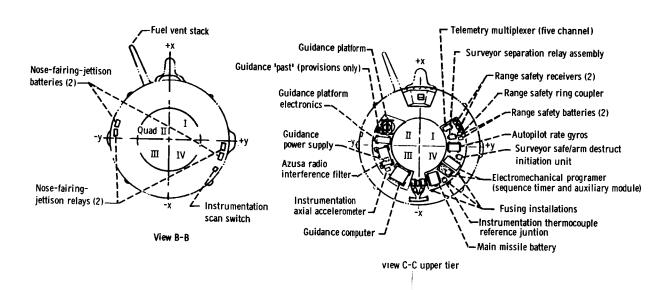
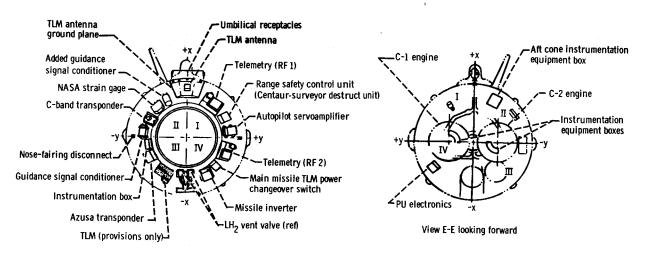


Figure II-2. - General arrangement of









View D-D lower tier

Centaur 2D (AC-6) (ref. 1).





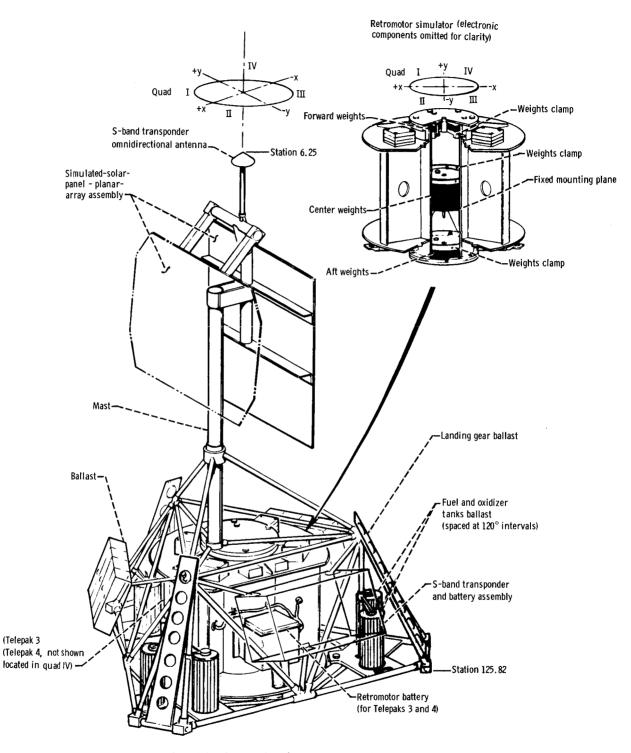
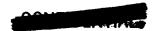


Figure II-3. - Surveyor dynamic model (SD-2) (ref. 1).





III. PRELAUNCH HISTORY

SUMMARY

Between the time the Atlas-Centaur launch vehicle arrives at ETR and launch day, it undergoes a series of preflight tests. These tests, which include (1) the Flight Control and Propellant Tanking Test, (2) the Flight Acceptance and Composite Test, and (3) the Composite Readiness Test, are to ensure that all airborne and ground-support systems are within specifications to support a successful launch. The tests were satisfactorily completed with only a few major anomalies.

ARRIVAL AND ERECTION

The Atlas-Centaur launch vehicle (AC-6) arrival at ETR began with the Atlas (151D) booster and the interstage adapter on May 14, 1965. The Centaur (2D) stage arrived May 25, 1965.

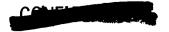
Vehicle erection on Complex 36B started on May 18 with the Atlas booster, followed by the interstage adapter on May 19, and the Centaur stage on May 27.

The Surveyor dynamic model arrived at ETR on May 14. The encapsulation of the model in preparation for preflight testing was accomplished on July 8 and it was mated to the launch vehicle on July 9. The encapsulated payload was demated on July 28 for final flight preparations and was remated to the launch vehicle on August 1 in preparation for launch.

PROPELLANT TANKING INTEGRATED TEST

The Propellant Tanking Integrated Test (Quad Tanking, ref. 2) is conducted to verify that the launch vehicle can be tanked with propellants and that all vehicle systems and the spacecraft can function properly under cryogenic and operational radiofrequency environments.

The Quad Tanking Test was conducted on July 13. The test began at 0520 EST and proceeded through to the scheduled 40-minute hold at T - 10 minutes at 0750 EST. Prior to T - 10 minutes, two major airborne equipment discrepancies were encountered. The first discrepancy occurred during the Guidance and Autopilot Test when the Atlas programer failed to act upon the guidance-generated BECO command. A rerun of this test was conducted successfully. After the Quad Tanking Test, the programer was removed from the vehicle and sent to GD/C, San Diego, for failure analysis. The second discrepancy occurred during LH₂ tanking when the C-1 pump inlet temperature would not meet the temperature requirements. The probable cause of this discrepancy was the hydrogen recirculation line. The





count was resumed at 0904 EST and, after several recycles between T - 5 minutes and T - 0, a simulated T - 0 occurred at 1000 EST. Other than the two major airborne equipment discrepancies, the results of the test were satisfactory.

PARTIAL TANKING TEST

A partial tanking test was conducted on July 29. The purpose of the test was to verify the fix of the hydrogen recirculation line by confirming the presence of LH₂ at the C-l pump inlet. The tanking consisted of 28 percent Centaur LO₂, 58 percent Centaur LH₂, and no propellants loaded in the Atlas. Liquid temperatures were not indicated at the pump inlet during LH₂ loading, but were indicated $5\frac{1}{2}$ minutes after the start of LHe chilldown of the Centaur main engines. The test was completed with satisfactory results.

FLIGHT ACCEPTANCE COMPOSITE TEST

The Flight Acceptance Composite Test (FACT, ref. 3) is conducted to verify that the combined Atlas-Centaur-Surveyor dynamic model system is capable of operation with no detrimental interference when subjected to conditions simulating flight.

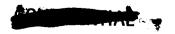
The FACT was conducted on July 28, beginning at 0905 EST. At T - 35 minutes a test to ensure that the Atlas inverter could be started and transferred to internal power was initiated. During the inverter start, trouble with a ground power supply was experienced and corrected. Subsequently, a second inverter start test was successfully performed. The test was resumed and proceeded normally with T - 0 occurring at 1226 EST. Other than the power supply problem, the test was completed with satisfactory results.

A second FACT was conducted on August 5. The purpose of the test was to check out the new Atlas programer that replaced the one that failed to start during the CRT test conducted on July 31. Prior to the start of the second test, the Atlas inverter was replaced because of the problems that were encountered during the first FACT. The test was satisfactorily accomplished.

COMPOSITE READINESS TEST

The Composite Readiness Test (CRT; ref. 4) is conducted to revalidate and verify the proper operation of the vehicle and GSE electrical systems.

The CRT was conducted on July 31. The test began at 1335 EST and proceeded until T - 5 minutes and 30 seconds at which time Atlas telemetry subsystem 1 was replaced because of a malfunction of two telemetry channels. The count was resumed and proceeded through to T - 0 at which time the count was recycled to T - 5 minutes because the second Atlas programer failed to start. The count was resumed and proceeded to the end of the test with a manual programer start and T - 0 occurred at 1559 EST. After the test, the programer was removed





and sent to GD/C, San Diego, for failure analysis.

A second CRT was conducted on August 6. The test was performed with satisfactory results.

LAUNCH

The first attempt to launch AC-6 was made on August 10 at ETR Complex 36B. The launch attempt was aborted at T - 1 minute because the Centaur destruct unit failed to arm. A recycle was started that enabled the second launch attempt to be conducted on August 11. The vehicle lifted off from ETR Complex 36B at 0931:04 EST. The vehicle systems performed nominally and injected the Surveyor dynamic model into a simulated lunar transfer orbit.

WEATHER

The atmospheric conditions on launch day were favorable, and permitted good photographic coverage. The cloud cover was from 20 percent between 20 000 to 40 000 feet to 80 percent between 250 000 to 300 000 feet. Surface winds ranged from 6 to 8 knots with visibility of 10 miles and a temperature of 84° F. Altitude variation of atmospheric pressure, temperature, and wind velocity component is presented in figures V-1 and 2.

LAUNCH ON TIME

The AC-6 launch and launch attempt demonstrated two important launch-on-time factors essential to the development of a capability to adjust to unknown factors that could cause the miss of a launch window. These factors were (1) the capability to preplan a countdown operation and execute the countdown to achieve a precise vehicle lift-off time and (2) the ability to turn around in 24 hours after an abort of a launch attempt.

The Atlas-Centaur AC-6 was launched on August 11, 1965, at 0931:04 EST, which was 4 seconds after the window-opening time. The ETR range countdown was scheduled for 280 minutes with preplanned holds of 60 and 40 minutes at T - 90 and T - 5 minutes, respectively. The countdown was successful thus demonstrating the ability to launch on time.

The launch attempt on August 10, 1965, was aborted after the countdown reached T - 1 minute and 35 seconds because the Centaur Range Safety Command system failed to arm. The vehicle was detanked, and preparations were made to attempt a launch on the following day. The second launch attempt was successful thus demonstrating the ability to turn a vehicle around and launch within a 24-hour period.

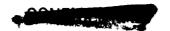




AC-6 PRELAUNCH HISTORY - 1965

Arrival of Atlas 156D	May 14
Arrival of interstage adapter	May 14
Arrival of payload	May 14
Erection of Atlas 156D	May 18
Erection of interstage adapter	May 19
Arrival of Centaur 6C	May 25
Erection of Centaur 6C	May 27
Arrival of insulation panels	June 1
Arrival of nose fairing	June 14
Erection of insulation panels	June 15
Encapsulation of payload	July 8
Mating of encapsulated payload	July 9
Quad tanking	July 13
Flight Acceptance Composite Test 1	July 28
Demating of payload	July 28
Partial tanking test	July 29
Mating of payload	August 1
Flight Acceptance Composite Test 2	August 5
Composite Readiness Test	August 6
Attempted launch	August 10
Launch	August 11





IV. MECHANICAL GROUND-SUPPORT EQUIPMENT AND FACILITIES

SUMMARY

All mechanical ground-support equipment and facility equipment functioned satisfactorily during the launch countdown. Minor problems, consisting of a failed hydrogen storage tank vent stack igniter and a possible leaking Centaur IO2 flow-control valve were encountered.

PROPELLANT-LOADING SYSTEM

Performance of the propellant-loading system was satisfactory throughout the countdown with only two minor problems encountered. The hydrogen storage tank vent stack igniter failed at approximately T - 200 minutes. It was decided, with Range Safety concurrence, to continue the countdown without the burner. At approximately T - 60 minutes it was reported that the Centaur LO2 loading flow-control valve leaked LO2 into the Centaur tank. It was speculated that the valve may not have been in a fully closed position when the storage tank transfer pressure was raised to 145 psig.

LH2 Systems

The liquid-hydrogen transfer system consists of a vacuum-jacketed LH₂ storage tank, a vaporizer for transfer pressure, a flow-control unit, and a vacuum-jacketed transfer line. The system delivers LH₂ at an approximate rate of 750 gpm. Gaseous helium is used for purging the transfer and storage-tank vent lines before and after tanking. The storage tank is pressurized to 12 psig for chilldown and 38 psig for transfer. On the AC-6 launch, however, the maximum transfer pressure achieved was 29.2 psig. This anomaly had also occurred on quad tanking but not on subsequent testing. This pressure, however, was adequate for LH₂ transfer.

LO2 Systems

The LO2 transfer system consists of a 38 000-gallon storage tank, a vaporizer for transfer pressure, a flow-control unit, and a topping system with an LN2 subcooler. The system performed satisfactorily with the only anomaly being the Centaur flow-control-valve leakage mentioned previously.

LIQUID-HELIUM CHILLDOWN

Liquid-helium chilldown was initiated at T - 23 minutes. The LHe flow-





control and line-dump valves are both opened for chilldown. When the dump-valve temperature reaches -200° F, it is closed. C-1 and C-2 pump temperatures are controlled by the flow-control valve and a -310° F temperature is required for both pumps at 15 minutes prior to T - O. There were no problems in the system, and approximately 180 gallons of LHe were used for pressurizing the storage Dewar, line chilldown, engine chilldown, and depressurizing the Dewar.

PRESSURIZATION SYSTEM

All pneumatic systems performed within required limits as follows:

Primary helium supply:

Minimum - 1500 psig from T - 90 minutes to engine start

Actual - 4500 psig

Emergency helium supply:

Minimum - 3500 psig from T - 90 minutes to engine start

Actual - 5000 psig

Routine GN, supply:

Minimum - 2300 psig from T - 90 minutes to engine start

Actual - 4500 psig

Environmental GN₂ supply:

Minimum - 900 psig from start of Centaur tanking to launch

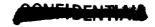
Actual - 1900 psig

UMBILICAL BOOMS

This was the first Centaur launch to use horizontal swing booms. This system consists of one upper and one lower boom that are swung in opposite directions by separate hydraulic rotary actuators. Boom rotation is actuated by solenoid firing valves that are energized by the 2-inch motion signal. The lower boom rotation starts 0.25 second later than the upper boom as a result of a time-delay relay in the lower-boom firing circuitry.

Upper Boom

The upper boom has four electric umbilical plugs, the GH2 vent line, and the Surveyor and Centaur air-conditioning ducts. The umbilical plugs are electrically ejected at approximately T - 4 seconds with a lanyard backup in the event of failure of the electric ejectors. This lanyard is retracted by a hydraulic cylinder. The upper boom rotation times are given in the following table:



POMEIDENTIAL

Degrees from rest	Time, sec	Required time, sec
3 21 50	T + 1.50	Prior to T + 1.50 Prior to T + 3.00 Prior to T + 4.70

The lanyard cylinder retraction started at T - 2.75 seconds and completed its stroke in 0.80 second. The required timing is between 0.80 and 0.96 second.

Lower Boom

This boom supports the $\rm IO_2$ and $\rm IH_2$ transfer lines, the aft pneumatic panel lines, $\rm IH_2$ and $\rm IO_2$ fill and drain valve actuation and purge lines, the T - O electric umbilical, the insulation-panel purge-bottle charge line, and the interstage-adapter air-conditioning duct.

This boom has two lanyard cylinders, one for the T-4 umbilicals and one for the T-0 umbilicals. In most cases, these lanyards act as a backup for the primary disconnect mechanism (electric, pneumatic, or static lanyard). The T-4 cylinder stroke started at T-3.05 seconds and stopped at T-1.78 seconds well within the 1.20- to 1.60-second requirement. The T-0 cylinder stroke started at T+0.20 second ending at T+1.02 seconds or 0.82 second total. The required time is between 0.80 to 0.96 second. The lower boom rotation times are presented in the following table:

Degrees from rest	Time, sec	Required time, sec
13 35 55	T + 2.63	Prior to T + 1.7 Prior to T + 3.2 Prior to T + 4.4

ENVIRONMENT CONTROL SYSTEM

The environmental control system provided the required air-conditioning supply temperatures and flow rates to the vehicle, except for the flow to the interstage adapter. After the launch it was discovered that the orifice plate was installed backwards in the test tool used to set the flow rate to the interstage adapter. Tests run on October 8, 1965 showed that reversing the orifice plate causes a 25-percent error in calculated flow rate. Consequently, flow rate to the interstage adapter during the countdown exceeded the specified upper limit of 178 pounds per minute.

Air-conditioning-system performance during the launch countdown, from the start of LO₂ tanking until lift-off, was as follows:





Payload:

Requirements - 85°±5° F; 75±3.5 lb/min

Actual - 84° to 85° F; 74 lb/min

(temperature measurement at disconnect, landline measurement number CN1560T; ref. 5)

Centaur electronic compartment:

Requirements - 48°±5° F; 79±4 lb/min

Actual - 47° to 49° F; 82 to 73 lb/min

(temperature measurement in duct on umbilical tower,

CNll9lT).

From 08:00 EST until lift-off, pressure oscillations of as much as ±3 in. of water occurred in the ducts, at about 6-min intervals. Flow rates noted are based on mean pressure values.

Interstage adapter:

Requirements - 137.50±7.50 F; 164±14 lb/min

Actual - Temperature at start of

- Temperature at start of LO₂ tanking was 120° F and rose to 130° F in 25 min. During the remainder of the countdown, temperature rose slowly to a maximum of 134° F at lift-off (temperature measured in duct on umbilical tower, CN1274T). Temperature measured at the disconnect (CN1557T) was 5° to 6° F lower than CN1274T. Flow rate was 195 lb/min.

Atlas pod:

Requirements - 50° F maximum; 32 lb/min minimum

- Temperature rose from 46.5° F at start of LO₂ tanking to

49.4° F at lift-off (temperature measured in duct at base of umbilical tower, AN1342T). Flow rate was between 40 and 41

lb/min.

Atlas thrust section:

Requirements - Over the range from 60 to 80 lb/min, minimum temperature ranges from 180° to 147° F.

ranges from 180° to 147° F

Actual - Temperature rose from 165°

- Temperature rose from 165° F at start of IO_2 tanking to 170° F at T - 5 min. After switch-over to GN_2 , temperature dropped to 169° F. Flow rate was 84 lb/min until T - 5 min and dropped to about 77 lb/min after switch-over to GN_2 .

The air-conditioning GN_2 supply was supplemented by operation of the LN_2 vaporizer at Complex 36A, from 03:00 to 09:31 EST. This accounts for consumption of 2250 gallons of LN_2 from the Complex 36A Dewar.

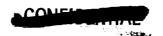
The available and consumed quantities of the propellants and gases and their usage are given in table IV-I.





TABLE IV-I. - PROPELLANT AND GAS USAGE

Propellant or gas	Usage	Available	Consumed
GN ₂	Routine use, scf	52 200	33 200 490 000 23 100 Negligible
GHe	Insulation-panel and engine purge, scf Primary, scf	440 000 95 200 49 000	111 000 20 100 15 100
LHe	gal	1 000	180
ro ^S	gal	38 100	30 600
LH ₂	gal	22 000	12 000
RP-1	gal	15 000	13 400
LNS	Complex 36B, gal	25 750 15 000	3 250 2 250



V. TRAJECTORY

SUMMARY

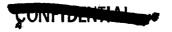
The Atlas-Centaur AC-6 vehicle, targeted for a September 28 launch opportunity, was launched on time August 11, 1965 at 0931:04.430 EST. The flight was so near nominal that the transfer orbit of the Surveyor model passed through the "paper moon" without the need of a midcourse correction. To place the payload in the desired target area on the lunar surface would have required a midcourse correction of only 4.25 meters per second. The booster launch vehicle exhibited the characteristic lofted trajectory profile, which has been observed in the previous flights (ref. 6). To account for this anomaly, a new drag model, which draws on flight observations as well as on wind-tunnel data, has been adopted. Most significant, aside from yielding a more satisfactory acceleration history, the new model reveals a substantial gain in payload capability for operational Surveyor flights. The Atlas sustainer engine operated with 1.6 percent higher specific impulse and 2.3 percent higher thrust levels than nominal. A further look at the engine model simulations may be suggested by this finding. Centaur engine specific impulse, though above acceptance test levels, was well within the three-sigma deviation of that predicted. The guidance system properly compensated for the "hot" booster and targeted to the proper injection conditions.

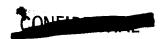
INTRODUCTION

Trajectory Definition

There are two main purposes for a postflight trajectory analysis effort. The first is to verify or improve the preflight trajectory simulation technique and thus to increase confidence in the FPR and payload capability calculations for operational flights. The second purpose is the determination of the best estimate of the actual vehicle performance. The analysis was performed first by comparing the preflight prediction with the observed trajectory and, second, by reconstructing the flight using the computer simulation.

The preflight or predicted trajectory was determined with the ground rules and weights of reference 7 and for the actual time of launch using a computer trajectory program. For trajectory evaluation, a guidance-based trajectory (GET) was accepted as the best estimate of the actual trajectory. Normally, the best estimate of trajectory (BET) consists of ground-based tracking data, which are received from AFETR in the form of position, velocity, and acceleration components. The reconstruction program, which was used as part of the trajectory analysis, required a smooth set of tracking data for matching. The GET data were found to be more consistent and smoother than the BET data. During the





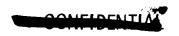
first 20 seconds of flight, the ETR determined BET data were of poor quality because of the absence of optical tracking. Beyond T+620 seconds, the noise level of the BET became excessive, because the range of the Glotrac, a high-precision tracking system, was exceeded at this time. After the loss of Glotrac, the three-sigma deviations of the tracking position and velocity components were one and two orders of magnitude, respectively, greater than prior to its loss. Even within the intermediate period between T+20 and T+620 seconds, the smoother GET provided a better opportunity to study trends and patterns in the component differences (residuals) of the actual and reconstructed trajectories.

The trajectory was reconstructed with the same computer program used to determine the preflight predicted trajectory. Performance and steering parameters were adjusted until the computed position and velocity components best matched the GET components in a weighted least-square sense. The adjusted values of the Atlas performance and steering parameters differed little for BET versus GET. However, the noise in the residuals was lower, and the selection of data points to be matched along the trajectory was less subjective with the smoother GET. The residuals, which resulted from the least-square match, were subjected to further investigation to determine changes in the model needed for a more satisfactory match and thus for a better simulation of the actual flight.

Rawinsonde Atmosphere Data

Atmospheric conditions and wind profiles at the time of launch are necessary for a proper postflight reconstruction. Launch conditions were determined at the site at 0940 EST, approximately 9 minutes after lift-off. Profiles of these measured temperatures and pressures as a function of altitude are compared with those assumed for the preflight trajectory (fig. V-1(a)). slight variations were evident between the measured and preflight values. Rawinsonde launch winds are presented in figure V-1(b). Zero magnitude winds, in lieu of light winds normal for September, were used in the preflight simulation of AC-6. The measured east-west components below 40 000 feet, where aerodynamic forces are most prevalent, agreed well with the preflight estimates; however, the north-south components in the same altitude region were approximately 20 feet per second out of the south. This wind, for an otherwise nominal flight, would have tended to bias the trajectory to the left of predicted. presence of winds also affected the angle of attack throughout booster operation, as discussed in section IX, VEHICLE STRUCTURES AND SEPARATION SYSTEMS. Above an altitude of 40 000 feet, the winds have much less effect on the trajectory.

Comparisons of profiles of dynamic pressure q and Mach number M of the preflight simulation with the profiles derived from Rawinsonde data and the observed trajectory are presented in figure V-2. Both q and M from T + 60 to T + 120 seconds were higher for the actual than for the preflight predicted trajectory. It is noteworthy that this time corresponds to the interval of highest drag, and also that values of q and M higher than those predicted were seen on earlier Atlas-Centaur flights through this time interval.





Telemetry and Other Measured Data

The preflight trajectory, as previously mentioned, was determined for nominal or predicted conditions. Variations in any actual condition, which may cause a change in the trajectory, should be incorporated, when possible, in the postflight reconstruction. The measured atmosphere and winds are included. The best estimate of the actual propellant and hardware weights were used in the reconstruction and are compared in table V-I with those of the preflight. Actual histories of several parameters, which affect engine operation and which are variables of the propulsion models, were obtained from telemetry data. The operation of the Atlas engines was simulated by a computer-programed detailed propulsion model (DEPRO), which includes effects due to ambient pressure, propellant densities, and pump inlet pressures and to operation of the sustainer propellant-utilization (PU) system.

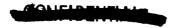
Ambient pressure was determined as a function of altitude from the launch atmosphere profile. The density of RP-1 was fixed at its launch time value of 50.38 pounds per cubic foot; that of $\rm IO_2$ was calculated from telemetry temperature-pressure data. Propellant-tank ullage pressures, which are used in DEPRO to determine pump inlet pressures, and the history of sustainer PU valve position were other telemetered data used in the reconstruction.

The telemetered inlet temperatures and pressures and the PU valve position for the two Centaur engines were used in the Pratt & Whitney (P & W) Regression equations to determine variations of the thrust and specific impulse of the engines. Because the telemetry history of the LH2 inlet temperature for the C-1 engine was not acceptable, it was replaced by the LH2 temperature history of the C-2 engine in the reconstruction.

Time histories of vehicle thrust attitude in pitch and yaw, relative to the launch inertial reference coordinate system, were derived from the telemetered values of the time integrals of the three guidance system accelerometers. These attitude histories were used to steer the vehicle during the guided portion of the postflight reconstruction in lieu of the guidance equations. Experience with the reassembly of AC-4 showed that a guidance simulation distorted the iteration process of the reconstruction. The guidance equation corrected for performance dispersions that had been introduced by the adjusting procedure used to search for the best performance values. Use of guidance-derived attitudes avoided this distortion.

RESULTS

Trajectory parameters are presented in table V-II for the predicted, observed, and reconstructed trajectories. A detailed trajectory listing is presented in appendix C. The observed and reconstruction values are in good agreement with each other and are in fair agreement with the predicted values. Another indication that the actual flight was near that desired is that the injection orbit elements (table V-III) are in reasonable agreement. The actual values were determined from 48 hours of spacecraft tracking by JPL. Based on these observations, a midcourse correction of only 4.25 meters per second would have been required to impact in the desired lunar target area. This is well within the projected capabilities of the AC-7 spacecraft, the first Surveyor that will attempt a midcourse maneuver and soft lunar landing.





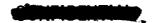
Values of vehicle performance were obtained from the trajectory reconstruc-In order to achieve a satisfactory fit of the observed trajectory, a modified aerodynamic drag model was used. A more detailed discussion of this model and its significance is presented later in this section. The reconstruction, as mentioned previously, was performed by adjusting vehicle performance and attitude parameters until the reconstructed trajectory best matched the observed velocity and position components in a weighted least-square sense (ref. 6). Prior to the reconstruction of the flight, several observations regarding the trajectory were apparent. As shown in figure V-3, the actual trajectory was to the right of and slightly lofted above the preflight profile. The bias to the right would appear to be a launch azimuth difference. The lofted trajectory had been the trend observed on previous Atlas-Centaur flights. Discrepancies in velocity (fig. V-4) and thrust acceleration (fig. V-5) indicated that there had also been greater-than-predicted acceleration during the booster phase. the lofted trajectory and the high thrust accelerations can result from betterthan-predicted booster performance and/or a variation of the flight aerodynamic drag characteristics from those predicted. The study of a similar phenomenon on the AC-4 flight indicated that a discrepancy in the drag characteristics was the principal cause (ref. 6). This anomaly for AC-6 is discussed later in more Velocity and thrust acceleration comparisons (figs. V-4 and 5) indicated performance other than the predicted performance during sustainer solo and Centaur phases. During sustainer solo operation, the differences, in part, can be attributed to the shift in BECO time for the predicted and actual flights.

For the reconstruction, five attitude factors were tuned during the Atlas phase of the reconstruction: (1) attenuation factor on the nominal booster pitch-rate profile, (2) initial pitch-over azimuth, (3) initial pitch attitude from T + 0 to T + 15 seconds, (4) and (5) attenuation factors on the sustainer pitch and yaw guidance-derived-attitude histories. In addition, the thrust and specific impulse levels, that is, reference values, of the booster and sustainer engines, and the effective time of BECO, were modified for the trajectory match. It should be noted that engine transient models, such as the booster engine decay model, were used in the reconstruction. Consequently, any deviation between the predicted booster engine shutdown model and the actual shutdown transient would be compensated for by a shift in the computed time of During Centaur phase, thrust and specific impulse of the engines were adjusted. Again, to compensate for any discrepancies in either the Centaur engine buildup model or the sustainer engine decay model, an effective time of MES was determined. Attenuation factors on the Centaur pitch- and yaw-attidude histories and constant drift rates in pitch and yaw completed the list of adjusted parameters for the Centaur reconstruction.

Atlas Parameters

The adjusted and the preflight propulsion parameters are presented in table V-IV. Preflight reference values and the reconstruction reference values of the propulsion model are compared. Additionally, specific inflight values, which are tabulated at T+2 seconds for the Atlas and T+300 seconds for the Centaur, are compared. These latter data show not only the difference in reference performance, but also the effect of deviations from predicted engine inlet conditions and PU valve histories.





Specific impulse and thrust of the engines were determined with the reference booster mixture ratio fixed at the preflight reference value. The adjusted reference specific impulse of the booster engines was slightly less (-1.3 percent) than the standard reference value, while engine thrust value maintained a near nominal value, up only 0.4 percent. Reference values of sustainer performance required larger adjustments. Increases in reference thrust and specific impulse of 2.3 and 1.6 percent, respectively, were needed. These adjustments were significantly greater than the three-sigma deviations of this engine and therefore were of concern. A similar increase in specific impulse was obtained over near-constant thrust regions of sustainer solo operation, when the slope-impulse technique (ref. 6) was applied to the reciprocal of guidance-based thrust accelerations. This check, in addition to the relatively small and random thrust acceleration residuals of the reconstruction during sustainer solo (fig. V-6) supports the higher sustainer performance.

An improvement in the match of observed position and velocity components was further attained by adjusting attitude parameters of the trajectory. A cross-range drift to the right by the actual trajectory from the predicted is indicated in figure V-3(c). In order to account for this cross-range drift, the initial roll to pitch-over azimuth was adjusted. The actual pitch-over azimuth was determined as 94.92°, which is 0.38° greater than that indicated for the launch time. Integration of the telemetered roll rate during the initial 15 seconds after 2-inch motion gave an azimuth of 94.9°, in good agreement with the computed adjusted value. An attenuation factor on booster pitch-rate history was increased 0.5 percent, possibly compensating for step errors in the autopilot or uncorrected drifting of the autopilot. The initial pitch attitude of both the booster and the sustainer steering profiles required minor adjustments to improve the trajectory match.

The final residuals of thrust acceleration, velocity, and position components during Atlas operation are presented in figures V-6(a), 7(a), and 8(a). Except during engine transient times, the velocity residuals were below 3 feet per second, and position residuals were below 60 feet.

Centaur Parameters

The match of position and velocity components during the Centaur phase was not as good as the Atlas match. Reconstruction residuals for this phase are presented in figures V-6(b), 7(b), and 8(b). Maximum velocity and position residuals were approximately 5 feet per second and 200 feet, respectively, except for the last 20 seconds of powered flight. During this portion of the flight, the pseudo-guidance simulation and possible limitation of the engine model may have contributed substantially to the relatively poor fit.

The thrust acceleration residuals (fig. V-6(b)) showed a pattern of error amplitudes that could be correlated with the larger amplitudes of the Centaur PU valve cycle shown in figure 5 of section VII. This correlation is particularly evident between T + 340 and T + 380 seconds, and after T + 660 seconds, at which time it was indicated that the PU valves were at the $\rm IO_2$ -rich limit. This correlation suggests that the PU valve may have, at times, exceeded the limits of





the engine performance model, which had been derived for small variations in inlet conditions and PU valve angle.

The reconstructed Centaur thrust level, derived with the P & W engine model for the measured engine conditions, was less than 1 percent below the acceptance test value (table V-IV). The adjusted reference specific impulse was determined as 435.9 seconds, well within the range of acceptable dispersion. An independent calculation of specific impulse was made with the slope-impulse technique, which requires a constant thrust (the mean of a sinusoidal thrust will satisfy the constant thrust requirement). For this method, a specific impulse of 435.5 seconds, consistent with the reconstruction value, was obtained.

An engine build-up model was derived for the reconstruction from the thrust acceleration history following the Centaur engine ignition signal. To compensate for errors in the engine transient models of sustainer shutdown and main engine startup, the time of the main engine start (MES) signal was adjusted in the reconstruction. The computed MES was 242.63 seconds, approximately 0.14 second earlier than the measured discrete event (table V-II).

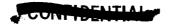
As in the Atlas reconstruction, it was necessary to adjust the guidance-based attitude histories used to orient the vehicle in the reconstruction. To reduce the residuals of velocity and position during the Centaur phase, the attitude histories, in pitch and yaw, respectively, were adjusted with attenuation factors of 0.9978 and 0.9976 and with a drift rate of 0.000ll degree per second to the left in the yaw plane and 0.00080 degree per second up in pitch plane.

Aerodynamic (Drag) Models

Reconstruction of the AC-4 trajectory (ref. 6) and preliminary attempts of reconstruction of AC-6 indicated that the standard drag coefficient C_X model did not accurately represent flight axial forces. This preflight model (Model I of fig. V-9) is employed to compute drag simply as the product q, C_X , and the reference area, A.

When this model was incorporated in the AC-6 reconstruction, a large residual pattern resulted during the high-dynamic-pressure (q) period of the flight from T + 60 to T + 110 seconds (fig. V-10). A similar pattern was observed in the AC-4 reconstruction, and the drag model was believed to be at fault. On the basis of AC-4 results, as well as flight data of other Atlas flights, GD/C formulated a new drag model (Model II of fig. V-9). This model separates the drag into three major components, q-sensitive drag, base force, and holddown force. The q-sensitive drag, with fore body and aft body contributions, is dependent on Mach number, dynamic pressure, and vehicle cross-sectional area. The base force results from recirculation of mass from the engine exhaust jets to the base of the vehicle. The magnitude of this base force is generally determined from flight measurements rather than wind tunnel tests.

The holddown force improves the match of thrust acceleration obtained by optical tracking during the first 10 seconds after 2-inch motion (fig. V-11).





This force is believed to be caused by the restraining forces of the launcher and effects of ground proximity. This force was included as an exponential force decaying from a maximum at lift-off to zero at 10 seconds.

The drag models and their reconstruction acceleration residuals are presented in figures V-9 and 10. The GD/C drag model (Model II) is of the form

$$DRAG_{II} = -4500(1.0 - P_{amb}/P_{sl}) + qAC_{x_{TI}} + 41.29(10.0 - t)^{2.3917}$$

where

 P_{amb}/P_{sl} ratio of ambient pressure to sea level pressure

A reference area, 78.5 sq ft

 C_{x} standard drag coefficient

t time from lift-off (0 < t < 10), sec

The first expression on the right of the equation gives the base force, with a vacuum value of 4500 pounds; the last term gives the holddown force with a maximum value of approximately 10 000 pounds.

The inclusion of Model II, which greatly improved the trajectory match, still left a residual pattern between T + 60 and T + 80 seconds (fig. V-10). Since the booster engine thrust was increased from 154 000 pounds for AC-4 to 165 000 pounds for AC-6, it could be anticipated that the vacuum base force would increase with the higher jet pressure associated with the uprated engines. Consequently, a third drag model, patterned after the GD/C Model II, was derived specifically for the AC-6 reconstruction. In addition to adjusting the base-force term and the drag coefficients, the initial holddown force was tailored to the optical tracking data (fig. V-11). The resulting drag model (Model III) is of the form

$$DRAG_{III} = -5000(1.0 - P_{amb}/P_{sl}) + qAC_{x_{III}} + 16.516(10 - t)^{2.3917}$$

where $0 \le t \le 10$. This model increased the vacuum base force from 4500 to 5000 pounds, readjusted the C_X function (fig. V-9), and reduced the holddown force to 40 percent of that of Model II. The effects on thrust acceleration residuals with this revised model are shown in figures V-10 and 11.

Model III did not significantly change the values of the reconstruction booster performance parameters from those determined by Model II. The thrust increased 0.03 percent, and specific impulse decreased by 0.04 percent for Model III. Sustainer performance showed no change in specific impulse and a 0.05-percent decrease in computed thrust level.

A net payload increase for an operational vehicle, AC-15, of 83 pounds for Model II and 85 pounds for Model III results when the new models replace the standard drag model, Model I. The results of the reconstruction presented in



the tables and figures were obtained with Model III. In summary, Model II, the new standard preflight drag model, yields a good acceleration match for AC-6. This can be further improved as indicated by the results based on Model III; however, the differences in residuals for the two models are small and may be within inherent flight-to-flight variation. Regardless of which model was used, there still existed large residuals in thrust acceleration and velocity during the 10 seconds prior to BECO. These residuals, evident in figures V-6 and 8, suggest the need for further study of the drag and/or propulsion models, if the same patterns of residuals repeat in future flights.

Atlas Propellant Residuals

An indication of the accuracy of the engine performance models is how well they predict the amount of each propellant remaining in the vehicle tanks. Previous reconstructions have indicated that the Atlas propulsion model could be improved by increasing the number of independent variables considered (ref. 8). However, this new model has not been incorporated into the simulations used in this analysis. The current Atlas propulsion model is referred to as the 6 variable DEPRO; the proposed new model (ref. 8) is referred to as the 12 variable DEPRO.

Estimates of the fuel and oxidizer residuals in the Atlas tanks were made on the basis of sensor uncovery times. It was indicated that approximately 294 pounds of RP-1 and 418 pounds of LO₂ remained. The postflight reconstruction, which included simulation of measured sustainer PU valve position that was on the LO₂-rich limit most of the flight, indicated that approximately 490 pounds of RP-1 and 123 pounds of LO₂ were left. Thus, the total residuals were about 100 pounds less than estimated and were accepted as adequate for the purposes of the reconstruction; however, the imbalance between fuel and oxidizer residuals was larger than desired. There is evidence that this may be a result of an inadequacy on the part of the 6 variable DEPRO model.

Using the data of reference 8, which indicated approximately a 0.5-percent decrease in booster mixture ratio when the 12 variable model was used rather than the 6 variable model, showed that the oxidant-fuel ratio of the residuals from the reconstruction could be changed from about 0.25 to 1.92. This value would be in better agreement with the estimated residual oxidant-fuel ratio of 1.42. Consequently, the use of the 12 variable model should yield a better estimate of the propellant residuals. An accurate means of predicting the residuals is needed in preflight simulations, so that the booster engines may be properly orificed and the sustainer PU valve suitably biased prior to flights.





TABLE V-I. - TRAJECTORY ANALYSIS WEIGHT SUMMARY

Weight, lb	Preflight ^a estimate	Postflight estimate	Trajectory reconstruction
Total at lift-off At BECO (before staging) Booster jettison ^C Insulation Nose fairing Total at separation Sustainer residual propellant ^d Sustainer jettison ^C Centaur and payload at lift-off Boost-phase Centaur loss: Oxidant Fuel Hardware and miscellaneous Centaur at separation Total weight at MECO Centaur residual propellant: ^d Oxidant Fuel (including PU residual) Centaur jettison	302 073 79 117 7 355 1 226 1 995 44 562 475 7 700 39 848 3 461 (126) (58) (3 277) 36 387 6 372 188 (107) (81) 4 084	303 536 7 354 1 225 2 005 44 833 712 7 713 39 892 3 484 (58) (129) (3 297) 36 408 6 474 294 (203) (91) 4 096	b303 536 80 529 b7 356 b1 225 b2 005 44 731 613 b7 710 b39 892 b3 484 (b58) (b129) (b3 297) b36 408 6 580 400 (333) (67) b4 096
Payload	2 100	2 084	^b 2 084

^aBased on data of appendix A of ref. 7. ^bBased on the best postflight weight estimate. ^cIncludes residual lubrication oil and trapped propellant. ^dPropellant above pump inlet.

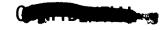


TABLE V-II. - TRAJECTORY PARAMETER COMPARISON

Parameter	BECO	Insulation jettison	Nose-fairing jettison	SECO	Separation	MES	
Time, a sec							
Planned ^b Actual Reconstruction	142.061 141 79 c141.879	172.061 171.62 171.72	197.061 196.47 196.49	235.268 234.10 234.39	237. 268 236. 22 236. 22	243.768 242.77 c242.634	
		Altit	ıde, n. mi.				
Planned Actual ^d Reconstruction	31.430 31.841 31.893	47.682 48.324 48.377	60.261 61.092 61.103	78.391 79.289 79.426	79.307 80.277 80.279	82.178 83.223 83.170	
		Rang	ge, n. mi.				
Planned Actual Reconstruction	42.024 42.271 42.383	80.056 80.488 80.624	115.444 116.076 116.106	177.484 177.921 178.441	181.019 181.716 181.720	192.494 193.434 193.200	
		Relative v	elocity, e ft/s	sec			
Planned Actual Reconstruction	8073 8152 8172	8861 8972 8976	9680 9810 9810	11 334 11 487 11 496	11 327 11 483 11 490	11 280 11 430 11 444	
		Inertial v	elocity, ft/se	ec			
Planned Actual Reconstruction	9313 9390 9410	10 141 10 251 10 254	10 984 11 113 11 113	12 664 12 817 12 827		12 616 12 767 12 780	
	Axial load factor, g's						
Planned Actual Reconstruction	5.700 5.69 5. 7 57	1.252 1.27 1.278	1.426 1.45 1.454	1.378 1.471	0.00024	0.00024	

^aTime from 2-in. motion (0931:04.430 EST). Planned and reconstruction times refer to the beginning of thrust decay or weight separation. Actual times are taken from table II-I.

^dAll actual values were determined from corrected telemetry guidance data. ^eVelocity referenced to a coordinate system fixed with rotating Earth.



bAll planned values are taken from a simulated trajectory based on ref. 7 and using the actual time of launch.

^CEffective time compatible with the engine build-up simulation used in reconstruction.

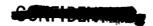


TABLE V-III. - SPACECRAFT ORBIT PARAMETERS

Parameter	Predicted ^a	Actual ^b	Reconstruction
Time ^c of epoch, sec Inclination, deg True anomaly, deg Semimajor axis, n. mi. Perigee altitude, d n. mi. Apogee altitude, d n. mi. Eccentricity Period, days Energy, sq ft/sec ²	678 28.59 -5.89 229 843.56 90.14 452 708.95 0.9846 31.989 -5 039 728	679.2 28.56 -5.76 224 365.98 90.19 441 753.77 0.9842 30.853 -5 162 766	90.94 441 749.52 0.9842
Injection conditions			
Latitude, deg Longitude, deg Radius, n. mi. Flight path angle, f deg Azimuth, deg Relative velocity, ft/sec	23.034 307.258 3 543.43 -3.039 108.143 34 647.21	22.981 307.449 3 543.20 -2.968 108.166 34 645.67	22.984 307.539 3 543.79 -2.966 109.249 34 640.18

^aData obtained from Lewis Research Center preflight nominal trajectory.



bData obtained by Jet Propulsion Laboratory from spacecraft tracking.

CTime measured from 2-in. motion (from 0931:04.430 EST).

dMeasured above a spherical 3444-nautical-mile-radius Earth.

eReconstruction trajectory terminated at Jet Propulsion Laboratory determined energy.

fAngle between relative velocity vector and local horizontal.

gAngle of relative velocity vector measured clockwise from true north.



TABLE V-IV. - PROPULSION PARAMETERS FOR RECONSTRUCTION

Parameter	Re	Reference values		Specific	Specific inflight valuesa	luesa
	Standardb	Reconstruction Ratio	Ratio	Preflight	Postflight	Ratio
	Booster	jer jer	;			
Thrust (sea level), lb Flow rate, lb/sec Specific impulse (sea level), sec Mixture ratio, 0/F	330 000 1306.9 252.5 2.28:1	331 155 1328.3 249.3 2.28:1	1.0035 1.0164 .9874 1.0000	325 536 1291.9 252.0 2.25:1	325 232 1298.7 250.3 2.18:1	0.9991 1.0053 .9936
ŭ	Sustainer and vernier	nd vernier				
Thrust ^c (sea level), lb Flow rate, lb/sec Specific impulse (sea level), sec Mixture ratio, O/F	59 000 275.2 214.4 2.27:1	60 351 2 77. 1 217.8 2.27:1	1.0229 1.0069 1.0159 1.0000	58 342 273.4 213.4 2.40:1	60 332 275.6 218.9 2.48:1	1.0341 1.0080 1.0258 1.0333
	Centaur	aur				
Thrust (vacuum), lb Flow rate, lb/sec Engine specific impulse (vacuum), sec Vehicle specific impulsed (vacuum), sec Mixture ratio (engine), O/F	29 939.00 68.904 434.5 434.0 5.045:1	29 684.5 68.045 435.9 435.4 5.045:1	0.9915 .9883 1.0033 1.0000	29 939.0 68.904 434.5 434.0 5.045:1	29 730.9 68.255 435.6 435.0 5.086:1	0.9930 .9906 1.0025 1.0024

^aFor Atlas booster and sustainer, values are for T + 2 sec, for Centaur, values are for T + 300 sec for the corresponding inlet conditions.

bThe standard reference values used in the reconstruction are the class values for Atlas engines and acceptance test values for the Centaur engines.

CIncludes total vernier thrust. dIncludes 8.72 lb of thrust and 0.103 lb/sec of flow charged to boost pumps.

CONFIDENTIAL.

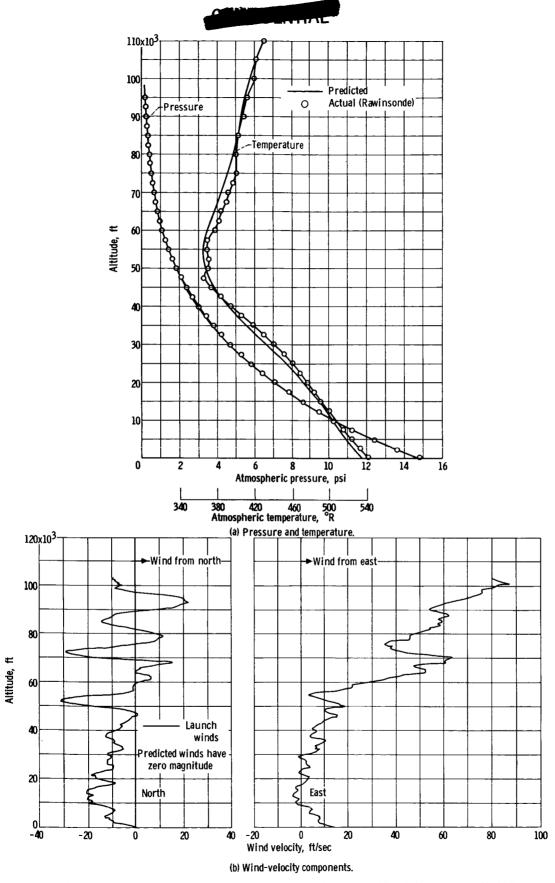
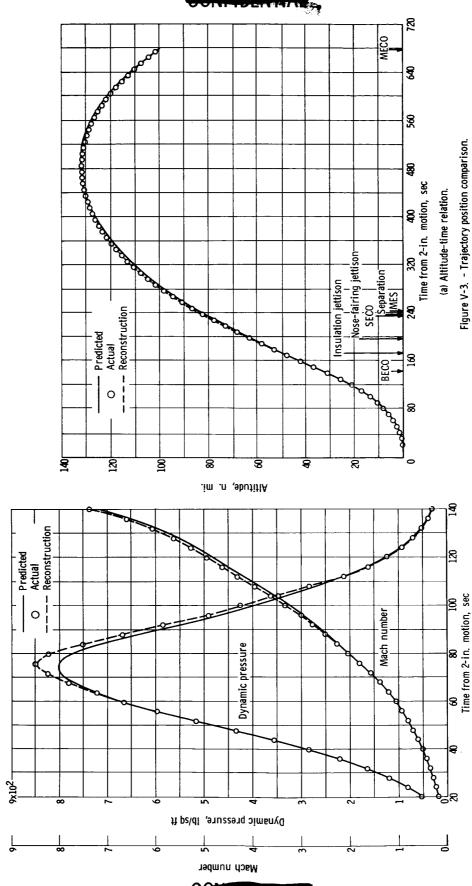


Figure V-1. - Atmospheric conditions at time of launch. Rawinsonde run 997 at 9:40 EST, August 11, 1965.





MINUENTER

Figure V-2. - Comparison of aerodynamic parameters for AC-6.



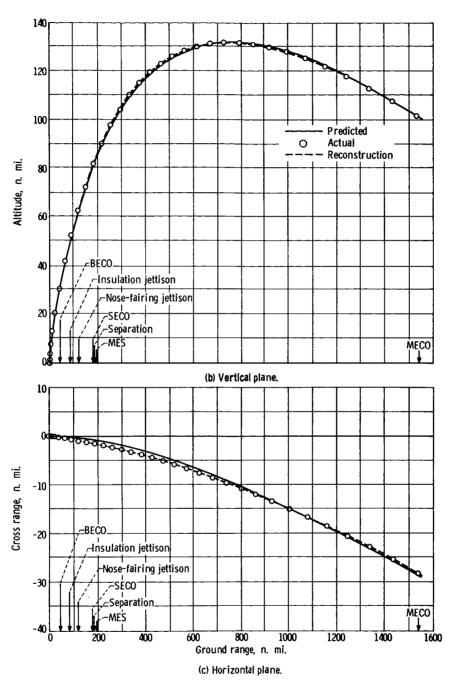


Figure V-3. - Concluded.

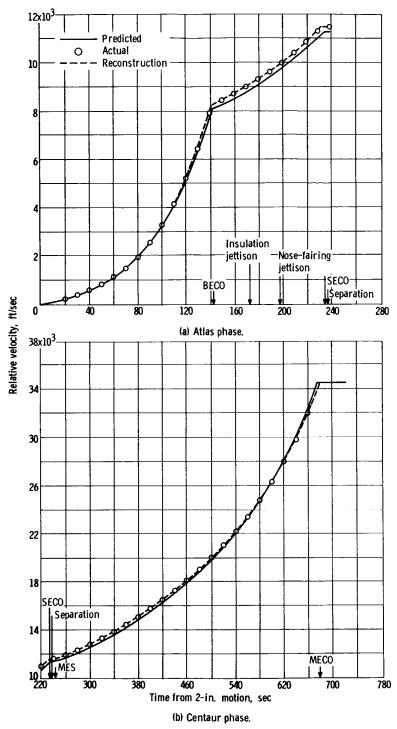


Figure V-4. - Trajectory comparison. Velocity relative to atmosphere including wind effects.





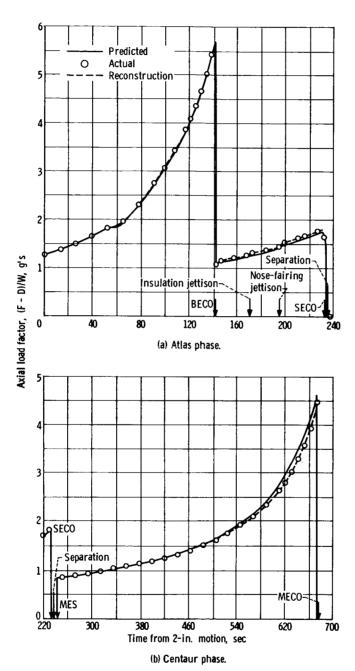


Figure V-5. - Trajectory comparison. Thrust acceleration (axial load factor).

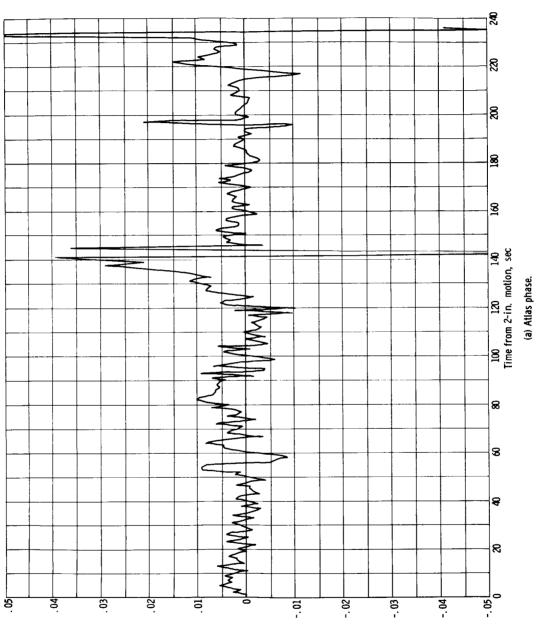
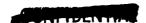


Figure V-6. - Thrust acceleration residuals (reconstruction minus GET).

Thrust acceleration residuals, g's



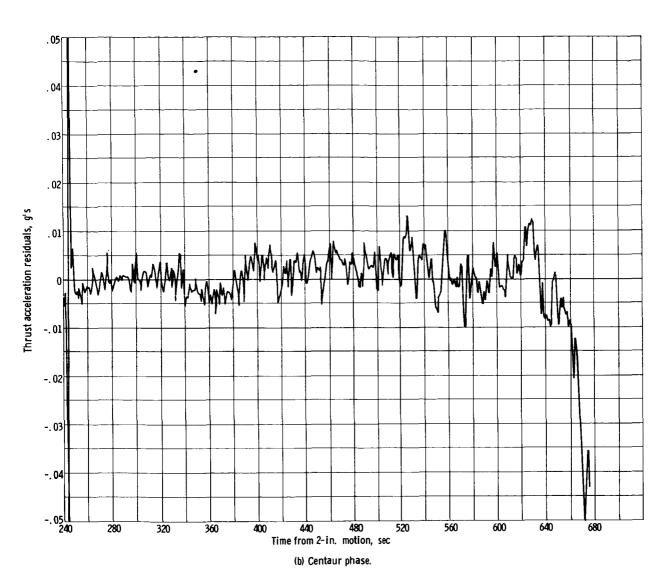
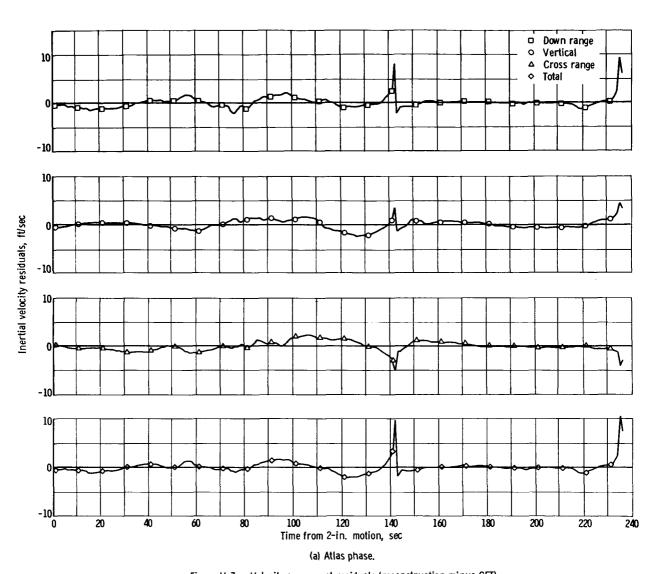


Figure V-6. - Concluded.





 $\label{eq:Figure V-7.} \textbf{Figure V-7.} \ \textbf{-} \ \textbf{Velocity component residuals (reconstruction minus GET)}.$

COMPLETE

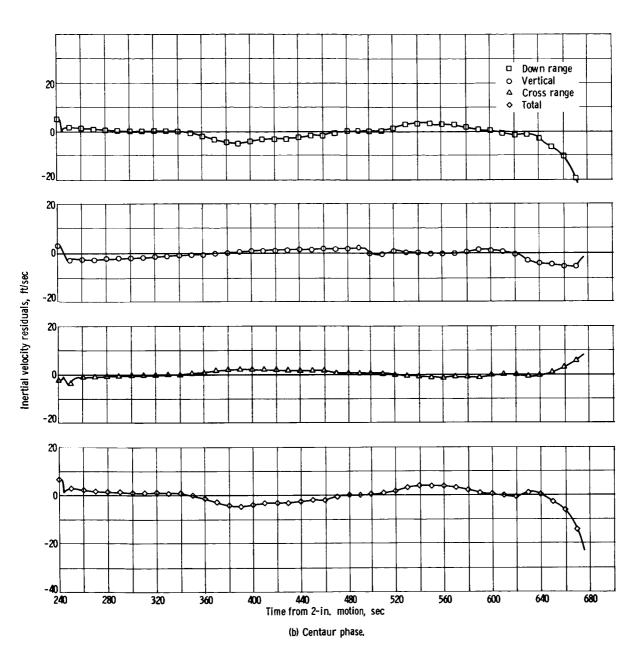


Figure V-7. - Concluded.



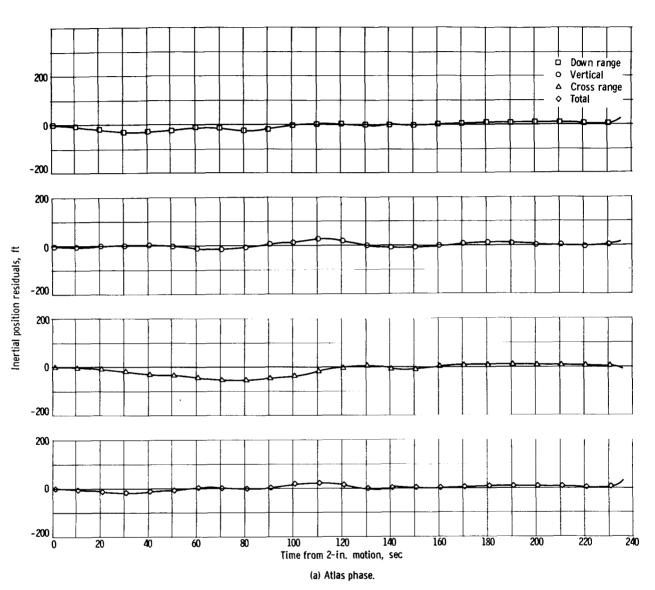


Figure V-8. - Position component residuals (reconstruction minus GET).

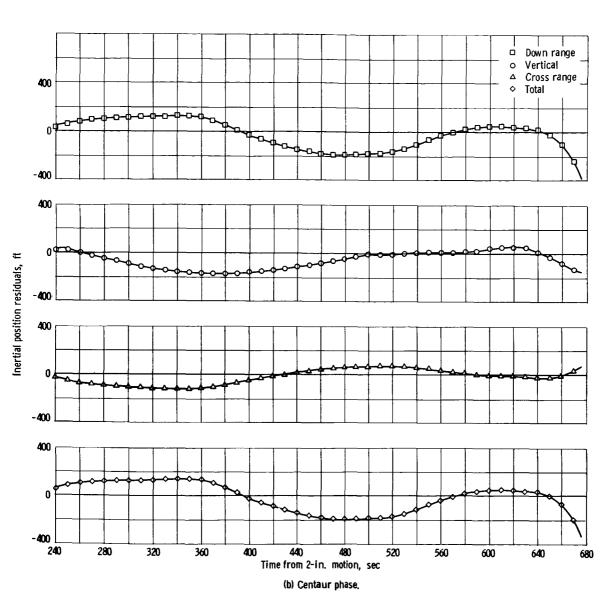
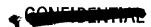
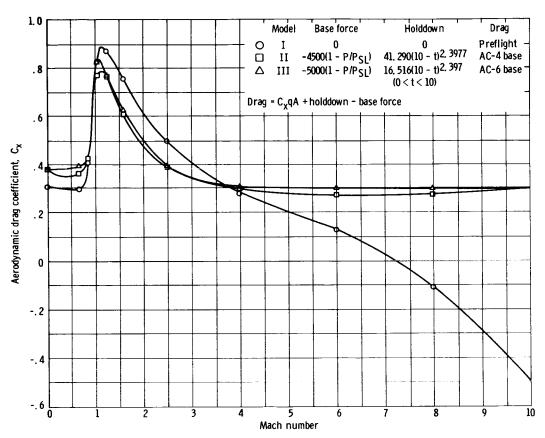


Figure V-& - Concluded.





 $\label{prop:prop:prop:signal} \textbf{Figure V-9.} \ \ \textbf{- Comparison of aerodynamic drag coefficient models}.$





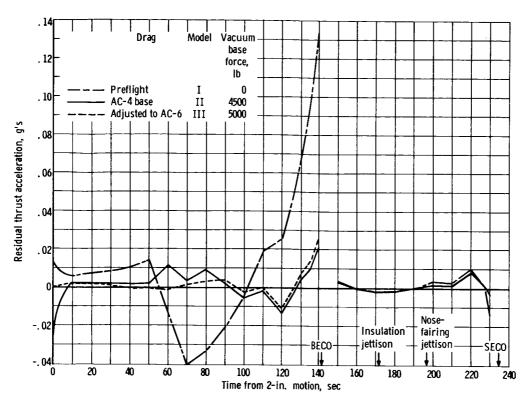


Figure V-10. - Comparison of residual thrust acceleration for three drag models.

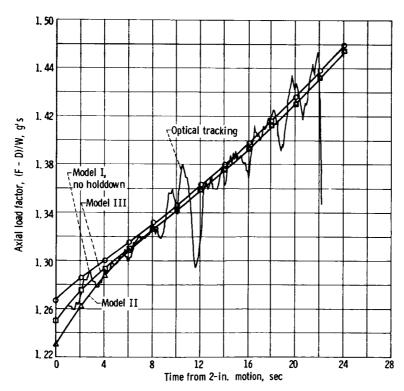


Figure V-11. - Effect of holddown force models on thrust acceleration.





VI. PROPULSION

SUMMARY

The Atlas and the Centaur propulsion systems both performed adequately for the AC-6 flight. For the first time, a successful vehicle retromaneuver was demonstrated.

ATTAS

The AC-6 was the first successful Centaur flight to utilize 165 000-pound-thrust booster engines. Some Atlas steady-state operating conditions are presented in table VI-I. All propulsion system parameters appeared normal through the booster phase of flight. Nominal performance adjusted for engine inlet conditions (ref. 6) in terms of thrust specific impulse, and mixture ratio is presented in table VI-II. The Atlas propulsion system appeared to operate nominally throughout the flight.

CENTAUR

Major changes in the AC-6 propulsion system included:

- (1) Installation of RL10A-3-1 engines
- (2) Strengthened propellant supply ducts to withstand RL10A-3-1 engineshutdown pressure spikes
- (3) Installation of a separate LHe chilldown manifold and overboard vent for each engine
- (4) Increase in boost-pump lead or deadhead time
- (5) Relocation of the venturi in the C-1 LO2 duct bleed system
- (6) Installation of duel-element temperature probes for both the LH₂ and LO₂ turbopump inlets

Additional system changes resulting from the failure of the C-l LH₂ turbopump inlet temperature probe to indicate liquid during quad tanking (see section III, PRELAUNCH HISTORY) include the following:

(1) Relocation of the venturis in the LH2 duct recirculation systems to the junction with the main LH2 supply duct





- (2) Insulation added on both the dual-element probes and the LH₂ recirculation system branch lines
- (3) Installation of foam insulation rings on the LH2 supply ducts extended to cover the engine inlet flange
- (4) Reversal of the flow direction in the LH2 duct purge system

One primary discrepancy occurred during the operation of the Centaur propulsion system: a thrust chamber pressure overshoot, in excess of that normally experienced, occurred on both engines during the start transient. Although the effect of this overshoot on the AC-6 flight was negligible, had conditions been more severe, the engines might have failed to accelerate.

MAIN ENGINES

During a typical engine start transient, the turbopump speed and engine chamber pressure rise to their peak at approximately the same time. When flow commences from the engine turbopumps to the combustion chamber, a corresponding drop in pump inlet pressure occurs. Following the peak transient flow, when flow rate begins to stabilize, pump inlet pressure increases toward a steady-state operating level. This recovery of pump inlet pressure normally takes place just prior to the peaking of engine chamber pressure and turbopump speed.

Turbopump speed and engine chamber pressure during the start transient for both the flight and the engine acceptance tests are presented in figures VI-1 and 2. Although chamber pressure and turbopump speed peaked at approximately the same time during flight, turbopump speed began its rise early relative to chamber pressure. The chamber pressure lag could have resulted from a temporary starvation of flow to the LO₂ turbopumps.

Turbopump inlet pressures and temperatures during the start transient for flight and for the engine acceptance tests are presented in figures VI-3 and 4. Both the $\rm IO_2$ and the fuel pump inlet pressures on AC-6 dropped to values considerably below those of the acceptance tests and also below those experienced on previous flights. The recovery of $\rm IO_2$ pump inlet pressure during the AC-6 start transient did not take place until approximately 0.2 second following the time of peak chamber pressure. This presents additional evidence of flow starvation to the $\rm IO_2$ turbopumps.

Plots of fuel and LO₂ pump NPSP during the flight start transient are presented in figures VI-5 and 6, respectively. The NPSP for both LO₂ and fuel dipped to near the saturation line, whereas on previous flights, the minimum values were well above the steady-state operating limit.

The foregoing sequence of events suggests that both LO₂ turbopumps momentarily cavitated. The combination of chamber pressure and turbopump speed overshoot, the fact that the turbopump speed led the chamber pressure during the start transient, and the lag in LO₂ pump inlet pressure recovery indicate that the LO₂ turbopumps were momentarily unloaded. The speed overshoot could have been caused by a combination of unloading the LO₂ turbopumps and the high pres-





sure ratio across the turbine that resulted from the lag in chamber pressure rise. A quick recovery of $\rm LO_2$ flow following the momentary cavitation would then account for the chamber pressure overshoot. The dip in fuel pump NPSP is considered a result of high transient flow rates and probably did not contribute to the overshoot.

The most likely causes of the LO2 turbopump cavitation are as follows:

- (1) Gas bubble formation in the sump at the ${\rm LO_2}$ boost-pump inlet causing the ${\rm LO_2}$ boost pump and the engine ${\rm LO_2}$ turbopump to cavitate during the flow transient following MES
- (2) Improperly filled propellant lines resulting from a combination of excessive air-conditioning heat input and minimum chilldown
- (3) Warm turbopump housing temperatures resulting from excessive heat input from air conditioning and insufficient cooldown

The adequacy of the propellant tank burp at SECO to suppress boiling and to provide boost-pump NPSH is evaluated by subtracting the saturation pressure corresponding to the boost-pump inlet temperature from the ullage pressure after burp. Although AC-6 did not have instrumentation to measure LO₂ boost-pump inlet temperature, a correlation was made by using data from past flights. The subtraction of the saturation pressure, corresponding to this temperature, from the ullage pressure resulted in a -1.0-psi effective burp pressure margin, whereas all previous flights had positive margins of at least 1.0 psi. This negative burp pressure margin could have created a quantity of gas at the boost-pump inlet. During the flow transient following MES, this gas could then have been drawn through the propellant feed system causing the boost pump and the engine LO₂ pumps to cavitate. To ensure against the recurrence of this problem, the burp pressure is to be increased for all future vehicles.

Although the LO₂ turbopump inlet temperature probes indicated liquid at main engine start, gas could have been trapped in the low-pressure ducts upstream of the probes or could have existed at the probes at saturated liquid temperatures. Ground tests are currently being conducted to determine the effects of propellant ducts partly filled with gas at main engine start.

Figures VI-7 and 8 demonstrate higher turbopump housing temperatures at engine start compared with those of previous flights. Failure of the fuel pump housing temperature to stabilize at 120° R during the booster phase, as experienced on previous flights, is considered to have resulted from the difference in ground air conditioning. The contention is that, on previous flights, the combination of LHe chilldown and GN₂ air conditioning was sufficient to create a layer of nitrogen frost on the turbopump housing. During the booster phase, the housing temperature could only warm to the melting temperature of the nitrogen frost; however, conditions on AC-6 were probably such that no nitrogen frost layer formed. The warm LO₂ pump housing temperature is also considered to be a result of excessive air conditioning. The effects of warm housing temperatures will be further investigated by additional ground testing.

The use of RL10A-3-1 as opposed to RL10A-3 engines is considered to have had a negligible effect on the problem of overshoot. Extensive ground testing





on both engines has revealed little difference during the start transient.

The start total impulse calculated to 95 percent of rated thrust was 2860 and 3095 pound-seconds for the C-1 and C-2 engines, respectively. The differential total impulse between engines was well within specifications.

Engine steady-state operation appeared normal. Table VI-III compares some flight steady-state values with their nominal or predicted values. The C-1 fuel pump inlet temperature, which had created problems during quad tanking (see section III, PRELAUNCH HISTORY), failed to record throughout the entire flight. Engine thrust, specific impulse, and mixture ratio during steady state are presented in table VI-IV. The high mixture ratios at MES + 100 seconds are a result of activation of the propellant utilization system at MES + 90 seconds (see section VII, PROPELLANT SYSTEMS).

Main engine cutoff appeared normal. The cutoff total impulse was calculated to be 2250 and 2400 pound-seconds for the C-l and C-2 engines, respectively. Although the differential impulse of 150 pound-seconds between engines was satisfactory, the engine specification value of total cutoff impulse, 1180±150 pound-seconds per engine, was exceeded. Even though excessive total cutoff impulse also occurred on all previous flights, it is not considered a major problem. The engine manufacturer bases its specification values on simple electrical circuitry used at the factory. The more complex vehicle electrical system creates a longer delay in engine valve closure at MECO. Preflight guidance corrections compensate for the "excessive" cutoff impulse obtained during flight.

Engine inlet temperatures and pressures for the engine retrothrust operation are noted in figures VI-9 to 12. All indications are that the retrothrust operation was highly successful. For further details on this subject see sections VII, PROPELLANT SYSTEMS; XII, FLIGHT CONTROL; and the attitude control portion of this section.

Boost Pumps

Boost-pump start command was initiated at approximately 39.1 seconds prior to main engine start compared with a predicted time of 39.2 seconds. First indications of turbine inlet pressures occurred 1.5 and 1.6 seconds after BPS command for the oxidizer and fuel units, respectively. These times are considerably below the preflight estimate of 6.7 seconds required to expel the gases trapped in the peroxide bladder and lines. As shown in figure VI-13, turbine inlet pressures reached steady-state values of 140 and 88 psia for the fuel and oxidizer units, respectively, which compare favorably with preflight acceptance test values of 139.5 and 89.9 psia. Inlet pressure oscillations similar to those experienced on previous ground and flight tests were evident. Maximum amplitudes were experienced at the fuel turbine for the last 65 seconds of boost-pump operation.

Both the oxidizer and the fuel turbines accelerated normally to steadystate speeds of 38 400 and 51 150 rpm, respectively (fig. VI-14) just prior to prestart command. No indications of overspeed tendencies were noted during the





separation sequence. The separation phase was of some concern because the overspeed control system had been found faulty and was intentionally disconnected prior to flight.

A momentary increase in oxidizer boost-pump turbine speed, approximately 500 rpm, occurred at MES + 1.2 seconds. At this particular time in the start sequence, the turbine speed should be decreasing steadily as a result of the increased boost-pump oxidizer flow as the engine accelerates. This slight increase in speed may be attributed to either (1) momentary reduction in liquid-oxygen flow to the engines caused by engine pump cavitation, or (2) ingestion of gas through the boost pump at MES resulting in momentary cavitation of the boost pump.

Both boost pumps operated normally during the Centaur burn portion of the flight with steady-state turbine speeds of 33 600 and 46 850 rpm for the oxidizer and fuel units, respectively. Based on the preflight acceptance test data and inflight peroxide bottle pressure of 307 psia, the corresponding turbine speeds expected during flight were 32 000 and 46 380 rpm. Variations in propellant flow rates during the period of propellant utilization system control resulted in essentially no change in turbine speeds, with the exception of the last 50 seconds of engine operation. During this period, a 600-rpm decrease in fuel-boost-pump turbine speed was evident. This slight reduction in turbine speed may have been caused either by the propellant utilization valve (which was in the fuel-rich position for the majority of this time period), or by the previously noted large oscillations in the fuel turbine inlet pressure during the last 65 seconds of operation. The cause cannot be determined, but the magnitude of the speed reduction is well within acceptable limits.

Post-MECO boost-pump turbine speed decay is shown in figure VI-15. Fuel unit speed decay is questionable because the data are of poor quality. The oxidizer unit trace is typical of previous flight data with the exception that the coastdown time is from 65 to 100 seconds longer than any previous flight. This extended coastdown time may have been a result of low propellant level of this flight resulting in quicker gas pullthrough in the weightless environment.

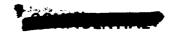
Boost-pump turbine bearing temperatures are shown in figure VI-16. The oxidizer unit temperature was 243° F at MECO and continued to increase to a maximum value of 300° F as a result of heat "soak-back." Corresponding values for the fuel unit were 320° and 372° F. The maximum values obtained were well below the 400° F upper limit permitted during acceptance testing. Landline instrumentation indicated turbine housing skin temperatures of 82° and 93° F for the oxidizer and fuel units, respectively, just prior to lift-off.

Instrumentation to monitor headrise across the boost pumps was not available on this flight; the performance of the pumps in this respect may be obtained from the engine inlet conditions. These data are presented in the section covering main engine performance.

Attitude Control and Hydrogen Peroxide Systems

AC-6 was the first vehicle to have the attitude control engines mounted in-





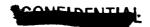
board of the interstage adapter. As a result of this relocation, the A or 1.5 pound-thrust engines were rotated 25° outboard to reduce exhaust gas impingement on adjacent equipment (see fig. VI-17).

The $\rm H_2O_2$ bottle pneumatic pressure is shown in figure VI-18. A relatively long time was required to pressurize the bottle but this was expected with the small quantity of $\rm H_2O_2$ tanked. The gradual drop in bottle pressure after lift-off was also normal since the pressure regulator is referenced to ambient pressure.

Data indicated proper conditioning of the H₂O₂ system prior to launch. Figure VI-19 shows the P-2 fuel supply temperature. The trace appears normal with a slight rise as the system was being pressurized and a drop after lift-off due to discontinuation of the ground air conditioning at that time. The supply lines were filled with gas until the H₂O₂ engines were first fired at MECO. Thus the lines had a small total mass and reacted rapidly to ambient temperature changes. At MECO, the attitude control engines were enabled and fired to correct for main engine shutdown disturbances. The flow of warm H₂O₂ from the bottle was responsible for the sharp increase in temperature at this time. After the end of the retromaneuver, when the tube heaters were turned off, the supply lines increased in temperature, followed by a decrease and then another increase. These changes are attributed to solar heating with the vehicle rolling so that the supply lines were alternately in and out of the sun's rays.

Data that indicate the attitude control engine firing times are shown in figure VI-20. The P-1, A-2, and A-4 engines were fired for a short period just after MECO to correct for small pitch and roll errors caused by main engine thrust cutoff. The small requirement for attitude control at this time indicates a very smooth main engine shutdown. At MECO + 73.7 seconds, P-2 and A-1 engines fired for about 15 seconds with intermittent firing of A-2. the result of a programed function to turn the vehicle 1800. The engines were cut off when the turning rate reached a limit of 1.6 degrees per second. At MECO + 146.7 seconds, P-1, A-3, and A-4 engines came on to stop the turning. The start of retrothrust began at MECO + 193.5 seconds. Shortly thereafter, a yaw-roll error was indicated by the firing of A-2, A-3, and A-4 engines. error continued for the duration of the retromaneuver, with constantly decreasing magnitude. Since the disturbance did not exist prior to the start of blowdown, and since the magnitude of the disturbance decreased with time, it is apparent that it was caused by misalinement of the retrothrust vector with the vehicle center of gravity and possibly a small amount of unbalanced impingement forces. With the exception of the preceding disturbances, the entire retromaneuver was performed relatively smoothly. Prior to the flight, there was some speculation that liquid hydrogen might freeze and partially block the cooldown valve discharge tubes through which the hydrogen is exhausted. However, the small requirement for the attitude control engines and the times at which they were fired indicate that there was no appreciable blockage of the discharge tubes.

The $\rm H_2O_2$ bottle was tanked with 109 pounds. Approximately 9 pounds were expended in ground tests, resulting in a lift-off weight of 100 pounds. Based on a nominal $\rm H_2O_2$ flow rate of 6.18 pounds per minute for the boost pumps, the total boost-pump requirement was calculated to be 49 pounds. The total weight





of $\rm H_2O_2$ expended by the attitude control system was less than 5 pounds, based on the indicated firing times of the attitude control engines and nominal flow rates of 0.0194 and 0.0097 pound per second for the 3- and 1.5-pound-thrust engines, respectively. Therefore, there were approximately 46 pounds of $\rm H_2O_2$ remaining in the tank at the completion of the mission.

HYDRAULTC SYSTEMS

At.las

The booster hydraulic system performance was nominal throughout the boost phase (fig. VI-21). Steady-state airborne hydraulic pressure levels were obtained approximately 7 seconds following engine start. The 7-second time period included accumulator charging and the gimbal flow requirements just after lift-off (fig. VI-22). Steady-state pressures of 3103 psia at the pump discharge and 3211 psia at the B-1 accumulator were maintained until BECO and then dropped to zero as expected.

The sustainer hydraulic power changeover occurred in approximately 8 seconds. This time period included accumulator charging, engine control valve, and gimbal flow requirements just after lift-off (figs. VI-22 and 23). Steady-state pressure levels of 3036 psia at the pump discharge and 3163 psia in the vernier engine portion of the circuit were maintained until BECO. Normal pressures in support of gimbal flow requirements commanded by the autopilot and the admission of guidance were observed during BECO and after booster-package jettison.

An unexpected drop of approximately 500 psi at lift-off + 137 seconds with no flow demand of any significance has been attributed to a pressure transducer malfunction. The dropout was not reflected in any form on the sustainer-vernier pressure trace, which is derived from the same hydraulic circuit downstream of the pump.

Centaur

Evaluation of the data received from the AC-6 flight shows that both the C-1 and C-2 hydraulic systems operated properly. Engine positions as a function of time are shown in figure VI-24. The new rematched recirculation system effectively started nulling both engines as MES - 7.6 seconds. 1.6 degrees per second maximum and a minimum of 0.5 degree per second were higher than those achieved on previous flights. A change in nulling rates occurred at MES - 6.4 seconds as a result of slight vehicle rate changes imparted by a minor Atlas-Centaur separation disturbance. Feedback positions at MES - 0.2 second indicate that the vehicle was pitching upward, yawing right, and rolling counterclockwise. Vehicle rates imparted by engine start differential impulse were effectively eliminated in the allotted time between MES and MES + 4 seconds. Guidance corrections, required after rate suppression, were accomplished in an 8-second interval between MES + 4 and MES + 12 seconds. whole start transient in terms of engine gimbal was milder than any that occurred on previous flights. The only other hydraulic demand of any significance was made at MES + 253.8 seconds in response to a guidance input.



The uprated recirculation system pressures just prior to MES reached values of 127 psia for C-1 and 126 psia for C-2, as shown in figure VI-25. Main system pressures reached and maintained steady-state values of 1112 psia for C-1 and 1116 psia for C-2. The expected drop in pressure at MES + 4 seconds with guidance readmission was not noticeable.

Engine position changes needed to compensate for the transient differential impulse during shutdown are shown in figure VI-24(b). The maximum engine positions reached were 1.6 degrees for C-1 pitch, 1.3 degrees for C-2 pitch, -2.6 degrees for C-1 yaw, and 0.7 degree for C-2 yaw. Movement to these positions during shutdown indicates that compensation was made for vehicle downward pitch, right yaw, and counterclockwise roll.

The recirculation system pumps were restarted by the programer and continued to function properly until the end of the retromaneuver. Engine positions during retromaneuver were basically those that existed just prior to MECO (fig. VI-24(b)). Attitude errors in the pitch plane were sufficient to cause a sinusoidal type response of the engines. A corresponding peak to peak displacement of approximately 0.4 degree occurred on both engines for three cycles lasting 300 seconds.

Hydraulic system manifold temperatures at lift-off were 66° F for C-1 and 72° F for C-2, as shown in figure VI-26. The expected temperature drop through boost phase occurred and was comparable to that observed on AC-4. At MES + 0, C-1 reached a low of 58° F and C-2 settled to 61° F. Temperature rise rates during main pump operation were nominal. Temperatures at MECO were 178° F on C-1 and 193° F on C-2. Rates of temperature drop after MECO + 300 seconds were linear at 1.7° F per minute. The temperatures at lift-off + 1500 seconds were 122° F for C-1 manifold and 125° F for C-2 manifold.



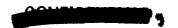


TABLE VI-I. - ATLAS STEADY-STATE OPERATING CONDITIONS

Parameter	Time from lift-off, sec	Nominal value	Flight value
Booster			
B-1 pump speed, rpm B-2 pump speed, rpm B-1 IO2 pump inlet pressure, psia B-2 IO2 pump inlet pressure, psia B-1 fuel pump inlet pressure, psia B-2 fuel pump inlet pressure, psia B-1 thrust chamber pressure, psia B-2 thrust chamber pressure, psia Gas-generator chamber pressure, psia	100 100 95.6 95.6 95.6 100 100	a6340 a6279 b58.7 b58.7 b56.2 b56.2 a577.5 a577.5	53.0
Sustainer			
Pump speed, rpm Fuel pump inlet pressure, psia LO2 pump inlet pressure, psia LO2 pump inlet temperature, OF Fuel pump discharge pressure, psia Gas-generator discharge pressure, psia LO2 injector manifold pressure, psia Thrust chamber pressure, psia	195 195 195 200	alo 114 b46.9 b41.5 b-284.2 a762	9984 51.1 42.1 -281.5 894 791 823 696
Vernier			
V-1 thrust chamber pressure, psia V-2 thrust chamber pressure, psia	200 200	^a 359 ^a 360	373 371

^aAcceptance test data. ^bDEPRO predicted value.



TABLE VI-II. - ATLAS PERFORMANCE (DEPRO PROGRAM) a

### Thrust at lift-off, lb Boosters		· · · · · · · · · · · · · · · · · · ·	
### Thrust at lift-off, 1b Boosters			
Sustainer Sustainer Sustainer Sustainer See 807 See 919 Sustainer Sustaine		Varue	Varue
Sustainer Verniers, axial 56 807 1 491 56 919 1 518 Total 385 063 385 059 Thrust at BECO, 1b Boosters Sustainer Verniers, axial 375 411 1 705 376 363 79 515 1 744 Total 457 628 457 622 Thrust at SECO, 1b Sustainer Verniers, axial 79 760 1 704 79 250 1 744 Total 80 464 80 994 Specific impulse at lift-off, sec Boosters Sustainer and verniers 251.8 213.0 252.9 213.9 Total 245.1 246.0 Specific impulse at BECO, sec Boosters Sustainer and verniers 288.0 306.8 287.7 304.2 Total 291.0 290.5 Specific impulse at SECO, sec Total 306.8 303.4 Lift-off BECO 2.30 2.39 2.28 2.34	Thrust at li	ft-off, lb	
Verniers, axial 1 491 1 518 Total 385 063 385 059 Thrust at BECO, 1b Boosters 375 411 376 363 Sustainer 80 512 79 515 Verniers, axial 1 705 1 744 Total 457 628 457 622 Thrust at SECO, 1b Sustainer Sustainer 79 760 79 250 Verniers, axial 1 704 1 744 Total 80 464 80 994 Specific impulse at lift-off, sec Boosters 251.8 252.9 Sustainer and verniers 213.0 213.9 Total 245.1 246.0 Specific impulse at BECO, sec Boosters Sustainer and verniers 306.8 304.2 Total 291.0 290.5 Specific impulse at SECO, sec Total 306.8 303.4 Lift-off BECO 2.30 2.28 2.30 2.34		1	
Total 385 063 385 059 Thrust at BECO, 1b Boosters 375 411 376 363 Sustainer 80 512 79 515 Verniers, axial 1 705 1 744 Total 457 628 457 622 Thrust at SECO, 1b Sustainer 79 760 79 250 Verniers, axial 1 704 1 744 Total 80 464 80 994 Specific impulse at lift-off, sec Boosters 251.8 252.9 Sustainer and verniers 213.0 213.9 Total 245.1 246.0 Specific impulse at BECO, sec Boosters 306.8 304.2 Total 291.0 290.5 Specific impulse at SECO, sec Total 306.8 303.4 LO2 to fuel mixture ratio Lift-off 2.30 2.28 BECO 2.39 2.34			
### Thrust at BECO, lb Boosters	Verniers, axial	1 491	1 518
Boosters 375 411 376 363 Sustainer 80 512 79 515 Verniers, axial 1 705 1 744 Total 457 628 457 622 Thrust at SECO, 1b Sustainer 79 760 79 250 1 704 1 744 Total 80 464 80 994 Specific impulse at lift-off, sec Boosters 251.8 252.9 Sustainer and verniers 213.0 213.9 Total 245.1 246.0 Specific impulse at BECO, sec Boosters 288.0 287.7 Sustainer and verniers 306.8 304.2 Total 291.0 290.5 Specific impulse at SECO, sec Total 306.8 303.4 Lift-off BECO 2.30 2.28 2.30 2.34	Total	385 063	385 0 59
Sustainer 80 512 79 515 Verniers, axial 457 628 457 622 Thrust at SECO, 1b Sustainer 79 760 79 250 Verniers, axial 1 704 1 744 Total 80 464 80 994 Specific impulse at lift-off, sec Boosters 251.8 252.9 Sustainer and verniers 213.0 213.9 Total 245.1 246.0 Specific impulse at BECO, sec Boosters 288.0 287.7 Sustainer and verniers 306.8 304.2 Total 291.0 290.5 Specific impulse at SECO, sec Total 306.8 303.4 Lift-off 2.30 2.28 BECO 2.39 2.34	Thrust at	BECO, 1b	
Verniers, axial 1 705 1 744 Total 457 628 457 622 Thrust at SECO, 1b Sustainer Sustainer Verniers, axial 79 760 1 79 250 1 744 Total 80 464 80 994 Specific impulse at lift-off, sec Boosters Sustainer and verniers 251.8 252.9 213.9 213.9 Total 245.1 246.0 Specific impulse at BECO, sec Boosters Sustainer and verniers 288.0 304.2 Total 291.0 290.5 Specific impulse at SECO, sec Total 306.8 303.4 Lift-off BECO Lift-off BECO 2.30 2.28 2.34	Boosters		· ·
Total 457 628 457 622 Thrust at SECO, 1b Sustainer 79 760 79 250 Verniers, axial 1 704 1 744 Total 80 464 80 994 Specific impulse at lift-off, sec Boosters 251.8 252.9 Sustainer and verniers 213.0 213.9 Total 245.1 246.0 Specific impulse at BECO, sec Boosters 288.0 287.7 Sustainer and verniers 306.8 304.2 Total 291.0 290.5 Specific impulse at SECO, sec Total 306.8 303.4 LO2 to fuel mixture ratio Lift-off BECO 2.30 2.28 ECO 2.39 2.34	Sustainer		
### Thrust at SECO, 1b Sustainer 79 760 79 250 1 704 1 744 Total 80 464 80 994 Specific impulse at lift-off, sec Boosters 251.8 252.9 213.9 Total 245.1 246.0 Specific impulse at BECO, sec Boosters 288.0 287.7 306.8 304.2 Total 291.0 290.5 Specific impulse at SECO, sec Total 306.8 303.4 LO2 to fuel mixture ratio Lift-off 2.30 2.28 2.34 BECO 2.39 2.34	Verniers, axial	1 705	1 744
Sustainer Verniers, axial 79 760 1 704 79 250 1 744 Total 80 464 80 994 Specific impulse at lift-off, sec Boosters Sustainer and verniers 251.8 213.0 252.9 213.9 Total 245.1 246.0 Specific impulse at BECO, sec Boosters Sustainer and verniers 288.0 306.8 287.7 306.8 Total 291.0 290.5 Specific impulse at SECO, sec Total 306.8 303.4 Lift-off BECO 2.30 2.39 2.28 2.34	Total	457 628	457 622
Verniers, axial 1 704 1 744 Total 80 464 80 994 Specific impulse at lift-off, sec Boosters 251.8 252.9 Sustainer and verniers 213.0 213.9 Total 245.1 246.0 Specific impulse at BECO, sec Boosters 288.0 287.7 Sustainer and verniers 306.8 304.2 Total 291.0 290.5 Specific impulse at SECO, sec Total 306.8 303.4 Lift-off 2.30 2.28 BECO 2.39 2.34	Thrust at	SECO, 1b	
Total 80 464 80 994 Specific impulse at lift-off, sec 251.8 252.9 Boosters Sustainer and verniers 213.0 213.9 Total 245.1 246.0 Specific impulse at BECO, sec 288.0 287.7 Sustainer and verniers 306.8 304.2 Total 291.0 290.5 Specific impulse at SECO, sec Total 306.8 303.4 Lift-off BECO 2.30 2.28 2.39 2.34	Sustainer	79 760	79 250
Specific impulse at lift-off, sec Boosters 251.8 252.9 Sustainer and verniers 213.0 213.9 Total 245.1 246.0 Specific impulse at BECO, sec 288.0 287.7 Sustainer and verniers 306.8 304.2 Total 291.0 290.5 Specific impulse at SECO, sec Total 306.8 303.4 IO2 to fuel mixture ratio 2.30 2.28 BECO 2.39 2.34	Verniers, axial	1 704	1 744
Boosters 251.8 252.9 Sustainer and vermiers 213.0 213.9 Total 245.1 246.0 Specific impulse at BECO, sec 288.0 287.7 Sustainer and vermiers 306.8 304.2 Total 291.0 290.5 Specific impulse at SECO, sec Total 306.8 303.4 Lift-off 2.30 2.28 BECO 2.39 2.34	Total	80 464	80 994
Sustainer and verniers 213.0 213.9 Total 245.1 246.0 Specific impulse at BECO, sec Boosters Sustainer and verniers 288.0 304.2 Total 291.0 290.5 Specific impulse at SECO, sec Total 306.8 303.4 Lift-off BECO 2.30 2.28 2.39 2.34	Specific impulse	at lift-off,	sec
Sustainer and verniers 213.0 213.9 Total 245.1 246.0 Specific impulse at BECO, sec Boosters Sustainer and verniers 288.0 304.2 Total 291.0 290.5 Specific impulse at SECO, sec Total 306.8 303.4 Lift-off BECO 2.30 2.28 2.39 2.34	Boosters	251.8	252. 9
Total 245.1 246.0 Specific impulse at BECO, sec Boosters 288.0 287.7 Sustainer and verniers 306.8 304.2 Total 291.0 290.5 Specific impulse at SECO, sec Total 306.8 303.4 Lift-off BECO 2.30 2.28 2.39 2.34			
Specific impulse at BECO, sec Boosters 288.0 287.7 Sustainer and verniers 306.8 304.2 Total 291.0 290.5 Specific impulse at SECO, sec Total 306.8 303.4 Lift-off BECO 2.30 2.28 2.39 2.34			246.0
Boosters Sustainer and verniers 288.0 304.2 Total 291.0 290.5 Specific impulse at SECO, sec Total 306.8 303.4 Lift-off 2.30 2.28 BECO BECO 2.39 2.34		L	
Sustainer and verniers 306.8 304.2 Total 291.0 290.5 Specific impulse at SECO, sec Total 306.8 303.4 Log to fuel mixture ratio Lift-off BECO 2.30 2.28 2.39 2.34	Specific impulse	e at BECO, se	eC
Total 291.0 290.5 Specific impulse at SECO, sec 306.8 303.4 Lift-off BECO 2.30 2.28 2.39 2.34	Boosters	288.0	287.7
Specific impulse at SECO, sec Total 306.8 303.4 L02 to fuel mixture ratio 2.30 2.28 BECO 2.39 2.34	Sustainer and verniers	306.8	304.2
Total 306.8 303.4 LO2 to fuel mixture ratio 2.30 2.28 BECO 2.39 2.34	Total	291.0	290.5
Lift-off 2.30 2.28 BECO 2.39 2.34	Specific impuls	e at SECO, se	ec
Lift-off 2.30 2.28 BECO 2.39 2.34	Total	306.8	303.4
BECO 2.39 2.34	LO2 to fuel m	ixture ratio	
	Lift-off	2.30	2.28
SECO 2.54 2.55	BECO	2.39	2.34
	SECO	2.54	2.55

^aSee ref. 6 for explanation of this technique.





TABLE VI-III. - CENTAUR ENGINE STEADY-STATE OPERATING CONDITIONS

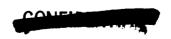
Parameter	Nominal	MES +	90 sec
		C-1	C-2
LH ₂ pump total inlet pressure, psia LH ₂ pump inlet temperature, ^O R LO ₂ pump total inlet pressure, psia LO ₂ pump inlet temperature, ^O R LO ₂ pump speed, rpm LH ₂ turbine inlet temperature, ^O R LH ₂ venturi upstream pressure, psia Chamber pressure, psia	35.0 38.8 59.8 176.6 11 350 331 649 300	34.4 59.6 173.5 11 125 326.9 672.8 293.5	33.4 38.9 59.9 174.0 11 462 337.1 681.5 291.1



TABLE VI-IV. - CENTAUR PERFORMANCE (AC-6 FLIGHT)

Parameter	Accep-				Ė	Time from	MES, sec	ပ			
	tance	50	06	100	150	200	250	300	250	400	435
Chamber pressure, psia	293.6	293.5	293.5	297.5	292.7	292.7	292.3	292.7	292.7	291.7	293.4
			C-1	engine	(SN 1895)						
Thrust, 1b: PWA regression method ^a PWA C* method ^a	14 934	14 930 14 580	14 928 14 575	15 131 14 977	14 965 14 473	14 934 14 494	15 014 14 515	14 869 14 512	14 884 14 465	14 901 14 438	15 111 14 670
Specific impulse, sec: FWA regression method FWA C method	434.0	433.7 436.4	433.8 436.5	430.6 432.8	433.2 437.3	433.6 437.0	432.5 436.5	434.7 436.8	434.5 437.4	434.2 437.1	431.1 434.6
Mixture ratio: FWA regression method FWA C* method	5.0	5.030	5.024 4.862	5.409	5.097	5.040	5.183 4.859	4.896 4.800	4.925 4.663	4.958 4.732	5.350
			C-2	engine	968T NS)						
Chamber pressure, psia	293.9	291.1	291.1	295.1	290.3	288.7	5.682	289.5	289.5	289.5	291.4
Thrust, 1b: FWA regression method FWA C* method	15 005	15 021 14 401	15 022 14 401	15 309 14 804	15 068 14 308	15 051 14 212	14 943 14 310	14 963 14 323	14 933 14 259	14 889 14 279	15 175 14 519
Specific impulse, sec: PWA regression method PWA C* method	435.0	434.1 438.1	434.1 438.1	429.3 435.0	433.3 438.8	433.6 439.1	435.3 438.3	435.0 438.1	435.5 439.0	436.1 438.7	431.8 436.8
Mixture ratio: PWA regression method PWA C method	5.09	5.151	5.150	5.693 5.264	5.242 4.565	5.212 4.511	4.986 4.687	5.025	4.961 4.534	4.869 4.595	5.417

 $^{\mathbf{a}}\mathbf{See}$ appendix C of ref. 6 for explanation of these techniques.





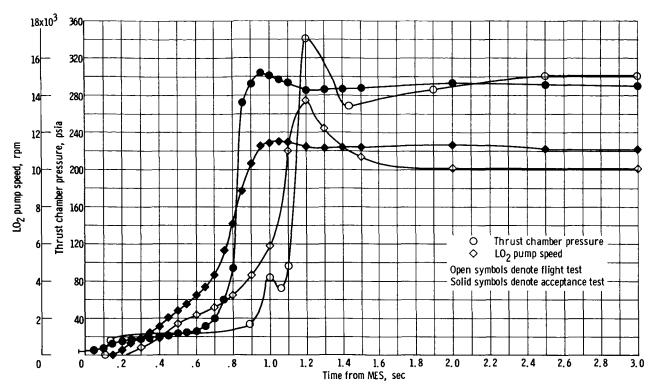


Figure VI-1. - C-1 engine (seria! no. 641895) flight and final acceptance test run start transient characteristics.

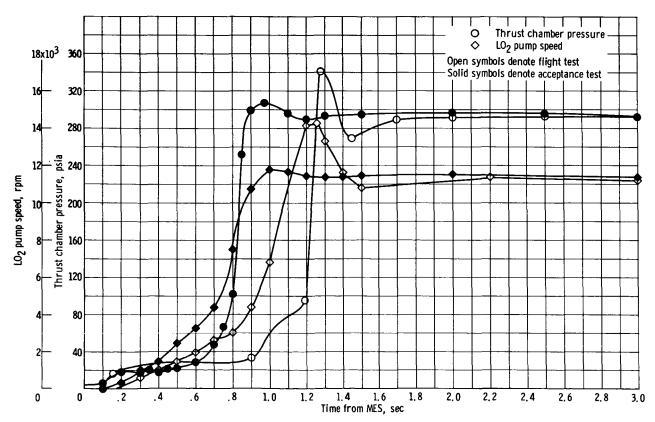


Figure VI-2. - C-2 engine (serial no. 641896) flight and final acceptance test run start transient characteristics.



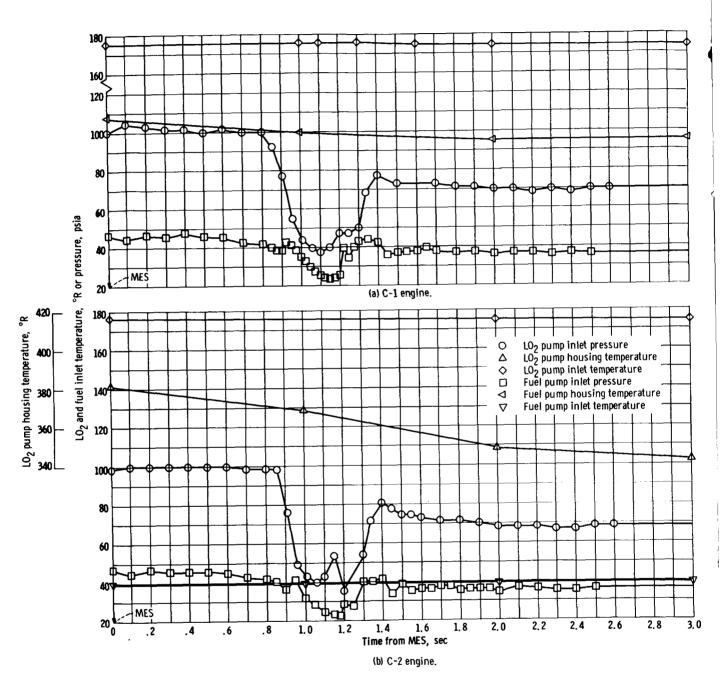
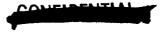


Figure VI-3. - AC-6 flight start transient fuel and ${\rm LO_2}$ pump conditions.



CONTIDENTIAL

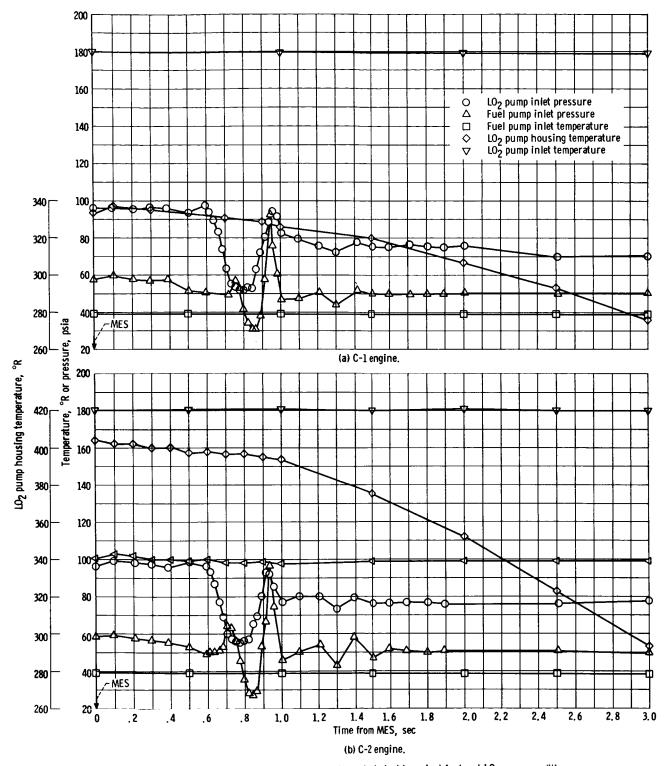


Figure VI-4. - AC-6 final acceptance test start transient fuel and ${\rm LO_2}$ pump conditions.





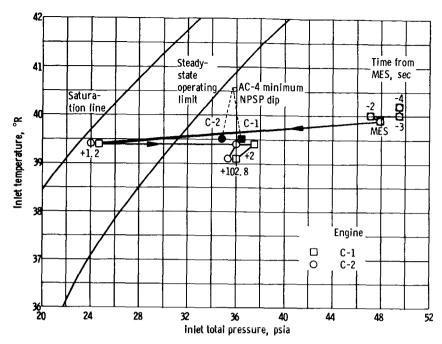


Figure VI-5. - Fuel pump inlet conditions near engine start. (C-2 engine temperatures used for C-1 engine; C-1 engine data not valid.)

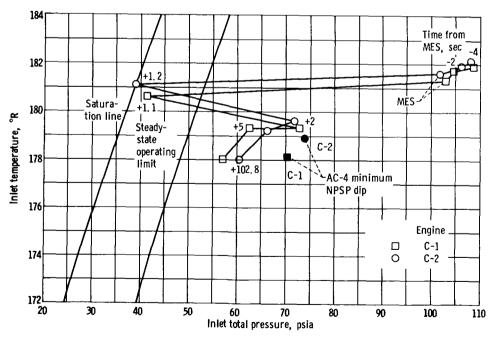
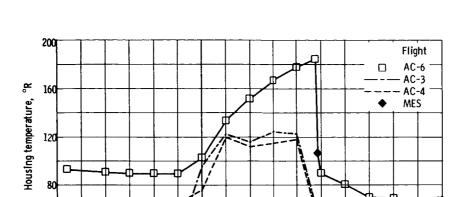


Figure VI-6. - LO₂ pump inlet conditions near engine start.





Time from lift-off, sec Figure VI-7. - C-1 engine fuel pump housing temperature.

100

200

300

400

500

-200

-100

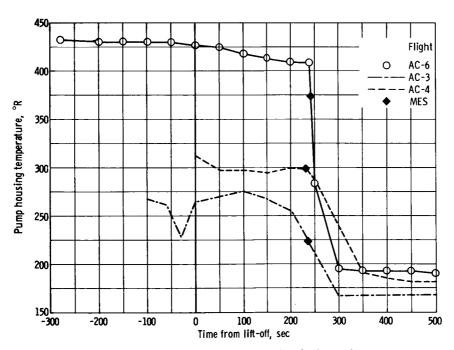


Figure VI-8. - C-2 engine ${\rm LO_2}$ pump housing temperature.





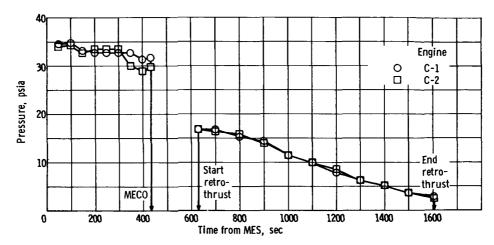


Figure VI-9. - Fuel pump inlet pressures through end of retrothrust.

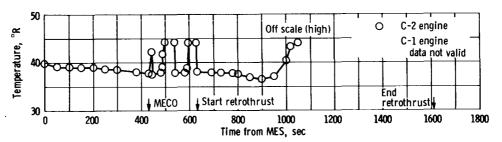


Figure VI-10. - Fuel pump inlet temperature through end of retrothrust.

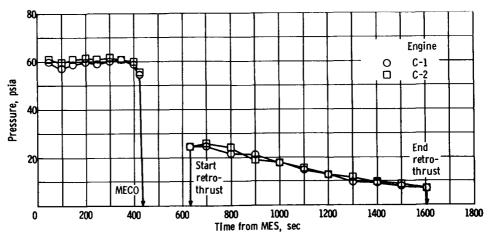


Figure VI-11. - LO₂ pump inlet pressures through end of retrothrust.



CONFIDENTIAL

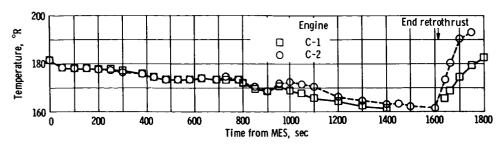


Figure VI-12. - ${\rm LO_2}$ pump inlet temperature through end of retrothrust.

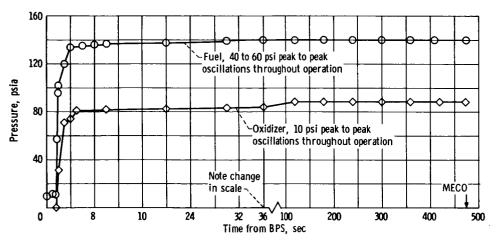


Figure VI-13. .- Boost pump turbine inlet pressure.





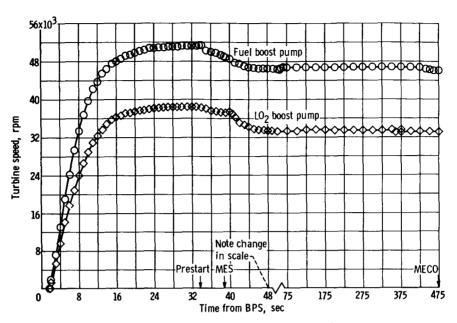


Figure VI-14. - Boost pump turbine speed.

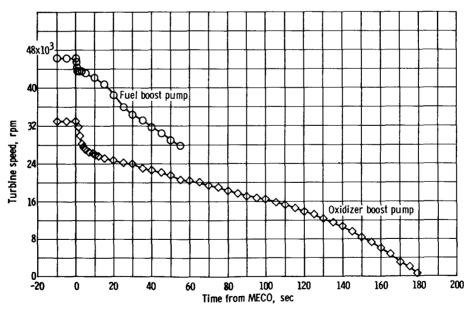


Figure VI-15. - Boost pump turbine speed coastdown (post-MECO). (Fuel boost pump data questionable from 0 to 55 sec, and completely invalid after 55 sec.)



CONEIN

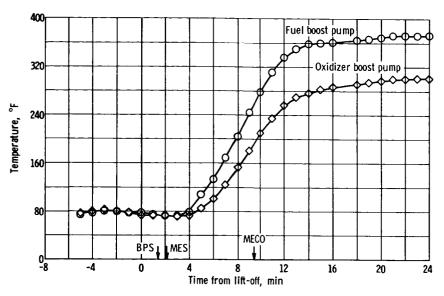


Figure VI-16. - Boost pump turbine bearing temperature.

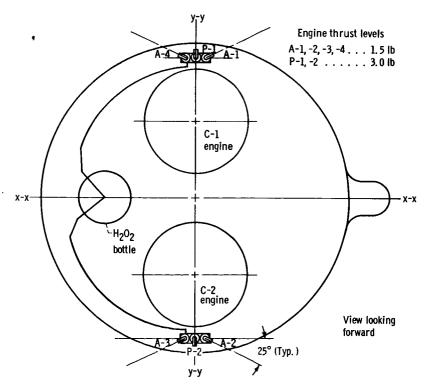


Figure VI-17. - Attitude control engines system schematic drawing.



100HPIDENTIN

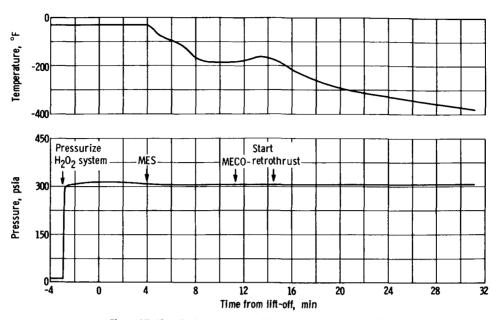


Figure VI-18. - Engine compartment temperature and $\rm H_2O_2$ bottle pressure.

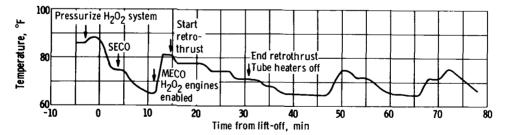


Figure VI-19. - P-2 engine ${\rm H_2O_2}$ supply temperature.

TO CHELD THE STATE OF THE STATE

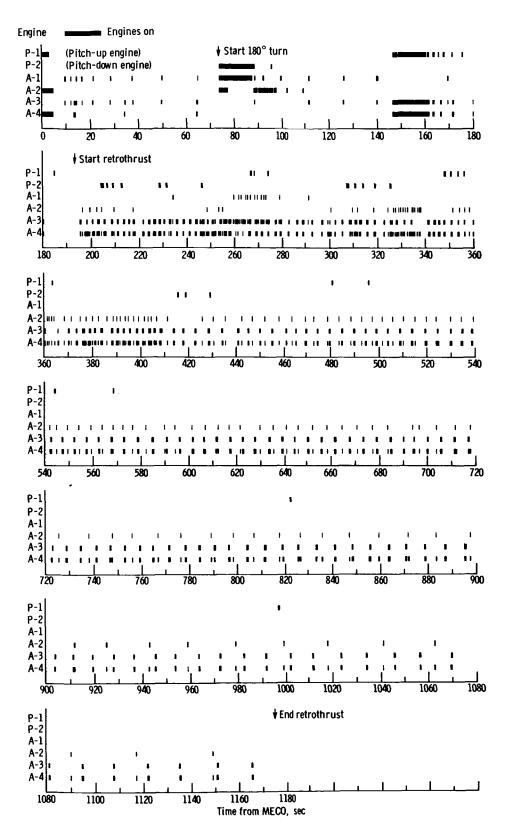


Figure VI-20. - Hydrogen peroxide engine commands history.



CONFIDENTIAL

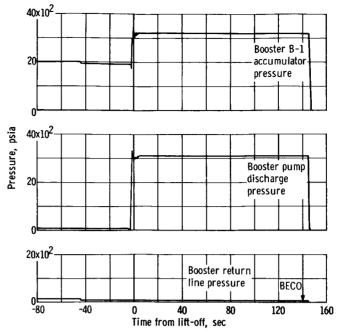


Figure VI-21. - Booster hydraulic pressures.

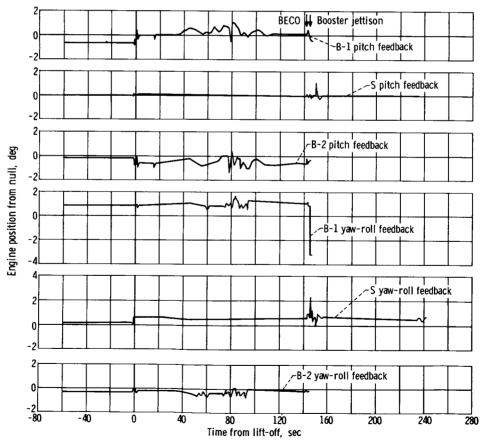


Figure VI-22. - B-1, S, B-2 engine positions.



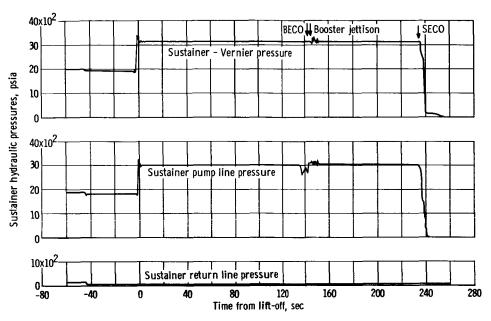


Figure VI-23. - Sustainer hydraulic pressures.



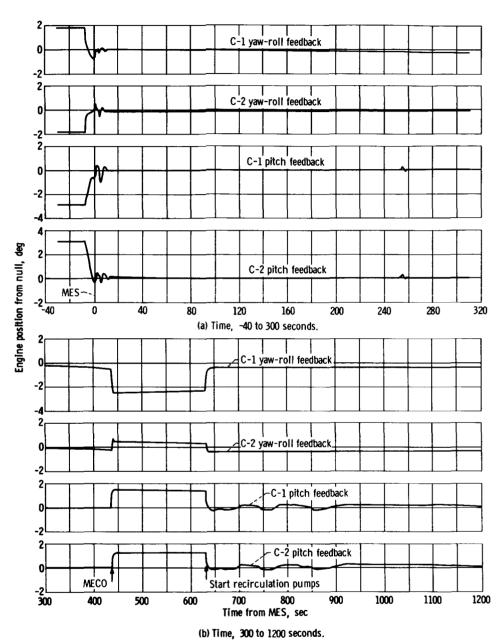
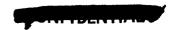


Figure VI-24, - C-1 and C-2 engine positions.





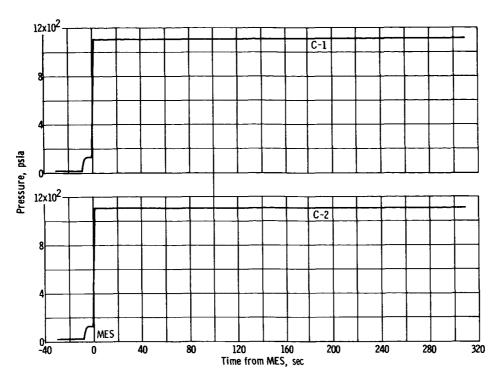


Figure VI-25. - C-1 and C-2 main hydraulic power package pressures.

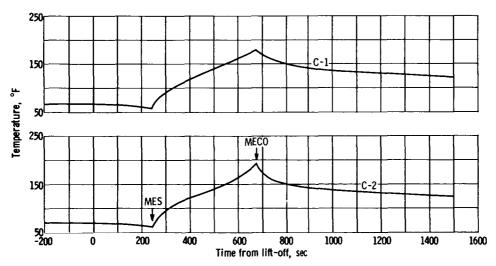


Figure VI-26. - Hydraulic manifold C-1 and C-2 temperatures.

VII. PROPELLANT SYSTEMS

SUMMARY

The Centaur propellant systems performed satisfactorily in support of the AC-6 flight. Additions to AC-6 were (1) a dual-element hot-wire liquid level sensor system for controlling precise topping levels during tanking and (2) a propellant utilization (PU) system to optimize propellant consumption. Topping rates were easily controlled to maintain minimum ullage levels. The PU system accurately controlled depletion of propellant quantities to within 5 pounds of LH2 at the time the liquid levels receded below the bottom of the PU probes in the tank.

Tank pressurization and venting were successful throughout the flight, and the vent valves controlled within specified pressure limits. The pressure rise rate (3.73 psi/min) in the LH₂ tank was lower than expected during initial primary vent-valve lockup, T - 7 to T + 67 seconds. This was believed to be a result of cold helium purge gas leaking through the forward bulkhead seal and possibly some GH_2 leakage through the vent valve. The AC-6 was tanked to a minimum ullage, and the boiling on unlocking the low-pressure relief valve appears to have resulted in about 50 pounds of LH₂ entrainment.

Blowdown of the residual propellants through the engines to provide retromaneuver thrust was accomplished without incident. Pressure decay rates in the LH2 and LO2 tanks were in good agreement with predicted values based on conditions with 50 percent of the propellants settled.

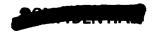
The Atlas sustainer stage operation was successfully terminated in a planned propellant depletion mode by the fuel-depletion system. This was the first time this system was utilized to initiate sustainer engine cutoff.

CENTAUR PROPELLANT LOADING

The AC-6 Centaur tank was the first to utilize a new propellant level indicating system (PLIS) for loading propellants to proper flight levels. The system consisted of three dual-element hot-wire liquid level sensors in the hydrogen tank and four dual-element hot-wire level sensors in the LO2 tank, as shown in figure VII-1. In conjunction with the PLIS, a refined topping system was installed to enable propellant "topping flow" rates as low as 3 gpm for fine level control.

To assure proper liquid levels at lift-off (T - 0), propellants were "topped" until T - 90 seconds. The requirement at this time was that the topping-low sensor be wet in the hydrogen tank and the topping-high sensor be





wet in the IO_2 tank. This requirement was adequately met, as shown in figure VII-2, with the IO_2 topping-high sensor indicating dry at T - 73.5 seconds and the LH₂ topping-low sensor going dry at T - 26 seconds. Propellant weights at lift-off are summarized in table VII-I.

CENTAUR PROPELLANT UTILIZATION SYSTEM

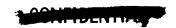
System Description

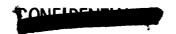
The AC-6 flight was the first test of the Centaur propellant-utilization (PU) system that demonstrated the capability of the system to operate in a closed-loop configuration. The system, as shown in figure VII-3, is used during tanking to indicate propellant masses and during flight to optimize propellant In flight, the mass of propellant remaining in each tank is sensed by a capacitance-type probe (transducer assembly) and compared in a bridge-type circuit. If the mass ratio of propellants (oxidizer to fuel ratio) in the tanks at any time varies from a predetermined value (usually 5), an error signal is sent to the proportional servopositioner that controls the IO2 engine flow If the mass ratio is greater than 5, the LO₂ flow to the engines is increased to return the mass ratio within the tanks to 5. If the mass ratio is less than 5, the LO2 flow to the engines is decreased. Since the sensing probes do not extend the full length of both tanks, PU control is not effected until approximately 90 seconds after main engine start. For this 90 seconds of engine burn, the LO2 flow-control valves are nulled (locked at a nominal flow mixture ratio of 5).

System Performance

All prelaunch checks of the system were within required limits and specifications. The PU LH2 and IO2 quantity readouts during tanking are shown in figure VII-4. Again, it should be noted that the PU probes do not extend the full length of the tanks and, therefore, do not indicate the final amount of tanked propellants. Table VII-II summarizes prelaunch checks of the PU system.

Inflight performance of the PU system was satisfactory. The liquid levels reached the top of the LO2 probe at MES + 89.5 seconds and the LH2 probe at MES + 95.1 seconds. The PU valves, as shown in figure VII-5, nulled by the programer until MES + 90 seconds, were unnulled properly and immediately moved to the LO2-rich position and remained there until MES + 193.5 seconds. During this time (MES + 90 to MES + 193.5 sec), 228±25 pounds of excess LO2 were consumed; 160 pounds of error bias, plus 68 pounds of tanking error and engine mixture ratio error accumulated during the first 90 seconds of engine burn. valves oscillated about null from MES + 193.5 to MES + 423.6 seconds (Δ time = 281.1 sec). During this time, the system corrected for a -514±100 pound steady-state IO2 error; that is, the valves decreased the IO2 flow so that the engines burned at a fuel-rich mixture ratio. All these calculations have been made with the assumption that nominal engine inlet conditions existed throughout engine burn. At MES + 423.6 seconds, the LO2 level passed the bottom of the LO2 probe, and 2.2 seconds later, the LH2 level receded below the bottom of the LH2





probe. At this time, the flow control valves went to the $\rm IO_2$ -rich stops and remained there until MECO. Figure VII-6 shows the propellant quantities as indicated by the PU probes as a function of time during engine burn.

System Accuracy

At IO2 probe uncovery (level passing the bottom of the probe) 25.8 pounds of IH2 were indicated by the IH2 probe (hydrogen remaining in tank above bottom of probe). This represents the 2.2-second uncovery time difference between the IO2 and IH2 probes. The error bias, which was 160 pounds of IO2, was effectively reduced to 123 pounds as a result of a larger amount of gaseous hydrogen than expected remaining in the tank. Therefore, at IO2 probe uncovery, 24.6 pounds of IH2 (123 lb IO2 at a ratio of 5 equals 24.6 lb IH2) indicated by the probe. The PU system error then would be 25.8 - 24.6 = 1.2 pounds of IH2. A conservative number for PU error would be less than 5 pounds of IH2 indicated by the IH2 probe above the probe bottom at the time the IO2 level passed the bottom of the IO2 probe.

PROPELLANT RESIDUALS AT MECO

Liquid Residuals

The $\rm IO_2$ and $\rm IH_2$ residuals were calculated by using the time that the propellant levels passed the bottom of the PU probes as a reference point. The total $\rm IO_2$ residual was 271.1 pounds with 202.8 pounds of this being burnable $\rm IO_2$. The total $\rm IH_2$ residual was 163.2 pounds with 91.3 pounds of this being burnable $\rm IH_2$. For calculations of these residuals see appendix B.

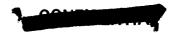
Gaseous Residuals

The gaseous residuals of 83 pounds of GH₂ and 165 pounds of GO₂ were calculated by using ullage temperature and pressure data at MECO obtained from figures VII-7 and 8, respectively. The hydrogen residual calculations were made by utilizing the temperature profile in the tank at MECO and reflect temperature stratification in the tank. The oxygen residual was based on the three ullage temperature measurements in the tank.

CENTAUR PROPELLANT TANK PRESSURIZATION

Powered-Flight Phase

The IO2 and IH2 tank pressures were controlled throughout the AC-6 flight, as shown in figure VII-7. It should be noted that the IH2 pressure rise rate during initial number 1 vent-valve lockup, T - 7 to T + 69 seconds, was low (3.73 psi/min). As a result, the number 2 vent valve did not relieve until T + 67 seconds, only 2 seconds before the number 1 vent valve was unlocked and tank pressure was relieved to allow pressures to remain within structural limits.



The cause of the low pressure rise rate is believed to be twofold. A leak in the forward station 208 seal allowed very cold helium purge gas, from between the IH2 tank and the insulation panels, to escape into the forward equipment area and cool the forward bulkhead. Evidence of such a leak was indicated by the low temperatures of electronic equipment in the forward bulkhead area prior to lift-off. (See section VIII for equipment temperatures.) In addition, the primary hydrogen vent valve may not have been fully seated. Photographic coverage gives evidence of continued hydrogen venting from the vent fin during the early seconds of flight.

Tank ullage temperatures are shown in figure VII-8. The LO₂ tank ullage temperature remained essentially at saturation, indicating thermal equilibrium in the tank throughout the flight. The LH₂ tank ullage temperature reflected changes in pressure as expected. The temperature measurement, which was located on the forward bulkhead, again indicated an abrupt temperature drop to LH₂ temperatures at MECO, which provided evidence of LH₂ spray from the boost-pump volute bleed hitting the forward bulkhead. In addition to the ullage temperatures shown in figure VII-8, several additional temperature measurements were made in the tank, as shown in figure VII-9 for the period of engine burn. These measurements were utilized to obtain a temperature profile in the tanks at MECO to enable accurate calculations of gaseous residuals and give some indication of temperature stratification.

Step pressurization of the propellant tanks (burp) to provide the proper NPSH for boost-pump start was normal. The pressure data are summarized in the following table:

Tank	Initial pressure, psia	Final pressure, psia	ΔP, psid
ro ^S	29.5	33. 3	3. 8
LH2	19.2	21.6	2.4 (1-sec spike)
		20.4	1.2

Pneumatic system operation was also normal and in good agreement with ground testing. Helium bottle pressure was 2820 psia at lift-off and had decreased to 2580 psia by T+550 seconds. The engine controls pressure regulator and the H_2O_2 controls pressure regulator were 448 to 460 psig and 307 to 314 psig, respectively. The latter was slightly higher until the boost pumps were started as a result of normal regulator lockup. Helium consumption for the burp prior to boost pump start was 0.292 pound.

Propellant Tank Venting

Venting of the LH $_2$ and LO $_2$ tanks, as required to maintain a scheduled tank pressure profile, was accomplished successfully on the AC-6 flight. The hydrogen vent flow rate, which was the only one monitored, was invalid because of a





loss of pressure instrumentation at the venturi flowmeter. However, based on known liquid levels at T - O and start of PU control, the total propellant ventage prior to Centaur staging has been estimated as follows:

	Propella	ants, lb
	ro ^S	TH ⁵
Total propellants tanked	25 521	5 278
Ground boiloff: LH ₂ = 0.45 lb/sec (T - 26 to T - 7 sec) LO ₂ = 0.326 lb/sec (T - 73.5 to T - 0 sec)	26	9
Total propellants at T - 0	25 495	5 269
Propellants consumption, engine chilldown to PU probe uncovery: IO2 T + 234.4 to T + 332.5 sec IH2 T + 234.4 to T + 338.5 sec Remaining propellants and ventage at PU start Actual propellants at PU start	5 197 20 298 20 240	1 122 4 147 4 018
Total propellants vented	58	129

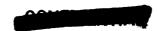
The $\rm GO_2$ vented was low as expected, but the indicated hydrogen ventage was high. Previous flights indicated that the total hydrogen vented during this time was about 70 to 80 pounds. This increased ventage on AC-6 (129 lb - 80 lb = 49 lb) may be attributed to liquid entrainment during periods of tank blowdown after vent-valve lockup periods. A sudden drop in pressure upon unlocking the lower relief valve produces boiling, and with a very low ullage (about 13 cu ft on AC-6), liquid droplets could easily be entrained in the vent discharge.

Retromaneuver Blowdown

Current separation requirements between the spacecraft and Centaur are 336 kilometers in 5 hours. To effect this separation distance, Centaur is turned 180° to the injection velocity at T + 752.8 seconds, and a retrothrust is applied at T + 872.8 seconds, terminating at T + 1853.8 seconds. The thrust force is provided by venting residual hydrogen through the chilldown valves and residual oxygen through the engine nozzles. Analysis of flight data indicated that the spacecraft-Centaur separation distance after 5 hours was 1300 to 1600 kilometers, which is considerably in excess of the minimum separation requirement.

Tank pressure histories during the retromaneuver, as shown in figure VII-10 were normal, and agreed well with analytical predictions for the 50 percent liquid settled case. Pressure in the IH₂ tank increased from MECO to start of retroblowdown at an average rate of about 0.77 psi per minute, then showed a





gradual decline. Pressure in the LO₂ tank continued to increase at an average rate of about 0.33 psi per minute until 87 seconds after the start of retroblowdown before the downtrend was observed. From the shape of the tank pressure profiles, it appeared that venting of mixed phase or trapped liquid occurred during this period.

Tank pressures in both tanks continued to decay from T + 960 seconds to the end of the retromaneuver at T + 1853.8 seconds. The average rate of pressure decay was 0.96 psi per minute in the LH₂ tank, and 1.18 psi per minute in the LO₂ tank. Tests (ref. 9) had shown that, under suitable conditions, solid hydrogen would form and tend to adhere to the vent duct when LH₂ was exhausted to an ambient pressure below its triple point. The tank pressure history and attitude control duty cycles in this period, however, showed no apparent evidence of any adverse effects due to solid hydrogen formation in the chilldown vent ducts. At T + 1853.8 seconds, the blowdown valves closed, and both tanks experienced a gradual rise in pressure.

BOOSTER FUEL DEPLETION SYSTEM

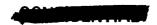
The flight of AC-6 was the first Centaur mission in which the sustainer stage flew to propellant depletion and utilized propellant depletion systems (IO₂ and fuel) to initiate SECO. The fuel depletion system had flown for the first time on AC-4 in an open-loop configuration. Pressure switches, used to detect IO₂ depletion, had served only as a backup for triggering engine shutdown on all previous flights. An additional backup signal to the propellant depletion scheme was provided by Centaur guidance, capable of SECO initiation at 0.7 g.

The most probable mode of shutdown, based on propellant tanking, is the depletion of LO₂ before fuel. This was the case experienced in the flight of AC-6. In order to detect LO₂ depletion, two series-connected sustainer-engine-fuel manifold-pressure switches are activated by a decay in fuel-manifold pressure that results from a drop in LO₂ pump NPSH. When both pressure switches close, a signal is transmitted to the autopilot to initiate SECO (fig. VII-11).

In the event that fuel depletes first, detection is made by two magnetostrictive sensors, mounted on a common probe and located in the fuel tank, with the sensing point at station 1194.27 (fig. VII-12). Two series-connected sensor controller units located in the B-1 pod receive the "dry" feedback signals from the sensors and, in turn, relay a 28-volt signal to the autopilot. Both sensors must indicate "dry" before a shutdown signal can be transmitted.

In addition to the functional system just described, there is a duplicate and independent evaluation system with similar sensors located in the fuel tank, with the sensing fuel level at station 1168.50. These sensors are positioned sufficiently high in the tank to be uncovered on all flights (evaluation system will be flown through AC-8 only). Outputs from this system are transmitted to the telemetry system alone and are not utilized for any command functions (fig. VII-13).

The fuel-depletion system operated without anomalies on AC-6 as indicated





by telemetry measurements of each of the four sensor controller relays. The data were quite similar to those obtained from the AC-4 flight. The evaluation sensors indicated approximately four uncover-cover cycles during a 2.2-second period commencing at T + 208.5 seconds (fig. VII-14). Slosh oscillations of this nature were expected because of the location of the probe near the tank wall with exposure to undampened fuel movement. At T + 210.7 seconds, the evaluation sensors remained dry until after retrorocket firing. At T + 237.2 and T + 241.8 seconds, sensor A indicated wetting for 1/2-second periods as a result of fuel sloshing.

The functional sensors remained covered with fuel until 2.5 seconds following SECO (T + 236.6 sec). At this time the sensors were uncovered due to the forward movement of the fuel after retrorocket firing. Sensor A gave three momentary wet signals at T + 240.6 and T + 246.1 seconds (2 cycles) before remaining dry, indicating continued fuel movement. Had not the engines sensed $\rm LO_2$ depletion, there would have been 2.5 seconds additional burn time remaining until the fuel-depletion system would have triggered shutdown.



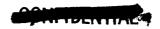
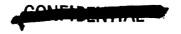


TABLE VII-I. - AC-6 PROPELLANT LOADING

	Propellant			
	LH ₂	ro ⁵		
Sensor required to be wet at T - 90 sec Sensor station number Volume ^a at sensor, cu ft Ullage volume at sensor, cu ft LH2 topping-low sensor dry at sec LO2 topping-high sensor dry at sec Ullage pressure, psia Density ^b , lb/cu ft Weight in tank at time sensor goes dry, lb	Topping low 174.99 1256.69 11.22 T - 26 21.8 4.2 5278	Topping high 373.16 370.94 6.58 T - 73.5 30.5 68.8 25 521		
LH2 boiloff to vent-valve lock at T - 7 sec, lb LO2 boiloff to T - 0 sec, lb Ullage volume at lift-off, cu ft Weight at lift-off, lb	13.5 5269	26 6.9 25 495		

 $^{^{\}rm a}\text{Volumes}$ include 1.85 cu ft LO $_{\rm 2}$ and 2.53 cu ft LH $_{\rm 2}$ for lines from boost pumps to turbopump inlet valves.



bDensities are taken from curves for vapor pressure against density from ref. 10.



TABLE VII-II. - PROPELLANT UTILIZATION SYSTEM

PREFLIGHT CHECKS

Time,	PU valve slew rates, deg/sec							
IIITI	C - 1	C - 2	Limits					
T - 44 T - 9	9.20 9.50	9.35 9.20	6 to 12 6 to 12					

PU valve crossover points (time of check, T - 59 min)

The following equation must be satisfied:

$$5 \text{ LH}_2 - \text{LO}_2 = 160 \pm 300 \text{ lb}$$

For check:

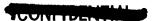
 $LH_2 = 2880$ $LO_2 = 14045$

therefore

 $5 \text{ LH}_2 - 0_2 = 355 \text{ lb}$

Full quantity check (time = T - 52 min)

Propellant	Quantity,	Requirement,
LH ₂	3 860	3 880±200
LO ₂	19 425	19 400±1000





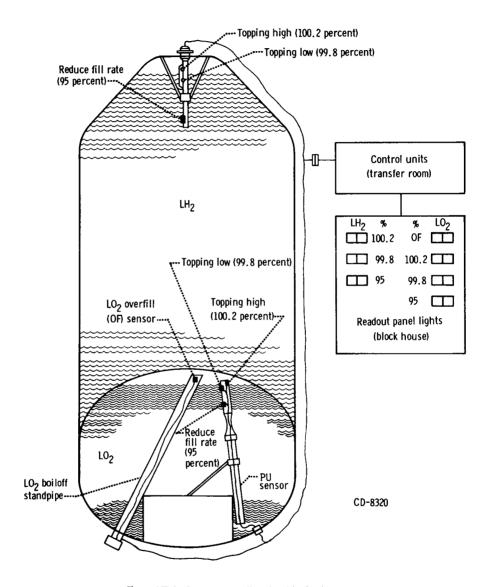


Figure VII-1. Centaur propellant level indicating system.

CONCIDENTIA

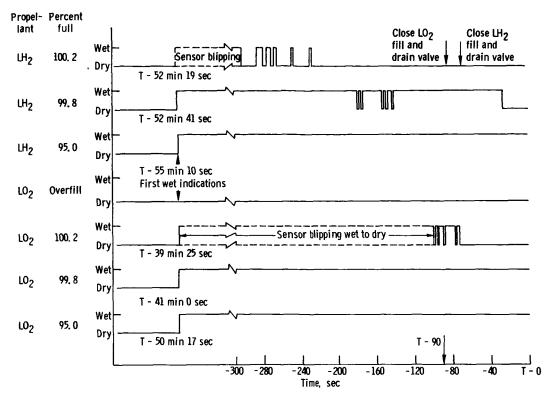


Figure VII-2. - Centaur propellant level indicating system operation,

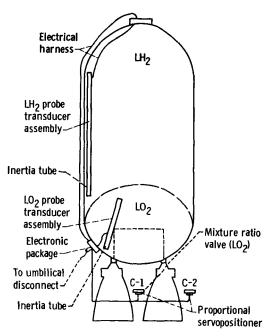
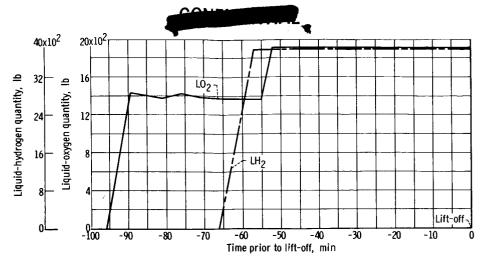
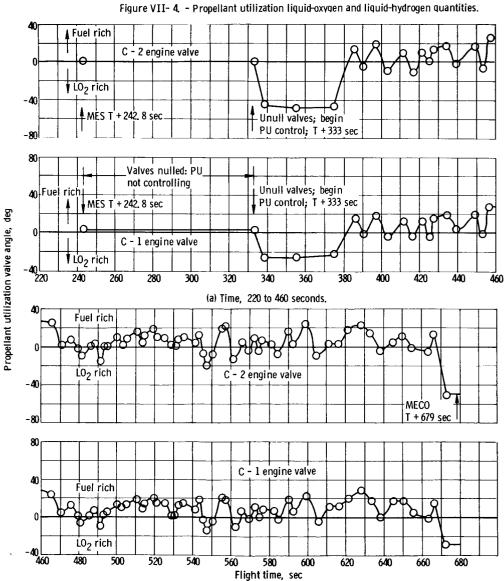


Figure VII-3. - Centaur propellant utilization system schematic.







(b) Time, 460 to 680 seconds.

Figure VII-5. - Propellant utilization valve angle as function of time.



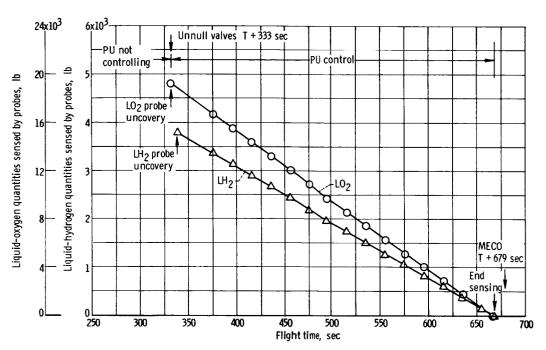
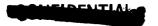
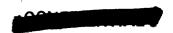


Figure VII-6. - Propellant quantities from propellant-utilization probes.





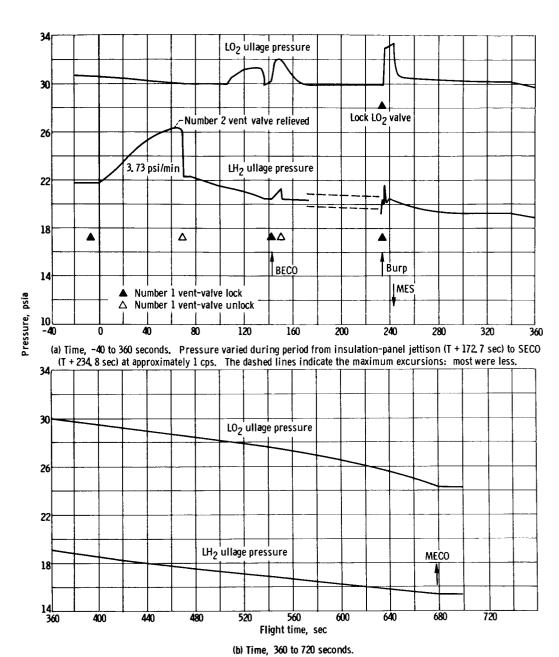
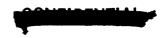


Figure VII-7. - Propellant tank pressures.



VVIIII

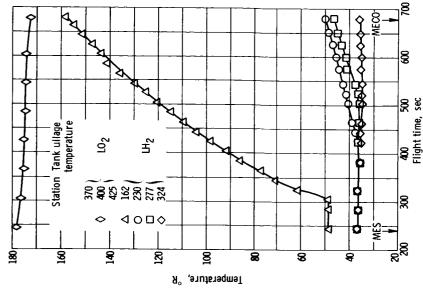
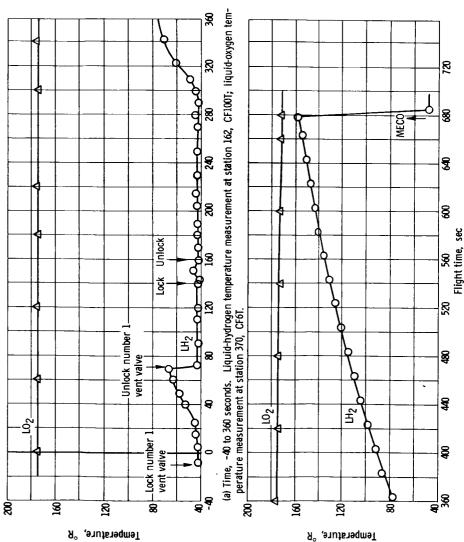


Figure VII-9. - Propellant tank ullage temperature during engine burn.



(b) Time, 360 to 720 seconds. Sudden temperature drop at MECO is spray from liquid-hydrogen boost-pump volute bleed hitting forward bulkhead. Figure VII-8. - Propellant tank ullage temperatures.





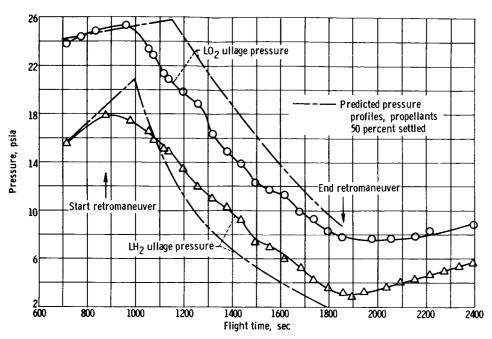


Figure VII-10. - Propellant tank pressures during retromaneuver.

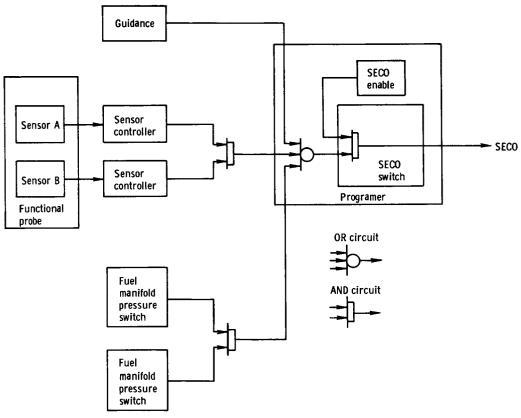


Figure VII-11. - Booster fuel depletion system circuit.





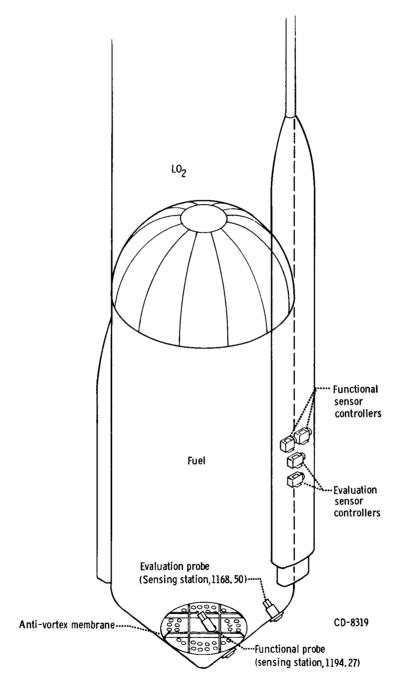
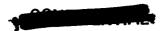


Figure VII-12. - Location of booster fuel depletion system sensors.





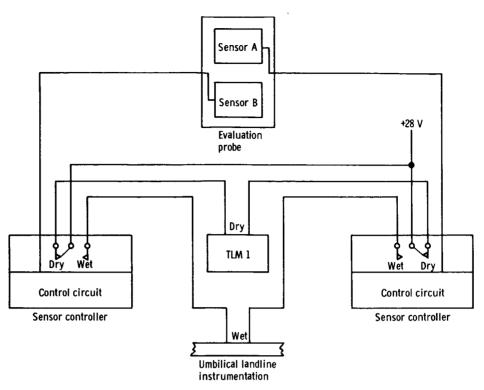


Figure VII-13. - Booster fuel depletion evaluation sensor system circuit.

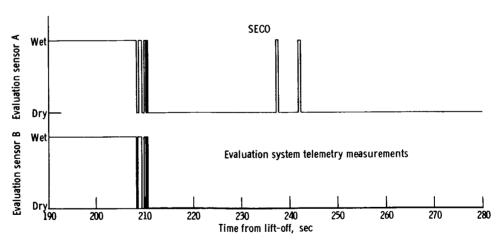


Figure VII-14. - Booster fuel depletion system evaluation sensors operation.



VIII. ENVIRONMENTAL TEMPERATURES

SUMMARY

The AC-6 environmental temperature profiles during flight were generally satisfactory, indicating adequate thermal control. Limited use of Thermolag provided additional protection for the nose-fairing and insulation panels, and the maximum skin temperatures due to aerodynamic heating were in good agreement with predicted values. Maximum measured flight temperatures were 1450° F at the nose-cap stagnation point and 826° F on the leading edge of the hydrogen vent stack. The high indicated nose-cap temperatures, however, were erroneous due to a poor thermocouple installation.

Internal temperatures in the payload compartment and the Centaur thrust section were nominal. In the Centaur forward equipment area some unusually low temperatures were experienced, particularly at the number 1 telemetry package, which had a skin temperature of -16° F or lower at lift-off. These low temperatures indicated the possibility of a cold helium gas leak through the station 208 seal.

EXTERNAL THERMAL ENVIRONMENT NOSE-FAIRING AND INSULATION PANELS

Measured external temperatures on the nose-fairing and insulation panels are shown in figures VIII-1 to 4. Table VIII-I also compares maximum measured temperatures with the predicted temperatures. The maximum measured temperature on the phenolic nose cap was 1450° F compared with a preflight prediction of 850° F. However, the nose-cap measurements were not valid because of a poor thermocouple installation. The thermocouples in the nose cap had been potted with a low-temperature epoxy that pyrolized at about 400° F. Consequently, the epoxy charred, insulated the thermocouple from the nose cap, and the small isolated mass sensed the higher response to aerodynamic heating as evidenced by the higher temperatures. The thermocouple did not accurately reflect the nose-cap temperature. This theory has been substantiated by postflight tests.

The maximum temperature experienced as a result of aerodynamic heating on the leading edge of the hydrogen vent stack was 826° F at a point 18 inches outboard from the nose fairing. This thermocouple installation was integral with the vent stack and was not compromised as in the case of the nose cap. The maximum temperature was less than the predicted 1025° F.

Heating effects on the conical surface of the nosecone were much less and did not exceed 265° F. These temperatures were well below the critical bond (glue) line temperature of 500° F. The effect of the Thermolag used to protect select areas can be noted by comparing figures VIII-2(a) and (b). Temperatures measured under the Thermolag at station 72 were approximately 80° F less than





those without Thermolag. Measured temperatures on the insulation panels along the positive x-axis without Thermolag indicated a peak value of approximately 300° F.

INTERNAL TEMPERATURE CONTROL

Payload Compartment

The payload compartment environmental control and temperature instrumentation are shown in figure VIII-5. The temperature histories of the payload compartment are shown in figure VIII-6. All the temperatures at lift-off gave assurance that a satisfactory thermal environment was maintained throughout the countdown. The Surveyor ambient temperature (CY7T), which was 85° F at lift-off, indicated that the environment in the vicinity of the retromotor was sufficient to meet the requirement of 85°±5° F at lift-off. The temperatures of the spacecraft separation latches, which have a lower temperature limit of 35° F, varied from 73° to 85° F at lift-off.

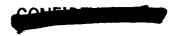
An attempt was made on this flight to determine the feasibility of monitoring and controlling the conditioning gas temperature at the ground side of the duct disconnect while maintaining the temperature of the gas within the lower airborne duct at 85°±5° F. Figure VIII-7 shows a comparison of these temperatures and indicates that a temperature setting of 83° F on the ground controlling sensor would have met the 85°±5° F requirement. These data will be verified by repeating this procedure on future vehicles.

Interstage Adapter

Extensive temperature instrumentation was installed on the AC-6 interstage adapter to measure the thermal environment. This instrumentation is shown in figure VIII-8. Table VIII-II is a summary of maximum measured temperatures on the AC-6 interstage adapter. Figure VIII-9 is a typical temperature history of the interstage skin.

INTERNAL THERMAL ENVIRONMENT CENTAUR ELECTRONICS COMPARTMENT

Temperatures in the forward equipment area are shown in figures VIII-10 and ll. It can be noted from the thermal mapping of figure VIII-11 that some of the components experienced abnormally low temperatures at lift-off. In particular, the temperature measurement on telemetry package number 1 went off scale at -16° F. These telemetry units have been tested over the range of 20° to 110° F, but the maximum or minimum allowable operating temperatures are not known. A summary of the critical measurements is given in the following table:





Centaur electronics compartment temperature survey								
Equipment	Lift-off temperature, or	Allowable range,						
Telemetry package number 1 Guidance platform Autopilot servoamplifier C-band transponder Inverter	Below -16 59 33 39 68	30 to 130 10 to 130 -35 to 160 200(max)						

Difficulties with the cold temperatures in the forward compartment were experienced during the quad tanking test and the first launch attempt. Inspection revealed a leak in the forward station 208 seal that allowed cold helium purge gas from between the insulation panels and the tank to leak into the area and cool the components. An attempt was made to repair the seal, but it appears that the failure recurred.

Centaur Thrust Section

Data from the Centaur thrust section indicated adequate thermal control. The $\rm H_2O_2$ manifold temperature of 80° F at lift-off was below the 120° F maximum allowable. The propellant-utilization electronics package skin temperature of 70° F was well within the 20° to 120° F range allowed.



TABLE VIII-I. - NOSE-FAIRING AND INSULATION-PANEL MAXIMUM TEMPERATURES

Remarks		Questionable	**************************************	dete invelid	3000									
Thermo-	20 35 -I) on	No	No N	No	No	Yes	Yes	No	No	No	No	No	No
ted	Time, sec	149	146	140	140	140	110	110	130	120	125	125	150	197
Predicted	Tempera- ture, of	850	751	375	375	375	180	180	200	165	092	092	1025	120
eđ	Time, sec	146	139	121	121	130	130	160	125	125	135	130	150	197
Measured	Tempera- ture, OF	1450	1352	292	230	220	152	188	155	184	270	295	928	100
Axis			! I	+ Y+	+	+	· ¥	×	<u>}</u>	¥	¥	¥	!	1
Station		1 1	1 1	13	72	125	72	72	185	314	362	400	!	!!!
Measurement		Nose-cap stagnation point	30° from stagnation point	Nose-fairing conical surface)				Nose-fairing barrel section	Wiring tunnel	Boost-num fairing		Leading edge of He vent stack	Umbilical island





TABLE VIII-II. - INTERSTAGE ADAPTER MAXIMUM TEMPERATURES

Measurement	Station	Quadrant	Measured		Predic	ted
			Tempera- ture, or	Time, sec	Tempera- ture, o _F	Time, sec
AA224T AA225T AA226T AA227T AA244T AA669T AA670T AA671T	444 465 484 499 418 430 450	I I III I I II	116 140 154 152 164 180 220 135	127 120 130 130 117 127 120 130	180 176 175 170 114 183 180 180	120 126 127 133 135 120 120
AA672T AA673T AA674T AA675T AA676T AA677T AA814T AA821T	461 490 510 419 422 503 507 535	II II II IV IV III -y-axis	130 110 105 230 150 120 250 262	137 120 120 126 120 160 130	180 169 215 290 188 230 290 290	120 133 170 142 160 170 142 142



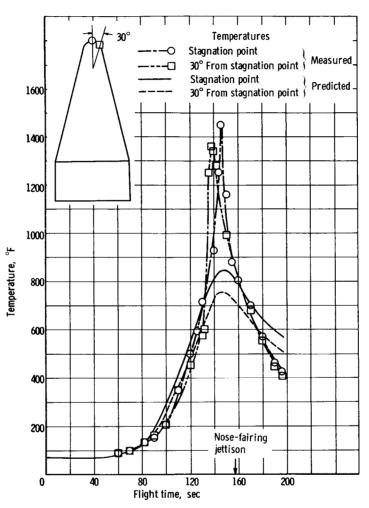
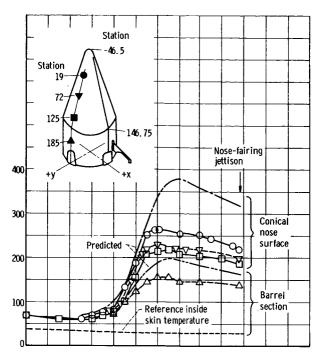
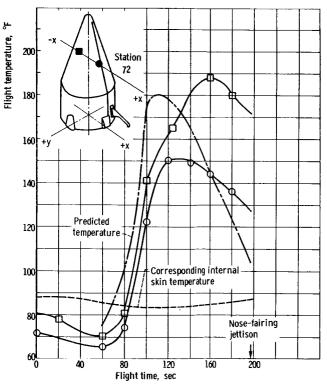


Figure VIII-1. - Nose-cap temperatures.





(a) y-Axis. Temperature measurements shown are in center of 4-inch-diameter area not covered with Thermolag. Other areas of nose fairing covered by Thermolag T-230.

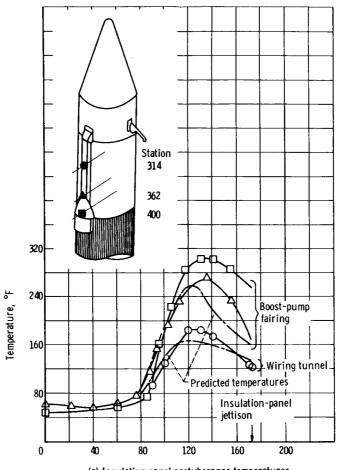


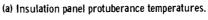
(b) x-Axis. Thermocouples covered with layer of Thermolag 0. 046 to 0. 056-inch thick.

Figure VIII-2. - Nose-fairing skin temperatures.









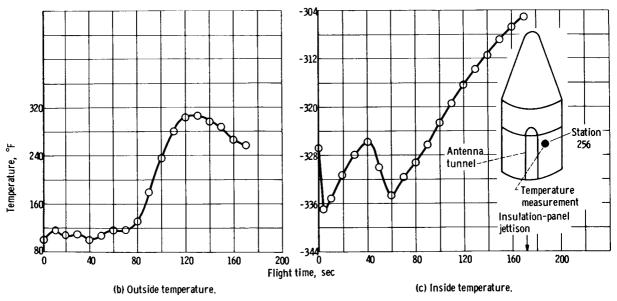


Figure VIII-3. - Insulation panel temperatures.



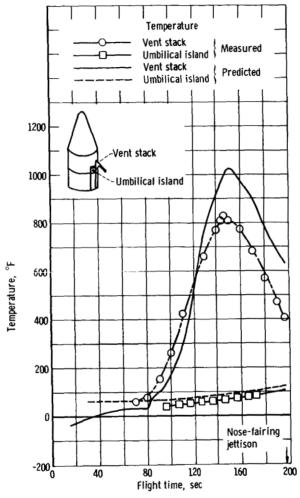
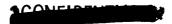
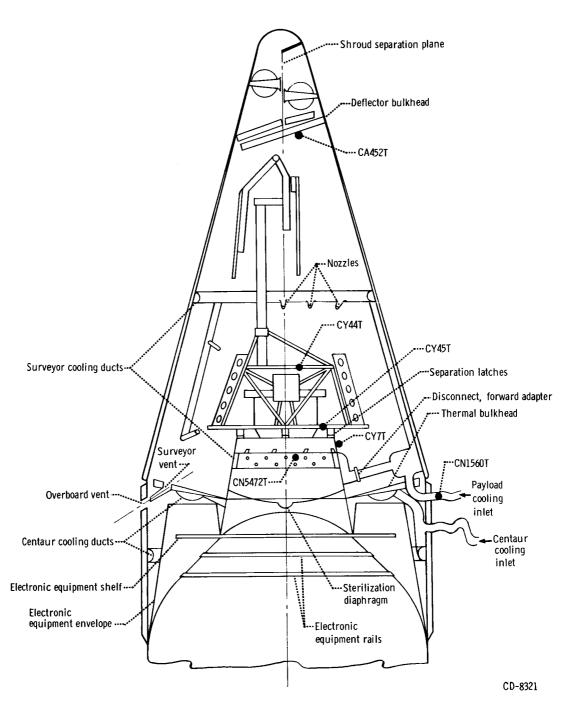
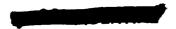


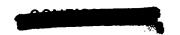
Figure VIII-4. - Protuberance temperatures.





 $\textbf{Figure VIII-5.} \ \, \textbf{-} \ \, \textbf{Surveyor compartment environmental control and temperature instrumentation.} \\$





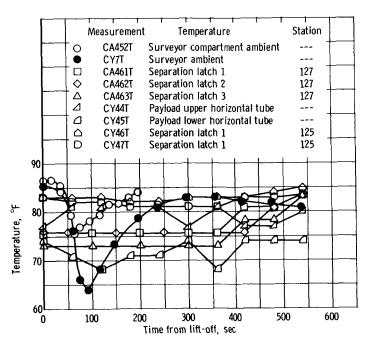


Figure VIII-6. - Payload compartment temperature history. (See fig. VIII-5 for temperature measurement locations.)

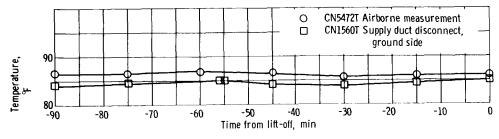


Figure VIII-7. - Payload compartment thermal conditioning gas supply temperature history.



3CONFIDENCE

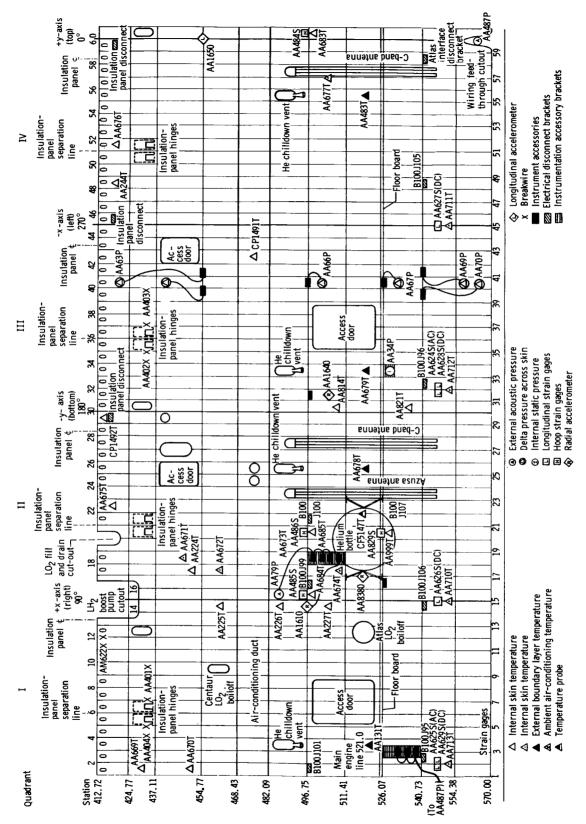
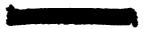
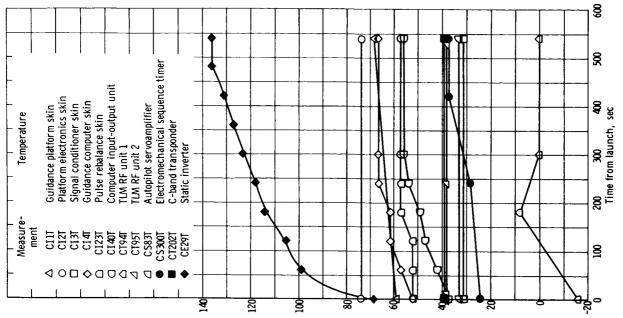


Figure VIII-8. - AC-6 interstage adapter instrumentation.





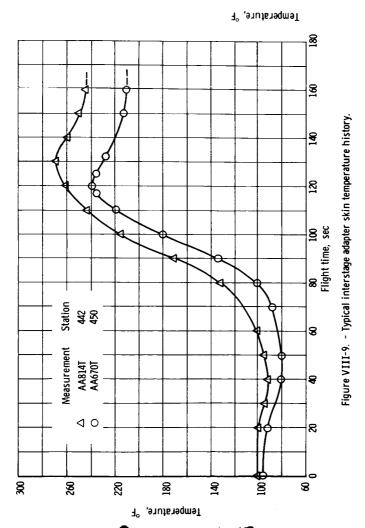
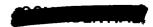
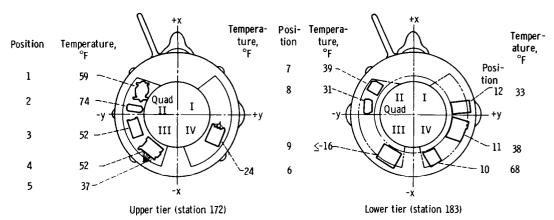


Figure VIII-10. - Electronics compartment temperature history.





- 1 Guidance platform
- 2 Electronics guidance platform
- 3 Guidance pulse rebalance
- 4 Guidance computer
- 5 Computer input-output unit
- 6 Electromechanical sequence timer

- 7 C-band transponder
- 8 Guidance signal conditioner
- 9 Telemetry package 1
- 10 Inverter
- 11 Telemetry package 2
- 12 Autopilot servoamplifier

Figure VIII-11. - Thermal mapping of Centaur electronics compartment at lift-off.



IX. VEHICLE STRUCTURES AND SEPARATION SYSTEMS

SUMMARY

The structural integrity was demonstrated, and all mission objectives of structural significance were achieved on the AC-6 flight. The peak longitudinal load factor experienced during the flight was 5.7 g's at BECO. Aerodynamic drag loads peaked during transonic flight as expected. Bending loads induced by wind shears and gusts on this flight were small. The peak bending moment occurred at T+82 seconds at station 812 and attained a value of 1.79×10^6 inchpounds.

Intimate contact was maintained between the Centaur IH2 tank and the insulation panels until panel separation. A minimum positive differential pressure of 10.7 psi across the Atlas intermediate bulkhead was experienced during launch. Interstage adapter panel excitation could not be evaluated due to the loss of the accelerometer on the panel skin.

The separation systems functioned properly within the established preflight limits, and all the separations were accomplished successfully. A tumbling rate of 1.82 degrees per second was encountered on the spacecraft subsequent to its separation from the Centaur stage. This compares with an allowable value of 3.00 degrees per second.

FLIGHT LOADS

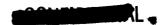
Longitudinal Loads

There are two sources of longitudinal loads on flight vehicles: one is the inertial load resulting from axial acceleration, and the other is a result of aerodynamic drag forces. Vehicle axial acceleration is known both from onboard accelerometers and from a knowledge of total engine thrust. The inertial loads can then be calculated from known mass distribution. For this flight, the total axial load and drag load history through atmospheric flight was calculated from strain gage data (station 547) and compared with analytical values based on wind-tunnel drag coefficient data. This comparison is shown in figure IX-1. It can be seen that the measured and calculated values agree quite well except at approximately T + 60 seconds (Mach 1) and after T + 104 seconds. This was attributed to the fact that the strain gage data were of poor quality and difficult to interpret accurately.

Vehicle Bending Moments

Though the Atlas-Centaur vehicle is launch restricted from inflight winds,





these winds during the month of August are usually very mild. The launch availability during this month was estimated to be 100 percent. This was the case on the AC-6 launch opportunity, as was shown both by preflight Rawinsonde runs and by measured (strain gage and angle of attack) bending moment data. All bending loads were well within the vehicle limit capability.

A comparison of predicted and actual bending loads encountered on this flight is shown in figure IX-2. The predicted range was based on T - 2 hours (0611 EST) Rawinsonde run and $\pm 30(1 - \cos)/2$ feet-per-second gust criteria loads. The measured bending moments are based on the flight angle-of-attack data. The bending moments were calculated in each case at station 812, which is the station of peak loading. The maximum bending moment occurred at T + 82 seconds, attaining a value of 1.79×10 6 inch-pounds. This is within the limit allowable of 5.6×10 6 inch-pounds at this station.

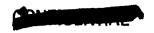
There were four strain gages mounted on the interstage adapter at station 547. One each of these gages was located on the principal axes. As previously mentioned, the data obtained from these gages were of poor quality. Further, because of the low bending moment amplitudes encountered on this flight, the relative magnitude of the errors resulting from the poor quality data could be sizeable. A comparison between the bending moment history calculated from strain gage responses, angle-of-attack data, and two Rawinsonde runs is shown in figure IX-3. The Rawinsonde balloons were launched at 0611 EST and 0940 EST, the latter approximately 10 minutes after vehicle lift-off. It is seen that the bending loads obtained from these various sources are in substantial agreement, leading to increased confidence in preflight analytical procedures.

The measured angle-of-attack histories in the pitch and yaw planes are shown in figures IX-4 and 5. In each case they are compared with calculated angles of attack based on the two previously mentioned Rawinsonde runs. It is seen that, in general, the trends are in agreement. The apparent divergence between measured and calculated values in the pitch plane could be a result of the relatively low angles of attack encountered on this flight. It is felt that, in a more severe wind environment, the agreement would be better. Comparison of the two Rawinsonde runs (figs. IX-4 and 5) gives an indication of the variability of winds aloft. As has been evidenced on past flights, the time dependence of these winds is relatively minor, particularly in the time domain of interest in establishing launch vehicle loads environment.

Gust Bending Moments

All previous Atlas-Centaur vehicles have been launched into mild wind environments, and the AC-6 flight was no exception. The gust loads encountered (with the exception of AC-2) have also been very small. These loads are monitored by the high-frequency strain measurements at station 547 on the interstage. A review of these high-frequency strain responses showed a maximum strain increment of 20 microinches per inch at T + 78 seconds, which is equivalent to a gust bending moment of 0.145×10⁶ inch-pounds. This bending moment increment represents a gust of approximately 4 feet per second. It is apparent that the gusts encountered on this flight were well below the design criteria of 30 feet per second.





PAYLOAD ADAPTER LOADS

There are three strain gages mounted on the payload adapter longerons directly aft of the separation latch points. Data from these gages indicate only compression loads in the adapter from launch to T + 700 seconds, at which time the vehicle went out of range of receiving stations at Antigua. The history of the adapter loads through T + 700 seconds, as calculated from the strain gages, is shown in figure IX-6. The loads increase steadily from launch to BECO attaining a peak value of 4000 pounds per latch point. There are subsequent lesser compression load discontinuities at SECO and MECO. From known values of payload weight, a peak longitudinal load factor of 5.78 g's can be calculated at BECO. At this time, measured axial acceleration showed a value of approximately 5.7 g's, which is within the accuracy of the strain gage data.

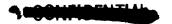
Payload adapter strain gage data from the AC-6 flight at the time of launch have been expanded and indicate the following results:

- (1) At T + 0.78 second, a bending moment of 80 000 inch-pounds occurred in the payload adapter at station 143. This is equivalent to a 1.2-g lateral load factor shown in figure IX-7.
- (2) Oscillation of the payload from T+0.6 to about T+1.1 seconds had a frequency of about 10 cps.
- (3) The relatively high bending (twice that encountered on AC-4 during launch) may have been a result of a dynamic load from the launcher kick struts that give a third kick at 0.5 to 0.6 second after lift-off.
- (4) The design load factors for this time of flight are 1.95 g's lateral and 1.8 g's longitudinal. The flight load factors are within these limits.

Insulation Panel Hoop Tension Loads

The Fiberglas honeycomb LH2 tank insulation panels are bolted to each other along four longitudinal seams and to the Centaur tank at station 412. At T + 171.9 seconds, the flexible linear-shaped-charge severence system was activated, and the panels were severed free from the vehicle. To preclude the possibility of panel flutter during the flight, the panels were installed on the tank with a pretension (hoop) load. This pretension load ensures intimate contact between the panels and the tank throughout the flight and further provides a built-in spring to assist in panel separation and jettison.

From a consideration of nominal preduction tolerances, temperatures, and tank internal pressure, it was estimated analytically that a panel hoop load of approximately 82 pounds per inch would be attained at launch. Landline strain gage data recorded during the quad tanking test revealed that the panel hoop load varied between 71 and 82 pounds per inch over the panel length at T + O second, indicating that approximately nominal pretension conditions were attained in the panels on this flight. Continuous strain gage data through the tanking test showed a constant hoop load. A return of all gage readings to the





ambient hoop load levels during detanking indicated that the structural integrity of the panels was maintained throughout the tanking process.

During flight, the hoop load in the panels varied because of changes in tank internal pressure and panel temperature. Based on this analysis, the maximum value attained during the flight was 115 pounds per inch at T + 70 seconds. This compares with an allowable hoop load in excess of 206 pounds per inch. It may, therefore, be concluded that the insulation panels were structurally intact throughout the flight. A history of the predicted range and the actual panel hoop loads is shown in figure IX-8.

Interstage Adapter Differential Pressure Environment

The AC-6 interstage adapter was the first of the operational lightweight adapters to be test flown. The operational adapter is approximately 400 pounds lighter than those flown on AC-4 and AC-5. This weight reduction was accomplished by a reduction in area of both stringers and frames, while the basic skin gage remained unchanged at 0.032 inch. The skin panel size of the AC-6 adapter is approximately 4.5 by 13.5 inches compared with 8.5 by 14.5 inches used on the previous adapters.

Differential pressure gages located in a vertical line at the negative y-axis of the adapter skin recorded a maximum crushing pressure of 2.1 pounds per square inch, which was well within the structural allowable of 3.5 pounds per square inch. The interstage adapter was subjected to a crushing pressure environment throughout most of the atmospheric flight as expected. Pressure data are shown in figure IX-9.

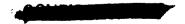
Centaur Propellant Tank Pressures

Recorded pressures in the Centaur $\rm IO_2$ and $\rm IH_2$ tanks were normal throughout suborbital flight as was the differential pressure across the intermediate bulkhead. Detailed plots of the variation of pressure as a function of time are shown in figure VII-7. The pressure curves fall well within the structural allowables of 25 psig for the $\rm IH_2$ tank and 42 psig for the $\rm IO_2$ tank throughout the flight.

Atlas Intermediate Bulkhead Differential Pressure

The Atlas $\rm IO_2$ tank ullage pressure programing system, incorporated to maintain sufficient bulkhead differential pressure during launch transient with 165K booster engines, was effective. It was designed to reduce Atlas $\rm IO_2$ tank pressure approximately 5 psi for the first 20 seconds of flight. A satisfactory differential pressure across the intermediate bulkhead of 10.7 to 13.6 psi was maintained for this period of time. At T + 20 seconds, the return to full flight pressure in the $\rm IO_2$ tank was initiated by the programer and completed approximately 3 seconds later.

A minimum value of 7.8 psi differential pressure across the bulkhead was





experienced at T + 92 seconds. The maximum value of 25.8 psi occurred immediately following BECO at T + 144 seconds. Though the upper and lower differential pressure limits have not been clearly established, a minimum value of 2.0 psi was considered desirable. The range of differential pressures encountered on the AC-6 flight was compatible with previous flight experience. Differential pressure, IO2, and fuel tank ullage pressure histories for this flight are shown in figure IX-10.

SEPARATION SYSTEMS

To optimize the payload, several structural elements were jettisoned during powered flight. In chronological order these were as follows:

- (1) Booster-package jettison
- (2) Centaur insulation-panel jettison
- (3) Nose-fairing jettison
- (4) Atlas-Centaur separation
- (5) Centaur-Surveyor separation

The booster-package jettison was fully developed during the Atlas research and development program, and no problems have been encountered with this system on any of the Atlas-Centaur flights. On the AC-6 flight, booster-package jettison was successfully accomplished at T + 144.9 seconds. The insulation-panel jettison and nose-fairing and Atlas-Centaur separations have been demonstrated on previous flights. Centaur-Surveyor separation was the only one to be demonstrated for the first time on the AC-6 flight. The performance of each of these systems (except booster-package separation) on this flight is given in the discussion that follows.

Insulation-Panel Separation

Four breakwires were located on the insulation-panel jettison hinges to record panel separation. These breakwires provided an "on-off" type of measurement. A review of these measurements reveals that all the panels were jettisoned simultaneously at T + 171.9 seconds. This conclusion can be verified by noting the cessation of all insulation-panel-instrumentation data at this time. A second verification of panel separation can be deduced from the tank hoop strain increase, which also occurred at this time. This increase indicates that the hoop stress relief provided by the panels had been removed showing intimate contact between the panels and the Centaur tank.

This successful separation serves to demonstrate the capability of the shaped-charge system to withstand repeated cryogenic cycling, particularly in the area of station 219 where temperatures of -320° F are encountered. The AC-6 linear-shaped-charge-separation hardware experienced one partial Centaur tanking and one full cryogenic abort without degradation of its pyrotechnic components.





On previous vehicles, aborts had been followed by a complete replacement of the pyrotechnic system hardware. Confidence in the abort capability of the system was based on the following preflight test program:

- (1) A series of cryogenic unlatch tests simulating flight aborts and rain
- (2) A system qualification test program consisting of 38 successive, successful flight-type hardware "breadboard" tests, subjecting all test hardware to the extreme limits of vibration, humidity, cryogenic and elevated temperatures, vacuum conditions, and flight aborts

The recovery and thorough inspection of the AC-6 wiring tunnel panel gave further indication that the insulation panels successfully separated and jettisoned from the vehicle. This panel, recovered by a U.S. Navy destroyer at 21°21' north lattitude and 71°17' west longitude (near Grand Turk Island in the Caribbean), was thoroughly inspected by cognizant GD/C and NASA engineers and found to be in reasonable condition considering the impact loads it obviously sustained during reentry and on contact with the water. The panel was intact with the exception of one missing hinge, one aft corner of the panel, and the "bolt-on" boost-pump fairing. The inside surface of the panel showed some local delamination of the skin. Charring of the detonator fairing and shaped-charge retainer indicates that the panel was in an aft end first attitude during reentry. Charring of the fracture surfaces indicates that the aft corner broke off prior to or during reentry.

Nose-Fairing Separation

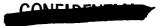
Separation of the nose fairing was signaled by the linear-motion indicator connecting the fairing halves to the spacecraft mast at T+196.49 seconds. The approximately 7-inch travel of these potentiometers was accomplished in 0.04 second. No excessive vibrations were observed on the accelerometers at this time.

The thrustor bottle compartment pressure dropped from 14.7 psia at launch to flight vacuum prior to nose-fairing jettison. At nose-fairing jettison there was a pressure peak of about 3 psi due to thrustor bottle pressure. This peak is slightly less than pressures developed during the Lewis Research Center Space Power Chamber tests of the nose fairing. Though this measurement may be somewhat inaccurate because of the 6-cycle-per-second maximum response of the transducer, it does indicate the pressure was within acceptable limits.

Atlas-Centaur Separation

The stage-separation process was initiated by the linear-shaped-charge firing at T+236.20 seconds which severed the interstage adapter at station 413. The retrorockets fired at approximately T+236.3 seconds to decelerate the Atlas. Acceleration data indicated that all eight rockets ignited.

Information obtained from rate gyros indicated that the Centaur did not rotate about its center of gravity appreciably during the separation process



(less than 0.05 deg). The rate and displacement gyros indicated that the Atlas rotated about its yaw axis approximately 0.27 degree at the time it cleared the Centaur. The predicted yaw rotation would result in a lateral motion of 2.3 inches at station 413 after 9 feet of axial motion relative to the Centaur. The observed motion due to rotation was 2.7 inches.

The gyros also indicated that the Atlas rotated somewhat about its pitch axis, but to a greater degree than is normally experienced. The departure noted from the norm appears to lie in a residual turning rate seen in the Atlas prior to separation. The Atlas was displaced in a negative direction prior to SECO and was initiating a corrective pitch when SECO occurred. The resulting positive pitch motion was not nulled out as the neutral position was passed after the engine was shut down, but continued into the separation interval. Therefore, the interstage adapter and the Centaur were moving together at the time of shaped-charge firing, and there was a vertical motion of the Centaur that moved it with the Atlas rotation, tending to prevent interference. considering the change in the Atlas angular rate during staging, it appears that the clearance between the vehicles was reduced by 0.3 inch (out of a nominal 15 in.) toward the positive y-direction, which still leaves approximately 14.7 inches clearance. The predicted vertical motion at station 413 after 9 feet of longitudinal travel is -2.7 inches.

Spacecraft Separation System

Separation latches. - The separation latches at the Centaur Surveyor interface were designed to hold the spacecraft rigidly to the payload adapter and to provide the impulse during spacecraft separation. A cross-sectional view of the latch assembly and strain gage location is shown in figure IX-11. Not shown are the springs that provide the separation impulse. The separation latches are preloaded in tension to eliminate relative motion between the spacecraft and spacecraft adapter. As seen in figure IX-12, all three latches maintained the preload until spacecraft separation. The initial preload in all the latches was set at 2400 pounds before launch. Two of the gages drifted away from their nominal value prior to lift-off. This is thought to be zero shift in the strain gage since there is no known mechanism by which this preload could be relieved during the countdown.

Variations in preload during the flight were all less than 300 pounds from their prelaunch value. This level of variation does not affect the functional performance of the latch mechanism. At spacecraft separation, data from the gages showed the expected sudden release of the preload, indicating that the latch pin-pullers functioned successfully. Data from three deflection gages, one on each of the latch springs, also confirms a successful separation. Analysis of the spacecraft tip-off rate induced by the latch springs is discussed in the following section.

Spacecraft separation. - Analysis of the variation of signal strength from the S-band transponder revealed a tumbling rate of 1.8 degrees per second of the Surveyor spacecraft after separation from Centaur. A check of the Surveyor polar signal strength patterns for the omnidirectional antenna reveals that the frequency rate of tumbling is the same as the frequency of signal strength.





Linear potentiometers are located at each of the three points where the spacecraft is locked to the payload adapter to measure the position of each of the attachment points with relation to the spacecraft. Figure IX-13 shows the location of these potentiometers and a time record of their output. These data show that initiation of separation at all three points is within 5 milliseconds, but that the potentiometers located on the positive y-axis (CY2D) reached full scale 90 milliseconds after the other two potentiometers. These potentiometers indicated that a positive pitch rate existed at separation, and this fact agrees with the tumbling rate based on S-band signal variation.

Each of the three latches holding the Surveyor to the Centaur payload adapter has two sets of springs tending to separate Centaur and the spacecraft. The stronger set of these springs provides force for separation, while the weaker set of springs is used to make the potentiometer follow the motion of the spacecraft as well as to impart a small force to the separation. Calculations by analog computer show that, if all the force derived from the spring of potentiometer CY2D were removed from the system, the tumbling rate of Surveyor would only be 0.85 degree per second. This calculated rate includes the initial tumbling rate before separation of the combined Centaur-Surveyor, which was determined from the pitch and yaw rate gyros as

Yaw rate = -0.244 deg/sec

Pitch rate = 0.12 deg/sec

From this calculation, indications are that a higher unbalanced force was necessary to obtain the 1.8-degree-per-second tumbling rate that existed and that there was a high probability of a partial "hang-up" of one of the main separation springs. Also noted was that one extensiometer travel was only about 90 percent as much as the other two.



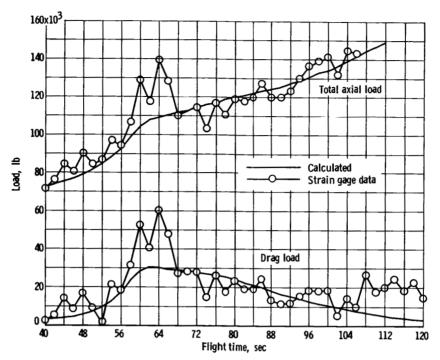


Figure IX-1. - Comparison of history of calculated and measured drag and total axial load on AC-6 flight.

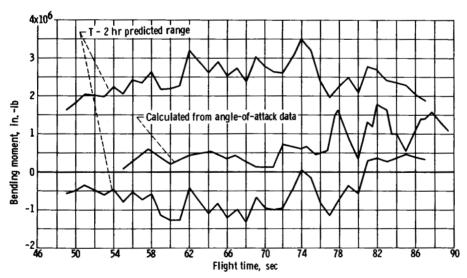
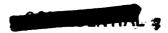


Figure IX-2. - AC-6 flight bending moment history at station 812 based on measured angle-of-attack data and range of bending moments predicted on basis of T - 2 hours (0611 EST) Rawinsonde run.



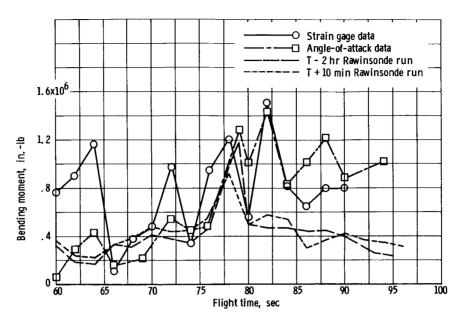


Figure IX-3. - AC-6 flight bending moment history at station 547.

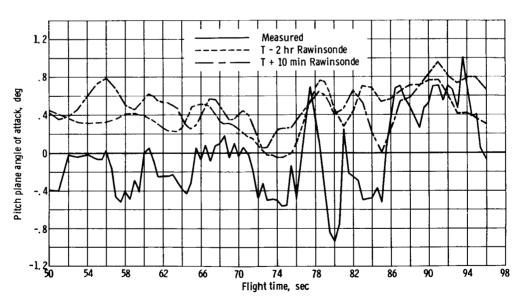


Figure IX-4. - Comparison of measured pitch plane angle of attack and computed values based on Rawinsonde soundings just before and after vehicle launch.





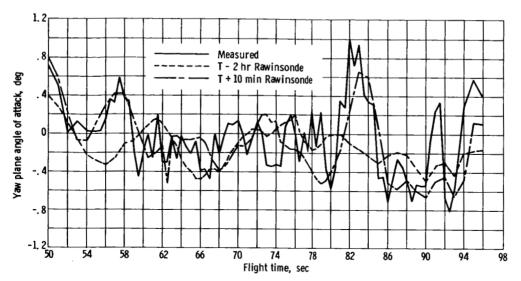


Figure IX-5. - Comparison of measured yaw plane angle of attack and computed values based on Rawinsonde soundings just before and after vehicle launch.

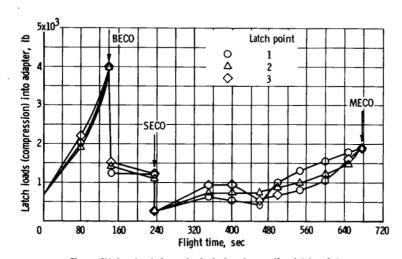


Figure IX-6. - Loads in payload adapter at separation latch points.



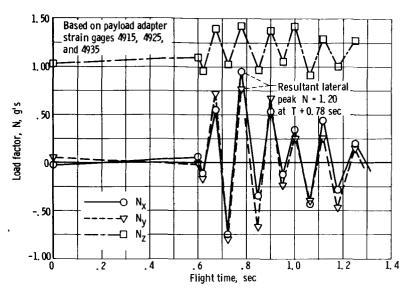


Figure IX-7. - Payload lateral and longitudinal load factors at launch. Design load factors at launch are 1, 8 g's longitudinal and 1, 95 g's lateral.

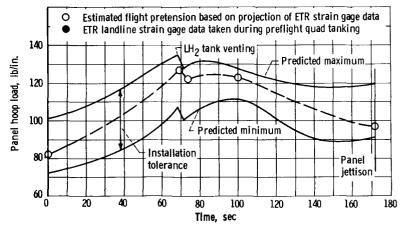
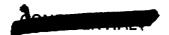


Figure IX-8. - AC-6 insulation panel hoop load as function of time. The spring rates are: K_{panel} = 0. 166 inch of radial motion/psi and K_{tank} = 0. 008 inch of radial motion/psi.





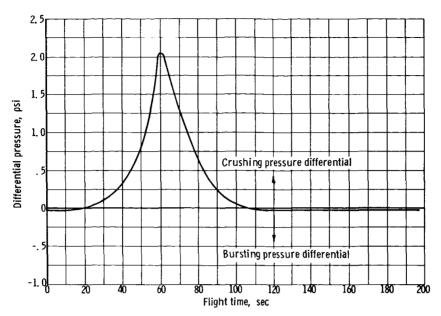
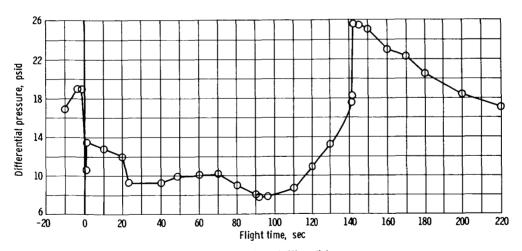


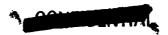
Figure IX-9. - Interstage adapter (AC-6) pressure differential history at station 557 in quadrant III (AA69P).

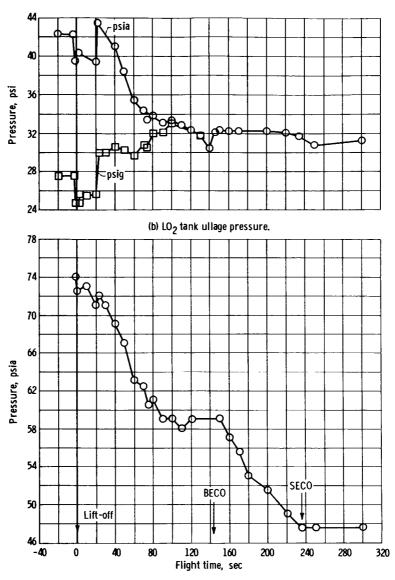


(a) Intermediate bulkhead differential pressure.

Figure IX-10. - Atlas pressure histories for AC-6.







(c) Fuel tank ullage pressure. Figure IX-10. - Concluded,







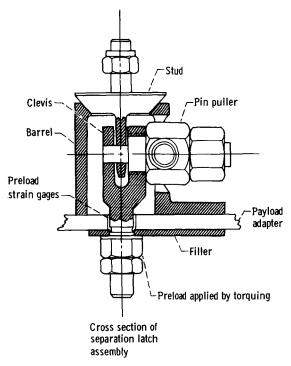


Figure IX-11. - Cross-sectional view of Centaur surveyor separation latch assembly.

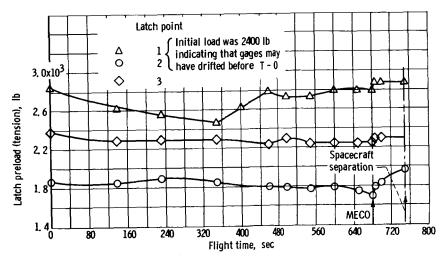


Figure IX-12. - Centaur-Surveyor separation latch preload.



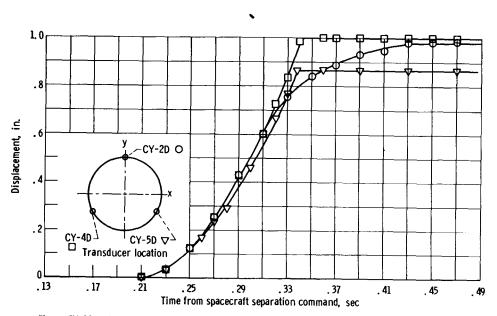


Figure IX-13. - Surveyor displacement from Centaur at separation. Spacecraft separation command issued at $\, T + 747.57 \,$ seconds.



X. VEHICLE DYNAMICS

SUMMARY

Longitudinal modal excitations and lateral payload excitation were high at lift-off for the AC-6 flight. The vehicle-flight-vibration environment as well as the lateral modal excitation were similar to previous flights. At SECO, an engine shutdown pressure oscillation caused a 90-cps longitudinal vibration unobserved on previous flights.

MODAL DYNAMICS

Longitudinal excitations were observed approximately at the same times as in previous flights, as is shown in figure X-1. Lift-off perturbations resulting from launcher release and from Atlas IO2 pressurization, as shown on z-axis accelerometers, were 0.47 g single amplitude around a 1.25-g centerline with a frequency of 7 cps. This amplitude was approximately three times greater than that observed on the AC-2, AC-3, and AC-4 flights, but about the same as that on the AC-5 launch. The peak disturbance occurred at about 0.2 second after 2-inch rise. At this time, struts bearing on the base of the Atlas vehicle were raised by the vehicle motion which caused the launcher holddown arms to ro-Another longitudinal acceleration peak observed at 0.6 second after 2-inch rise had a single amplitude of 0.4 g (around a 1.25-g centerline) with a frequency of 7.0 cps. At the same time, large disturbances were indicated by the roll-rate gyro, displacement gyro, Surveyor separation-plane y-axis accelerometer, and Surveyor mast tip y-axis accelerometer. The roll signals indicated that, up to 0.6 second, the vehicle had rolled 0.160 whereupon it snapped back to 00 in less than 0.01 second. The Surveyor separation-plane accelerometer signals indicated a single amplitude of 0.80 g about a 0-g centerline, and the Surveyor mast tip accelerometer indicated a single amplitude of 4.0 g's about a 0-g centerline. Specifications for the Surveyor allows a 1.25-g singleamplitude vibration at the Surveyor-Centaur separation plane.

Surveyor displacement potentiometers measuring relative motion between the mast tip and the nose fairing showed a single-amplitude displacement of 0.48 inch at this time. These disturbances (at 0.6 sec) occurred at approximately 22 inches of vehicle rise and coincided with a load peak measured on the launcher kick strut at the same rise during tests conducted before this flight.

"Pogo" type oscillations occurred slightly earlier in the AC-6 than in the AC-4 flight and had a maximum single amplitude of 0.16 g about a centerline varying from 2.0 to 5.4 g's, as shown in figure X-1. The frequency for "pogo" was 12 cps. An engine cutoff transient was observed at BECO on z-axis accelerometers with a single amplitude of 0.7 g around a 1.28-g centerline and a frequency of 70 cps. This amplitude was approximately half that noted on pre-





ceding flights. Unlike previous flights, the AC-6 flight also had longitudinal oscillations caused by an engine cutoff transient at SECO detected on z-axis accelerometers (one located at station 1057 and the other at station 450 on the interstage adapter) that indicated a single amplitude of 5.3 g's about a 1.6-g centerline with a frequency of 90 cps. At the same time, a y-axis accelerometer and a tangential accelerometer on Surveyor were excited at the same 90-cps frequency. The y-axis accelerometer (on spacecraft mast tip) had a single amplitude of 0.30 g around a 0-g centerline, and the tangential accelerometer had a single amplitude of 0.35 g about a 0-g centerline. Again these disturbances did not exceed specifications for the Surveyor vehicle.

Lateral bending mode deflections are shown in figure X-2 as calculated from Centaur pitch- and roll-rate gyros (located at station 173). The design allowable modal deflections at station 173 are also shown in figure X-2. allowable deflections are only critical from 44 to 80 seconds after 2-inch rise. During this period, only deflections in the yaw plane were observed since the low-range pitch-rate gyro was off scale. The observed yaw-plane first-modal deflection during the critical time period was less than 10 percent of the design deflection, and the yaw-plane second-modal deflection during the critical time period was less than 5 percent of the design deflections. The pitch-plane modal deflections observed before and after the critical time period for both first and second modes were approximately the same as the yaw-plane modal deflections at the same times. Since the deflections in both planes were nearly equal for both the actual case and for the design criteria, it can be assumed that the pitch-plane modal deflections do not exceed the design criteria during the critical time period.

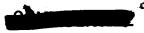
Figure X-3 shows the comparison of first-mode maximum bending deflections during AC-2, AC-3, AC-4, and AC-6 flights. From this comparison it can be seen that the lateral first-mode deflections for this flight were about the same as in other flights. The first- and second-mode frequencies plotted against time are shown in figure X-4 and are very close to the theoretical values calculated before the flight.

VIBRATIONS

The vibration profile of AC-6 was similar to previous flights. At launch and transonic/max Q, the vibration environment was predominantly Gaussian with sinusoids superimposed. After the transonic region, the only vibrations evident were caused by flight events such as booster engine cutoff, Atlas-Centaur separation, etc.

All the accelerometers indicated a perturbation at booster jettison that is believed to be noise, since it was also visible on some temperature measurements. At 197.5 seconds after launch, the accelerometer indicating outboard acceleration located on compartment A of the spacecraft (CY58 ϕ) oscillated between data channel band edge in a mode that is typical of instrumentation failure. The transducer located on the LH₂ duct (CA601 ϕ) gave a questionable vibration indication starting at approximately 243 seconds after 2-inch rise.

The maximum vibrations are given in table X-I. Radial vibration in the



interstage adapter was fairly low; AAl6l ϕ (Q₁ + Q₂ station 497) gives the highest level, which was 40.0 g's (double amplitude) and occurred during launch. The maximum vibration indicated by the spacecraft accelerometers was 32.0 g's (double amplitude) retromotor attachment 1 z-axis (CY52 ϕ), which occurred at 235.8 seconds after launch. The foot of the spacecraft experienced maximum vibration at launch that was equal to 2.0 g's (double amplitude) with a frequency of 8.7 cps and was measured on CY50 ϕ located at station 125 and sensitive to the y-direction. The maximum vibration that the mast of the spacecraft experienced was 8.4 g's (P-P) indicated by an accelerometer located at the top of mast that read in the y-direction (CY55 ϕ).

In order to gain an insight into how the actual flight vibration compares with the qualification levels that were used in designing vehicle and spacecraft components, a power spectrum analysis was performed on all usable accelerometer measurements. The power spectral density plots (fig. X-5) included in this report are for the flight times at which maximum vibration occurred. The densities were obtained by using very short analysis times (0.5 sec or less) to eliminate variations with flight time. The spectrum analyzer used was a General Applied Science Laboratories Model SA12 real-time low-frequency heterodyne analyzer.

Examination of the power spectral density (fig. X-5(b)) for the maximum radial vibration in the interstage adapter (quoted previously as 40 g's double amplitude) shows that there are sinusoids at 200, 300, and 400 cps, and the data channel starts to attenuate at 220 cps. If the 400-cps component is assumed to be noise (inverter crosstalk) the maximum energy level is $0.88~\rm g^2/cps$ at a frequency of 300 cps.

As seen from figures X-5(f) to (o), the vibration profile of the spacecraft was predominantly sinusoidal, with the maximum levels being below the separation plane qualification level. The foot area accelerometer (CY50 ϕ) indicated 0.036 g²/cps, at a frequency of 25 cps, retroattachment area accelerometer (CY549) indicated 0.1 g²/cps at a frequency of 25 cps, and the top-of-the-mast accelerometer (CY55 ϕ) indicated 1.15 g²/cps at a frequency of 50 cps.

AC-6 instrumentation included two microphones, one located on compartment A (CY61Y) and the other at the top of mast (CY60Y). The maximum dynamic sound pressure measured in each microphone area was 0.0695 psi (single amplitude) and 0.0727 psi (single amplitude), respectively, these values being close to the qualification level (ref. 11) of 145 decibels (rms) (fig. X-6 gives the amplitude as function of spectrum for launch).

At shaped-charge firings, Centaur insulation-panel jettison, the Atlas-Centaur separation there were shock loads induced in the spacecraft. This shock vibration was not indicated by all spacecraft accelerometers because of their low-frequency response (the frequency of this shock was of the order of 600 to 700 cps). Accelerometer (CY54 ϕ) (best frequency response) indicated a 12.0-g (single amplitude) maximum amplitude shock lasting for approximately 0.05 second. The other high-frequency response accelerometers in the area (CY53 ϕ and CY52 ϕ), indicated 12.5 g's (single amplitude) and 16.0 g's (single amplitude), respectively, after correcting for roll-off. The nature of this shock is such that it could conceivably cause damage to the spacecraft packages if it is





not quickly damped out. Spacecraft amplification factors are currently being investigated to evaluate this situation better. Figures X-7 to 9 show both the raw data and amplitude spectrum (resulting from Fourier analysis) of this shock. The amplitude indicated by the amplitude spectrum is less than the raw data value. This is to be expected since the raw data is triangular in appearance.

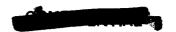




TABLE X-I. - MAXIMUM VIBRATIONS OBSERVED DURING COMPLETE AC-6 FLIGHT

Location	Measurement number	Time after 2-inch motion, sec	Maximum g's, double amplitude	Frequency band of data channel, cps	Comments
Interstage adapter z-axis Q1 and Q2, station 455	ΑΑ165φ	142	4.2 g's	0 to 45	BECO
Panel radial Q_2 and Q_3 , station 503	AA164φ	Only deflection was at Atlas booster jettison (noise)			
Interstage adapter radial Q_1 and Q_2 , station 497	AAl6lφ	1	40.0 g's	0 to 220	Launch
Interstage adapter radial helium bottle, station 519	ΑΑ838φ	236.2	10.0 g's	0 to 1200	Atlas-Centaur separation shock-type transient
LH ₂ duct near y-section, station 453 Q ₂	CA6Olφ	171.7	13.03 g's	0 to 160	Transducer failed at 242.9 sec
Spacecraft vibrations: Compartment A, strain normal	CY59S		1200 μin./in.	0 to 660	Launch
Foot accelerometer, 0° at station 125 x-axis sensitivity	СΥ49φ	0.6	1.2 g's	0 to 160	90 cps
Foot accelerometer, 0° at station 125 y-axis sensitivity	СҰ50ф	0.45	2.0 g's	0 to 220	8.7 cps
Foot accelerometer, 270° at station 125, sensitive in tangential direction	СУ51ф	0.65	1.6 g's	0 to 330	8.7 cps
Retroattachment 1, z-axis sen- sitivity	CY52p	171.7 235.8	11.2 g's 32.0 g's	0 to 600	Shock-type transient
Retroattachment 2, z-axis sen- sitivity	СΥ53φ	235.8	25.0 g's	O to 790	Atlas-Centaur separation shock-type transient
Retroattachment 3, z-axis sen- sitivity	СΥ54φ	235.8	24.0 g's	0 to 1000	Atlas-Centaur separation shock-type transient
Top of mast, y-axis sensitivity	СҮ55ф	0.68	8.4 g's	0 to 80	10 cps
Top of mast, x-axis sensitivity	СҰ56ф	0.5	3.0 g's	0 to 60	10 cps
Compartment A, accelerometer outboard sensitivity	СҰ57ф	0.68	3.0 g's	0 to 450	10 cps
Compartment A, accelerometer z-axis sensitivity	СҰ58ф	171.7	1.6 g's	0 to 110	
Compartment A, outboard sen- sitivity	CY61Y	Launch	147.6 decibel	s 0 to 2100	0.0695 psi single amplitude
Top of mast	CY6OY	Launch	148.0 decibel	s 0 to 1200	0.0727 psi single amplitude

CONTRACTOR



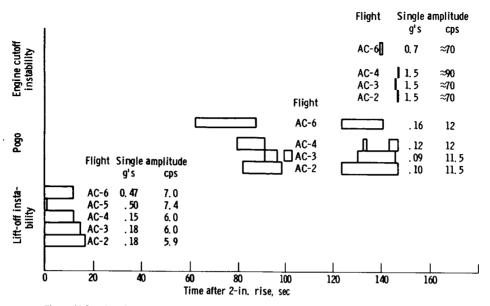


Figure X-1. - Longitudinal oscillation occurrences, frequencies, and maximum amplitudes for Atlas-Centaur flights.

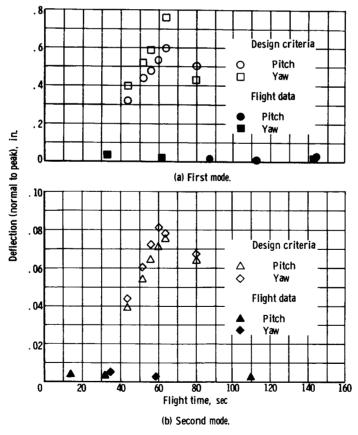


Figure X-2. - Flight data and design criteria for wind-gust modal amplitudes (pitch and yaw planes at station 173).





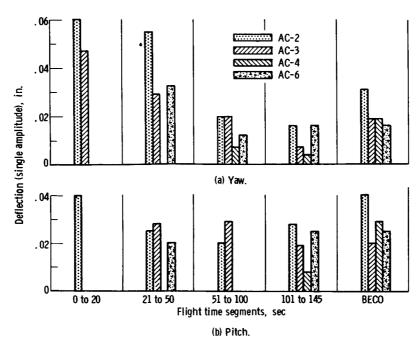


Figure X-3. - Maximum first modal amplitudes at station 173 for AC-2, AC-3, AC-4, and AC-6 flights.

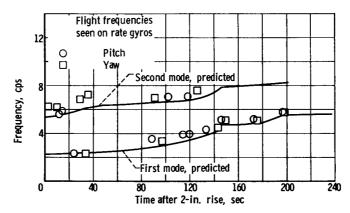
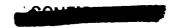


Figure X-4. - Comparison of flight bending frequencies with theoretical bending frequencies.





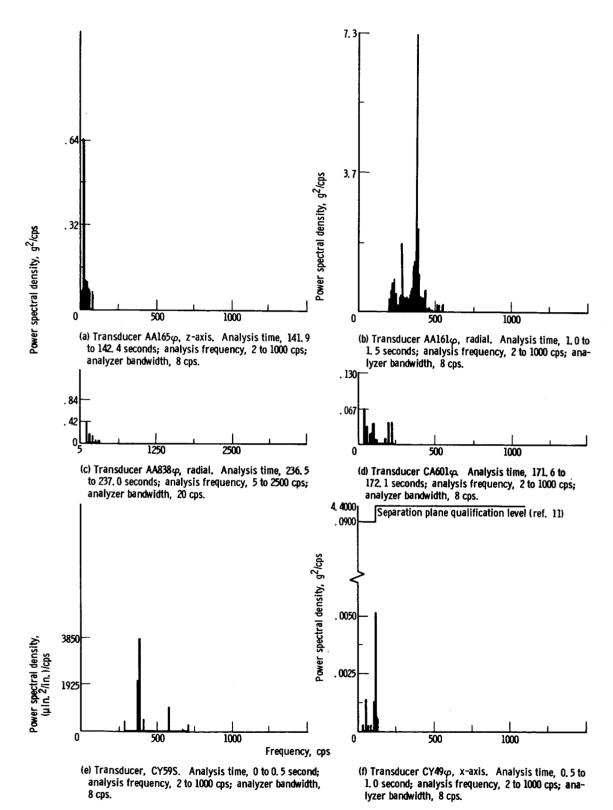
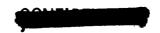


Figure X-5. - Vibration power spectrum.





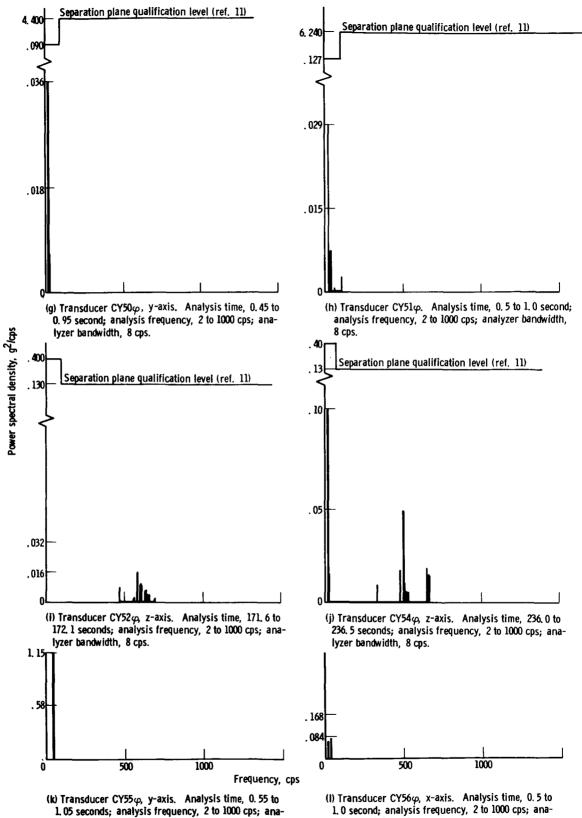
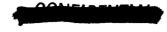


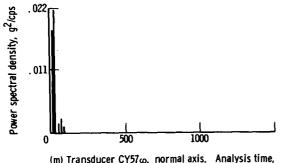
Figure X-5. - Continued.

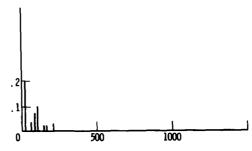
lyzer bandwidth, 8 cps.



lyzer bandwidth, 8 cps.

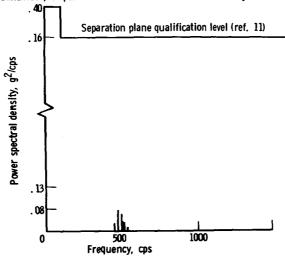






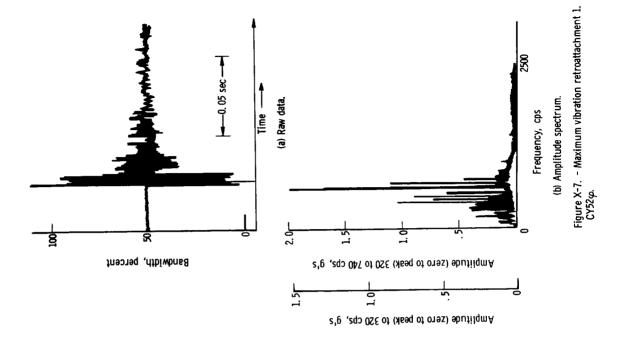
(m) Transducer CY57 φ , normal axis. Analysis time, 0.5 to 1.0 second; analysis frequency, 2 to 1000 cps; analyzer bandwidth, 8 cps.

(n) Transducer CY58 φ , z-axis. Analysis time, 171.5 to 172 seconds; analysis frequency, 2 to 1000 cps; analyzer bandwidth, 8 cps.



(o) Transducer CY53 φ , z-axis. Analysis time, 235. 6 to 236. 1 seconds; analysis frequency, 2 to 1000 cps; analyzer bandwidth, 8 cps.

Figure X-5. - Concluded.

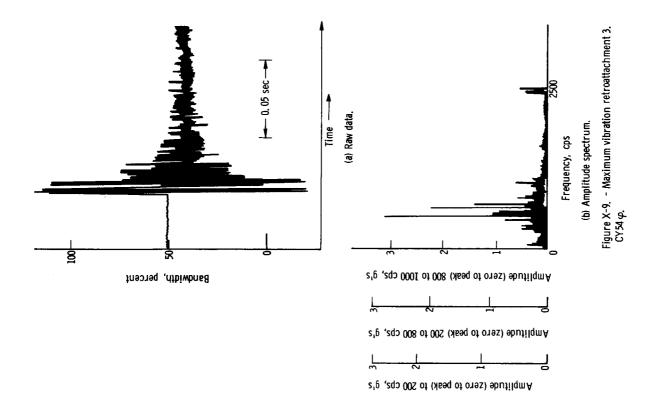


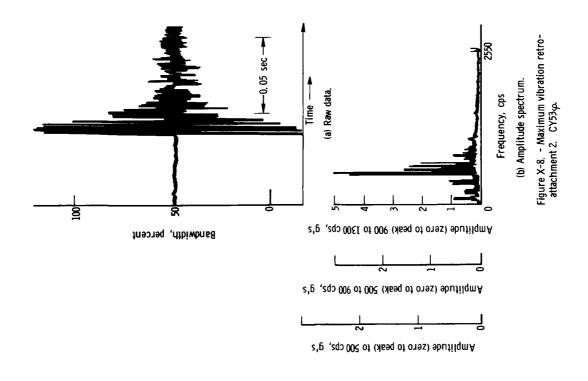
(b) Transducer CY60Y. Analysis time, 1.0 to 1.2 seconds; analysis frequency, 5 to 2500 cps; analyzer bandwidth, 20 cps. (a) Transducer CY61Y. Analysis time, 0.1 to 0.2 second; analysis frequency, 5 to 2500 cps; analyzer bandwidth, 20 cps. Frequency, cps .073 ⊢ . 037 .035 T

Ymplitude spectrum (zero to peak), psi

Figure X-6. - Sound pressure level.









XI. FLIGHT CONTROL

SUMMARY

Analysis of the Atlas-Centaur flight-control telemetry data indicated satisfactory system performance throughout flight.

ATLAS

Flight-control measurements during Atlas-powered flight were taken from the Centaur rate gyros. Since the Centaur autopilot is not activated for control purpose until sustainer engine cutoff (SECO), the flight control measurements are monitored for correlation with the Atlas flight-control data and to supply supporting data during the booster phases of flight.

At lift-off the Centaur rate gyros indicated the usual clockwise roll transient at a frequency of 3.5 cps and a maximum rate of 1.2 degrees per second just prior to Atlas autopilot activation at 42-inch motion. Following lift-off, the axial accelerometer indicated longitudinal oscillations at a frequency of 6 cps reaching a maximum of 1.2 g's peak to peak at T + 0.5 second. The oscillations decayed to negligible levels by T + 15 seconds. All past Atlas-Centaur vehicles have shown similar oscillations (refs. 7 and 12).

Integration of the roll-rate gyro verified satisfactory accomplishment of the Atlas roll program, indicating a clockwise roll maneuver of 20.1 degrees, at an average rate of 1.55 degrees per second. The desired launch azimuth was 94.539 degrees, and the pad heading of 115 degrees resulted in a desired roll program of 20.46 degrees.

Low-order rigid-body and propellant slosh oscillations were observed throughout booster and sustainer flight. A comparison of analytical and flight telemetered data is shown in figure XI-1. Good correlation is evident indicating present methods of analysis in determining flight frequencies are acceptable.

The diverging oscillations in the pitch plane at the frequency of the Atlas LO₂ sloshing mode observed on AC-4 and to a lesser extent on AC-3 prior to booster engine cutoff (BECO) appear to have been stabilized on AC-6. Although the oscillations are evident prior to BECO, they approach a limit cycle with amplitudes reaching peak to peak rates of 0.12 degree per second as measured by the Centaur pitch-rate gyro.

Rates imparted to the vehicle during insulation-panel jettison were 1.96 degrees per second peak to peak in roll and less than 0.2 degree per second peak to peak in pitch and yaw. Telemetry received at the insulation-panel-jettison event indicated a roll transient of a higher magnitude than the roll





transients seen on AC-3 or AC-4. Figure XI-2 pitch- and yaw-rate gyro data showed little activity during the event other than high-frequency vibration at approximately 25 cps, which corresponds to the frequency of the third bending mode.

The area of interest, however, is the response that occurred in roll. By differentiating the roll-rate-gyro output, calculating resultant roll torques, and subtracting the torques due to vernier engine deflections, the net external torque on the vehicle can be calculated. The results are shown in figure XI-3.

The net torques on the vehicle were substantial in magnitude and changing in direction. A torque as shown in figure XI-3 is difficult to conceive since insulation-panel-hinge reactions are the only source of external forces on the vehicle. The hinges are mounted in such a manner as to cancel torques due to reactions normal to a line passing through the hinge points. No satisfactory explanation is known as to the source of the observed torques.

Rates due to nose-fairing-jettison were 0.64 degree per second peak to peak in pitch and less than 0.2 degree per second peak to peak in yaw and roll. During both insulation-panel and nose-fairing-jettison events, rates were reduced to less than 0.2 degree per second peak to peak within 1.5 seconds.

Sustainer engine cutoff was commanded at T + 234.3 seconds. Residual vehicle rates due to sustainer and vernier engine cutoff (SECO/VECO) were 0.2 degree per second in pitch and essentially zero in yaw and roll, at a point just prior to vehicle separation. These rates compared similarly with those observed during the AC-4 flight. Atlas-Centaur separation was commanded at T + 236.3 seconds following firing of the shaped charge, cutting the interstage adapter at T + 236.2 seconds. By T + 237.8 seconds, the previously mentioned residual vehicle rates had increased to 0.54 degree per second in pitch, 0.17 degree per second in yaw, and -0.16 degree per second in roll, indicating small external torques acting on the Centaur vehicle. These were probably the result of Atlas retrorocket gas impingement on the Centaur vehicle and also small torques due to the Centaur boost-pump exhaust gases (started at T + 203.8 sec).

CENTAUR

Main engine prestart was commanded at T + 237.8 seconds. The hydraulic circulating pumps were energized at T + 234.8 seconds (SECO + 0.5 sec). Main engines were then gimbaled toward a null position at an average rate of 0.6 degree per second. The engines, however, are enabled to respond to vehicle rates and approach gimbal positions in an attempt to reduce the vehicle rates, although engine thrusts are not yet available. Engine positions just prior to MES were C-1 pitch, 0.64 degree; C-2 pitch, 0.51 degree; C-1 yaw, -1.02 degrees; and C-2 yaw, -0.04 degree.

The AC-6 vehicle start transients were mild compared with AC-2 and comparable in magnitude to AC-4. Rates imparted to the vehicle due to the main engine ignition transients were -1.35 degrees per second in pitch, 0.11

142



degree per second in yaw, and 3.26 degrees per second in roll. These rates were primarily the result of engine differential thrust buildup, relative engine positions, and the residual vehicle rates. Corresponding maximum engine deflections due to these rates were C-1 pitch, 0.38 degree; C-2 pitch, 0.38 degree; C-1 yaw, 0.83 degree (peak to peak); and C-2 yaw, 0.45 degree (peak to peak).

At a point just prior to enabling the guidance steering signals (MES + 4 sec) vehicle rates had been reduced to 0.54 degree per second in pitch, -0.04 degree per second in yaw, and 0.7 degree per second in roll. Engine positions at this time were essentially at null.

The guidance steering commands were enabled at T + 246.8 seconds (MES + 4 sec). The guidance resolver chain outputs indicated errors of 5 degrees (nose up) in pitch and 3 degrees (nose right) in yaw. These errors had been accumulated during the separation and MES flight phases. Vehicle rates due to steering enable were -1.81 degrees per second in pitch and -1.40 degrees per second in yaw. Corresponding engine deflections were C-1 pitch, 0.64 degree; C-2 pitch, -0.64 degree; C-1 yaw, -0.64 degree; and C-2 yaw, -0.51 degree. This error was nulled in approximately 3 seconds.

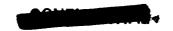
Following the settling out of the MES and steering enable transients, the engines indicated trim positions of C-l pitch, 0.014 degree; C-2 pitch, 0.17 degree; C-l yaw, 0.01 degree; and C-2 yaw, -0.09 degree. At MES + 220 seconds, trim positions were C-l pitch, 0.13 degree; C-2 pitch, 0.11 degree; C-l yaw, -0.25 degree; and C-2 yaw, -0.12 degree. Low-level engine-limit cycling in the pitch and yaw planes was also observed during this period at a frequency of approximately 0.25 cps (rigid body) and peak-to-peak amplitudes of 0.12 degree.

Low-order slosh and rigid-body oscillations were observed throughout the powered phase at peak-to-peak amplitudes (average) of 0.2 degree per second. Frequency components agreed with the predicted engine-limit cycle frequencies as shown in figure XI-1.

CENTAUR COAST PHASE

At T + 747.8 seconds, spacecraft separation was commanded. A complete discussion of separation dynamics is presented in section X, <u>VEHICLE DYNAMICS</u>. Approximately 9 seconds prior to the separation sequence, vehicle rates were below the rated control engine switching thresholds, and no engines were commanded on during this time. The following table shows the residual rates of the Centaur vehicle just prior to separation, the rates imparted the Centaur vehicle after separation, and the differential change:

Plane of motion	T + 747.8 sec, deg/sec	T + 748.1 sec, deg/sec	Differential postseparation, deg/sec
Pitch	-0.12	-0.11	0.01
Yaw	.19	.14	05
Roll	.04	.03	01



CENTAUR RETROMANEUVER

Centaur turnaround was commanded at T + 752.8 seconds as indicated by both attitude engine commands and rate-gyro data. At the initiation of turnaround, the guidance resolver-chain outputs indicated that the vehicle was approximately 18 degrees nose down and 12 degrees nose right with respect to the guidance steering vector generated at MECO. In response to the turnaround command, the vehicle reached maximum rates of 1.48 degrees per second in pitch and 1.45 degrees per second in yaw. Vehicle roll rates were maintained within the control thresholds. At T + 845 seconds, vehicle steering completed the turnaround maneuver approximately 15 seconds before the start of blowdown.

The blowdown maneuver was commanded at T + 872.8 seconds and enabled oxygen to be vented through the main engine and hydrogen through the chilldown valves, to produce thrust of sufficient magnitude in order to alter the orbital path of the expended Centaur stage. Coincident with the blowdown command, the hydraulic recirculating pumps were started to aline the thrust vector as commanded by attitude and rate errors. This was done in order to minimize blowdown torques and maximize the effect of the small axial thrust. Comparison of the Surveyor and Centaur orbital data indicates the separation distance was 1300 to 1600 kilometers 5 hours after separation.

Torquing moments were generally about the yaw and roll axes and were well within the capability of the attitude control system. During the first 100 seconds of blowdown, torquing moments were at their greatest, resulting in maximum duty cycles of approximately 65 percent. This duty cycle, however, was not maintained for long periods, and the average duty cycle was of the order of 10 percent. Duty cycles decreased with time thereafter as a result of tank pressure decay and subsequently lower torques.

Attitude control engine firings are plotted in figure VI-22, which show the attitude engine activity from MECO through the blowdown maneuver.



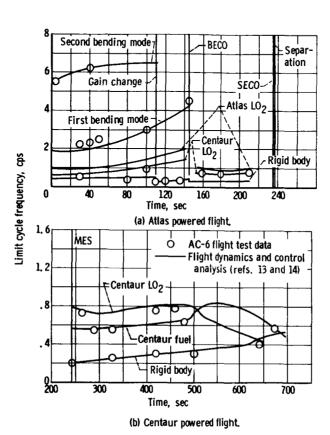
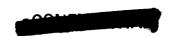
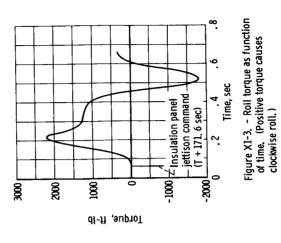


Figure XI-1. - Comparison of experimental and analytical frequencies.





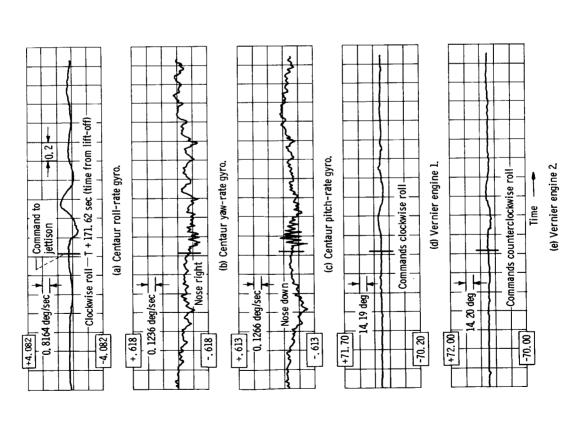


Figure XI-2. - AC-6 flight response at insulation-panel jettison.



XII. GUIDANCE

The Centaur guidance system flown on the AC-6 vehicle exhibited nominal performance throughout the flight. Velocity errors at $T_{\rm C}$ + 689 seconds were as follows: $\delta V_{\rm U}$ = -0.4 foot per second, $\delta V_{\rm V}$ = -0.4 foot per second, and $\delta V_{\rm W}$ = 0.2 foot per second. One of the prime objectives of this flight was to demonstrate the capability of the inertial guidance system to inject the SD-2 Surveyor spacecraft on a lunar intercept trajectory. The maximum allowable spacecraft midcourse correction for miss only is 50 meters per second. Tracking data indicated a midcourse correction of 4.25 meters per second for the AC-6 flight.

The system was calibrated on F - O day, and the Day 2 Plan I "J" values (launch-on-time constants, ref. 15) were loaded into the airborne computer. After completion of calibration, the system was optically alined to an azimuth of 115 degrees from north. The system was advanced to the inertial mode 8.97 seconds prior to lift-off.

The computed steering vector successfully guided the vehicle during the sustainer and Centaur powered phases and provided a retrovector to which the vehicle was steered during retromaneuver and blowdown. The airborne computer generated booster cutoff, sustainer cutoff backup, and main engine cutoff discretes, as planned, with the significant times shown in the following table:

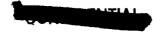
Function	Time, sec	Data source (ref. 5)	
BECO	141.800	TLM CI21X	
SECO backup	236.573	TLM CI22X	
MECO	679.08	TIM CI19X	

Table XII-I is a summary of the 21 digital words that were telemetered during each computer cycle by the digital data link.

A discussion of system performance is presented in the following sections. The times preceded by the symbol T are referenced to 2-inch motion, and those preceded by $T_{\rm C}$ are referenced to computer zero time. Figure XII-l is a functional schematic drawing of the guidance system.

GIMBAL SERVOSIGNALS

Telemetry measurements of the gimbal torque motor input voltages and the 7.2-kilocycle demodulator outputs indicate that the platform remained stable throughout the flight. The maximum gimbal servoloop errors are shown in table XII-II. Gimbal 1, 2, and 3 demodulator error voltages indicate equivalent gyro





error angles well within the 60 arc-seconds of required dynamic accuracy. Gimbal 4 demodulator error does not represent an inertial misalinement but rather the gimbal 2 resolver error.

At T + 2.3 seconds, gimbal 2 reflected the start of the roll program and at T + 15.3 seconds, gimbal 3 responded to the initiation of the Atlas pitch program. At T + 43.6 seconds, gimbal 4 uncaged at a pitch angle of 160 (fig. XII-2(a)), as computed from the nominal Atlas pitch profile. During the Atlas powered phase of flight, gimbals 1 and 2 oscillated at approximately 1 cps, which is indicative of propellant sloshing. From T + 50 seconds until BECO, low-frequency oscillations from 0.25 to 0.33 cps observed on gimbal 1 were attributed to rigid body dynamics. During the Centaur phase of flight, oscillations of approximately 0.2 cps, which are characteristics of rigid body dynamics, were observed on gimbal 1. Propellant sloshing caused oscillations of 0.5 to 0.75 cps to appear on gimbal 2 during Centaur phase. At T + 496 seconds, the pitch gimbal voltage reflected a computer steering command for perigee correction. At T + 753 seconds, gimbals 1 and 3 responded to the beginning of retromaneuver and indicated satisfactory performance throughout the vehicle Telemetered analog signals of gimbal 3 torque motor input and demodulator output show the occurrence of both the perigee correction and the beginning of retromaneuver (figs. XII-2(b) and (c)).

TORQUING LOOPS

The digital and analog torquing signals indicated that the guidance system went into the flight mode 7.8 seconds prior to lift-off. Analog signals revealed two unexplained shifts in the W-torquing loop. The first shift occurred at T - 0 and was equivalent to a 0.45 degree per hour change in the W-torquing rate. The second occurrence was at T + 204 seconds (same time as nose-fairing jettison) and was equivalent to a torquing change of 0.30 degree per hour. An equivalent change in torquing at the time of nose-fairing jettison occurred during the flight of the AC-4 vehicle. The digital torquing output did not give any indication of the two changes in W-torquing. The digital and analog data were reduced to the same units, "differenced," and the results are plotted in figure XII-3. The bias in the differences is a result of signal conditioner null offset, and figure XII-3(c) clearly indicates the two shifts previously discussed.

ACCELEROMETER LOOPS

Oscillograph recordings of the 14.4-kilocycle demodulator output voltages are shown in figure XII-4. These measurements indicate satisfactory performance of the accelerometer loops throughout the flight. Prior to T - O and U- and V-demodulator outputs showed a saw-toothed oscillation with a frequency from 0.17 to 0.25 cps. Similar cycling occurred in all three loops during the coast phase of flight. This is normal operation of the accelerometer loops when the inertial components are sensing zero gravity. The following table lists the largest pendulum offsets observed during flight:



LOONEIDENTIAL

Event	Accelerometer direction									
	A_{u}	-A _u	A_{V}	-A _V	$A_{\overline{W}}$	-A _w				
	Maximum pendulum excursion, arc-sec									
Lift-off Mach 1 BECO Booster jettison Insulation-panel jettison Nose-fairing jettison SECO Atlas-Centaur separation MES	30 27 18 14 28 30 20 20	38 22 12 20 36 37 22 40	20 8 8 12 16 6 8	7 12 8 16 8 16 14 8	24 18 15 15 20 36 12 8	36 16 8 12 24 50 8 8				

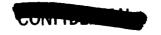
The demodulator outputs indicated small error voltages throughout powered flight with maximums occurring at the time of maximum shocks. At T+742 seconds, the U and W demodulator outputs were no longer monitored. The two available channels allowed more spacecraft measurements to be telemetered. A histogram of the incremental velocity pulses (ΔV 's) required to rebalance the pendulous accelerometers indicates that there were no large limit cycles or bursting of the loops.

STEERING LOOPS

The guidance steering loop performed exceptionally well throughout the flight. During the boost phase, the computer outputs were zero, and the X- and Y-resolver-chain outputs were maintained at null. Steering was enabled by the flight control system at T + 148 seconds, at which time the X- and Y-resolver-chain outputs moved off null indicating that the computer was compensating for trajectory errors built up during boost phase (fig. XII-5). Guidance steering was closed loop during sustainer and Centaur powered phases of flight. The steering vector was locked out by the flight control system at SECO until MES + 4 seconds when the autopilot reinitiated acceptance of guidance steering commands. At T + 497 seconds, the Y-resolver-chain output reflected a computer command perigee correction in the pitch plane. After MECO had been generated, guidance steering was disabled until T + 706 seconds, at which time the steering vector was switched to the negative of the velocity vector to provide the retrovector to which the vehicle was steered after separation of the spacecraft (fig. XII-5).

FUNCTIONAL PERFORMANCE

The computer digital steering value minus the telemetered analog value as a function of time is shown in figure XII-6. Analysis indicates that the difference is a result of signal conditioner null offset. The computer-generated missile actual velocity is shown in figure XII-7, and the difference of nominal velocity from total velocity is shown in figure XII-8. The guidance computer correctly calculated the missile velocity, which was close to the nominal expected velocity as a function of time. Figure XII-9 shows plots of computer calculated position, and figure XII-10 shows the difference of the calculated posi-





tion from the nominal as a function of time. Figure XII-ll indicates that the platform skin temperature stayed within the 50° to 120° F specifications throughout the flight. It is also apparent that the inertial component temperatures were within their control bands.



Discrete words length (W.T.) ^a	16	ω	Ø	Ø	ω	۵	8	۵	æ	8	8	80	80	80	80	80	æ	ω	80	8	ω	12	12	12	
Units	ft/sec	သ လ လ	ft	ff	ft	ft/sec	ft/sec	Ĥ	ft	သ မ င	none	ft	ft/sec	ft/sec	rad/sec	rad/sec	rad/sec	$(ft/sec^2)^2$	$(ft/sec)^2$	သဓဋ	ft/sec	 	1 1 1 1 1 1 1 1 1 1 1 1 1 1 1 1 1 1 1 1	1 1 1 1 1 1 1 1 1 1 1 1 1 1 1 1 1 1 1 1	
Function	Sigmator W-velocity	Time	Signator V-position	Signator W-position	Signator U-position	Sigmator U-velocity	Signator V-velocity	Total V-position	Total W-position	Guidance launch time into window (first cycle)		Total U-position	Total W-velocity	Total V-velocity	V-gyro torquing rate	U-gyro torquing rate	W-gyro torquing rate	Thrust acceleration squared; boost phase	Energy to be gained; sustainer-Centaur phase		Total U-velocity	U-steering vector	W-steering vector	V-steering vector	where one W.T. = 0.15625 msec.
Symbol	$V_{\Gamma W}$	ئړ. ژ	, h	row	ម	Vou	V	r	r mm	نوړ	Codeword	rmu	VmW	Vmv	Omega $d_{\mathbf{V}}$	Omega പ്പ	Omega dw	28 24	, υ	Δt_{co}	Vmu	* [†]	*,≯	*,>	word time
Word	7	c ₃	23	4	വ	9	7	80	o.	10		77	12	13	14	15	16	17			18	19	82	12	aw.T.,

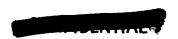
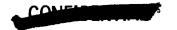


TABLE XII-II. - GIMBAL SERVOLOOP MAXIMUM ERRORS

Gimbal	Gimbal demod	ulator ma	ximum errors	Torquer motor maximum errors				
Signal conditioner output, V(dc)		Demodu- lator output, V(dc)	Displacement error, arc-sec	Signal conditioner output, V(dc)	Torque motor input, V(dc)			
1	0.40	5.00	7.2	-0.28	-2.80			
	25	-3.13	-4.5	.40	4.00			
2	.30	1.03	10.6	20	-2.00			
	18	62	-6.18	.15	1.50			
3	. 45	. 74	16.4	30	-3.00			
	20	33	-7.31	.34	3.40			
4	. 20 30	1		10 .20	-1.00 2.00			





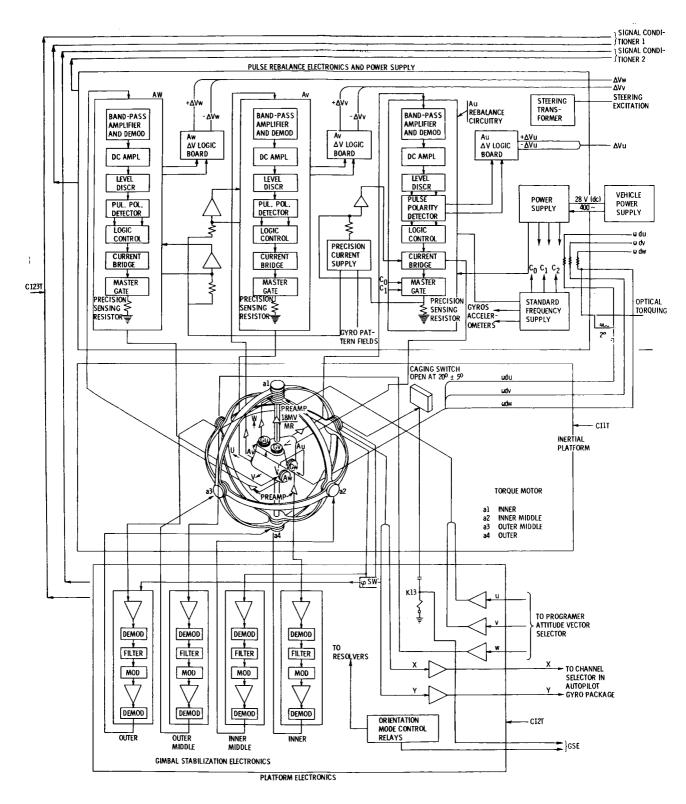
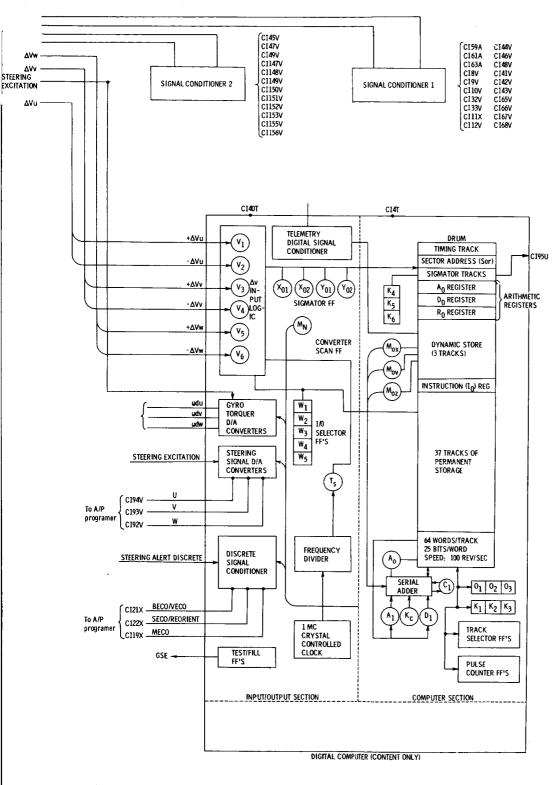


Figure XII-1. - Guidance system







simplified schematic drawing.





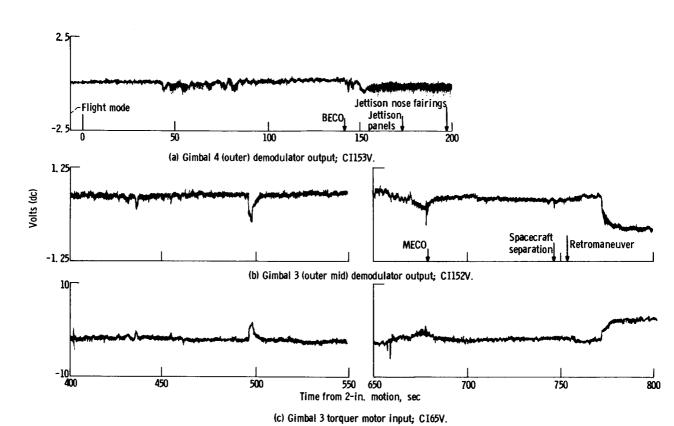
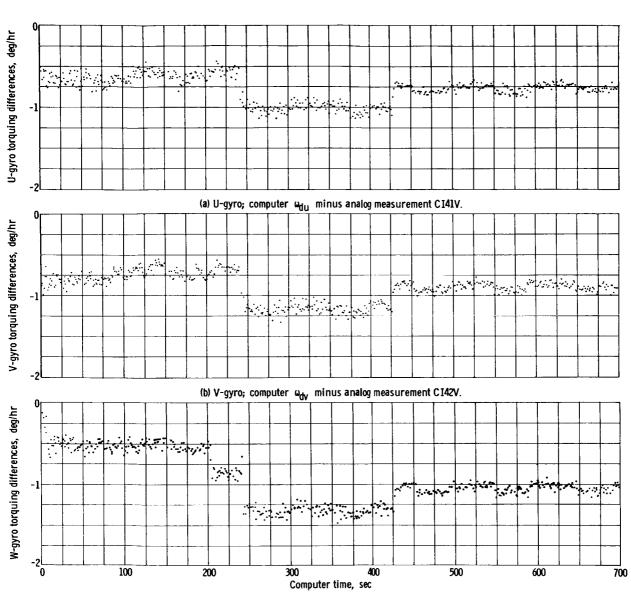


Figure XII-2. - Centaur guidance system telemetered data.

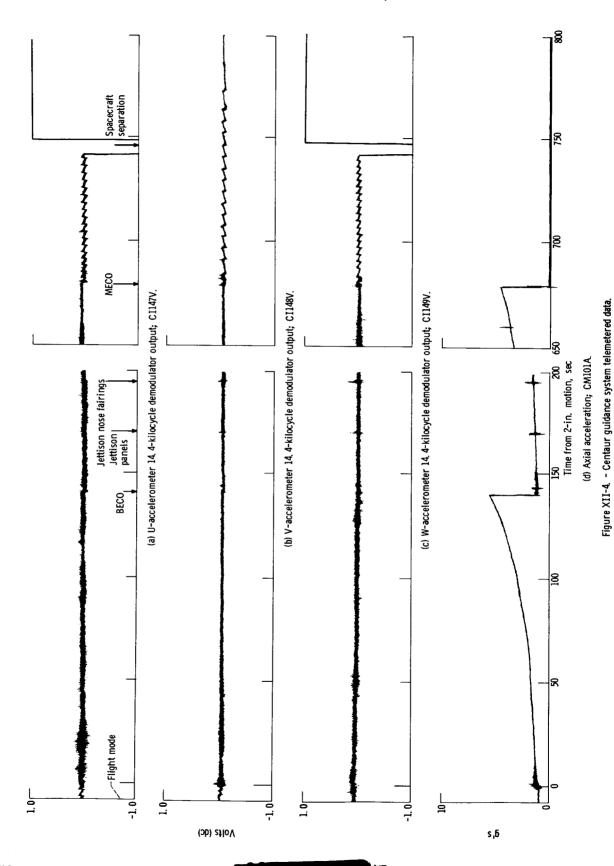




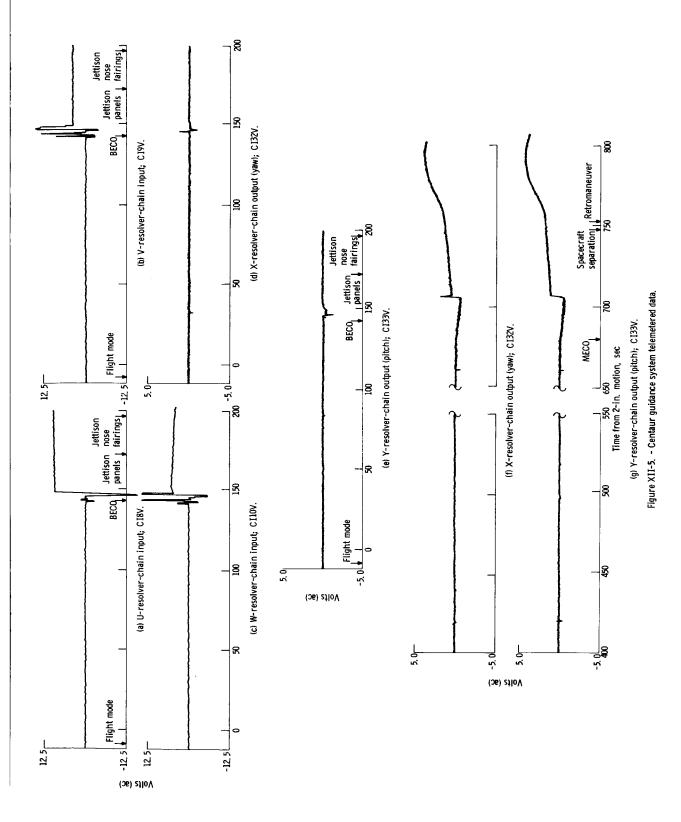
(c) W-gyro; computer $\omega_{\mbox{\scriptsize dW}}$ minus analog measurement CI42V.

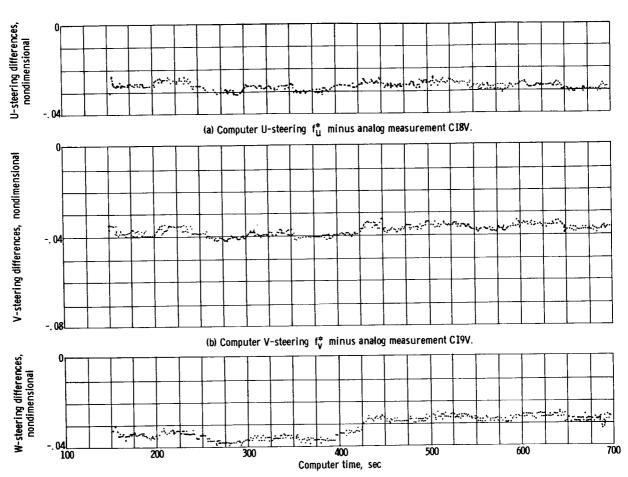
Figure XII-3. - Torquing differences.





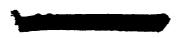






(c) Computer W-steering $\,f_{W}^{*}\,$ minus analog measurement CI10V.

Figure XII-6. - Steering differences.



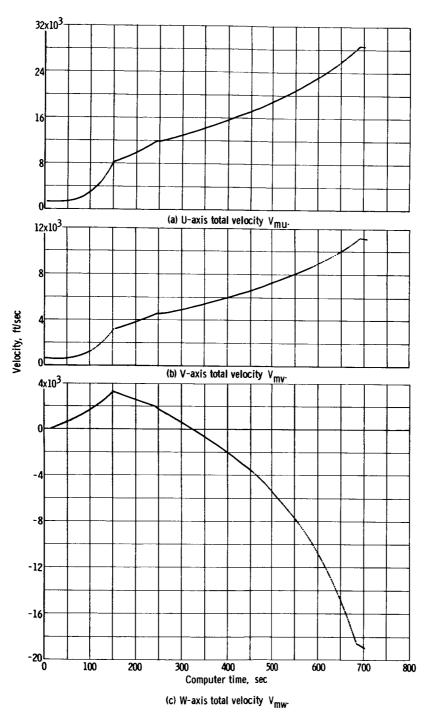
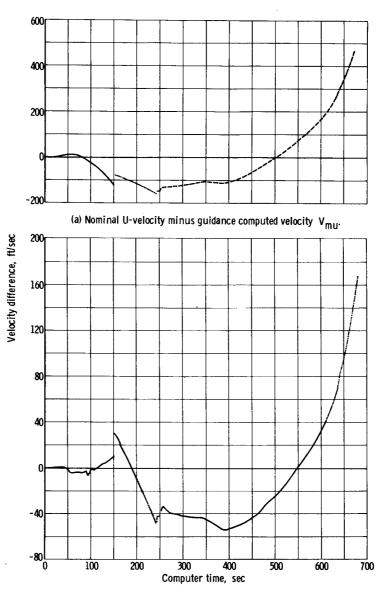


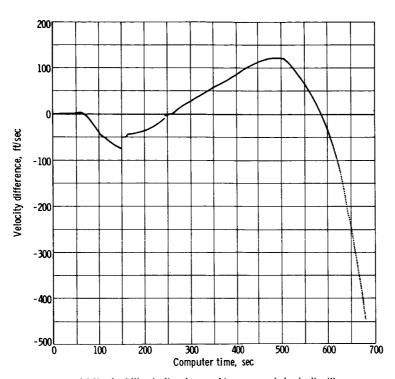
Figure XII-7. - Guidance computer total velocity.





(b) Nominal V-velocity minus guidance computed velocity $\, {
m V}_{mv} . \,$ Figure XII-8. - Total velocity differences.





(c) Nominal W-velocity minus guidance computed velocity $\,W_{mw}$. Figure XII-8. - Concluded.



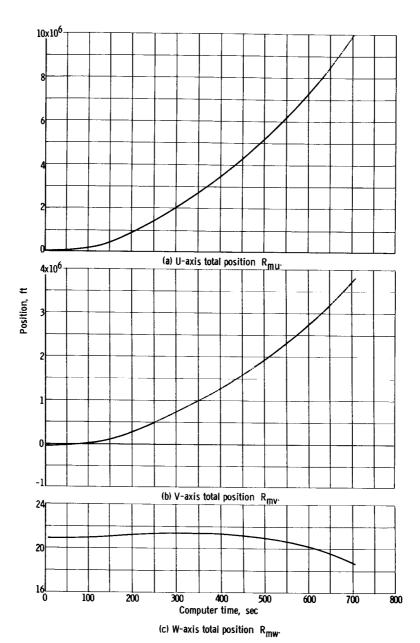
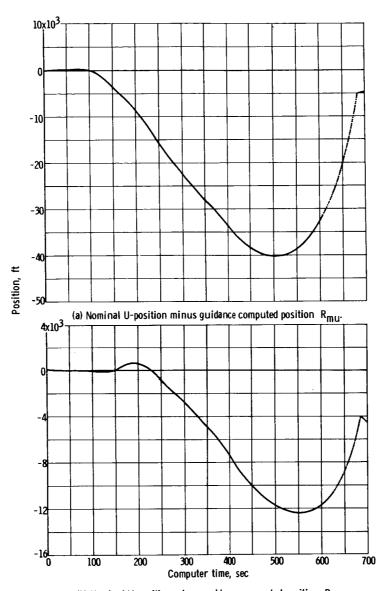


Figure XII-9. - Guidance computer total position.

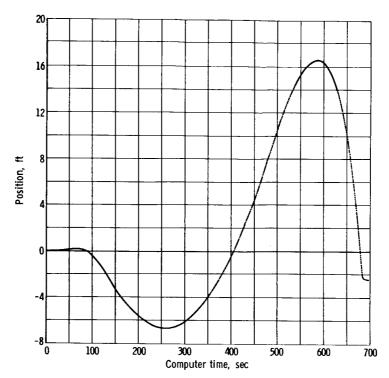




(b) Nominal V-position minus guidance computed position $\, R_{mv} . \,$ Figure XII-10. - Total position differences.







(c) Nominal W-position minus guidance computed position $R_{\mbox{\scriptsize mw}}$

Figure XII-10. - Concluded.

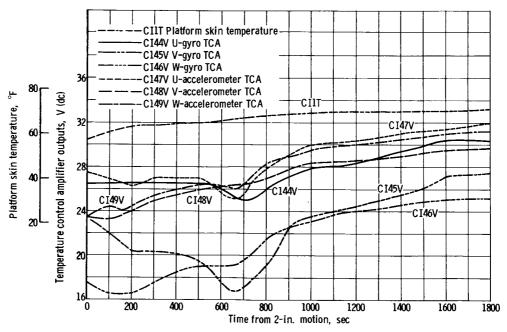


Figure XII-11. - Platform temperature history. Gyro and accelerometer temperature control amplifier outputs and platform skin temperature.





XIII. ATLAS-CENTAUR INSTRUMENTATION, RADIO FREQUENCY, AND ELECTRICAL SYSTEMS

SUMMARY

The Atlas-Centaur electrical system performed satisfactorily during ground operations, launch, and through all phases of programed flight. All electrical functions, voltage and current levels were within specifications. This was the first Centaur flight in which the new high-energy (1 amp - 1 W) squibs, that provided greater protection from stray currents and static discharges, were used exclusively. Squib simulators were used successfully during ground tests to provide assurance of adequate current flow to all pyrotechnics. Atlas-Centaur RF system performance was also satisfactory. Telemetry coverage was provided well beyond the end of retromaneuver. Main power cutoff was accomplished on schedule, and data quality was generally good. Approximately 98 percent of all instrumentation yielded valid data. Range Safety Command systems experienced no malfunctions during flight. The August 10, 1965 launch attempt, however, was scrubbed because of the failure to obtain a positive indication of an armed Centaur destruct system.

C-band tracking of the Centaur was adequate to provide acquisition of the spacecraft by the deep-space network, although it was intermittent. The JPL deep-space network acquired and tracked the SD-2 dynamic model S-band transponder as planned; signal strength from the spacecraft dropped off 2 hours sooner than the expected 20-hour minimum. Glotrac functioned normally and will permit a precision powered flight trajectory to be generated for the guidance component error analysis program.

Launch countdown logic and event times were modified from those at Complex 36A to improve probability of a successful launch. Upper umbilicals were ejected earlier in the countdown, while the time from engine start to vehicle release was reduced approximately 1/2 second to gain maximum thrust from the lower stage.

ELECTRICAL SYSTEM

Atlas

The major Atlas electrical system components were a manually activated main vehicle battery, two telemetry batteries, and a three-phase 400-cycle rotary inverter. The main battery bus voltage indicated near nominal voltage throughout powered flight. On transfer to internal power, the battery voltage dropped momentarily to 25.8 volts, recovering to 27.6 volts in approximately 200 milliseconds. A steady-state low of 27.3 volts was recorded at lift-off and reached a high of 27.8 volts at loss of signal.





The Atlas main power changeover switch satisfactorily transferred the launch vehicle load from external ground power to internal battery supply. Operation of the telemetry batteries was satisfactory, as verified by the performance of the telemetry system.

The Atlas vehicle utilizes a rotary inverter to deliver ac power at a nominal 115 volts, 400 cycles, three phase. The inverter operation was satisfactory with no recorded malfunction during flight. At launch, the voltage was 114.43 volts and the frequency was 402 cycles. Recorded data showed good recovery from load variations with the voltage varying from 114.33 to 114.72 volts during flight. The terminal value was 114.53 volts at T + 520 seconds when Atlas telemetry ended. The frequency varied from 402 to 402.7 cycles which maintained a differential frequency of two to three cycles with the Centaur 400-cycle inverter, required to avoid dangerous oscillations in the servo-amplifier electromechanical loop.

Centaur

The Centaur vehicle power requirements were adequately supplied by one 100-ampere-hour battery, two range safety batteries, two pyrotechnic batteries, and a 400-cycle static inverter. Three notable configuration changes were made to the Centaur electrical power system:

- (1) The main missile, telemetry, and tracking system power was supplied by a single 100-ampere-hour battery.
- (2) A battery preload was used to precondition the main battery prior to power changeover to internal.
- (3) The Range Safety Command system was supplied by two batteries of a new design.

The main battery voltage and current were near nominal throughout the flight. Vehicle system dc input (CE28V) indicated a level at lift-off of 27.8 volts. A low of 27.1 volts was recorded during main engine start sequence (maximum loading) and a high of 28.1 volts was reached during retromaneuver.

The 14-ampere preload of the main battery prior to changeover to internal power preconditioned the battery to accept Centaur load. Preconditioning of the battery minimized the voltage drop at changeover that could be detrimental to the user systems. The resulting battery voltage level dropped to approximately 26.5 volts on transfer (specification limit is 26 V minimum). The main missile battery current (CEIC) at lift-off was 56 amperes, reaching a high of 69 amperes at main engine start. Comparison of the profile for ground test battery load current with the flight recorded profile showed close correlation between sequential events (see fig. XIII-1). Several small spikes were noted on the current recording from T + 103 to T + 117 seconds, which were not identified with any specific event. The spikes appear to be valid data, although they could be attributed to spurious noise from a source as yet undetermined.

Transfer of the Centaur load was successfully accomplished by the main





power changeover switch in less than 250 milliseconds. No abnormal voltage or current transients occurred on transfer of load from external power source to internal battery supply.

On completion of the Centaur flight requirements at T + 1853.8 seconds the power changeover switch satisfactorily disconnected the main vehicle load from the battery while maintaining connection of the battery to the telemetry, C-band, and Azusa systems.

Satisfactory operation of the pyrotechnic batteries and relay system was verified by the successful jettison of the nose-fairing and insulation panels. The battery voltages were 35.0 volts at lift-off (minimum specification limit is 34.7 V).

Two new range safety system batteries, used for the first time, performed satisfactorily as verified by the range safety command receiver operation. The batteries were specially designed to provide the proper voltage level for receiver operation and vehicle destruct capability. The battery voltages at lift-off were 32.3 and 32.5 with receivers in operation (minimum specification limit is 30 V).

The staging disconnect functioned normally at T + 234.9 seconds after withstanding the shock produced by the jettison of the insulation panels. The actuator temperature was 72° F at lift-off (minimum value is 60° F).

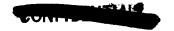
The Centaur static inverter functioned normally and within specifications delivering three-phase 400-cycle power to the autopilot, guidance, and propellant-utilization systems. The inverter also supplied reference frequency to telemetry and gyros. The addition of the PU system on AC-6 caused a slightly leading power factor which accounts for the somewhat higher ac voltage. The voltages remained fairly constant throughout flight and were 116.3 to 116.5 volts for phase A, 115.5 to 115.7 volts for phase B, and 114.6 to 114.8 volts for phase C.

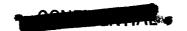
Since the inverter frequency was crystal controlled and was independent of load conditions, the frequency remained at 400.00 cycles throughout the flight. The ambient air temperature of the inverter at launch was 68° F and the inverter skin temperature was 87.5° F rising to a maximum of 183° F at termination of the programed flight. In figure XIII-2, it can be seen that the inverter immediately started to cool down and fell to 137° F at T + 3600 seconds when telemetry was lost.

INSTRUMENTATION SYSTEM

There were 442 measurements telemetered on AC-6, of which 267 were Centaur measurements, 150 were booster measurements, and 25 were payload measurements. The number of measurements by vehicle system is shown in table XIII-I. Three measurements were deleted prior to launch as a result of malfunction:

(1) C-1 engine pump LH2 inlet temperatures (CP6OT)





- (2) LH2 tank stem temperature (CP127T)
- (3) Helium-purge-bottle discharge pressure (CP1146P)

The two temperature transducers were damaged during installation and were not easily accessible for repair or replacement during the countdown. The third measurement was deleted as a result of a transducer failure.

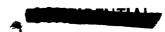
The following measurement anomalies were noted during the AC-6 flight:

- (1) The high rate LH₂ vent dynamic pressure (CF190P) was consistently low during GH₂ venting and actually went negative during the early portion of flight. The cause of failure has not been determined; however, a more reliable transducer will be installed in an environmentally improved location on future vehicles.
- (2) The low rate LH_2 vent dynamic pressure (CF191P) data was questionable. This transducer will also be relocated.
- (3) The nose-cap surface-temperature (CA80T and CA958T) readings were erratic; at approximately T+130 seconds, these readings increased abruptly and reached about twice the expected value. This failure has been attributed to improper installation.
- (4) The LH_2 duct vibration (CA6010) operation was intermittent throughout the flight. A similar failure in this mode was caused by a defective coaxial cable. A new design has been initiated for a more reliable cable; however, the availability and implication have not been established.
- (5) The spacecraft compartment A accelerometer (CY580) oscillated from band edge to band edge 0.7 second after nose-fairing jettison for no apparent reason.
- (6) The interstage adapter panel radial vibration (AAl640) exhibited no useful data during flight. No resolution of this problem has been made.

TELEMETRY

The AC-6 telemetry system consisted of six RF links. Two of these links were on the Atlas booster. Atlas RF 1 transmitted booster operational measurements at 229.9 megacycles. Atlas RF 2 was used primarily for interstage adapter R&D measurements and operated at 232.4 megacycles. The Atlas transmitters radiated through a ring-coupler from two antennas, one on each Atlas pod.

The four telemetry links on the Centaur vehicle were coupled to a single antenna mounted on a ground plane located on the umbilical island. Signals were radiated through the nose fairing until nose-fairing jettison at T + 196.6 seconds. Centaur operational measurements were telemetered on SS 1, and Centaur R&D measurements were telemetered on SS 2. These two subsystems were located in the forward equipment area on the Centaur vehicle. Subsystems 3 and 4 were located in the retromotor simulator portion of the Surveyor dynamic model and





transmitted payload environmental information until spacecraft electrical disconnect, which occurred at T+740 seconds. Subsystems 1 and 2 functioned until loss of signal at T+6950 seconds. Telemetry transmitter frequency and nominal power were as follows:

Telemetry link	Frequency, Mc	Nominal power, W				
Atlas RF: 1 2 Centaur SS: 1 2 3 4	229.9 232.4 225.7 235.0 243.8 251.5	10 4 4 4 4 4				

Six measurements of telemetry parameters were made on AC-6. These were skin temperature measurements of SS 1 to 4 and thermocouple reference junction temperatures on the Atlas and Centaur. All measurements were as expected with the exception of telemetry SS 1 skin temperature (CT94T). This measurement went off scale (low) indicating a temperature less than 0° F shortly after the start of tanking. This low temperature was probably caused by the leakage of helium through the forward insulation-panel seal. The temperature remained off scale (low) until approximately T + 8 minutes. At that time, the measurement came on scale, and the temperature increased slowly to 24° F at T + 17 minutes. No data loss or anomalies resulted from this low temperature. Summary of the AC-6 telemetry coverage from time of lift-off to loss of signal at Pretoria is given in figures XIII-3 and 4.

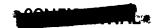
Analysis of the signal strength records indicated that the performance of all the telemetry links was satisfactory throughout the flight. The only dropout of telemetry data was experienced by the TEL II ground station at booster engine jettison (T + 145 sec) for a period of 0.2 second. This dropout had occurred on previous vehicles also and may have been caused by flame attenuation (fig. XIII-5). At this time, flame attenuation is more prevalent because of the backscattering effect of the sustainer engine's flame impinging on the booster section as it is jettisoned. However, because of a different look angle, the telemetry data that is recorded from Grand Bahama Island at this same time does not have any dropout (fig. XIII-6).

RANGE SAFETY SYSTEM

A lightweight Range Safety Command system for the second stage (Centaur) and spacecraft (Surveyor) was flown on AC-6 for the first time. A block diagram of the system is shown in figure XIII-7. The functions of the system are to

(1) Cut off the Centaur main engines to an RF command, resulting in zero thrust





- (2) Destroy the LH₂ and LO₂ tank structure, in response to an RF command to disperse the propellants
- (3) Destroy the Surveyor engine, in response to an RF command, by causing a conical-shaped explosive charge to detonate and bore a hole through the engine housing, penetrate the propellant, and emerge through the opposite side (the shaped charge was inert for AC-6)
- (4) Cause the actions in (2) and (3) on detection of premature separation of the Surveyor from Centaur (disarmed for AC-6)

The first-stage (Atlas) Range Safety Command system was the same for AC-6 as on previous Atlas-Centaur flights. Both systems performed properly except for the failure to obtain an armed destructor command during the August 10 attempted launch countdown. The launch was scrubbed at approximately T - 2 minutes as a result of a failure of the Centaur destructor to respond properly to the "ARM" command. The failure was subsequently determined to be due to inadequate design of the frost plug. It is inserted after removal of the safe-lock plug which mechanically prevents arming of the destructor. The design of this plug is such that it can be inserted improperly with resultant distortion of the plug that interferes with the arming of the destructor.

On August 11, 1965, after suitable replacement of the frost plug, the "ARM" function worked properly, and launch was successfully accomplished. Both Atlas and Centaur RSC systems performed satisfactorily throughout the flight. Signal strength was adequate to transmit commands to both the Atlas and Centaur RSC systems. The minimum gain margin for the Atlas system was 55 decibels, while the gains for the upper stage were 20 and 18 decibels, respectively, for receivers 1 and 2. The only command to the system was sent from the Antigua (station 91) transmitter shortly after main engine cutoff to disable the range safety system. Figure XIII-8 shows the operation of the various ground transmitters in supporting AC-6 range safety.

TRACKING SYSTEMS

C-Band

The Centaur stage C-band radar transponder and the pair of antennas under the insulation panels used in conjunction with ETR and Bermuda ground radar stations provided adequate tracking of the Centaur vehicle through the powered-flight phase. Real time computation of the Antigua and Twin Falls (ship) C-band tracking data after MECO enabled an early orbit to be determined. Look angles were transmitted to the DSIF station at Johannesberg permitting early acquisition of the S-band transponder in the dynamic model. C-band operation was satisfactory for the first 500 seconds of flight. Stations tracking later portions of the flight experienced tracking difficulty. The C-band radar coverage is shown in figure XIII-9. Extracts from the station logs follow:

Station 1. Cape Kennedy. - Beacon performance was satisfactory. All commitments were met. At loss of signal, the frequency deviation was 3 megacycles (see fig. XIII-9).

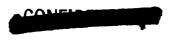


- Station 19. Merritt Island. The average signal strength was 45 decibels above the receiver threshold. Slight deterioration of the beacon return was noted from T + 90 to T + 100 seconds. At T + 500 seconds, the beacon return deteriorated both in amplitude and pulse width until the end of tracking.
- Station 3. Grand Bahama Island. FPS-16 lost tracking from T + 266 to T + 283 seconds, and the FPS-18 lost tracking from T + 412 to T + 447 seconds. Other stations operating showed no anomalies so these losses may be attributed to station problems or poor look angles. Final loss of signal occurred at T + 543 seconds, and at this time, the frequency deviation was down 7 to 9 megacycles.
- Station 7. Grand Turk Island. The beacon shifted in frequency and dropped 15 to 20 decibels in signal strength at approximately T + 435 seconds. The pulse was extremely narrow and the loss of signal frequency deviation was -6 megacycles.
- Station 9. Antigua Island. Shortly after 500 seconds, the signal dropped to approximately 15 decibels. A weak signal was confirmed by Grand Turk, and tracking was maintained to the horizon. The final beacon frequency reading was off -3 megacycles.
- Station 86. Twin Falls Ship. Tracking was complicated by locally generated noise interference.
- Station 12. Ascension Island. Lock-on was late as a result of computer program input and the beacon frequency shift.
- Station 13. Pretoria. This station reported negative tracking. The beacon transmitter frequency shift could have exceeded the radar receiver local oscillator tuning range of ±13 megacycles.

Indications are that the C-band transponder experienced the following symptoms:

- (1) Width and amplitude deterioration of the return pulse
- (2) Frequency deviation that may have gone out of specification

A magnetron failure within the transponder will produce frequency and pulse behavior identical to that recorded for AC-6. Conditions necessary include pulling, pushing, temperature change, or movement of the tuning mechanism which will produce a frequency shift. Temperature is discounted based on the telemetry data of the transponder skin temperature indicating normally (~36° F at T - 0, rising to ~65° F at T + 75 min). Pulling may be caused by either a change of VSWR and/or cable losses, while pushing may be caused by a power supply change. Analysis of this anomaly has been made with design engineering testing. The probable cause of failure was loss of internal cannister pressure through one of the seals. Future preflight checkout shall include more extensive testing of the electrical and mechanical aspects of the unit.



Glotrac

A Centaur stage Azusa type-C transponder and antenna system in conjunction with Glotrac segment 1 enabled powered flight position and velocity data to be determined with precision through the measurement of Doppler shift at three or more widely separated ground stations. Glotrac station coverage is shown in figure XIII-10. Handover at 400 seconds from the MARK II transmitter at the Cape to the Bermuda transmitter was satisfactorily accomplished within 4 seconds.

The Azusa interstage adapter antenna is used to provide coverage through the early flight phase when insulation panels cover the Centaur mounted antenna. At nose-fairing jettison (T + 197 sec) the dc power to the coaxial switch circuit is interrupted causing the switch to connect the Centaur mounted antenna to the transponder.

S-Band

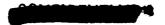
The SD-2 dynamic model contained an S-band transponder assembly and an omnidirectional antenna mounted on top of the forward mast. The transponder operated on low-power (100 mW) mode until approximately 11 seconds prior to space-craft separation, at which time the Centaur programer initiated a switchover command to the high-power (10 W) mode. The spacecraft was acquired by the Johannesberg DSIF approximately 20 minutes after injection, and two-way lock was obtained. Deep-space tracking of the spacecraft by Johannesberg, Goldstone, and Canberra continued for approximately 18 hours, at which time there was a marked dropoff in transponder power due to battery depletion. The precision deep-space tracking of the spacecraft after separation enabled an overall guidance system evaluation to be made. Tracking data indicated that the injection accuracy was excellent and that the spacecraft was well within the midcourse correction capability allowables. See section VI for discussion of trajectory (also ref. 17).

ELECTRICAL GSE

A modification to the ETR 36B GSE facilities provided the capability to monitor and record 23 channels of voltage and current data for the Atlas and Centaur electrical systems continuously through the preflight, countdown, and postflight operations.

A dual industrial power source was provided to the complex by completing an alternate route with capability for remote manual switchover in the event of an outage. The critical power shortage was relieved by requesting priority beforehand via an "express" bus which essentially provides preferential service similar to the service afforded manned launch complexes at ETR. This was provided to minimize outage possibilities such as occurred on previous Centaur countdowns.

No major electrical GSE anomalies occurred during either the aborted launch attempt of August 10 or the successful launch of August 11. Several minor GSE





problems were experienced during major preflight testing. A brief outline of these significant incidents appears in section III, PRELAUNCH HISTORY, and is discussed in greater detail, with corrective actions taken, in the analysis and evaluation of the corresponding system.

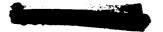
There were two significant problems observed in the electrical GSE both involving the dc power supplies:

- (1) The 7-volt dc battery simulator supply to the Atlas vehicle exhibited an unstable voltage characteristic during the composite readiness test and necessitated replacement by a flight-type battery in order to complete the test. This same problem had occurred in an earlier test. The power supply was subsequently returned to the vendor.
- (2) It was noted that a potential difference exists between the ground returns of the 28-volt dc power supplies in the transfer room and the blockhouse as well as with the battery simulator supply in the gantry. This potential difference is manifested by changes in landline calibrations and becomes evident at power transfer to the battery simulator supply, or when either the blockhouse or transfer room supplies are cut off. This is a condition that is prevalent at all Atlas launch complexes but which can be improved considerably by extensive modification to a single-point grounding system.

Corrective action is now in process to rectify two other anomalies in the GSE:

- (1) Cooling air to the propellant level control unit chassis was inadequate resulting in improper operation of the tanking system. A supplementary source of cooling air effected a temporary fix to permit completion of tanking tests and launch preparations for the AC-6 flight.
- (2) Unreliable operation of the vehicle optical alignment door and lack of position monitoring made it necessary to monitor the door position visually during launch preparations.

A listing of significant events and the time at which they occurred is shown in table XIII-II.



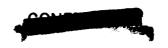


TABLE XIII-I. - AC-6 MEASUREMENT SUMMARY

	Total		67	no a	186	d L w		150		91	7 8 1	482	4 4 2 4	9 /	1	2	292
	Digital		1 1	111	11	111	;;	: ;		11		¦ =	11	1 1		;	1
	Acous- tic		11	111	11	111	11	: :		11		! !	11	; ;	! ~	1	O.
	Discrete position		41		1 00 1	-	11	21		L 13	10		14 28	0	: !	-	52
	Volt- age		10	۱۱ ۵	11	-	11	; 5		10	4 1	- 58	۱∞	۱ ۵	11	:	44
	Temp- era- ture		40	^{(N}	0		1 1	45		63	Hб	ณ ๛	120	9 7	- 9		108
type	Strain		21	111	; ;	111	11	: ដ		20	: :	::	::	: :	ļH	!	21
Measurement type	Rate		; ;		"	o	11	! 8		11	; ;	;;	1 1	; ;	1 1	!	;
Measur	Fre- quency	3.8	11	٠;;	11			;		::	٦l	1 1	11	! !	11	-	1
	Pres- sure	Atlas	6	1 ~ 9	202	! ! ^Q	: :	- 44	Centaur	9 ;	7	۱ ۵	15			:	28
	Vibra- tion		4 -	111	11	111	11	1 4		۲:	1 1	1 1	!!	1 1	101	:	11
	Power		11	111	11	111	: :	: :		1:	1 1	1 1		1 !	۲ :	1	1
	Deflec- tion		1 1	1 1 1	100	111		13		11	1 1	; ;	1 1	į o	۱ ۵	1	8
	Cur- rent		11		11	: : :	1 1	: :		::	۱ ٦			1 1	1;	:	-
	Rota- tion rate		::		۱,			1 6		11	; ;	;;	4 0		1 1	!	10
	Accel- eration		11	111	::	111	! !			11	; ;	۱'n	1 1	11	11	1	4
Vehicle system	-		Airframe Range safety	command Electrical Pneumatic Hydraulic	Guidance Propulsion	right control Telemetry Propellant level	control Azusa Payload	Miscellaneous Total		Airframe Range safety	command Electrical Premmatic	Hydraulic Guldance	Propulsion Fiight control	Telemetry Propellant level	control Azusa Pavload	Miscellaneous	Total

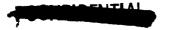




TABLE XIII-II. - SIGNIFICANT FLIGHT EVENTS

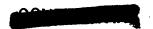
Event	Landline	Time of occurrences, sec				
	measurement number (a)	Nominal	Actual			
Engine start command Upper umbilicals ejected Ignition complete (main stage limiter) Vehicle release 2-in. motion ^b Lower boom solenoid valve Auxiliary 2-in. motion Upper boom solenoid valve ^c 8-in. rise 42-in. rise (final umbilical ejected)	APll61X (347) CNl615X (354) APl617X (28) APl577X (363) AMl030X (364) CNl465X (88) CNl474X (365) CNl464X (84) ANl827X (366) ANl066X (469)	T - 0 T - 0 T + 0.03 T + 0.25	T - 8.27 T - 3.20 T - 2.15 T - 0.78 T - 0 T - 0 T + 0.04 T + 0.26 T + 0.27 T + 0.85			

^aNumbers in parentheses refer to pen recording numbers.



bThere was no evidence of erratic 2-in. rise switch operation, observed on previous flights between lift-off and 42-in. rise, which had been attributed to flame impingement. The switch cabling was wrapped with Blastape to prevent this from happening.

^cThe upper boom solenoid valve received its signal at T + 0.260 sec, indicating that the primary actuating device (240-msec time-delay relay) initiated upper boom motion rather than the backup signal from the 8-in.-rise switch that occurred at T + 0.270 sec.



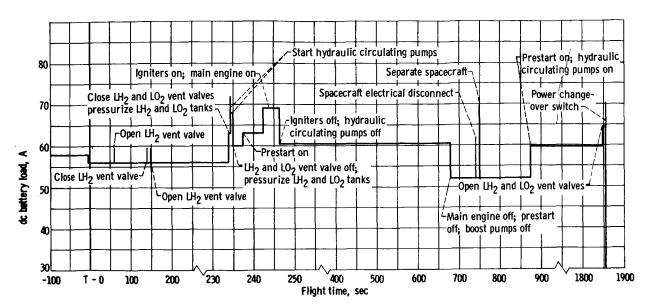


Figure XIII-1. - AC-6 main vehicle battery composite lead profile.

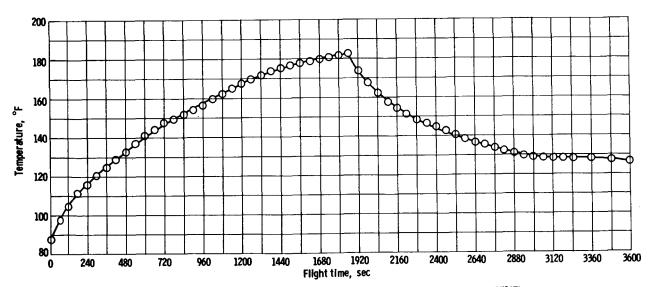


Figure XIII-2. - Variation of inverter skin temperature as function of flight time (CE29T).





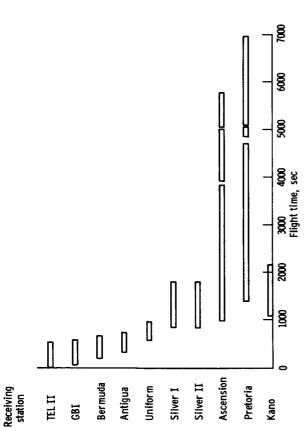


Figure XIII-3. - AC-6 Telemetry coverage.

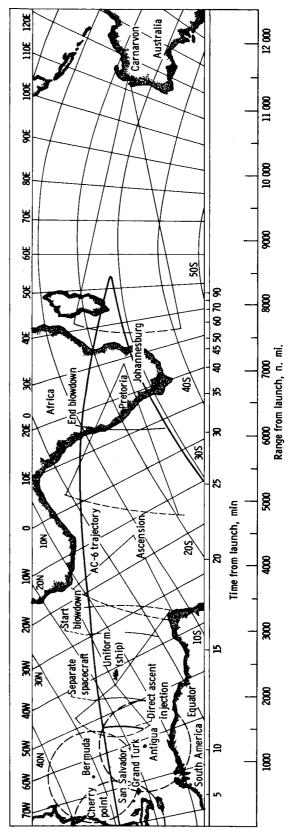


Figure XIII-4. - Centaur AC-6 direct ascent flight plan and data coverage. Axial rotation rate of Earth exceeds spacecraft angular rate about Earth center, thus, apparent westerly motion of spacecraft.

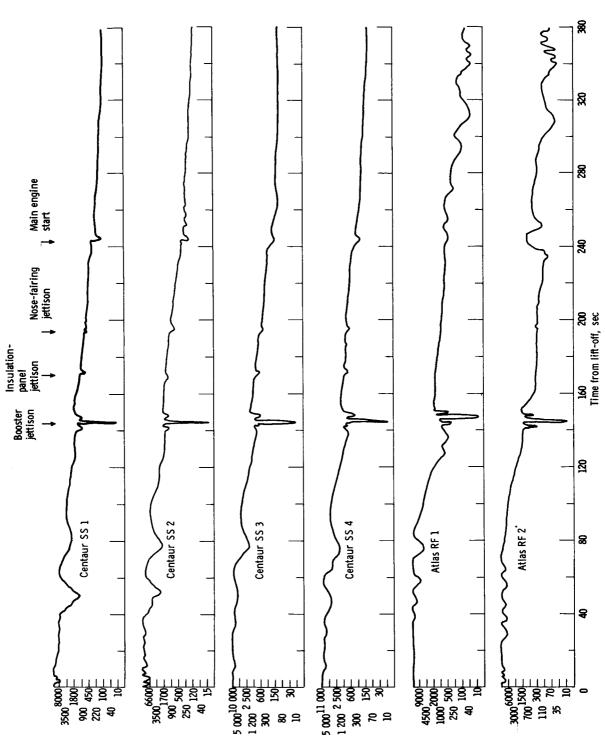
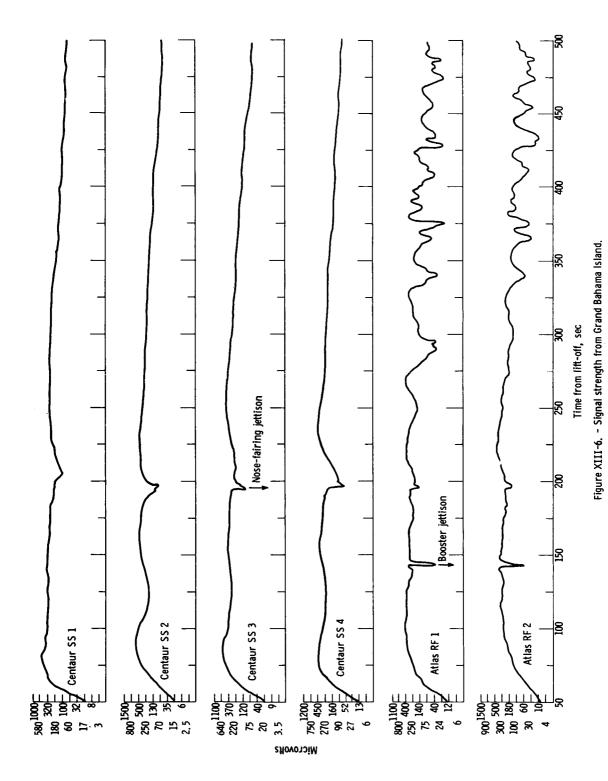


Figure XIII-5. - Signal strength from TEL II station at Cape Kennedy.

Microvolts







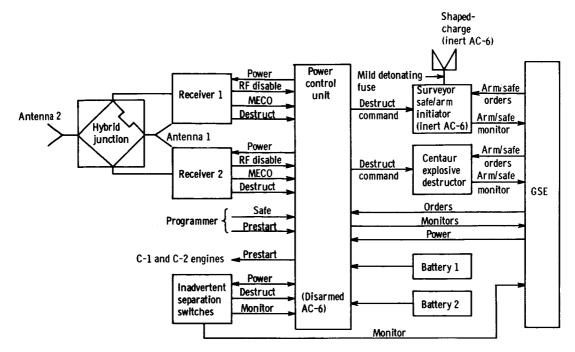


Figure XIII-7. - Block diagram of second stage range safety command subsystems.

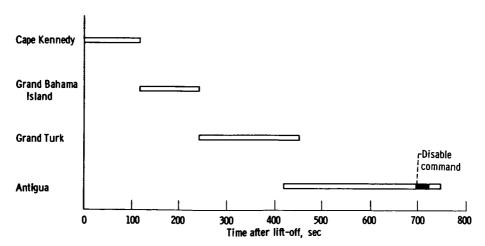


Figure X111-8. - AC-6 Range Safety Command System transmitter utilization.



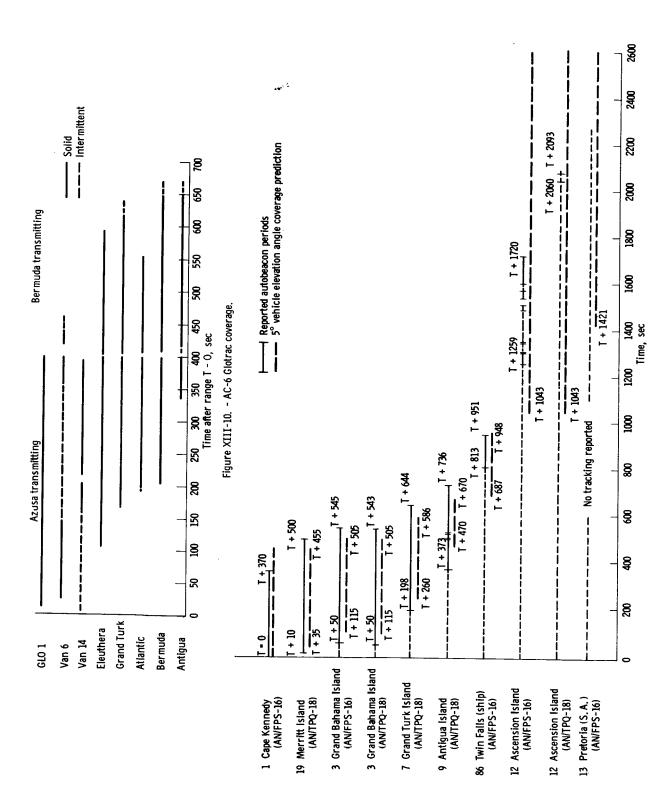


Figure XIII-9. - C-band transponder coverage and performance.



APPENDIX A

SYMBOLS

A reference area

A-C Atlas-Centaur

AFETR Air Force Eastern Test Range

A/P autopilot

ac alternating current

BECO booster engine cutoff

BET best estimate of trajectory

BPS boost-pump start

burp step pressurization of propellant tank

 $\mathtt{C}_{\mathtt{X}}$ standard aerodynamic drag coefficient

C-band frequency band used in radar (range, 3.9 to 6.2 gigacycles)

CRT composite readiness test

cps cycles per second

D drag

D/A digital-analog

DSIF deep-space instrumentation facility

dc direct current

EST Eastern Standard Time

ETR Eastern Test Range

F - days prior to launch

FPR flight performance reserve

GD/C General Dynamics/Convair

GET best estimate of trajectory based on guidance data

GH2 gaseous hydrogen



Glotrac Global tracking

GMT Greenwich Mean Time

gpm gallons per minute

GN₂ gaseous nitrogen

GO₂ gaseous oxygen

GSE ground support equipment

H₂ hydrogen

H₂O₂ hydrogen peroxide

JPL Jet Propulsion Laboratory

LH₂ liquid hydrogen

LHe liquid helium

LN₂ liquid nitrogen

LO₂ liquid oxygen

M Mach number

MECO main engine cutoff

MES main engine start

max Q maximum aerodynamic load

N load factor, g's

 $N_{\mathbf{x}}$ load factor in x-direction

 N_z load factor in z-direction

NPSH net positive suction head

NPSP net positive suction pressure

02 oxygen

186

P-P peak to peak

PLIS propellant level indicating system

psi pounds per square inch

psia pounds per square inch absolute

psid pounds per square inch differential

psig pounds per square inch gage

PU propellant utilization

Q,QUAD quadrant

q dynamic pressure

RF radio frequency

rms root mean square

rpm revolution per minute

RP-1 rocket propulsion fuel

RSC Range Safety Command

S-band frequency band used in radar (range, 1.55 to 5.20 gigacycles)

SD-2 Surveyor dynamic model 2

SECO sustainer engine cutoff

T time from lift-off (2-in. motion)

 $\mathbf{T_c}$ time referenced to computer zero time

t MECO backup

TCA temperature control amplifier

TEL telemetry receiving station

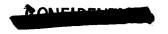
Telepak telemetry package

TLM telemetry

 ΔV incremental velocity impulse

VECO vernier engine cutoff

VSWR voltage standing wave ratio



APPENDIX B

CALCULATIONS OF PROPELLANT RESIDUALS

The ${\rm LO_2}$ and ${\rm LH_2}$ residuals at MECO were calculated by using the time that the propellant level passed the bottom of the PU probe as a reference point. The calculations are summarized as follows:

Liquid oxygen:

Š	Station level at bottom of probe 443	. 4
1	Sevel lag ^a in probe, in	. 4
1	Actual propellant level station in tank	. 8
	otal volume below station 443.8, cu ft	
	lass remaining at probe uncovery	
	$(69.5 \text{ lb/cu ft} \times 14.9 \text{ cu ft})^{\circ}$, lb	35
]	Do burned from probed uncovery to MECO, lb	
	C-1 engine:	
	29.2 lb/sec for 4.6 sec	. 3
	31.3 lb/sec for 8.0 sec	
r	Total LO2 burned by C-1 engine, lb	
	U-2 engine:	•
·	29.2 lb/sec for 7.2 sec	. 2
	31.3 lb/sec for 5.4 sec	
r	Fotal IO_2 burned by C-2 engine, lb	
	Total LO ₂ consumed from probe uncovery to MECO, 1b	٠.,
•	384.7 + 379.2	. 9
r	Total IO ₂ residual ^e , ib	
•	1035 lb - 763.9 lb	. ז
1	Jable IO2 residual ^f , 1b	• -
`	271.1 lb - 68 lb	. 1
		• -
Tri avri	l hydrogen:	
DI GUI	11 at 05011.	
:	Station level at bottom of probe	. 5
	Level lag ^a in probe, in	. 2
	Actual propellant level station in tank	. 7
	Total volume below station 372.7, cu ft	
	Mass remaining at probe uncovery	
•	(4.29 lb/cu ft \times 62.3 cu ft) ^c , lb	. 7
-	LH2 burned from probed uncovery to MECO, lb	•
	C-1 engine:	
,	5.58 lb/sec for 2.4 sec	. 4
	5.43 lb/sec for 8.0 sec	. 5
ı	Fotal LH ₂ burned by C-1 engine, 1b \cdots 56	
	C-2 engine:	
,	5.57 lb/sec for 5 sec	· _ c
	5.43 lb/sec for 5.4 sec	
ı	Fotal LH ₂ burned by C-2 engine, lb	-5
•	rocar rus partied by c-s engine, in	• 4



Total LH2 consumed from probe uncovery to MECO, 1b				
56.9 lb + 57.2 lb	 	 	•	104.1
Total LH ₂ residual ^e , lb				
267.3 lb - 104.1 lb	 • •	 		163.2
Usable residual ^f , lb				
163.2 lb - 71.8 lb	 	 	•	91.4



^aThe level lag is the difference in level inside the PU probe (level sensed) and the level outside the probe (actual level in tank).

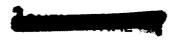
bVolumes include 2.01 cu ft LO2 and 3.47 cu ft LH2 for lines, pumps, etc.

CDensities obtained from curves for vapor pressure against density from ref. 10.

dFlow rates based on PU valve positions.

eAccuracy of residuals is ±10 percent as a result of uncertainties in density, probe location, and volume.

fA total of 68 lb of LO₂ represents the LO₂ remaining in the boost-pump sump when zero NPSH point is reached; 71.8 lb of LH₂ represents the LH₂ remaining in tank and sump when the boost pump will cause vapor pull-through in the liquid (ref. 18).



APPENDIX C

SYMBOLS AND DETAILED LISTING OF TRAJECTORY RECONSTRUCTION FOR AC-6 FLIGHT

DESCRIPTIONS

Standard Output (OP 1)

TIME elapsed time from lift-off

WEIGHT total weight of vehicle

TOTAL FLOW total weight flow

GRND RANGE ground-range great-circle distance (spherical earth, R₀ = 3441.3

n. mi.) from launch pad to vehicle subpoint

THETA I inertial range angle, measured between launch radius vector and

present radius vector

Q*ALPHA TOT product of dynamic pressure and total angle of attack

ALTITUDE altitude above oblate spheroidal earth, ft

RADIUS magnitude of radius vector from Earth center to vehicle

VEL E magnitude of velocity with respect to Earth

VEL R magnitude of velocity with respect to air

VEL I magnitude of velocity in inertial system

ALT altitude above oblate spheroidal earth, n. mi.

ALPHA angle of attack in pitch (XI, ZETA) plane, positive for ship

above relative velocity vector, VR

BETA angle of attack in yaw (XI, ETA) plane, positive for ship left of

relative velocity vector, VR

PSI inertial attitude angle, measure of angle between ship longitu-

dinal axis and inertial u,v plane, positive above plane

PSIDOT time rate of change of PSI

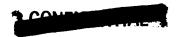
CROSS RANGE minimum ground distance from vehicle subpoint to plane formed by

launch vertical vector and launch down-range vector

DOWN RANGE distance from vehicle subpoint to launch site along Great Circle

at 94.5390 azimuth through launch site





GEOCENT LAT geocentric latitude, degrees north of equator

LONGITUDE degrees from Greenwich, positive east

AZI E azimuth of VEL E, angle between projection of VEL E into azimuth plane (plane perpendicular to radius vector) and north direc-

tion, positive clockwise from north

AZI R azimuth of VEL R

AZI I azimuth of VEL I

PHI inertial attitude angle - angle between projection of minus ZETA

axis in u,v plane and the u-axis

THRUST FIXED fixed thrust magnitude - nongimbaled engines thrust

THRUST CONTL controlled thrust magnitude - gimbaled engines

GAMMA E flight path angle of VEL E, measured angle between velocity vec-

tor and local horizontal, positive above horizontal

GAMMA R flight path angle of VEL R

GAMMA I flight path angle of VEL I

EAST WIND magnitude of wind velocity component from east

AXL FORCE net aerodynamic force and holddown force along longitudinal

axis, XI

SIDE FORCE aerodynamic force along side axis, ETA

NORM FORCE aerodynamic force normal to vehicle along ZETA

AXL LD FCTR instantaneous value of (thrust - drag)/weight

WIND VEL magnitude of wind velocity

NORTH WIND magnitude of wind velocity component from north

ATM PRESS atmospheric (ambient) pressure

DYNM PRESS dynamic pressure, $\frac{1}{2} \rho_{\mathbf{a}} V_{\mathbf{r}}^{2}$

HEAT PARAM heating parameter; time integral from lift-off of product of

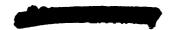
time, DYNM PRESS, and VEL R

MACH NUMBER Mach number, ratio of VEL R and local speed of sound

RHO-VR CUBED product of air density and VEL R cubed

CONTRACT OF THE PARTY OF THE PA

192



TOTAL ISP

instantaneous quotient of total axial thrust by total flow

Detailed Propulsion (DEPRO)

THRUST () total thrust of booster (B), sustainer (S), or vernier (V) engines, respectively, (vernier gimbaled)

THRUST TOT total thrust of all engines

THRUST CORR (B) change in booster thrust from C star table

THRUST CORR (S) change in sustainer thrust from C star and PU tables

PC (B) effective chamber pressure of booster engines

FUEL FLOW () total fuel flow rate of booster (B), sustainer (S), or vernier (V) engines, respectively; vernier flow included in sustainer

FUEL FLOW TOT total fuel flow rate for all engines

F FLOW CORR (B) change in booster fuel flow rate from C star table

F FLOW CORR (S) change in sustainer fuel flow rate from C star and PU table

PC (S) effective chamber pressure of sustainer engine

OXID FLOW () total LO₂ flow rate of booster (B), sustainer (S), or vernier (V) engines, respectively; vernier flow included in sustainer

OXID FLOW TOT total LO₂ flow rate for all engines

O FLOW CORR (B) change in booster LO2 flow rate from C star table

O FLOW CORR (S) change in sustainer LO2 flow rate from C star and PU tables

PC (V) effective chamber pressure of vernier engines

FP INLTP () fuel pump inlet pressure, booster (B) or sustainer (S)

FUEL DENSITY fuel density

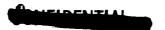
OXID DENSITY LO2 density based on telemetry measurements

MIX RATIO (B) ratio of LO₂ to fuel (booster)

MIX RATIO (S) ratio of LO₂ to fuel (sustainer)

BASE FORCE force of interaction of jet exhaust and base configuration

OP INLTP () LO2 pump inlet pressure, booster (B) or sustainer (S)





weight of fuel above sustainer pump inlet FUEL WEIGHT weight of LO2 above sustainer pump inlet OXID WEIGHT AXL LD FCTR axial load factor, required by propulsion model to calculate effect of headrise on pump inlet conditions CAP RATIO (PU) capacitance output from fuel manometer divided by capacitance output from oxidizer manometer; this ratio is calculated from telemetry values of PU valve angle position restraining force on vehicle during first 10 sec HOLD - DOWN weight of lubrication oil remaining, booster (B) or sus-OIL WEIGHT () tainer (S) FUEL LEVEL height of fuel above sustainer pump inlet OXID LEVEL height of LO2 above sustainer pump inlet net positive suction head of sustainer LO2 pump NPSH propellant utilization fuel valve angle, value used is from VALVE ANGLE (PU) telemetry atmosphere (ambient) pressure ATM PRESS vapor pressure of LO2 VAPOR PRESS FUEL TNK PR (G) gage pressure of fuel tank (telemetry) OXID TNK PR (G) gage pressure of LO2 tank (telemetry) ACS ITER internal counter Vehicle Dynamic Parameters (OP 5) thrust components in vehicle axes system THRUST XI ETA ZETA thrust deflection angle in XI-ETA plane to compensate for DEL XI-ETA center-of-gravity offset and aerodynamic moments thrust deflection angle in XI-ZETA plane to compensate for DEL XI-ZETA center-of-gravity offset and aerodynamic moments center of gravity measured from zero station along longi-CG XI tudinal (XI) axis CG ETA center of gravity measured from longitudinal axis along pitch (ETA) axis

COMPANY

194

center of gravity measured from longitudinal axis along yaw CG ZETA

(ZETA) axis

center of pressure measured from zero station for forces CP NORM

perpendicular to pitch (XI-ETA) plane

center of pressure measured from zero station for forces CP SIDE

perpendicular to yaw (XI-ZETA) plane

aerodynamic moments about center of gravity in vehicle axes AERO MOM XI

> ETA system

ZETA

INERTIA XI

moments of inertia in vehicle axes system

ETA ZETA

INERTIA XI-ETA

ETA-ZETA XI-ZETA

products of inertia in vehicle axes system

Centaur

total Centaur thrust THRUST

total LH2 flow LH2 FLOW

LO2 FLOW total LO2 flow

ratio of LO2 to LH2, total RATIO

C-1 THRUST thrust of C-l engine

C-1 LH2 FLOW LH2 flow for C-1 engine

C-1 LO2 FLOW LO₂ flow for C-l engine

C-1 RATIO ratio of LO2 to LH2 for C-1 engine

percent change in thrust due to inlet pressures, temperatures, PERCENT T1

and PU valve setting for C-1 engine

C-2 THRUST thrust of C-2 engine

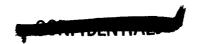
C-2 LH2 FLOW LH2 flow for C-2 engine

C-2 LO2 FLOW IO2 flow for C-2 engine

C-2 RATIO ratio of LO2 to LH2 for C-2 engine



PERCENT T2	percent change in thrust due to inlet pressures, temperatures, and PU valve setting for C-2 engine
LH2 WEIGHT	weight of LH2
LO2 WEIGHT	weight of LO2
C-1 LH2 PRESS	pump inlet pressure for C-1 engine LH2 (telemetry)
C-2 LH2 PRESS	pump inlet pressure for C-2 engine LH2 (telemetry)
PERCENT ISP1	percent change in engine specific impulse due to inlet conditions and valve setting for C-1 engine
C-1 ISP	specific impulse of C-l engine equals ratio of C-l thrust to C-l flow
C-1 FLOW	total propellant flow for C-1 engine
C-1 LO2 PRESS	pump inlet pressure for C-1 engine LO2 (telemetry)
C-2 LO2 PRESS	pump inlet pressure for C-2 engine LO ₂ (telemetry)
PERCENT ISP2	percent change in engine specific impulse due to inlet conditions and valve setting for C-2 engine
C-2 ISP	specific impulse of C-2 engine equals ratio of C-2 thrust to C-2 flow
C-2 FLOW	total propellant flow for C-2 engine
C-1 LH2 TEMP	pump inlet temperature for C-l engine LH ₂ (telemetry)
C-2 LH2 TEMP	pump inlet temperature for C-2 engine LH2 (telemetry)
PERCENT MR1	percent change in propellant mixture ratio due to engine inlet conditions and PU valve setting for C-1 engine
C-1 PU VALVE	propellant utilization valve setting for C-1 engine (telemetry)
C-2 PU VALVE	propellant utilization valve setting for C-2 engine (telemetry)
C-1 LO2 TEMP	pump inlet temperature for C-1 engine LO2 (telemetry)
C-2 LO2 TEMP	pump inlet temperature for C-2 engine LO2 (telemetry)
PERCENT MR2	percent change in propellant mixture ratio due to engine inlet conditions and PU valve setting for C-2 engine





Orbit Elements (OP 4)

PERIGEE RAD radius at perigee of instantaneous conic

APOGEE RAD radius at apogee of instantaneous conic

PERIGEE ALT perigee altitude (above spherical Earth with radius = 3443.9

n. mi.)

APOGEE ALT apogee altitude (above spherical Earth with radius = 3443.9

n. mi.)

PERIGEE VEL velocity at perigee

APOGEE VEL velocity at apogee

SEMI LAT REC semilatus rectum of trajectory

PERIOD period of eliptical trajectory

SEMI MAJ AXIS semimajor axis

ENERGY energy, $v^2/2 - \mu/r$

ECCENTRICITY orbit eccentricity

INCLINATION orbit inclination

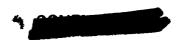
TRUE ANOMALY true anomaly

ASCEND NODE ascending node

ATM PRESS DYNM PRESS HEAT PARAM MACH NUMBER RHO-VR CUBED TOTAL ISP PSI LBS/FT SQD FT'LBS/FT SQD	ATM PRESS VAPOR PRESS FUEL TWK PR (G) OXID TWK PR (G) ACS ITER PSI PSI PSI	INERTIA XI-ETA INERTIA ETA-ZETA INERTIA XI'ZETA SLUG-FT SQD SLUG-FT SQD SLUG-FT SQD SLUG-FT SQD SLUG-FT SQD 0.8414420E-01 0 0.7545577E-02 46.660424 243.51833 14.661513 28.611137	58.338486 24.838486 4.0000000 0 0
AXL FORCE SIDE FORCE NORM FORCE AXL LD FCIR MIND VEL WORTH WIND LBS LBS LBS FT/SEC	DIL WEIGHT (B) DIL WEIGHT (S) FUEL LEVEL DXID LEVEL NPSH VALVE ANGLE (PU) LBS LBS INCHES INCHES INCHES DEG	INERTIA XI INERTIA ETA INERTIA ZETA SLUG-FT SQD SLUG-FT SQD SLUG-FT SQD SLUG-FT SQD SLUG-FT SQD 10.59.5250 43.532346 32.380253 1.2503855 8.6176623 -5.0132224 166.000000	937.69234 551.35773 59.660548 14.100000 0
THRUST FIXED THRUST CONTL GAMMA E GAMMA R GAMMA I EAST WIND LBS DEG DEG DEG FT/SEC	UP INLTP (B) UP INLTP (S) FUEL WEIGHT OXID WEIGHT AXL LD FCTR CAP RATIO (PU) HOLD-DOWN PSI PSI LBS LBS	AERO MOM XI AERO MOM ETA AERO MOM ETA FT-LBS FT-LB	76103.000 172286.00 1.2503862 0.4516520 4070.0978 0 -16140.178 7518.2086
GEDCENT LAT LONGITUDE AZI R AZI R AZI I PHI DEG DEG DEG DEG	FP INLTP (B) FP INLTP (S) FUEL DENSITY OXID DENSITY MIX RATIO (B) MIX RATIO (S) BASE FORCE PSI PSI LBS/CUBIC FT LBS/CUBIC FT	CP NDRM CP SIDE INCHES INCHES INCHES 102.03122 125.57289 90.000001 -0.2834380E-01 69.597418	50.380000 68.889999 2.1796546 1.9069072 13.090707 298.47157 624.74978
ALPHA BETA PSIDOT PSIDOT CROSS RANGE DOWN RANGE DEG DEG DEG DEG N.MI.	OXID FLOW (B) OXID FLOW (S) OXID FLOW (V) OXID FLOW TOT O FLOW CORR (S) C FLOW CORR (S) PC(V) LBS/SEC	CG XI CG ETA CG ZETA INCHES INCHES INCHES INCHES 90.202411 91.089153 90.079948 0 0.5519358E-04 -0.1039724E-05 180.76768	0 1070.6204 0.2591751 -9.9399999 315.27214 797.99998 0.5000000
ALTITUDE RADIUS VEL E VEL R VEL I ALT FT FT FT FT FT FT FT FT/SEC	FUEL FLOW (B) FUEL FLOW (S) FUEL FLOW (V) FUEL FLOW TOT FUEL FLOW CORR (B) F F	DEL XI-ETA DEL XI-ZETA DEG DEG 0.2090976E 08 0.2543216E-04 8.6176617 1342.4258 -0.1555270E-01 408.25398	0 503.05025 0.1100356 9.9359999 688.40168 0.7191021E-01
1 TIME 2 WEIGHT 4 GRND RANGE 5 THETA I 6 Q*ALPHA TOT 1 SEC 2 LES 2 LES 2 LES 4 N. MI. 5 DEG 6 DEG-PSF	1 THRUST (8) 2 THRUST (S) 3 THRUST (V) 4 THRUST TOT 5 THRUST CORR (B) 6 THRUST CORR (S) 7 PC(B) 1 LBS 2 LBS 4 LBS 5 LBS 6 LBS 6 LBS 7 PSIA	1 THRUST XI 2 THRUST ETA 3 THRUST ETA 1 LBS 2 LBS 2 LBS 3 LBS 3 LBS 4 0.5520337E-04 5 0.7227983E-06 6 7.5562331 1 325075.55 2 56955.596	1526.0075 4 383597.15 5 -181.84886 6 -976.4999 7 574.20450 1 383596.55 2 481.44076 3 400.34498
			וב בם ביים

CONCIDENTAL

14.653006 0.4083280 5.336091 0.1662689E-01 498.8660 244.36092 14.653006 28.640030 58.286993 25.046994 42.000000	0 0 0 14.653006 0.4083280 5.3360091 0.1662689E-01 498.86660 244.36092	14.653006 28.640030 58.286993 25.046994 43.000000	14.431659 10.675694 2446.3177 0.8566623E-01 67006.851 244.94400 14.431659 28.75585 58.268339 26.068340 120.00000
-2383.0916 7.8699333 46.328034 1.2739783 8.7409658 -4.6198340 164.10000 52.700000 941.49165 556.97995 60.712587	0 0 0 0 1.2383.0916 7.8699333 46.328034 1.2739783 8.7409658 -4.6198340	164.10000 52.700000 941.49165 556.97995 60.712587 -4.1022221 0	-229.81629 -112.90607 295.86516 1.3416770 12.576276 -0.8333253E-01 156.50000 51.500000 954.32954 576.73292 63.608242 -2.3900001
59635.999 325231.59 88.981075 63.563803 0.7256804 7.4203514 53.040716 57.683414 75113.631 170127.41 1.2739782 0.4347981 2386.8503	0 -22994.848 1257.5164 59835.999 325231.59 88.981075 63.563803 0.7256804 7.4203514	53.040716 57.683414 75113.631 170127.41 1.2739782 0.4347981 2386.8503 0	60053.484 326274.95 88.881361 83.467972 4.1335449 12.576000 54.473969 59.177110 71216.876 1.34167569 0.43463835 0.2390502E-14
28.307490 -80.541179 40.868798 121.29905 89.990241 -0.2834380E-01 69.567023 71.671313 50.380000 68.885999 2.1817685 2.4756669	299.21912 624.74998 28.307490 -80.541179 40.868798 121.29905 89.990241 -0.2834382E-01	69.567023 71.671313 50.380000 68.885999 2.1817685 2.4756669 15.984401 299.21912 624.74998	28.307505 -80.541198 53.842976 84.661310 89.952325 12.330644 69.307250 71.491478 50.380000 68.869999 2.1879211 2.3683569 91.272480 299.95150
26.487728 3.2316061 90.079948 0.1431421E-04 -0.3523774E-04 890.52763 196.27811 0.2496105 5.573776	799,19998 0.5013333 0.3926667 26.487728 3.2316061 90.079948 0	890.52763 196.27811 0 1086.8057 0.2496105 5.573776 315.29380 799.19998 0.5013333	6.3960503 -1.8904111 90.079948 0 -0.8233720E-03 -0.1130550E-02 892.33156 193.69303 0 1086.0246 0.2217726 3.0655001 315.98254 803.99999 0.5066667
-77.500000 0.2090978E 08 17.003596 18.986295 1342.3367 -0.1275486E-01 408.1679 79.282924 0 47.45071 0.1059643 -5.573776 699.46621	6.7003726E-01 0.6278981E-01 -77.550000 0.2040976E 08 17.003596 18.986295 1342.3367 -0.1275486E-01	408.1679 79.282924 0 81.45071 0.1059643 -5.573776 699.46621 0.7003726E-01	366.50000 0.2091023E 08 96.926457 97.541192 1344.4248 0.6031814E-01 407.84449 81.783713 0 0.9911472E-01 -3.0655001 698.21640
2.C0C0000 300384.92 1575.8149 0.3803400E-04 0.7354352E-C2 10.875362 325231.59 58309.886 1526.1134 385067.58 324.1999 574.40135	385066.96 470.69867 421.99080 2.0000000 30384.92 1575.8149 0.3803400E-04 0.7356352E-C2 10.87536352E	325231.59 58309.886 1526.1134 385067.58 324.40135 385066.96 470.65867	9.999998 287772.32 1577.2112 0.1390597E-02 0.367668E-01 71.155015 326274.95 5E524.003 1529.4817 38632.43 186.2000 574.88435 421.71669
# D D D D D D D D D D D D D D D D D D D	D 4 M Q 4 4 4 4 4 4 4 4 4 4 4 4 4 4 4 4 4		04-1 0 0 0 0 0 0 0 0 0 0 0 0 0 0 0 0 0 0 0



14.122938 26.686758 14134.999 0.1369163 267212.30 245.95676 14.122938 28.177062 26.327062 184.00000	0 0 0 14.122938 26.686758	14134.999 0.1369163 267212.30 245.95676 14.122938	8.84586 8.17706 6.32706 85.0000	000	13.671721 52.564540 51217.801 0.1953010 748671.20 247.38813	13.671721 28.936138 58.228279 26.728279 231.00000	000
-609.05181 152.98536 323.95700 1.383737 10.471728 -4.2699992 151.75000 50.750000 961.7539 588.68318 64.151505	0 0 0 -609.05181 152.98536	323.95700 1.383737 10.471728 -4.2699992 151.75000	50.750000 961.75739 588.68318 64.151505 -3.2999999	000	-1242.5184 566.98078 94.896011 1.4297302 12.500988 -9.1618992	147.00000 50.000000 969.07626 600.65314 64.803958 -3.5600000	000
60617.316 32722.43 88.803411 87.325059 6.6179438 9.5615999 54.780973 59.521639 68770.167 155992.63	0 -125605.86 20339.905 60617.316 327292.43	88.803411 87.325059 6.6179438 9.5615999	9.52163 8770.16 55992.6 .383773	0 -125605.86 20339.905	61364.505 328767.26 89.418265 86.983444 9.3439264 8.5049576	55.136643 59.918281 66332.392 150552.79 1.4297303 0.4353002	0 -28849.076 89894.970
28.307525 -80.541231 58.725236 110.86109 89.927983 20.055011 68.891796 71.125731 50.880000 68.857499 2.1897129	385,32631 624,74998 28,307525 -80,541231	58.725236 110.86109 89.927983 20.055011	74.125731 50.380000 68.857499 2.1897129 2.4225807	385,32631 624,74998	28.307551 -80.541260 19.979073 127.26459 89.810045 20.055011	68-487040 70.775239 50.380000 68.844999 2.1916705 2.4373941 349.75491	277.20958 624.74997
MNB 40 0H 604	806.99999 0.5100000 C.4100000 2.7548628 0.8847233	90.079948 0.4824402 -0.1815362E-02 -0.2973084E-02	194.89441 0 1087.5018 0.213653 4.384998 316.95485	806.99999 0.5100000 0.4100000	0.3394084 1.7606265 87.667747 0.4824402 -0.3282023E-02	892.87419 195.12217 0 1087.9964 0.2048088 4.762000	809.49998 0.523333 0.423333
	0.7956819E-01 0.1038117 994.50000 0.2091085E 08		401.03911 60.449087 0 488.08580 0.9066373E-01 -4.3849998 698.68919	0.7956819E-01 0.1038117	1932-5000 0.2091179E 08 221.04637 221.34168 1361.3854 0.3180486	407.39435 80.053598 0 487.44795 0.8689382E-01 -4.762000 698.72547	0-1072969 0-7078773E-01
5.00000 577.666 577.1466 .348348 .3512948 7.20546 27292.4 871292.4 871292.4 871292.4 871292.9	387908.54 538.69938 702.83543 15.000000 279886.42	1577-1461 0.3483488E-02 0.5512978E-01 77-205461	36162643 1534.2367 387909.74 -149.83090 258.99999	387908.54 538.69938 702.83543	26.000000 272001.01 1577.0027 0.56481726-02 0.73497036-01 94.248358	328767.26 59823.258 1541.2472 390131.76 -143.59997 279.80000 574.86661	390130.59 730.59205 481.99838
			3 m c & c 4 C w 4 c & c 6	5 2 2 3	0 4 4 5 6 7 8 8 8	U W 4 4 4 4 4 4 4 4 4 4 4 4 4 4 4 4 4 4	0 h 7 2 3 3

1		

13.671721 52.564540 51217.801 0.1953010 748671.20 247.38813	13.671721 28.936138 58.228279 26.728279 232.00000	000	12.323769 141.44509 337622.74 0.3374364 3444909.8 251.65744	12,323769 29,174477 58,376230 30,176230	000	11. 984071 165.46576 459216.98 0.3701022 4409616.9 252.74279	11.984071 29.227917 58.375928 30.155929 343.00000	000
-1242.5184 566.98078 54.896011 1.4297302 12.500988 -9.1618992	147.00000 50.000000 969.07626 600.65314 64.803958 -3.5600000	000	-3477.6857 1116.8508 93.158265 1.5376206 14.494280 -12.590074	137.50000 48.500000 983.63178 624.62925 71.088127 -5.2339998	000	-4089,9925 968,89505 25,988382 1,560558 12,143299 -11,097624	135.60000 48.200000 986.53320 629.42239 70.714839 -5.4000000	000
61364,505 328767.26 89,418265 86,983444 9,3439264 8,5049576	55.136643 59.918281 66332.392 150552.79 1.4297303 0.4353002	0 -28849.076 49894.970	63678.811 343745.11 84.13222 82.842731 15.209443 7.1815171	58.267037 63.144728 61484.417 139619.30 1.5376209 0.4337502	0 8002.0820 171950.05	64236.952 334747.04 82.86258 82.053832 16.394400 4.9297504	58.118064 63.016154 60517.920 137431.07 1.5605557 0.4335965	0 55259.610 138249.88
28.307551 -80.541260 19.979073 127.26459 89.910045 20.055011	68.487040 70.775239 50.380000 68.844999 2.1916705 2.4373941 349.75491	277.20958 624.74997	28.307602 -80.540757 88.295714 103.99221 89.950727 20.055011	67.316554 69.732149 50.380000 68.811998 2.2067693 2.5594373	267.96249 624.74998	28.307607 -80.560479 89.361306 100.53530 89.974133 20.055011	66.979795 69.422471 50.380000 68.804599 2.2066022 2.5745810 923.78552	265.49998 624.74998
0.3394084 1.7606265 87.667747 0.4824402 -0.3282023E-02 -0.4596777E-02	892.87419 195.12217 0 1087.9964 0.2048088 4.7620000 318.38836	809.49998 0.523333 0.4233333	0.7137683E-01 1.2596738 82.843346 0.4824402 -0.8444539E-02 0.2166229E-01	896.66630 197.50739 0 1094.1737 0.1529197 7.5913997 322.67717	814.49997 0.5500000 0.4500000	-0.4671421E-01 0.9060293 81.878466 0.4824402 -0.9902581E-02 0.3633315E-01	896.31729 197.73874 0 1094.0560 0.1532686 7.939999 323.75830	815.69998 0.5566667 0.4553333
1932.5000 0.2091179E 08 221.04637 221.34168 1361.3854 0.3180486	407.39435 80.053598 0 487.44795 0.8689382E-01 -4.762000 698.72547	0.1072969 0.7078773E-01	4889.7500 0.2091475E 08 377.51923 378.49046 1431.4609 0.8047493	406.32534 77.168285 0 483.49362 0.6483061E-01 -7.5913997 699.53279	0.1416411 C.6196086E-01	5675.2500 0.2091553E 08 413.37678 414.1500! 1453.2396	406.19794 76.804242 0 483.00218 0.6497855E-01 -7.939999	0.1305776 0.4580654E-01
20.000000 272001.01 1577.0027 0.5648172E-02 0.73497G3E-C1 94.248358	328767.26 59823.258 1541.2472 390131.76 -143.59997 279.80000 574.86661	390130.59 730.59205 481.99838	29.99999 256203.96 1579.2258 0.232.998E-01 0.1107239 178.46029	333745.11 62116.589 1562.2215 357423.91 -107.13534 423.71999 575.69186	397422.19 982.47101 429.78085	32.000000 253046.12 1578.6167 0.376832E-01 0.1183263 150.11588	334747.04 62669.444 1567.5087 398983.98 -107.37981 437.00000	398982.59 909.28635 318.97668
	1 2 E 4 S O F	0 1 7 2 3 3 3	10 C C C C C C C C C C C C C C C C C C C	O W & K O P	0 1 2 5 3 3	0 1 1 1 3 4 4 8 6	O W & K O P P P P P P P P P P P P P P P P P P	0 1 6 2 8 3

_	

•		567E 2500	-0-46716216-01	28.307607	64236.952	-4089,9925	11.984071
,	253046-12	0.2091553F 08	0.9060293	0	334747.04	968.89505	165.46576
	1578-6167	•	81-878466	89,361306	82.862528	25.988382	459216.98
	0.3765832E-01	414-15001	0.6633552	100.53530	82.053832	1,5605558	0.3701022
S	0.1183263	1453.2396	-C.9902581E-02	89.974133	16.394400	12.143299	4409616.9
9	150.11588	0.9340260	0.3633315E-01	20.055011	*0C1676**	+70160*11.	61741.767
	334747.04	406-19794	896.31729	66.979795	58.118064	135.60000	11.984071
	62669-444	76-804242	197.73874	69.422471	63.016154	48.200000	29.227917
9 00	1567.5087		3	50.380000	60517.920	986.53320	58.375928
	398983.98	483.00218	1094.0560	68.804599	137431.07	629,42239	30,155929
	-107,37981	0.6497855E-01	0.1532686	2.2066022	1.5605557	70.714839	344.00000
•	437.00000	-1.9359999	7.9399999	.574581	0.4335965	-5-4000000	
1	575.51145	699.52277	323.75830	923.78552	0		
	03 00000	0 1205776	×15. 60008	3.65_4999A	C	0	0
	378362=37 GFG 28635	0.45804546-01	0.556667	624.74998	55259.610	•	0
7 10	318-97668		0,4553333		138249.88	0	0
4	000000	0052 7700	-0.4978502	28,307579	66760.001	-1182.2672	10.416903
4 6	000000000000000000000000000000000000000	0 20010406	1 1805944	£ 36 8 £ 5 · 0 8 ÷	339422.28	2122. 7864	283.35539
	240421-51		76716376	91.638327	77.189988	-492.35731	1346492.7
	1010-0013	57. 5172B	0.4433650	99,791181	77-223469	1.6595304	0.5194768
	0000000	1573-5309	-0-1716748F-01	90-135064	20.859241	18,267021	04753
• ۱	• 5	1.5708638	0.1490035	20.055011	-2.1476239	-18.140336	257.71975
					705003 1.3	00000 861	10.416903
	339422.28	405-63434	894.90906	02-034130	21 575514 52 575514	000000	,
	65168.047	16.131241	191.22219	6.0561.00	56656-365	998-12705	58.583097
	1591.9544	0	1002 1318	68.775000	128686.29	648.58788	30.283097
3 €	406182-28	462+3/139	0-1541162	2,2061965	1.6595300	69,375080	417.00000
	79616-701-	ĺ	7. 11111	2.5701051	0.4335965	-5.3999999	
~ ه	574.76060	- •	328.75695	1456.8356	0		
•					,	,	(
	406178.70		820.49999	265.49999	0	ɔ (.
	1470.5832	-0.7341166E-01	0. 5833333	624.74998	397359.00	.	-
5 3	-520-42699		0.4766667		338 795. 74	9	5
				0.000	100 07277	-7162 2672	10.414903
-	40-000000		-0.4978502	28.301319	320623	7107*7011	283 25520
P 2	240427.31	0.2091940E 08	1.1895844	-80.538343	337476	- 400 25721	1366607
	1576.0619	574.59356	16.5/1624	91.038321	006601-11	101000364	0.5194768
•	0.1499887	5/4-51/58	U-1556121 -0 1716768-01	99-171101	20.859241	18.267021	0.1047538E 08
io 4	0.1496333	1515-5509	0.1490035	20.055011	-2.1476239	-18.140336	257.71975
0	17006.600						1 1 1 1 1 1 1 1 1 1 1 1 1 1 1 1 1 1 1 1
	339422.28	405.63434	90606*468	65.634136	57.589394	128.00000	10.416903
E 2	65168.047	76.737247	197.22279	68.193679	62.575516	4 7. 000000	680144*67
ь 3	1591-9544	0	0	50.380000	56656.365	50121.846	30.383097
	406182.28	82.37159	1092-1318	68.775000	47.686821 1.4606309	040-30100	30.000 ot 3
	-107-97362	0	0.1541162	2.2061965	0050469-1	0000000000000	00000
9	66665*965	8666666-1-	7.939998 330.36406	1456 8356	0.4333363	0.5555555	
-	514.16060	044.04400	• • 500)	•		
	406178.70	0.2074403	820.49999	565.49699	0	0	0
P 2	1470.5832	-0.7341166E-01	0.5833333	624.74998	397359.00	0	0 ;
	-520.42699		0.4766667		338795.74	0	9

POMELDENT

8.1278249 473.75257 3991657.0 0.7604285 0.2507961E 08 264.96236 8.1278249 29.781147 58.772173 30.172175 515.00000	0 0 0 1.165341 556.47168 5807963.2 0.3365747E 0.3365747E 267.99087 7.1655341 29.951584 58.734464 30.014466 567.00000	0 0 0 1.1655341 556.47168 5807963.2 0.33657422 0.3365747E 267.99087 7.1655341 29.951584 58.734664 30.014666 568.00000
-12962.776 1629.9621 -140.35732 1.7928995 -17.735429 118.50000 45.500000 1012.6114 672.47033 66.410231	0 0 0 0 17006.413 300.56964 752.7845 1.84.7884 11.733509 -11.621925 114.70000 1018.4329 681.97313 64.570889	-17006.413 300.56964 352.77845 1.84.7884 11.733509 -11.621925 114.70000 44.900000 1018.4329 681.97313 64.570889 -2.777778
70323.914 346122.16 69.339205 69.422889 25.421510 -2.5999983 56.370275 61.477274 51832.165 11.786.89 1.7957392 0.4348105	0 314749.67 164422.83 164422.83 71756.412 348862.14 66.092517 26.5225939 66.092517 1.6143385 1.6143385 55.606063 60.759252 49893.521 113449.16 1.8479884	-51869.189 -5535.863 -35535.863 -35535.863 348862.14 66.252539 66.092517 26.552263 1.6143385 55.606063 60.759252 49893.521 113449.16 1.8479884 0.4360245 0
28.307378 -80.532060 92.565230 96.001675 90.438298 20.055011 63.521492 66.241867 50.38304 2.4556870 2235.4337	.6054 .9087 30720 30720 52791 09286 71920 55501 77181 25388 70439 70439	352.96625 654.47407 28.307204 -80.527917 94.719205 90.656147 20.055011 62.471813 65.253882 50.380000 68.704399 2.2019618 2.3706549 2562.7435
-0.1536195 0.4604396 69.033498 0.7538127 -0.3146654E-01 0.4812297 892.22288 194.06062 0 1086.2835 0.1590578 5.5511119	825.49999 0.623333 0.506667 0.1814791 -0.174148E-01 66.018245 0.7538127 -0.3841509E-01 0.7004257 890.74864 191.79130 0 1082.5399 0.1629607 3.6277777	827.09999 0.6420000 0.5200000 0.1814791 -0.174148E-01 6.7538127 -0.3841509E-01 6.7004257 191.79130 0.1629607 3.6277777 339.10563 827.09999 0.6420000
16179.250 0.2092604E 08 823.13828 822.68612 1806.1353 2.6627621 464.85096 79.024981 0 483.87594 0.6743291E-01 -5.5511119 697.28925	0.1509342 -0.3693258E-01 19437.500 0.2092930E 08 938.98008 939.94690 1924.3290 3.1990011 404.52502 80.902243 0 485.42726 0.6908752E-01 -3.627777	C.8299099E-01 0.9576332E-01 19437.500 0.2092930E 938.98008 938.94690 1924.3290 3.1990011 404.52502 80.90243 0.6908752E-01 -3.627777 695.99680 C.8299099E-01 0.9576332E-01
49.99998 224688.13 1571.7179 0.4822555 0.1919506 229.95380 346122.16 68696.297 1627.6173 416446.08 -111.43574 323.00005 573.46545	416444.23 1097.0411 268.43795 54.000000 218405.53 1569.5257 0.7014757 0.103119 101.45327 70113.849 1642.5641 420618.55 114.17005	420617.30 609.25031 7C3.01424 54.000000 218405.53 1569.5257 0.2103119 101.45327 348862.14 70113.849 1642.5641 420618.55 217.22222 217.22222 572.80334 420617.30

COVEY	
	124

5.7465147 661.77822 9601208.2 1.0688671 0.4784195E 08 272.59055	30.207253 58.653484 29.753485 649.00000 0	4.84/433/ 718.4284 0.1288145E 08 1.2125666 0.5791630E 08 275.51013 4.8474337 30.513477 58.512565 30.132566 702.00000	0 0 0 4.8474337 718.42864 0.1288145E 08 1.2125666 0.5791630E 08 275.51013 4.8474337 30.513477 58.512565 30.132566 703.00000
-40268.783 -70.192196 1073.3900 1.8474448 9.6854819 -9.4040829	44.000000 1027.1888 696.16972 58.293776 -1.9900001 0	-41003.099 674.99542 674.83930 1.9217867 10.836292 -10.776166 105.20000 43.4000000 1033.0146 705.56561 58.216013 -2.8521428	0 0 0 0 0 10 10 10 10 10 10 10 10 10 10
73938.029 352457.52 61.695132 61.652378 27.778962 2.3177105	58.005692 46977.882 106973.57 1.8474444 0.4367539 0 -172801.15 -378027.34	75442.659 355204.43 355204.43 58.725282 58.725282 28.240415 -1.1399394 53.040431 58.257692 45038.653 102664.68 1.9217867 0.4359556	0 -6889.2000 -387291.21 75442.699 355204.43 58.738745 28.738745 28.740431 53.040431 58.257692 45038.653 102664.68 1.9217867 0.4359556 0
28.306786 -80.519473 93.552414 94.424048 90.973541 20.055011	63.278974 50.380000 68.38099 2.1931191 2.3191053 3045.4032 327.30995 594.59126	28.30380 -80.512154 93.667531 94.695011 91.219602 20.055011 59.475126 62.344336 50.380000 68.626598 2.1944459 2.3675240 3351.2130	199.31581 560.76283 28.306380 -80.512154 94.695011 91.219602 20.055011 59.475126 62.344336 50.880000 68.62598 2.194459 2.3675240 3351.2130
. 197743 1. 49536 1. 49536 . 753812 . 487474	190.07869 0 1076.5213 0.1982561 2.4870002 343.60028 829.49998 0.6700000	0.473.167.1E-01 -0.9627425E-01 58.480117 0.7538127 -0.5517574E-01 1.5352763 886.07830 190.99717 0 1077.0755 0.1922536 3.7356071	829.8999 0.694000 0.553333 0.4731671E-01 -0.9627425E-01 58.480117 -0.5517574E-01 1.5352763 886.07830 190.99717 0 1077.0755 0.1922536 3.7356071 346.42609 829.89999 0.6940000
24986.250 0.2093485E 1122.4698 1123.4698 2119.6921 4.1122078	81.962076 0 486.15474 0.8410458E-01 -2.4870002 694.68038 -0.3244040E-01 0.1415932	29102.200 0.2093896E 08 1252.8798 1252.8011 2263.2494 4.7896555 403.78225 80.673805 0 484.45605 0.8154953E-01 -3.7356071 694.88876	-0.3078844E-01 0.8537090E-01 29102.500 0.209389E 1252.9798 1252.9798 1252.9798 4.7896555 403.78225 80.673805 0 484.45605 0.8154953E-01 -3.7356071 694.88876 -0.3078844E-01
* ~~~~~~~~~~~~~~~~~~~~~~~~~~~~~~~~~~~~	1 1	D 1 2 202750.59 1 3 1563-615 5 1.5362615 5 0.2609775 6 77.068320 0 1 355204.43 F 2 73764.335 P 3 1678.3645 R 4 430647.13 0 5 -134.76689 6 223.17142	D 1 430646.47 P 2 -231.41209 S 3 641.66511 C*1 64.000000 P 2 202750.59 1 3 1563.0000 1 3 1563.0000 C 1 5560975 6 77.068320 D 1 355204.43 E 2 73764.335 P 3 1678.3645 R 4 430647.13 D 5 -134.76689 C 223.17142



		•
	 	,

3.6022101 798.06741 0.1913052E 08 1.4825352 0.7613855E 08	3.6022101 30.972809 58.197790 30.597789 780.00000	3.2208212 814.12049 0.2158183E 08 1.5835463 0.8185734E 08 280.68248 3.2208212 31.169250 58.319179 30.859178	0 0 0 0 0 0.2158183E 08 1.5835463 0.4185734E 08 280.68133 3.2208212 31.169250 58.319179 30.859178 826.00000
-38010.769 621.40588 1233.5948 2.0608637 14.078476 -10.219595	99.500004 42.500000 1041.7423 719.67327 58.997292 -2.7364286 0	-36406.338 983.75119 171.39251 2.1128588 12.784745 -11.917643 97.600001 42.200000 1044.6501 724.35887 59.615111	0 0 0 0 0 171.375119 171.39251 2.142758 12.784745 -11.917643 97.600001 42.200000 1044.6501 724.35887 59.672296 -2.6978571
77421.375 359112.83 54.429804 54.101485 28.605528 9.6831489	53.723474 59.063304 42133.489 96204.347 2.0608637 0.4360628 0 0 -208704.59 -514570.11	78037.719 360345.33 53.0345.33 53.03749 52.846965 28.627741 4.6281191 54.157149 59.542648 41165.729 94051.390 2.1128581 0.4360985	0 589751.66 -179760.81 78038.062 360352.40 53.009749 52.846965 28.627741 4.6281191 54.183101 59.569865 41165.729 94051.390 2.1142758 0.4360985 0
28.305532 -80.498178 94.26.2465 94.749709 91.607092 20.055011	58.010647 61.044076 50.380000 68.562999 2.3564341 3774.7585 254.39101 522.62182	28.305175 -80.492613 94.337140 94.895601 91.723411 20.055011 20.884874 50.380000 68.535799 2.1991587 2.3529638	260.68024 510.53974 28.305175 -80.492613 94.337140 94.337140 91.723411 20.055011 57.795889 60.892386 50.380000 68.535799 2.1992582 2.3529693 3904.4825 260.68024
0.1960529 -0.1105525 53.957243 0.7534127 -0.6308133E-01 2.2760558	886.12786 190.37016 0 1076.4980 0.1758991 3.5678214 350.33264 830.49998 0.7300000	-0.4436596E-01 -0.3533762E-01 52.449615 0.7538127 -0.6512023E-01 2.5711233 886.25642 190.19986 0 1076.4563 0.1709323 3.5118927	83C.69999 0.7420000 0.5800000 -0.4436596E-01 -0.3533762E-01 52.449615 0.6533552 -0.6512023E-01 2.5711233 886.29077 190.20075 0 1076.4915 0.1704819 3.5118927 3.5118927 3.516999 0.7420000
35914.250 0.2094578E 08 1476.5203 1482.6205 2508.4913 5.9107254	403.14074 80.787389 0 483.92812 0.7458803E-01 -3.5678214 694.28184 -0.6739856E-01	38360.000 0.209482E 1559.1994 1562.5499 2599.3485 6.3132440 402.99794 80.834163 0 483.83210 0.7247386E-01 -3.5118927	0.4587541E-01 -0.1149960 38360.000 0.209482E 08 1559.1994 1562.5499 2599.3485 6.3132440 402.99532 80.834353 0 483.82967 0.7228211E-01 -3.5118927 694.18685
0*1 69.999997 P 2 193375.74 1 3 1561.9846 6 2.2769209 5 0.2953583 6 179.62441	D 1 359112.83 E 2 75723.906 P 3 1697.4693 R 4 436534.20 O 5 -123.26088 6 213.91428 7 570.51235 D 1 436531.82 P 2 -513.50431 5 3 1203.1004	0*1 72.000000 P 2 190251.91 1 3 1561.8468 4 2.5719378 5 0.3076177 6 46.176349 D 1 360345.33 E 2 76334.428 P 3 1703.2918 R 4 438383.04 0 5 -119.76657 6 210.82857	0 1 438381.77 P 2 381.63768 5 3 -679.85899 D*1 72.000000 P 2 190127.91 1 3 1561.8796 4 2.5719378 5 0.3076177 6 46.176389 D 1 360352.40 E 2 76334.771 P 3 1703.2926 R 4 438390.46 0 5 -119.44965 6 210.82857 7 570.48617 0 1 438385.18 P 2 381.65210 5 3 -879.84770





1.9054108 800.99030 0.3314835E 08 2.0421567 0.1002913E 09 284.84699 1.9054108 31.955032 58.594589 31.694589	0 0 0 0 1.4136417 73.846455 0.3946415E 08 2.2693606 0.1019412E 09 286.36740 1.4136417 32.460587 32.460587 32.026358 1008.0000	1.4136417 733.84932 0.3946615E 08 2.2693606 0.1019412E 09 286.36740 1.4136417 32.460587 32.460587 32.026358 1009.0000
-26827.323 728.9931 1074.9363 2.3537276 17.754376 -11.310751 90.000004 41.000000 1056.2610 743.15416 62.939945 -3.2216854	0 0 0 0 0 0 0 104.52480 -604.52480 -604.52480 14.056833 -13.345383 -13.345383 -13.345383 -1062.0600 1062.0600 1752.55274 64.832405 -3.0980898	-20689.299 694.52480 -604.56066 2.4897463 14.056833 -13.345383 -13.345383 86.200002 40.400000 752.5274 64.832405 -3.0980898
80214.780 364714.47 47.704864 47.387495 28.418681 13.685203 56.266192 61.863307 37301.017 85434.026 2.3537274 0.4356134	0 49053.990 -51362.280 81006.406 366388.44 45.258921 45.155064 28.149349 4.4153482 57.520584 63.236619 35371.182 81121.520 2.4897462 0.4357279 0	81006.406 366388.44 45.258921 45.155064 28.149349 4.4153482 57.520584 63.236619 35371.182 81121.520 2.4897462 0.4357279 0 589977.91
28.303324 -80.465013 94.665470 94.950631 92.217043 20.055011 56.945216 60.324452 50.380000 68.426998 2.2051560 4351.9011	303.57721 481.51730 28.302113 -80.447586 94.689645 95.396637 92.396637 20.055011 56.678370 60.218370 60.218370 60.218606 2.3713606 2.3713606 4519.1694 314.92267	28.302113 -80.447546 94.689645 95.010857 92.396632 20.055011 56.678370 60.218215 50.38000 68.356998 2.2078606 2.3713692 4519.1694
0.1619624 -0.4513068E-01 47.142775 0.6633552 -0.7053696E-01 4.0348567 887.40678 190.55957 0 1077.9664 0.1562896 4.2714438	830.49997 0.8000000 0.6166666 -0.2288800 -0.2452971E-01 4.4689352 0.6633552 -0.7157366E-01 4.9593081 888.06609 190.23522 0 190.23522 0 1078.3013 0.156409 4.0922302 357.09929 0.8320000 0.6380000	-0.2288800 -0.2452971E-01 44.489352 0.5427452 -0.7157366E-01 4.9593081 888.06609 190.23522 0.1506409 4.0922302 357.09428 836.09999 6.8320000
49057.000 0.2095892E 08 1935.9767 1945.8123 3009.0066 8.0737438 402.42358 80.045456 0.6625932E-01 -4.2714438	0.1028109 0.7605617E-01 5498C.750 0.2096485E 2154.8955 2154.3918 9.0486677 402.22923 80.221678 0.482.45090 0.6386452E-01 -4.0922302 694.13302	54980.750 0.2096485E 08 2154.8955 2158.771 3244.3918 9.0486677 402.22923 80.221678 0.63.86452E-01 -4.0922302 694.13302 0.1134047E-01
041 79.999997 P 2 177633.37 1 3 1561.9939 4 4.0354576 5 0.3613634 6 134.67257 0 1 364714.47 F 2 78491.515 F 2 78491.515 R 4 444929.25 0 5 -109.49634 6 252.73483	0 1 444927.89 P 2 798.37482 S 3 550.61123 0*1 84.000000 P 2 171384.79 1 3 1562.3107 4 4.9598052 5 0.3914360 6 168.92526 0 1 366388.44 E 2 79275.870 P 3 1730.5368 R 4 447394.84 0 5 -105.53883 7 570.61189 1 447393.96 P 2 88.552048 P 2 88.552048	0*1 84.000000 P 2 171384.79 1 3 1562.3107 4 4.9598052 5 0.3914360 6 168.92526 1 366388.44 E 2 79275.870 R 447394.64 0 5 -105.53883 6 242.84719 7 570.61189 1 447393.96 P 2 88.552048 5 3 -797.43538



0.9	80 80	8 0 0	
0.8781079 621.06242 0.4902291E 2.648869 0.1023797E 288.00530 0.8781079 33.218918 58.721891 32.321891 1100.0000	0 0 0 0 0.3732913 417.78825 0.6380302E 3.3321451 0.8829805E 289.53931 0.3732913 34.598362 58.726708 1247.0000	0 0 0 0 0.3732913 417.78825 0.6380302E 3.3321451 0.8829805E 289.53931 0.3732913 34.598362 58.726708 32.726708 1248.0000	, 0
-13724.656 -1046.9921 2262.2521 2.6932505 52.078544 1.7816021 80.500004 39.500000 1070.7606 766.69379 67.237117	0 0 0 0 -5864.0319 -278.35962 3.0529718 50.531514 -0.6184507 71.000002 38.00000 1085.2409 790.34962 71.240017	0 0 0 0 -359.07388 -278.35962 3.0529718 50.531514 -0.6184507 71.000002 38.000000 1085.2409 70.5409 70.5409 70.5409	• •
81856.938 368214.56 41.943488 41.170140 27.637731 52.048060 59.193958 65.087443 32476.428 74650.546 2.6932502 0.4358995	-898758.25 -674946.99 -674946.99 370022.88 37.106089 36.575709 26.462590 50.527729 62.064084 68.269659 27658.672 63.0529715	0 349172.89 -119356.35 -119356.35 -119356.35 82732.088 37.106089 36.575709 26.462590 50.527729 62.064084 68.269659 27658.672 63852.851 3.0529715 0.4352002	349112.03 -119356.35
28.299865 -80.416162 94.932760 94.573563 92.768343 20.055011 56.189951 59.970090 50.380000 68.251999 2.2112626 2.3574958		4873.0301 331.04511 466.48006 28.294727 -80.347588 95.144146 94.864855 93.252341 20.055011 55.608608 59.813499 50.380000 68.06999 2.2159070 2.4013420 4873.0301 331.04511	0000+
0.5471212 -0.3897452 41.232882 0.5427452 -0.7006521E-01 6.6265729 888.89971 189.78486 0 1078.6846 0.1435359 3.8234101 358.66869	825,49999 0.8800000 0.6700000 -0.1873564 -0.2396710 35.805429 0.5427452 -0.5418506E-01 10.266196 890.27828 190.69325 0.1338362 4.9185999	360.02112 825.49999 0.9800000 0.7300000 0.7300000 35.805429 0.3316776 -0.5418506E-01 10.266196 890.27828 190.69325 0.1338362 4.9185999 360.02112 825.49999	0.7300000
64623.000 0.2097449E 08 2523.0804 2561.7915 3635.4705 10.635578 401.98740 80.489079 0.6085233E-01 -3.8234101 693.87267	-0.9282521E-01 0.3994690 82836.750 0.2099271E 08 3244.0965 3284.4287 4392.0134 13.633176 401.76698 79.411119 0 481.17810 0.5674614E-01	694.25728 0.1061975 -0.6110547E-02 82836.750 0.2099271E 08 3244.0965 3284.4287 4392.0134 13.633176 401.76698 79.411119 0.6574014E-01 -4.9185999 694.25728 0.1061975	
D*1 89,999997 P 2 162009,71 1 3 1562,7195 4 6,6269175 5 0,4412073 6 417,18775 D 1 368214,56 E 2 80118,702 P 3 1736,2364 R 4 450071,50 O 5 -100,56106 6 228,01573 7 570,70670	0 1 450057.40 P 2 -729.14117 5 3 3138.0305 0 1 100.00000 0 2 146378.68 1 3 1563.7081 4 10.266299 5 0.5384671 6 127.09540 D 1 370022.88 F 2 80987.238 P 3 1744.8504 R 4 452754.97 C 5 -93.765494 6 288.43999	0.00 0 0 0 0 0 0 0 0 0 0 0 0 0 0 0 0 0	2 839-1780 3 -48.28583

0.1382768 240.41963 0.7591387E 08 4.1531726 0.6461732E 08 290.13695	0.1382768 34.598362 58.661722 32.661723 1339.0000 0	0.1132131 211.99531 0.7784418E 08 4.3100717 0.5960296E 08 290.22416 0.1132131 34.598362 58.626786 32.586786 1381.0000	0.1132131 211.99531 0.7784418E 08 4.3100717 0.5960296E 08 290.22416 0.1132131 34.598362 58.626786 32.586786 1382.0000
-817.89899 -20.406121 1050.3627 3.4720770 81.007221 -9.8999945	61.500006 36.500000 1099.6938 814.55772 78.201544 -4.2224985 0	-106.20795 -23.899064 926.48615 3.2657082 81.007221 -9.8999945 59.600001 36.2000000 1102.5736 819.42146 79.617698 -5.0074999	-106.20795 -23.899064 924.48615 3.5657082 81.007221 -9.8999945 59.600001 1102.5736 819.42146 79.617698 -5.0074999
83163.939 371546.97 33.168719 32.561096 25.164263	64.983003 71.559996 22851.902 53021.137 3.4720776 0.4346868 0 -341291.73 53099.321	83275.170 371784.33 32.495080 31.924701 24.918927 80.400000 65.569366 72.229335 21894.140 50846.828 3.565074 0.4339599 0	83275-170 371784-33 32-495080 31-924701 24-918927 80-400000 65-569366 72-22935 21894-140 50846-828 3-5697074 0-4339599 0
28.287572 -80.254949 95.288598 95.115643 93.642538	55.075521 59.775286 50.380000 68.060999 2.2304088 2.4360382 4952.9670 391.89264 488.04763	28.285867 -80.23159 95.312285 95.132676 93.710711 20.055011 24.951464 59.761785 50.380000 68.060999 2.2333777 2.4975342 4961.4921	28.285867 -80.233159 95.312285 95.312285 93.712711 20.055011 54.951464 59.761785 50.380000 68.060999 2.2333777 2.4975342 4961.4921
0.6297035 -0.1067720 32.488655 0.3316776 -0.2329492E-01 15.184417	894.55809 191.49406 0 1086.0521 0.1035511 5.7782474 360.78038 820.49998 1.0933333 0.8100000	0.629370 -0.1072034 31.825298 0.331676 -0.1520386E-01 16.341397 895.43654 192.82417 0 1086.2607 0.9735098E-01 7.1157498 360.86115	0.629370 -0.1072034 31.825298 0.2713726 -0.1520386E-01 16.341397 895.43654 192.82417 0.9735098E-01 7.1157498 360.86115 819.29999 1.1186667 0.8300000
103822.50 0.2101370E 08 4108.7977 4176.8026 5286.6202 17.086986	401.07361 78.544322 0 479.61793 0.4390069E-01 -5.7782474 694.63880	108378.50 0.2101826E 08 4300.7429 4369.2462 5483.6980 17.836807 400.93377 77.205817 0 478.13958 0.4127215E-01 -7.1157498 695.23403 0.1177559	108378.50 0.2101826E 08 4300.7429 4369.2462 5483.6980 17.836807 470.93377 77.205817 0 478.13558 0.4127215E-01 -7.1157498 695.23403
D#1 110.00000 P 2 130724.61 1 3 1567.2285 4 15.184375 5 0.6569918 6 153.55361	D 1 371546.97 E 2 81415.316 P 3 1748.5635 R 4 454710.91 D 5 -72.547753 6 335.02486 7 572.08279 D 1 454703.82 P 2 1405.4716 5 3 1812.5205	0*1 112.00000 P 2 127589.42 1 3 1567.9587 4 16.341340 5 0.6835804 6 135.33801 D 1 371784.33 E 2 81526.212 P 3 1784.33 F 455059.50 0 5 -68.203983 6 405.59999 7 572.32082	#1 112.0000 2 127589.4 4 16.34.958 4 16.37.958 5 0.683580 6 135.3380 6 135.3380 6 135.3380 6 135.3380 7 572.3398 7 65552.8 1 455052.8 1 455052.8

*

0.5008224E-01 123.29157 0.8407769E 08 4.9419070 0.4132525E 08 290.27877	0.5008224E-01 34.598362 58.449916 32.249917 1435.0000	0.1743915E-01 59.541084 0.8912985E 08 5.8198995 0.2467363E 08 290.12980 0.1743915E-01 34.598362 58.382560 31.682561 1477.0000	0 0 0 0 0 0 0 1403299E-01 52.08704 0.2250557E 08 290.08723 0.1403299E-01 34.598370 58.345966 31.445967 1522.0000
2076.0753 -26.517287 687.17193 3.9827958 81.007221 -9.8999945	52.000007 35.000000 1114.0498 838.93031 85.816302 -5.3999999	3591.8757 -17.480006 4.6415567 41.007221 -9.8994945 42.500008 33.500001 1128.3802 863.43147 -5.399999	3768.5769 -16.259134 181.74630 4.7981248 81.007221 -9.8999945 40.600002 33.200000 1131.2461 868.34584 97.380700 -5.3999999
83407.472 372676.64 30.112420 29.665610 23.994365	68.129482 75.159080 18077.570 42119.657 3.9827964 0.4335965 0 -228889.20	83466.654 373841.88 27.588688 27.351969 22.950859 80.400000 72.052947 79.666346 13314.575 31162.472 4.6415563 0.4335965	0 -68987.466 9726.4092 83472.563 374075.25 27.258000 22.754069 80.400000 72.872801 80.624950 12363.057 28963.618 4.7981248 0.4335965 0
28.278013 -80.133874 95.410323 95.205853 93.967766 20.055011	54.392137 59.694948 50.380000 68.060999 2.5464195 2.5350932 4982.9652 416.80429	26554 54158 54158 30894 30894 30899 30899 30809 308099 4-068	436.72728 503.42917 28.262651 -79.43766 95.331303 94.319118 20.055011 53.554498 59.820034 50.380000 68.060998 2.5351049 4995.2268 432.51684
0.8345654 -0.1080218 29.654319 0.2713726 0.2381848E-01 21.613858	899.30342 193.62590 0 1092.9293 0.7011673E-01 7.9399997 361.06385 814.49998 1.2199999	0.6078844 -0.1089386 -26.940593 0.2713726 0.8993392E-01 29.82695 905.17761 193.63243 0 1098.8100 0.2936173E-01 7.939998	796.49999 1.393332 1.0699999 0.5142667 -0.1092412 26.397846 0.213726 0.1058057 31.712221 906.42423 193.63241 0 1100.0566 0.2058606E-01 7.9399997 361.18320 792.89999
127904.75 0.2103779E 08 5138.7155 5208.9130 6339.8630 21.050415	400.32746 76.378215 0 476.70567 0.2972613E-01 -7.939997 695.47523 0.1832561	155529.50 0.2106543E 6368.1218 6439.9314 7587.9616 25.556864 399.47159 76.3E0358 0 475.85194 0.1244797E-01 -7.935998	0.1950672 0.1683508 161527.25 0.2107143E 08 6642.5963 6714.6787 7865.7748 26.583966 399.28114 76.380434 0 475.66157 0.8727504E-02 -7.939997 695.52384 0.1976454
0*1 120.00000 P 2 115033.21 I 3 1571.1934 4 21.613785 5 0.8006616 6 103.75298	0 1 372676.64 E 2 81657.522 P 3 1749.9499 R 4 456084.11 O 5 -49.123694 6 436.99998 7 573.37318 O 1 456077.73 P 2 1458.7346 5 3 1619.9242	*1 129.9999 2 1976.744 4 29.82620 5 0.974017 6 36.77062 1 373841.8 1 373841.8 4 457368.5 6 436.9997 7 574.9997	0 1 457302.87 P 2 1556.9234 5 3 1343.6858 0 1 132.00000 P 2 96143.960 1 3 1577.2767 4 31.77.2767 6 37.384243 6 27.384243 6 27.384243 6 27.384243 7 575.34138 7 575.34138 7 575.34138 7 575.34138

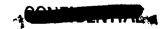
0.1403299E-01 52.087046 0.8986292E 08 6.0681943 0.2250557E 08 290.08723	0.1403299E-01 34.598370 58.345966 31.445967 1523.0000 0	0.5455301E-02 29.919180 0.9217494E 08 7.3762429 0.1526615E 08 289.82277 0.5455301E-02 34.504475 58.194544 30.494545 1579.0000	0.4236529E-02 25.976219 0.9259921E 08 7.792455 0.1378277E 08 289.69246 0.4236529E-02 34.469185 58.083007 30.815237 1627.0000
3768.5769 -16.259134 181.74630 4.7981248 81.007221 -9.8999945	40.600002 33.200000 1131.2461 868.34584 97.380700 -5.3999999	4293.5477 -11.725822 90.113364 5.5445865 81.007221 -9.8999945 33.000008 32.000001 1142.9212 888.03210 107.61306 -5.3999999	4386.8190 -10.308137 69.797919 5.7566136 81.007221 -9.8999945 31.214708 31.214708 31.718112 114.82030 -5.3999999
83472.563 374075.25 27.258000 26.941560 22.754069	72.872801 80.624950 12363.057 28963.618 4.7981248 0.4335965 0 -49719.153 8106.5056	83490.743 37525.34 25.735468 25.481408 22.038323 80.400000 76.962441 85.377053 851.2512 20149.411 5.5445864 0.4335965 0	83489.146 375704.14 25.419181 25.419181 25.419181 25.419181 80.400000 78.731556 81.334471 7669.5076 18057.486 5.7566133 0.435965 0
28.262651 -79.943766 95.569283 95.331303 94.319118 20.055011	53.554498 59.820034 50.380000 68.060998 2.2701404 2.3551049 4995.2268 432.51684 501.89474	28.249502 -79.784641 95.685866 95.427241 94.54048 20.055011 52.747653 59.894597 50.380000 68.013998 2.2916091 2.5352634 4998.1444	88.24 44.13 6.0591 6.0591 6.0591 6.0591 6.0591 6.0591 6.0591 6.0591 6.0591
0.5142667 -0.1092412 26.397846 0.2110676 0.1058057 31.71221	906.42423 193.63241 0 1100.0566 0.2058606E-01 792.89999 1.4280000	0.4559739 -0.1111630 24.709307 0.2170676 0.1795291 40.167442 912.83003 193.64279 0 1106.4728 0.9693052E-02 7.939998 361.23143	1.2599999 0.4068391 -0.1118575 24.312655 0.2310676 0.194283 42.382753 42.382753 915.59789 193.63386 0 1.09.2318 7.939998 361.24060 765.48636 1.6634468 1.6634468
161527.25 0.2107143E 08 6642.5963 6714.6787 7865.7748 26.583966	399.28114 76.380434 0 475.66157 0.8727504E-02 -7.9399997 695.52384 0.1976454	187286.75 0.2109721E 08 7856.4606 7929.4821 9091.5914 30.823435 398.33584 76.379750 0.4120998E-02 -7.939998 695.55748	193784.50 0.2110371E 08 8172.4529 8245.6636 9410.0952 31.892827 397.93916 76.376708 0 474.31587 0 -7.9359998 695.52660 0.2144120
0*1 132.00000 P 2 96143.960 1 3 1577.2767 4 31.712270 5 1.0127279 6 27.384243	D 1 374075-25 E 2 81722-030 P 3 1750-5335 R 4 457547-81 O 5 -14-422571 6 436-9998 7 575-34138 D 1 457542-15 P 2 1578-3266 5 3 1321-7146		P Z 1088.9411 5 3 1362.1093 BEGIN BOOSTER DECAY 0*1 141.87926 P 2 80528.882 1 3 1585.1061 4 42.383048 5 10.265490 6 10.960281 D 1 375704.14 E 2 81738.332 R 4 459193.29 R 4 459193.29 C 436.99999 7 577.79671 D 1 459186.84 P 2 1718.3749 5 3 1373.8065

•

0.4236529E-02 25.976219 0.9259921E 08 7.7992455 0.1378277E 08 289.69246	0.4236529E-02 34.469185 58.083007 30.815237 1629.0000	0.3296921E-02 21.205621 0.9294685E 08 7.9880532 0.1133504E 08 307.37687 0.3296921E-02 34.435753 57.977102 31.118902 1854.0000	0 0 0.3296921E-02 21.205621 0.9294685E 08 7.9480532 0.1133504E 08 307.37687 0.3296921E-02 34.435753 57.977102 31.118902 1855.0000
4386.8190 -10.308137 69.797919 5.7563255 81.007221 -9.8999945	31.214708 31.718112 1145.8246 892.63190 137.13160 -5.3999999	4499.4861 -8.0839808 99.041218 1.0973489 81.007221 -9.8999945 30.560654 31.451000 1146.5996 893.90269	0 0 0 0 0 4499.4861 -8.0839808 99.041218 11.0973489 81.0073489 81.6999945 31.560654 31.51000 1146.5996 893.90269 15.131007 -5.3999999
377454.95 81738.301 25.419181 25.177662 21.887357 80.400000	78.728235 99.300896 7669.5076 18057.486 5.7563259 0.4335965 0 -15863.483 3444.9427	1749.6677 81234.123 25.119306 24.882207 21.649071 80.400000 25.146922 41.589726 7435.0162 17487.162 1.0973490 0.4335965	2946.1647 2946.1647 1749.6677 81234.123 25.119306 24.882207 21.649071 80.400000 25.146922 41.589726 7435.0162 17487.162 17487.162 10973490 0.4335965 0
28.246017 -79.742957 95.714700 95.451375 94.591716 20.055011	52.412944 59.809906 50.380000 68.078885 2.308489 2.5352470 4948.5590 444.13515 506.22935	28.242609 -79.702397 95.745293 95.746019 94.621459 20.055011 46.837747 48.733476 50.380000 68.083514 0	440.32893 506.47728 28.242609 -79.702397 95.745293 94.621459 20.055011 46.837747 48.733476 50.880000 68.083514 2.5273584 4998.8785 440.32893
0.4068391 -0.1118575 24.312655 0 0.1994283 42.382753	915.59789 193.63378 0 1109.2317 0 7.9399998 361.24059 765.48636 1.6634468	0.7447207 -0.1095624 24.312655 0 0.2190349 44.538476 0 192.32026 0 192.32026 0 192.32026	759.78798 1.7109333 1.3405200 0.7447207 -0.1095624 24.312655 0.2190349 44.538476 0 192.32026 0 192.32026 0 192.32026 0 7.9399998 361.00615 759.78798 11.7109333 1.3405200
193784.50 0.2110371E 08 8172.4529 8245.6636 9410.0952 31.692827	397.93916 76.376691 0 474.31585 0 -7.9399998 695.52633 0.2144120	200022.00 0.2110995E 08 8233.4742 8306.8647 9473.9805 32.919387 0 76.095363 0 76.095363	0.2212744 0.2100168 200022.00 0.2110995E 08 8233.4742 8306.8647 9473.9805 32.919387 0 16.095363 0 16.095363 0 16.095363 0 0.2212744 0.2212744
0*1 141.87926 P 2 80528.882 1 3 1585.1060 4 42.383048 5 1.2265490 6 10.960281	D 1 375704.14 E 2 81738.301 P 3 1750.8142 R 4 459193.25 D 5 0 6 436.59999 7 577.79671 D 1 459163.64 P 2 1718.2885 S 3 1373.7389 END 800STER DECAY	0*1 143.66000 P 2 79721.291 1 3 269.97408 4 44.538830 6 12.689589 6 15.962216 D 1 0 E 2 81234.123 R 4 82983.790 6 436.59999 7 0.1670513E-01	0 1 82982.587 P 2 320.47763 5 3 304.17278 0*1 143.66000 P 2 79721.291 1 3 269.97408 4 44.538830 5 12.68930 6 15.962216 1 0 0 E 2 81234.123 P 3 1749.6677 R 4 82983.790 6 436.9999 6 436.9999 7 0.1670513E-01 P 2 320.47763 5 3 304.17278

4	CONCIDENT

0.2693984E-02 17.928368 0.9317436E 08 8.1253605 9619093.2 307.38057 0.2693984E-02	34,409454 34,409454 31,357505 1889,0000	000	0,2693984E-02 17,928368 0,9317436E 08 8,1253605 9619093,2 308,91942	0.2693984E-02 34.409454 57.893705 31.357505 1892.0000	000	0.1281268E-02 9.6752533 0.9372681E 08 8.6552763 5265308.6	0.1281268E-02 34.317448 57.601118 32.191917 1926.0000	000
4576.8705 -6.5914937 111.33262 1.1035186 81.007221 -9.8999945	31.241000 1146.9602 894.50337 15.3999999	000	-398.28766 -4.5431647 100.92751 1.1472364 81.007221	0 31.241000 1146.9602 894.50337 16.940733 -5.3999999	0 00	-214.94059 -1.9861772 102.34720 1.1710559 81.007221 -9.8999945	0 30.506000 1148.2220 696.61456 19.310499 -5.3999999	000
1749.6942 81231.550 24.885732 24.651568 21.456987 80.400000	41.8788 7328.4847 17217.920 1.1035186 0.4335965	-30934.578 2582.9734	1749.7051 81236.175 24.885732 24.651568 21.456987 80.400000	0 42.419498 7328.4847 17217.920 1.1472363 0.4335965	0 -27077.188 2822.1667	1749,7874 81226,141 24,088884 23,864960 20,804523 80,400000	0 43,449690 6955,6415 16275,609 1,1710559 0,4335965	0 -30739.068 1671.2987
28.239901 -79.670302 95.769596 95.499256 94.643554 20.055011 46.749217	48.655231 50.380000 68.087155 0 2.5273335 4999.0836	43/ _{-15/36} 506 ₋₆₃₀₃₃	28.239901 -79.670302 95.769596 95.499256 94.643554 20.055011	0 48.753485 50.380000 68.087155 0 2.5274062	379-35316 381-32268	28.230213 -79.556559 95.857449 95.576365 94.723979 20.055011	0 48.471570 50.380000 68.099895 0 2.5273221	364.41623 381.29531
1.0088991 -0.1075611 24.312655 0 0.2347615 46.24410 0	192,31146 0 192,31146 0 7,9399998 361,01159	155.30799 1.7482666 1.3713200	1.008891 -0.1075411 24.312655 0 0.2347615 46.244410	0 192.32348 0 192.32348 0 7.939998 361.01381	689,46999 0,9251800 1,3753000	1.9141677 -0.9843878E-01 24.312655 0 0.2921421 52.291050	0 192.29313 0 192.29313 0 7.9399998 361.03064	687.01999 0.9398800 1.3998000
204900.75 0.2111483E 08 8264.4025 8337.9316 9507.1560 33.722326 0	76.092633 0 76.092633 0 -7.9399998 691.19325	0.2188126	204900.75 0.2111483E 08 8264.4025 8337.9316 9507.1560	0 76.095197 0 76.095197 0 -7.9399998	0.1051755 0.1865798	221792.50 0.2113173E 08 8383.2032 8457.1969 9633.4974 36.502351	0 76.085722 0 16.085722 0 -7.9399998 691.12762	0.1047757 0.1932037
1 145.06000 2 79343.336 3 269.96255 46.244815 1 1.3024867 1 18.190376 0			145.06000 71987.775 268.63277 46.244815 1.3024867 18.190376	0 81236.175 1749.7051 82985.880 0 436.99999 0.1670513E-01	82985,286 152,33286 270,23683	149.96000 70671.572 268.59295 52.291647 1.4210998 18.544494	0 81226.141 1749.7874 82975.928 0 436.99999 0.1670513E-01	82975-302 151-73554 279-79712
10 m 0 m 0 m 0 m 0 m 0 m 0 m 0 m 0 m 0 m		300		□ M O M O O O O O O O O O O O O O O O O	0 d 20 11 2 W	0 d - 1 0 w 4 20 0	O W O & O	0 P 2 5 3



- ONIT DENTINA

-214.94059 7.980308 50.780005 11.710572 81.007221 -9.8999945 0 0 1148.2220 896.61456 19.310533 -5.3999999 0 0 0 0 0 0 0 0 0 0 0 0 0 0 0 0	0
1749.7874 81226.141 24.088884 23.864960 20.804523 80.400000 0 43.449707 6955.6415 16275.609 1.1710572 0.4335965 0 -1344.460 4718.1420 1749.7880 8122.6.053 24.082330 23.85848 80.400000 0 43.458073 6952.5984 1626.919 1.1712498 0.04335965 0 -14167.644 5076.9587 1749.9039 81193.173 22.634534 22.6335965 0 43.345477 0.4335965	4947.9620
28.230213 -79.556559 95.857449 95.976365 94.723979 20.274927 0 48.471573 50.380000 68.099895 0.5273212 0.5273212 0.68.099999 0.68.099999 0.2.5273215 0.28.209517 48.469260 68.099999 0.2.5273215	
0. 9377259 0. 1049550 23.336219 1. 2470491 0. 2921421 52. 291050 0 192. 29313 0 192. 29313 0 192. 29313 0 192. 29313 0 192. 29313 0 192. 29313 0 0. 9946426 0. 1318016 23.3458999 0. 9946426 0. 1388709 1. 3998999 0. 9946426 0. 1388709 1. 2999999 0. 9400000 1. 40000000 1. 40000000 1. 40000000 1. 40000000 1. 40000000 1. 40000000 1. 40000000 1. 40000000 1. 40000000 1. 40000000 1. 40000000 1. 40000000 1. 40000000 1. 40000000 1. 40000000 1. 40000000 1. 40000000 1. 40000000 1. 40000000 1. 400000000 1. 400000000 1. 400000000 1. 400000000 1. 400000000 1. 4000000000000000000000000000000000000	1.4756960
221792.50 0.2113173E 08 8383.2032 8457.1969 9633.4974 36.502351 0.6.085722 0.1087833 0.1087833 0.1087833 0.1087833 0.1087833 0.1087833 0.1087833 0.1085645 0.1703244 0.1703245 0.1703245 0.1703245 0.1703245 0.1703245 0.17032645 0.1704255 0.1714225 0.255488.25 0.1714225	
	5 3 264.88273

A.A.	
"	

0.2252039E-03 2.2718402 0.9417438E 08 10.003931 1274291.6 308.93327	0.2252039E-03 34.129669 56.802973 32.299374 1988.0000 0	0.2234756E-03 2.2572568 0.9417517E 08 10.010255 1266269.0 308.93328 0.2234756E-03 34.128922 56.799776 22.299776	0 0.3036552E-04 0.3455333 0.9426720E 08 10.624887 200120.56 308.93183 0.3036552E-04 33.941143 55.799970 32.299969 2046.0000
-50.470066 15.377543 69.019829 1.2192477 81.007221 -9.8999945	0 29.006000 1150.8718 900.93486 20.737648 -5.3999999	-50.146088 15.252473 68.541359 1.2194431 81.007221 -9.8999945 0 29.000001 1150.8827 900.95213 20.743291 -5.3999999	0 0 1.8594637 10.2695647 10.2695647 81.007221 -9.8999945 0 27.500001 1153.6532 21.958819 -5.3999999
1749,9039 81193,173 22,634534 22,429673 19,618159 80,40000	0 43.940578 6194.9068 14353.108 1.2192477 0.4335965 0 0 -19341.995	1749,9043 81193.036 22,628936 22,424149 19,613595 80,400000 0,43,942515 6191,8647 14345,421 1,2194431 0,4335965 0	-19206.961 4973.8473 1749.9847 81149.132 21.251595 21.064726 18.468795 80.400000 0 44.333764 5431.4031 12423.909 1.2695547 0.4335965 0 -2772.9939 604.40023
28,209517 -79,317452 95,969178 95,667006 94,830535 21,613437	0 47.688020 50.380000 68.125895 0 2.5270047 0 388.25328 384.95829	28.209431 -79.316477 95.969642 95.667365 94.830976 21.611071 0 47.684862 50.380000 68.125998 0 2.5270034 0	384.95128 28.187522 -79.067693 96.096657 95.773297 94.951149 21.341142 0 46.692647 50.380000 68.151999 0 2.5265375 0 386.66686
5.0319546 1.3194320 25.752568 -0.2170110 0.4138775 65.005762	0 192.20691 0 192.20691 0 7.9399998 361.05446 676.24318 0.9798400	5.0298378 1.3170945 25.743894 -0.2166517 0.4143712 65.057631 0 192.20657 0 7.9399998 361.05455	0.9800000 1.4759999 4.9312296 1.0405019 24.02501 -0.126828 0.5365364 78.291817 0 192.09579 0 192.09579 0 7.939998 361.07098 665.39999 1.5519999
255488.25 0.2116545E 08 8641.9751 8716.7780 9905.8162 42.047958	0 76.061161 0 76.061161 0 -7.935998 690.83247 0.1112527	255621.25 0.2116558E 08 8643.0554 8717.8613 9906.9476 42.069847 0 76.061063 0 76.061063 0 7.9399998 690.83128	0.1825984 288400.00 0.2119838E 08 8924.9739 9000.5022 10201.154 47.464535 0 76.031240 0 76.031240 0 0.1078827 0.1661898
0*1 159,96000 P 2 67986,195 1 3 268,48217 4 65,006801 5 1,6694172 6 11,814363	1 0 2 81193.173 3 1749.9035 5 0 182943.076 6 436.99999 7 0.1670513E-01 1 82942.484 2 161.05185 3 264.56012		F 2 160.98796 5 3 264.33345 041 165.99999 P 2 65291.343 1 3 268.34113 5 1.9274075 6 1.7410565 6 1.7410565 1 749.9847 R 4 82899.116 0 5 0 6 436.59999 7 0.1670513E-C1 0 1 82898.610 P 2 155.80128
0 & ~		Q 4 	מיע סַמייי טיחידיגט טיליע



	The state of the s
TOTAL	

0.2164278E-04 0.2490738 0.9427177E 08 10.685067 145071.70 308.93118 0.2164278E-04 33.908848 55.576378 32.299978	0 0 0 0.2164278E-04 0.2490738 0.9427177E 08 110.685067	0.2164278E-04 33.908848 55.576378 32.299978 2077.0000	0.4717097E-05 0.5012373E-01 0.9428112E 08 10.267247 30038.573 308.92809 0.4717097E-05 54.499995 33.753365 54.499995 2102.0000
-5.5332985 1.3575226 7.5062259 1.2784719 81.007221 -9.8999945 0 27.242000 1154.1393 1054.00820 22.171682 -5.3999999	0 0 0 2.1273192 6.3648424 1.3031321 81.007221	0 27.242000 1154.1393 906.00820 22.792469 -5.3999999	-1.1135236 0.2442007 1.7297105 1.3495718 81.00721 -9.8999945 0 26.000001 1156.5539 909.57455 -5.3999999
1749,9925 81139,158 21.021062 20.837168 18.300278 80.400000 0 44.402901 5300,6346 12093,525 1.2784719 0.4335965	-2011,6221 437,92041 1749,9981 81141,530 21,021062 20,837167 18,300278	0 44.696724 5300.6346 12093.525 1.3031320 0.4335965 0 -2188.0710 649.04272	1750.0353 811093.434 19.961176 19.791080 17.435264 80.400000 0 45.060406 4671.2674 10503.634 1.3495718 0.4335965 0
28.183620 -79.023890 96.119612 95.792627 94.972841 21.359342 0 46.469842 50.380000 68.156470 0 2.5264199	387.73414 384.16321 28.183620 -79.023890 96.119612 95.792627 94.972841	22.008304 0 46.521795 50.380000 68.156470 0 2.5264573 0 394.95061 386.01665	28.164272 -78.208665 96.2025278 95.880940 95.073740 21.260047 0 45.448225 50.380000 68.177999 0 2.5258901 0 396.84588 343.80950
4.9989934 1.0544031 23.821645 -0.1113769 0.5578567 80.622444 0 192.07055 0 192.07055 0 7.9399998 361.07258	663.54239 1.0268800 1.5650720 5.4571823 1.6722167 24.284797 -0.1875684 0.5578557	0 192.07671 0 192.07671 0 7.9399998 361.07372 663.54239 1.0268800 1.5650720	5.5775167 0.9365026 23.132205 -0.1045595 0.6609394 92.076468 0 191.95511 0 191.95511 0 7.9399998 361.08131 653.09999 1.0640000
293947.25 0.2120393E 08 8975.8356 9051.4811 10254.020 48.377495 0 76.024791 0 76.024791 0 -7.9399998 690.37006	0.1078270 0.1660334 0.1660334 293947.25 0.2120393E 8975.8356 9051.4812	0 76.C26107 0 76.C26107 0 -7.939998 690.39024 0.1080930	320309.75 0.2123032E 9237.0756 9313.2421 10524.329 52.716205 0 75.995037 0 75.995037 0 75.999998 689.98077 0.1091721 0.1680433
1 171.72000 2 64829.822 2 268.30944 4 80.624016 5 1.9725140 6 1.2722395 1 0 2 81139.158 3 1749.9925 4 82889.150 6 436.59999 7 0.1670513£-01	1 E2888.643 2 155.99129 3 240.19780 1 171.72000 2 63604.822 4 80.624016 5 1.972514C	1 0 2 81141.530 3 1749.9981 4 82891.528 5 0 436.59999 1 0.1670513E-C1 1 82891.019 2 156.38067 3 240.5263C	1 179.99999 2 61383.791 3 61383.791 5 68.16425 5 2.1935618 6 0.2834305 1 0 0 0 0 0 0 0 0 0 0 0 0 0 0 0 0 0 0 0
	040 04-		



	NO.	
* • • • • • • • • • • • • • • • • • • •		

0.2500467E-05 0.2536565E-01 0.9428246E 08 10.031876 15415.504 0.2500467E-05 33.678997	32.29997 2138.0000 0 0	0.250046/E-05 0.2536565E-01 0.9428246E 08 10.031876 15415.504 306.92607 0.2500467E-05 33.678997 53.905997 2141.0000	000	0.1043130E-05 0.980158E-02 0.9428340E 08 9.6549072 6087.9615	0 0 0 0 0 0 0 0 0 0 0 0 0 0 0 0 0 0 0
-0.5635106 0.1234966 0.9151411 1.3728920 81.007221 -9.8999945 0 25.406000	911.27843 24.420465 -5.3999999 0	-0.5635106 0.1234966 0.9151411 1.3745808 81.007221 -9.8999945 0 25.406000 1157.7754 911.27843 24.462218	5.3999999 0 0 0	-0.2177465 0.5299308E-01 0.3749056 1.4118419 81.007221 -9.8999945	24.506001 1159.7076 913.87397 25.312187 -5.3999999
1750.0441 81065.678 19.47404 19.310596 17.037537 80.400000 0 45.242815 4370.3602	9743.6249 1.3728920 0.4335965 0 0 -220.62623 38.555439	1750.0444 81066.832 19.47404 19.310596 17.037537 80.400000 0 45.262587 4370.3602 9743.6249	0.4335965 0 0 -220.62623 38.555439	1750.0576 81025.890 18.760216 18.60216 16.453644 80.400000	0 45.554422 3911.5305 8584.9379 1.4118418 0.4335965 0 0 -85.698168 15.830154
28.154663 -78.703108 96.281992 95.929336 95.127479 21.266625 0 44.852823 50.380000	68.188295 0 2.5255596 0 400.02328 383.80747	28.154663 -78.703108 96.281992 95.929336 95.127479 21.266625 0 44.856202 50.380000 68.188295	2.5255620 0 400.02328 383.80747	28.139540 -78.538732 96.367897 96.002604 95.209130 21.393719	43.945.216 50.380000 68.203999 0 2.525057 0 404.55706
5.7792558 0.9358240 22.745321 -0.9396356E-01 0.7111145 97.695623 0	191.88723 0 7.9399998 361.08312 647.63519 1.6688480	5.779258 0.9358240 22.745321 -0.9396356E-01 0.7111145 97.695623 0 191.88763 0	7,9399998 361,08319 647,63519 1,6688480	6.0454653 1.0455839 22.139122 -0.1140688 0.7889973 106.44782	0 191.78375 0 191.78375 0 7.939997 361.08588 639.30000 1.1119999
332727.25 0.2124274E 08 9368.0630 9444.4507 10659.369 54.759862 0 75.978102	75.978102 -7.9359998 689.75310 0.1059969	332727.25 0.2124274E 08 9368.0530 9444.4507 10659.369 54.759862 0 75.978188	-7,939998 689,75441 6,109969 0,1696957	351443.00 0.2126147E.08 9575.8160 9652.5427 10872.997 57.840079	0 75.952286 0 75.952286 0.7.939997 689.40603 0.1112690
183.96000 60322.027 268.07943 97.697765 2.3016316 0.1484784 0 81066.678 1750.0441		163.96000 60248.027 268.07991 97.697765 2.3016318 0.1484784 0. 81066.832 1750.0444 82816.876		189,99999 58629,217 267,95013 106,45025 2,4694904 0,6012180E-01	0 1750-890 1750-0576 82775-946 0 436-99998 0.1670513E-01 82775-403 160.75096 249.03952
O d a a a a a a a a a a a a a a a a a a	•			# C = = = = = = = = = = = = = = = = = =	O 4 4 6 6 6 7 7 7 7 7 7 7 7 7 7 7 7 7 7 7



CONFIDENTIAL

0.5187425E-06 0.3396376E-02 0.9428377E 08 8.0593816 2160.7643 308.91986	0,5187425E-06 33,443718 52,091399 32,299999 2203,0000	000	0.5187425E-06 0.3396376E-02 0.9428377E 08 8.0593816 2160.7643 308.92035 0.5187425E-06 33.443718 52.091399 32.299999	000	0.3913642E-06 0.2233373E-02 0.9428386E 08 7.5241905 1440.6316 308.91866	0.3913642E-06 33.377808 51.60000 32.29999 2222.0000
-0.754520E-01 0.1623956E-01 0.1288981 1.4542639 81.007221 -9.8999945	0 23.526500 1161.9297 916.67464 26.263580 -5.3999999	000	-0.7545220E-01 0.159706E-01 0.1319033 1.5074723 81.007221 -9.8999945 0 23.526500 1161.9297 916.67464 27.554563 -5.3999999	000	-0.4961549E-01 0.1055120E-01 0.8199426E-01 1.5333230 81.007221 -9.8999945	0 23.000001 1163.2179 918.24320 28.117105 -5.3999999
1750,0779 80984,568 18,026230 17,880978 15,852757 80,400000	0 45.886248 3418.6851 7340.5993 1.4542639 0.4335965	0 -28,398346 4,8043609	1750.0887 80989.137 18.026230 17.880978 15.852757 80.400000 6.497859 3418.6851 7340.5993 1.5074722 0.4335965	0 -28.792240 4.8914393	1750.0995 80966.666 17.647196 17.506851 15.543490 80.400000	0 46.700238 3152.2017 6667.8649 1.5333230 0.4335965 0 -18.668248
28.122641 -78.357434 96.461128 96.082316 95.297943 21.278160	0 43.024888 50.380000 68.220873 0 2.5245534	403.82230 383.75370	28.122641 -78.357434 96.461128 96.082316 95.297943 21.300278 0 43.124900 50.380000 68.220873 0	405.99702 383.81859	28.113205 -78.251277 96.513433 96.127316 95.348135 21.273994	0 42.624504 50.380000 68.229999 0 2.5243518 0 407.36976 383.71851
6.0138624 0.9179036 21.197631 -0.1845008 0.8741577 116.10384	0 191.67908 0 191.67908 0 7.939997 361.09004	630.34379 1.1431520 1.7791120	6.1073989 0.9395306 21.291260 -0.1143397 0.8741577 116.10384 0 191.69095 0 191.69095 0 191.69095 3.9399997 3.9399997	630-34379 1-1431520 1-7791120	6.1664414 0.9061711 20.874284 -0.1232002 0.9209298 121.43958	0 191.63403 0 191.63403 0 7.9399997 361.09444 625.50000 1.1599999
371268.75 0.2128132E 08 9809.7651 9886.8177 11112.853	0 75.925937 0 75.925937 0 -7.9399997 689.05444	0.1126112 0.1752839	371268.75 0.2128132E 08 9803.7651 9886.8177 11112.853 61.102978 0 75.928469 0 75.928469 0 75.928469	0.1126113	381878.50 0.2129194E 08 9947.1448 10024.361 11253.236 62.849118	0 75.914152 0 75.914152 0 -7.9399997 688.90211 0.1133251
196.49000 56890.644 267.81911 116.10658 2.6540487 0.2065845E-01	0 80984.568 1750.0779 82734.646 0 436.99998 0.1670513£-01	82734.086 162.60883 253.10758	196.49000 54885.644 267.83352 116.10658 2.6540487 0.2098338E-01 0 60989.137 1750.0887 82739.225 0.36.99998	82738-664 162-61798 253-12226	199,99999 23945,674 267,76228 121,44250 2,7557535 0,1391761E-01	0 80966.666 1750.0995 82716.765 436.99998 0.1670513E-01 82716.196 163.60419 255.30260
0 4 4 4 4 4 4 4 4 4 4 4 4 4 4 4 4 4 4 4	0 W D K O	- 0 d &	0d- 0mex0 *	5 2 2 6	0 c ~ * ~ u u u u u u	OH4KO O45 1275420 1275



	•	
0.2131879E-06 0.9238404E-03 0.9428401E 08 6.5567246 620.42271 308.91375 0.2131879E-06 33.190029 50.200000 32.299999 2270.0000	0.1373659E-06 0.5000750E-03 0.9428408E U8 6.0096308 350.10317 307.30963 0.1373659E-06 33.002254 49.400000 32.199999 2289.0000	0 0 0 0.9741856E-07 0.9428413E 08 5.6735187 5.6735187 231.03834 308.91048 0.9741856E-07 32.814476 49.000000 32.09999 2321.0000
-0.2052358E-01 0.4221280E-02 0.3603481E-01 1.6121042 81.007221 -9.8999945 0 21.500001 1167.3432 923.51154 29.691376 -5.399999	-0.1110942E-01 0.2260061E-02 0.1814379E-01 1.6911839 81.007221 -9.8999945 0 20.000001 1172.6462 930.92700 30.700494 -0.1153652	0 0 0 0 0 0.1010562040E-02 0.1010562E-01 1.7983982 81.007221 -9.8999945 0 18.500001 1179.9930 950.10765 30.479685 -5.3999999
1750.1275 80901.594 16.621532 16.494331 14.705274 80.400000 0 47.263741 2393.2661 4752.3450 1.6121042 0 0.4335965 0 -6.9638214 1.1550139	1750.2121 80432.083 15.665887 15.65887 15.550702 13.921779 80.400000 0 47.559432 1609.9981 2862.8318 1.6911839 0.4384497	0 -3.2473018 0.5749956 1750.3298 80833.339 14.769499 114.769499 114.76999 14.76999 14.76999 14.76999 14.76999 14.76999 10.49999 10.493996 0.4335965 0.4335965 0.4335965
28.085092 -77.963299 96.667636 96.260781 95.496182 21.263946 0 41.175731 50.380000 68.255999 0 2.5235548 0 406.40974 383.62293	28.055032 -77.655950 96.827682 96.400215 95.650148 21.277319 0 40.250416 50.380000 68.281999 0	0 400.43332 383.59221 28.022850 -77.334395 96.994871 96.994871 95.811407 21.221523 0 39.633230 68.307999 0 2.5229379 0 2.5229379
6.1251504 0.8743115 19.522741 -0.1466710 1.0575911 137.10616 0 191.46910 0 191.46910 0 7.939997 361.10019 605.70000 1.2319999	5.8052907 0.8640732 17.949611 -0.1995772 153.49410 0 183.56474 0 183.56474 0 361384383	361.11747 585.90001 1.3039999 2.0419999 2.0419999 0.7856002 16.181139 -0.1887396 1.3477408 170.64930 0 191.30008 0 191.30008 0 191.30008 0 7.939999 361.60001 1.3839999 2.1599999
411737.25 0.2132182E 08 10358.878 10436.519 11672.944 67.763236 0 75.872774 0 75.872774 0 75.872774 0 0 0 0 0 0 0 0 0 0 0 0 0 0 0 0 0 0 0	441102.75 0.2135122E 08 10801.908 10879.923 12123.217 72.596176 0 83.646213 0 83.646213 0 684.35364	684,35364 0.1193324 0.1868708 470029.00 0.2138018E 08 11280.697 11280.697 11359.044 12608.633 77.356824 0 75.824331 0 75.824331 0 75.824331 0 15.824311 0 0 15.824311 0 0 15.824311 0 0 15.824311 0 15.824311 0 0 15.824311 0 0 15.824311 0 15.824311 0 15.824311 0 15.824311 0 15.824311
209.99999 51269.078 267.55598 137.10957 3.0532554 0.57151546-02 0 80901.594 1750.1275 82651.721 0 436.99998 0.16705136-01 82651.119 167.94875 262.56475	219.99999 48594.156 267.42506 153.49802 3.3627704 0.2934629E-02 0 80432.083 1750.2121 82182.295 0.6523916	
	0 d	0 4 0 4 0 0 4 0 0 0 0 0 0 0 0 0 0 0 0 0



BEGIN SUSTAINER AND VERNIER SOFT SHUT-DOWN

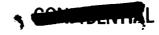
TOMELDENTIAL.

0.9177719E-07 0.2925857E-03 0.9428413E 08 5.6237873 215.72197	0.917719E-07 32.777481 48.960599 32.099999 2351.0000	0.917719E-07 0.2925857E-03 0.9428413E 08 5.6237873 215.72197 308.91035 0.9177719E-07 32.777481 48.960599 32.099999 2353.0000	0.8554827E-07 0.2670774E-03 0.9428414E 08 5.5652245 198.91729 311.11274 0.8554827E-07 32.732037 48.912199 32.099999
-0.6499937E-02 0.1166402E-02 0.9057020E-02 1.8191525 81.007221	0 18.204500 1181.9408 1031.0915 18.764413 -5.3999999	-0.6499937E-02 0.1166402E-02 0.9057020E-02 1.8191671 81.007221 -9.8999945 0 18.204500 1181.9408 1031.0915 1031.0915 1031.99999	-0.593258E-02 0.1061380E-02 0.8847232E-02 1.4710636 81.007221 -9.8999945 0 17.841500 1184.8256 1135.6877 0.9539811
1750.3538 80828.319 14.598986 14.496888 13.043493	0 41.679256 693.65654 581.24782 1.8191525 0.4335965 0 0 -1.4386914	82578.673 0 14.598986 14.496888 13.043493 80.400000 0 41.679358 693.65654 581.24782 1.8191671 0.4335965 0	65879.554 0 14.389217 14.289569 12.869223 80.400000 0 33.184644 506.00121 159.36938 1.4710636 0.4335965
28.016242 -77.269289 97.029104 96.577128 95.844449 21.194378	0 39.518604 50.380000 68.313121 0 2.5229040 0 389.47039 383.26373	28.016242 -77.269289 97.029104 96.577128 95.84449 21.194378 0 39.518623 50.380000 68.313121 0 2.5229040 0 389.47039 383.26373	28.007998 -77.188501 97.073732 96.616808 95.887000 21.194378 0 38.895282 50.380000 68.319413 0 1.7643088
5.1092315 0.7545784 15.811982 -0.1890199 1.3769484 174.12402	0 191.28786 0 191.28786 0 361.14645 555.92639 1.4013360 2.1836399	5.109 0.754 0.754 1.376 174.1 0 0 191.2 0 0 361.1 1.401 1.401	5.3972446 08 0.7520142 15.811982 0 14.140325 178.43625 0 135.01486 0 135.01486 0 0 0 0 0 0 0 0 0 0 0 0 0 0 0 0 0 0 0
475680.00 0.2138584E 08 11379.525 11457.933 12708.702 78.286860	0 15.820504 0 75.820504 0 687.72500 0.1223806 0.1907010	475680.00 0.2138584E 08 11379.933 11457.933 12708.702 78.286860 0 75.820504 0 75.820504 0 0 687.72500	\$\text{482600.50}\$ \text{482600.50}\$ \text{0.2139277E}\$ \text{11495.968}\$ \text{11574.449}\$ \text{12826.655}\$ \text{79.425827}\$ 0 \text{76.525639}\$ 0 \text{76.525639}\$ 0 \text{76.525639}\$ 0
0*1 231.97000 P 2 45393.667 1 3 267.32246 4 174.12856 5 3.7501380 6 0.1510933E-02	E 2 80828.319 P 3 1750.3538 R 4 82578.673 0 5 0 7 0.1670513E-01 0 1 82578.012 P 2 176.38235 5 3 274.65038	0*1 231.97000 P 2 45993.667 1 3 267.32246 4 174.12856 5 3.7501380 6 0.1510933E-02 0 1 0 E 2 80828.319 P 3 1750.3538 R 4 82578.673 0 5 0 7 0.1670513E-01 P 2 0	FUEL MANIFOLD PRESSURE BEGIN SUSTAINER DECAY BEGIN VERNIER DECAY 0*1 234.39000 P 2 44783.616 1 3 211.75460 4 178.44093 5 3.8308082 6 0.1455244E-02 6 0.1455244E-02 P 2 6421.894 P 3 1457.6602 P 3 1457.6602 P 0 6 0 0 1670513E-01



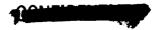
1	
3	

999	0.8554827E-07 0.2670774E-03 0.9428414E 08 5.5652245 198.91729 311.11274	0.8554827E-07 32.732037 48.912199 32.099999 2370.0000	•••	0.8204448E-07 0.2498129E-03 0.9428414E 08 5.4960726 186.01141	0.8204448E-07 32.703873 48.882199 32.099999 2449.0000	000	0.8204448E-07 0.2498129E-03 0.9428414E 08 5.4960726 186.01141	0.8204448E-07 32.703873 48.882199 32.099999 2450.0000
000	-0.5933258E-02 0.1061380E-02 0.8847232E-02 1.4710636 81.007221 -9.899945	0 17.841500 1184.8256 1135.6877 0.9539811 -5.3999999	000	-0.5549718E-02 0.9968817E-03 0.8681616E-02 0.6081972E-02 81.007221	0 17.662236 1185.1326 1144.4845 -7.8373277 -5.399999	000	-0.5549718E-02 0.9968817E-03 0.8681616E-02 0.6081972E-02 81.007221	0 17.662236 1185.1326 1144.4845 -7.8373277 -5.3999999
0 -1,3079836 0,2387682	65879.554 0 14.389217 14.289569 12.869223 80.40000	0 33.184644 506.00121 159.36938 1.4710636 0.4335965	0 -1,3079836 0,2387682	272.05860 0 14.226611 14.128041 12.722930 80.400000	0 28,985316 490,49810 122,63571 0,6081960E-02 0,4335965	0 -1.2199229 0.2196983	272.05860 0 14.226611 14.128041 12.722930 80.400000	0 28.985316 490.49810 122.63571 0.6081960E-02 0.4335965
394.00660 383.25604	28.007998 -77.188501 97.073732 96.616808 95.887000 21.194378	0 38.895282 50.380000 68.319413 0 1.7643088	394 <u>,</u> 00660 383,25604	28.002832 -77.138151 97.106560 96.646553 95.913820 21.194378	0 37.089516 50.380000 68.323313 0	397.34234 383.26618	28.002832 -77.138151 97.106560 96.646553 95.913820 21.194378	0 37.089516 50.380000 68.323313 0
548.95679 1.4226320 2.2126800	5.3972446 0.7520142 15.811982 0 1.4140325 178.43625	0 135.01486 0 135.01486 0 0	548.95679 1.4226320 2.2126800	5.6090377 0.7553962 15.811982 0 1.4373103 181.12417	0 0 0 0 0 0 58.864788	544.63680 1.4358320 2.2306800	5.6090377 0.7553962 15.811982 0 1.4373103 181.12417	00000
00	482600.50 0.2139277E 08 11495.968 11574.449 12826.655	0 76.525639 0 76.525639 0 0 548.13148	••	486857.75 0.2139703E 08 11492.962 11571.500 12824.769 80.126480	0 0 0 0 0 0 0 0.1138524E-05	00	486857.75 0.2139703E 08 11492.962 11571.500 12824.769 80.126480	00000
1 65879.554 2 0 3 0	*1 234,39000 2 4478,616 3 211,5460 4 178,44093 5 3,8308082 6 0,1455244E-02	1 0 2 64421. 3 1457.6 4 65879. 5 0 6 0 7 0.1670	0 1 65879.554 P 2 0 5 3 0 END SUSTAINER DECAY	D#1 235.89000 P 2 44731.058 I 3 0.2141025 4 181.12893 5 3.8810611 6 0.1413700E-02	1 0 2 0 3 272.05860 4 272.05860 5 0 6 0 7 0.1670513E-01	1 272 05860 2 0 3 0	0*1 235.89000 P 2 44731.058 1 3 0.2141025 4 181.12893 5 3.8810611 6 0.1413700E-02	1 0 2 0 3 272.05860 4 272.05860 5 0
D	O 0	0 4 4 4 0	ס פי אי ייי	Ö 0. →	0 4 5 4 0	0 4 10	Ö ⊶	0 4 6 8 0



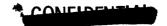
_	

		0.8130972E-07 0.2461712E-03 0.9428415E 08 5.4804612 183.26136 432.03589	0.8130972E-07 32.697674 48.875599 32.099999		0.8130972E-07 0.2461712E-03 0.9428415E 08 5.4804612 183.26136 432.03589	0.8130972E-07 32.697674 48.875599 32.099999	
	000	0.5468816E-02 0. 0.9833829E-03 0. 0.8645652E-02 0. 0.2067795E-02 5. 81.007221 18	7.662236 185.1326 144.4848 .8454711 .399999	000	-0.5468816E-02 0. 0.8645652E-03 0. 0.2540499E-02 5. 81.007221 16	7.662236 185.1326 144.4848 .8429626 .3999999	000
	29 0 83 0	i i	1.1	23 0 53 0	1	E-02	23 0 53 0
0	0 -1.2199229 0.2196983	92.499965 0 14.189969 14.091626 12.689763 80.400000	0 28.975206 490.49810 122.63571 0.2067818E-02 0.4335965	0 -1,2008023 0,2157253	92.499965 0 14.189969 14.091626 12.689763 80.400000	0 28.976397 490.49810 122.63571 0.2540499E-02 0.4335965	0 -1,2008023 0,2157253
0	397.34234 383.26618	28.001692 -77.127077 97.113898 96.653214 95.919726 21.194378	0 37.078086 50.380000 68.324171 0	398.09001 383.26877	28.001692 -77.127077 97.113898 96.653214 95.919726 21.194378	0 37.078655 50.380000 68.324171 0	398.09001 383.26877
58.864788	544.63680 1.4358320 2.2306800	5.6565087 0.7562588 15.811982 0 1.4424902 181.71541	0 0 0 0 0 0 58. 864788	543.68639 1.4387360 2.2346400	5.6565087 0.7562588 15.811982 0 1.4424902 181.71541	0 0 0 0 0 22.148656	543.68639 1.4387360 2.2346400
0.11385246-05	90	487787.50 0.2139796E 08 11490.524 11569.075 12822.580 80.279497	0 0 0 0 0 0 0.1138524E-05	00	487787.50 0.2139796E 08 11490.524 11569.075 12822.580 80.279497	0 0 0 0 0 0 0 0 0 0 0	00
0-1670513E-01	272.05860 0 0	236.22000 44730.987 0.2141025 181.72018 3.8921148 0.1404700E-02	0 0 92.499965 52.499965 0 0.1670513E-01	92.499965 0 0	236.22000 0.2141025 181.72018 3.8921148 0.1404700£-02	0 92.499965 92.499965 0 0.1670513E-01	92.499965 0 0
7	1 2 E	2 4 H 4 H A W A W A		0 1 5 3	0 4 H 4 H 1 H H H H H 1 H H H H H	126450 126450	0 1 5 2 8 3



CONTINUAL

ATM PRESS DYNM PRESS HEAT PARAM MACH NUMBER RHO-VR CUBED TOTAL ISP	PSI LBS/FT SQD FT'LBS/FT SQD LBS/SEC CUBED SEC	TRUE ANDMALY ASCEND NODE DEG DEG	0.9130972E-07 0.242839TE-03 0.9428415E 08 5.4432505 179.55378 1.9639639 175.97983	0 0.9428415E 08 0 1.9639639 175.10643
AXL FORCE SIDE FORCE NORM FORCE AXL LD FCTR WIND VEL NORTH WIND	LBS LBS LBS FT/SEC FT/SEC	ECCENTRICITY INCLINATION DEG	-0 0 0.2395078E-03 0 -0 0.7649055 28.570975	-0 0 0.2396183E-03 0.7640039 28.571106
THRUST FIXED THRUST CONTL GAMMA E GAMMA R GAMMA R EANMA R	LBS LBS DEG DEG DEG FT/SEC	SEMI MAJ AXIS ENERGY NM FT**2/SEC**2	8.7199999 0 14.189969 14.189970 12.689763 0 2012.2975 -0.5756356E 09	8.7199999 0 13.768950 13.768951 12.308842 0 2012.2989 -0.5756352E 09
GEOCENT LAT LONGITUDE AZI E AZI R AZI I PHI	0 E G 0 E G 0 E G 0 E G	SEMI LAT REC PERIOD NM MIN	28.001692 -77.127077 97.113899 96.650549 95.919726 21.194378 837.71051	27.988566 -77.000321 97.197918 96.727356 95.987320 21.194378 837.71625
ALPHA BETA PSI PSIDOT CROSS RANGE DOWN RANGE	DEG DEG DEG/SEC N.MI.	PERIGEE VEL APOGEE VEL FT/SEC FT/SEC	5.5581583 0.7534464 15.811982 0 1.4424891 181.71541 92765.799	0 0 15.811982 0 1.5027681 188.48362 92765.393 12410.560
ALTITUDE RADIUS VEL E VEL R VEL I	FT FT/SEC FT/SEC FT/SEC N.MI	PERIGEE ALT APOGEE ALT NM NM	487787.50 0.2139796E 08 11490.524 11490.524 12822.581 80.279497 -2969.0424	498254.00 0.2140844E 08 11462.597 11462.597 12797.473 82.002062 -2969.0387
TIME WEIGHT TOTAL FLOW GRND RANGE THETA I Q*ALPHA TOT	SEC LBS LBS/SEC N· MI. DEG DEG-PSF	PERIGEE RAD APUGEE RAD NM	236.22000 36408.000 4.440C000 181.72018 3.8921148 0.1361933E-C2 474.89109	24C.0000C 36391.216 4.44CC000 186.48861 4.0186629 0 474.89479 3549.7030
041 12445	00-11 1125-1136	10 4 0 7 7 7 7 7 7 7 7 7 7 7 7 7 7 7 7 7	10 0 0 0 4 0 0 1 0 0 0 0 0 0 0 0 0 0 0 0	07-1 04 #1264-20 12



l .
ſ

ATM PRESS DYNM PRESS HEAT PARAM MACH NUMBER RHO-VR CUBED TOTAL ISP	PSI LBS/FT SQD FT·LBS/FT SQD LBS/SEC CUBED SEC	TRUE ANDMALY ASCEND NODE DEG	C-1 PU VALVE C-2 PU VALUE C-1 LO2 TEMP C-2 LO2 TEMP PER CENT MR2 DE5 DE5	DES R 0 0.9428415E D8 0 84.660193	175,19457 -178,59629	0 180.94650 180.67325 109.73651	0 0.9428415F 08 0 434.35867	176.24557 -178.59589
AXL FORCE SIDE FORCE NORM FORCE AXL LD FCTR WIND VEL	LBS LBS LBS FT/SEC FT/SEC	ECCENTRICITY INCLINATION DEG		0EG R -0 0 0.2396953E-03	0.7640027 28.571198 433.04969	0 39.444650 39.444650 109.73913	-0 0 0.8223239 0	0.7632888 28.571254
THRUST FIXED THRUST CONTL GAMMA E GAMMA R GAMMA I EAST WIND	LBS LBS DEG DEG DEG FT/SEC	SEMI MAJ AXIS ENERGY NM FT**2/SEC**2	C-1 1SP C-1 FLOW C-1 LO2 PRESS C-2 LO2 PRESS PER CEVT ISP2 SEC LBS/SEC	PSI 8.7199999 0 13.474454 13.474455 12.042634	2012.2998 -0.5756350E 09 432.07177	0 103.05217 102.10522 99.223093	29834.589 0 13.251060 13.251060 11.842956 0	2013.2017 -0.5753771E 09
GEOCENT LAT LONGITUDE AZI E AZI R AZI I	DEG DEG DEG DEG DEG	SEMI LAT REC PERIOU NM MIN	LHZ WEIGHT LOZ WEIGHT C-1 LHZ PRESS C-2 LHZ PRESS PER CENT ISP1 LBS LBS	PSI 27.979340 -76.912107 97.256376 96.780796 96.034350 21.194378	837.72028 37.736249 4974.0000	25180.000 47.383130 46.889234 99.227134	27.971935 -76.841798 97.301565 96.821985 96.071736	840,29067 37,761621
ALPHA BETA PSI PSIDOT CROSS RANGE DOWN RANGE	DEG UEG DEG DEG/SEC N.MI.	PERIGEE VEL APOGEE VEL FT/SEC FT/SEC	C-2 THRUST C-2 LH2 FLOW C-2 LD2 FLOW C-2 RATIO PER CENT T2 LBS LBS/SEC	0 0 15.811982 0 1.5459533 193.19508	92765.107 12410.592 0	0 0 5.5855885 101.97909	0 0 15.811982 0 1.5810801 196.95081	92585.635 12429.079
ALTITUDE RADIUS VEL E VEL R VEL I	FT FT SEC FT/SEC FT/SEC FT/SEC N.MI	PERIGEE ALT APOGEE ALT NM	C-1 THRUST C-1 LH2 FLOW C-1 LOZ FLOW C-1 RATIO PER CENT T1 LBS LBS/SEC	505349.00 0.2141554E 08 11443.644 11780.439 83.169748	-2969.0361 105.76871 0	0 0 5.4869566 102.00125	510893.00 0.2142109E 08 11449.048 11449.049 12787.285	-2967,3861 105,92245
1 TIME 2 WEIGHT 3 TOTAL FLOW 4 GRND RANGE 5 THETA I 6 Q*ALPHA TOT	1 SEC 2 LBS 3 LBS/SEC 4 N. MI. 5 DEG 6 DEG-PSF	1 PERIGEE RAD 2 APOGEE RAD 1 NM 2 NM	1 THRUST 2 LH2 FLUW 3 LU2 FLUW 5 RATIO 5 LUSSEC 2 LBS/SEC 2 LBS/SEC		1 474.89740 2 3549.7022 1 8.715999	2 0 3 0 4 1.0000000 5	1 244.73374 2 36280.825 3 68.666529 4 156.55605 5 4.1769956 6 0	1 476.54739 2 3549.8560
04-	0 4 -	04 24	שני אבשני			w z ⊢	04-	04



*	

0 0 177.31291 178.62532 102.33869	0 0.9428415E 08 0 0 434.55317	176.26281 -178.59715 0 0 177.16917 178.58460 101.82378	0 0 0.9428415E 08 0 434.74652	175.27970 -178.59740 0 177.02800 178.54460 101.31591	0 0.9428415E 08 0 0 435.05894	176.32772 -178.61301 0 0 175.68171 178.39720 100.54240	© ©
435,51556 34,302166 38,917097 38,917097 103,01233	-0 0 0 0.8247197 0	0.7613946 28.571279 435.70755 34.254728 38.912306 102.48709	-0 0 0.8271044 -0	0,7595217 28,571303 435,89861 34,20903 38,907599 38,907599	-0 0 0.8343483	0.7544581 28.572819 436.19161 34.142034 38.905914 101.10251	0 0
434.25336 34.281364 69.121115 68.650145 99.788089	29806,243 0 13.056136 13.056138 11.672452	2015.5970 -0.5746938E 09 434.232827 66.845295 66.422236 99.832079	29779.044 0 12.867025 12.867026 11.506991	2017.9681 -0.5740181E 09 434.64842 34.185396 64.610001 64.23400 99.875857	29737.400 0 12.362873 12.362875 11.065454	2024,3606 -0,5722054E 09 434,98328 34,107544 60,704285 60,69999 99,942990	29738.643 0
4958.1744 25097.344 36.916965 36.393592 99.728148	27.964690 -76.773428 97.343127 96.859673 96.107919	847.11161 37.829035 4935.5434 24980.419 36.449823 35.722824	27.957508 -76.706020 97.384048 96.896791 96.143565	853.85622 37.895806 4913.2518 24865.829 35.064000 35.064000	27.938136 -76.526156 97.501077 97.003757 96.245858	872.08022 38.076018 4853.9020 24563.224 35.250000 34.0000000	27.915898 -76.322742
14939.099 5.5245527 28.777613 5.2090394 100.41331	0 0 15.811982 0 1.6156466 200.60352	92113.074 12477.997 14925.044 5.5402990 5.1828302 100.31865	0 0 17.661339 -1.5982462 1.6500899 204.20537	91650.996 12526.172 14911.696 5.5561482 28.652944 5.1569798 100.22893	0 0 12.989772 0.2413857 1.7446191 213.81877	90427.334 12655.586 14892.469 5.5809450 28.561089 5.1176079 100.09969	00
14886.770 5.5736467 28.707718 5.1506166 100.53730	516199.25 0.2142641E 08 11488.447 11488.447 12827.947	-2963.0012 106.32819 14872.479 5.589621 28.643205 5.1243545 100.44059	521354.25 0.2143157E 08 11527.474 11527.474 12868.188 85.803874	-2958.6561 106.72519 14858.628 5.6056353 28.579760 5.0983980	534741.25 0.2144498E 08 11632.835 11632.835 12976.684 88.007091	-2946.8683 107.72244 14836.211 5.6328387 28.474705 5.0551252 100.19566	549230.00 0.2145949E 08
C 1 29834.589 E 2 11.098199 N 3 57.48531 I 4 5.1796988	0*1 246.77000 P 2 36141.059 1 3 68.590554 4 200.60894 5 4.2452785 6 0	0 1 480.53233 4 2 3550.2617 C 1 29806.243 E 2 11.129921 N 3 57.357634 T 4 5.1534628	0*1 248.77000 P 2 36003.971 I 3 68.497487 4 204.21093 5 4.3125613	0 1 455.27745 4 2 3550.6587 C 1 29779.044 E 2 11.161784 N 3 57.232705 T 4 5.1275591	0*1 254.07000 p 2 35641.471 l 3 68.352577 4 213.82471 5 4.4920747	0 1 497.05527 4 2 3551.6560 C 1 25737.400 E 2 11.213784 N 3 57.035794 T 4 5.0862220	0*1 260,00000 P 2 35236,124

CONFIDENTIAL

3428415E 38 5.04724 3.38463 3.59358 3.19454 3.65627	9428415E 08 5.04831 6.42320 8.58569 5.32878 8.17151	.9428415E 08 35.05070 76.51082 78.58243 75.19509 78.11803	3415E 08 5212 5471 7815
0.9428415E 0 0 435.04724 175.38460 -179.59358 0 0 0 175.38635 176.38635	0 0,9428415E 0 435.04831 176.42320 -178.58569 0 0 175.32878 175.32878	0 0.9428415E 0 0 435.05070 176.51082 -178.58243 0 0 175.19509 178.11803 100.58666	0 0.9428415E 0 0 435.05212 176.56471 -178.57815
0.8439817 0.0.8439817 0.7486301 28.570899 436.14727 34.151490 38.916316 38.916316	-0 0.8509510 0.8509510 -0 0.7444160 28.570106 436.15540 34.150001 38.900772 101.06997	-0 0.8675883 0.8675883 -0 0.7343631 28.569774 436.17422 34.146544 38.864674 38.864674	-0 0 0.8780639 0 0.7280182 28.569327
11.803724 11.803725 10.575107 0 2031.7110 -0.5701353E 09 435.00389 34.102785 60.013642 60.699999	29738.744 0 11.423797 11.423798 10.241812 0 2037.0568 -0.5686392E 09 434.99793 34.104338 60.071214 60.69999	29738.979 0 10.582086 10.582087 9.5027418 0 2049.8759 -0.5650831E 09 434.98400 34.107959 60.204911 60.699999	29739.124 0 10.089115 10.089116 9.0692749 0 2058.0023 -0.5628517E 09
97.612599 97.104046 96.343241 21.833292 893.04468 38.283586 4787.4126 24224.977 35.246589 34.000000	27.899714 -76.176572 97.695782 97.179249 96.416053 21.519128 908.21111 38.434772 4740.0996 23984.257 35.232195 34.000000	27.860914 -75.832545 97.898937 97.363935 96.594481 21.652579 944.40012 38.798153 4630.2211 23425.243 35.198771 34.000000	27.836373 -75.619422 98.022842 97.476609 96.703617 21.336598 967.23946 39.029096
13.949902 0.9273585E-01 1.8539603 224.69543 89062.786 12802.997 14895.079 5.5772066 5.1234042	0 14.172476 0.1875443E-01 1.9334036 232.51402 88103.180 12908.482 14894.707 5.5779365 28.5779365 28.572064 5.1223359	0 13.807991 -0.7929710E-01 2.1254779 250.92588 85900.745 13156.651 14893.842 5.5796276 28.566916 5.1198606	0 13.321577 -0.8178531E-01 2.2483083 262.33904 84569.982 13310.910
11754.155 11754.155 13101.407 90.391632 -2933.2225 108.77747 14834.844 5.6342619 28.468523 5.0527511 100.18643	559235.50 0.2146951E 08 11842.413 11842.414 13191.917 92.038326 -2923.2945 109.54041 14835.316 5.6338230 28.470515 5.0534983	581531.75 0.2149185E 08 12053.762 12053.762 13408.062 95.707817 -2899.4108 111.29550 14836.417 5.6327982 28.475161 5.0552425	594508.00 0.2150485E 08 12187.263 12187.263 13544.255 97.843432 -2884.1944 112.33200
66.357274 224.70182 4.6549115 0 0 10.71104 3552.7110 29738.643 11.211468 57.042807	264.22000 364.22000 68.357337 232.52073 4.8405625 0 520.63905 3553.4739 11.211755 57.042578 5.0877454	274.02000 3427.754 66.357502 26.93340 5.1830500 0 544.52272 3555.2290 29738.975 11.212426 5.0873984	28C.400C0 3368.976 6E.357613 262.34709 5.3950042 0 555.73916 3556.2655
1 04 OUST 6456 10 14645	12 04 DT T T T T T T T T T T T T T T T T T T	O	040 0400

CONPIDENTING

0 176.11350 178.08540 100.55705	0 0.9428415E 08 0 0 435.05349	175.61944 -178.57446	0 176.03165 178.05266 100.52741	0 0.9428415E D8 0 0 435.05659	176.75303 -178.56759	0 175.84065 177.97626 100.45846	0 0.9428415E 08 0 0 435.06068	175.94209 -178.55903	0 0 175.56780 177.86712 100.36050	0 0 0.9428415E 38
34.144433 38.842646 38.842646 101.12625	-0 0 0 0.8888318 0	0.7214815 28.568933	436.19716 34.142317 38.820545 38.820545 101.14781	-0 0 0.9150141 0	0.7055295 28.568180	436.22384 34.137378 38.768976 38.768976 101.19845	-0 0 0 0.9552101 -0	0.6809257 28.567194	436.26176 34.130322 38.695306 38.695306 101.27163	000
34.110180 60.286493 60.699999 99.941632	29739,272 0 9,6088505 9,6088514 8,6464853	2066.4034 -0.5605634E 09	434,96682 34,112420 60,368349 60,69999	29739.622 0 8.5425262 8.5425272 7.7058287	2087.0416 -0.5550202E 09	434.94650 34.117676 60.559345 60.699999 99.950375	29740.136 0 7.1526613 7.1526613 6.4752083	2119.3260 -0.5465653E 09	434.91703 34.125272 60.832196 60.699999 99.959063	30284.195 0 5.9112587
23084.132 35.178376 34.000000 99.893978	27.811071 -75.403105 98.148410 97.590938 96.814479 21.357634	990.76687 39.268322	4495.8914 22741.882 35.157912 34.000000 99.891995	27,749292 -74,888461 98,445976 97,862415 97,078238 21,346988	1048.1710 39.858078	4338,8998 21943,305 35,110163 34,000000 99,887328	27.653966 -74.128322 98.880898 98.260407 97.466240 21.333874	1136.6797 40.786491	4114,6045 20802,494 35,041950 34,000000 99,880562	27.549632 -73.337325 99.327509
5.5806569 28.563776 5.1183537 100.10537	0 0 12.742861 -0.7433578E-01 2.3758754 273.92896	83243.735 13468.003	14892.782 5.5816875 28.560629 5.1168450 100.10180	0 0 11.638535 -0.8182717E-01 2.6907936 301.52600	80182.224 13843.970	14891,538 5,5840839 28,553294 5,1133354 100,09344	0 9.8789929 -0.9252915E-01 3.1848411 342.34957	75886.479 14404.815	14889.754 5.5874870 28.542835 5.1083491 100.08145	0 0 7.9054109
5.6321699 28.478010 5.0563124 100.20160	607058,75 0.2151742E 08 12324,710 12324,710 13684,235 99,909020	-2868,4020 113,34171	14837,771 5.6315374 28.480883 5.0573902 100.20619	634551.75 0.215449EE 08 12659.126 12659.127 14023.958	-2829,3613 115,57745	14839.364 5.6300514 28.487625 5.0599227 100.21695	669635.50 0.2156016E C8 13170.263 13170.264 14541.349 110.20783	-2767.7111 118.49600	14841.662 5.6279069 28.497365 5.0635815 100.23247	700036.00 0.2161067E 08 13725.170
E 2 11.212827 N 3 57.041786 T 4 5.C871904	0*1 286.00000 P 2 33458.830 I 3 66.357737 4 273.93756 5 5.6099750	0 1 575.53151 4 2 3557.2752	C 1 29739.272 E 2 11.213225 N 3 57.041512 T 4 5.0869854	D#1 300.00000 P 2 32501.819 1 3 66.358053 4 3C1.536C4 5 6.1207976 6 0	0 1 614.57218 4 2 3559.5110		0*1 320.00000 P 2 31134.653 1 3 68.358593 4 342.36197 5 6.8738444	0 1 676.22243 4 2 3562.4295	C 1 29740.136 E 2 11.215394 N 3 57.040200 T 4 5.0858847	0#1 340.0000C P 2 29755.643 I 3 70.317154

3 COMPANY

Maria Contraction of the Contrac

0 0 430.68005	177,13946	-29,500000 -50,300303 175,30897 177,74949	0 0.9428415E 38 0 0 430.72551	177.33996	-29,500000 -50,299999 175,10384 1,77,64692 112,41638	0 0.9428415E 08 0 0 432.95934	177.55636 -178.53995	-11,195566 -22,995673 174,91521 177,54391	0 0.9428415E 08 0 0 435.75904	177.80954 -178.53552 6.0000152 4.7615561
1.0177631	0.6537803 28.566300	430,99743 35,292764 38,616666 38,616666 109,57602	-0 0 0 1.0681652 0	0.6235000 28.565480	431,04317 35,285685 38,549999 38,549999 109,48634	-0 0 0 1.1138467 0	0.5900593 28.564745	433,37825 34,782000 38,486956 38,486956 104,59885	-0 0 0 1.1589213 0	0.5537068 28.564106 436.85296 33.995002
5.9112587 5.3709641 0	2155.6833 -0.5373471E 09	431,37985 34,921392 53,500000 59,000000 98,752866	30281.871 0 4.8104792 4.8104801 4.3871155	2197.2979 -0.5271703E 09	431.42534 34.915653 58.499999 59.000000 98.763348	30013.437 0 3.8314514 3.8314524 3.5072632	2244.7260 -0.5160319E 09	433.57798 34.436609 59.804346 60.304347 99.298374	29647.786 0 2.9525204 2.9525204 2.7125034	2298.2392 -0.5040164E 09 435.72884 33.939109
98.670536 97.867832 21.323225	1234.2823 41.840526	3893.8517 19646.297 35.801281 35.000000 99.068233	27,435382 -72,513191 99,786161 99,093211 98,283712 21,315041	1343.0933 43.057926	3681,0613 18454,932 36,057692 35,000000 99,078679	27,310239 -71,653749 100,25801 99,529645 98,714612 21,309322	1463.1799 44.459515	3467.5619 17266.816 35.315217 34.130435 99.573042	27,173193 -70,757221 100,74413 99,981000 99,161038 21,306068	1593.6194 46.058792 3241.5930 16131.318
-0.1032311 3.7342681 384.91237	71648.233	15211.090 5.2466937 30.046070 5.726675 102.24131	0 5.717894 -0.1139331 4.343053 429.35128	67427.048 15636.760	15209.654 5.2492899 30.036396 5.7219934 102.23165	0 0 3.3161281 -0.1246351 5.0156596 475.79971	63270.225 16311.997	15073.762 5.3817102 29.400289 5.4630013 101.31826	0 0.7004272 -0.1353371 5.7570011 524.37240	59239.541 17016.214 14850.817 5.6414865
13725.170 15101.185 115.21111	-2697.593 6 121.09308	15064,385 5,3901013 29,531291 5,4788007 101,73662	726054.75 0.2163680E 08 14330.847 14330.847 15710.694 119.49324	-2616.6510 123.37973	15063,498 5,3929477 29,522706 5,4743171 101,73063	747941.75 0.2165881E 08 14981.204 14981.204 16363.996 123.09538	-2523,7289 125,31390	14930,955 5,5275967 28,909012 5,2299424 100,83551	765873.50 0.2167688E 08 15665.732 15665.733 17050.744 126.04657	-2418,2449 126,85623 14788,249 5,6995702
4 384.92752 5 7.6558534 6 0	0 1 746.33996 4 2 3565.C266	C 1 30284.195 E 2 10.636795 N 3 59.577360 T 4 5.6010631	0*1 36C.00000 P 2 28345.428 1 3 70.304338 4 429.36962 5 8.4691036 6 0	0 1 827.28255 4 2 3567.3133	C 1 30281.871 E 2 10.642236 N 3 55.559102 T 4 5.5964835	0*I 38C.000CC p 2 269C.500CC 1 3 69.321608 4 475.82170 5 9.3158166 6 0	0 1 920.20463 4 2 3569.2474	C 1 30013,437 E 2 10,909307 N 3 58,309301 T 4 5,3449135	0*1 4C0.C0000 P 2 5582.225 1 3 6E.037110 4 524.39856 5 10.197904	0 1 1025.6886 4 2 3570.7898 C 1 25647.786 E 2 11.341057

.00	
1	

174.80030 177.43230 98.740558	0 0.9428415E 08 0 0 435.62105	178.10171 -178.53166	5.2461421 3.1307555 174.64538 177.32846 99.153554	0 0.9428415E 08 0 0 435.07437	178.46180 -179.52826	0.3428455 -1.5285848 174.46285 177.25286 100.63993	0 0.9428415E 38 0 0 436.94972	178.93113 -178.52516	17.000011 18.000012 174.30000 177.10000	0 0 0.9428415E 38
38.420768 38.420768 99.093575	-0 0 1.2252172 0	0.5132614 28.563518	436.70519 34.031163 38.353076 38.353076 99.435711	-0 0 0 1.3013498 -0	0.4684645 28.562970	436.14763 34.161150 38.273571 38.273571 100.90421	-0 0 0 1.3709489 0	0.4185379 28.562443	438.21425 33.668281 38.199999 38.199999 95.986451	-0 0 0 1.4760659
	29667.267 0 2.1685009 2.1685019 1.9993973	2360.4441 -0.4907340E 09	435.59909 33.969220 61.269229 61.446152 100.06067	29743.319 0 1.4642372 1.4642382 1.3548336	2433.0044 -0.4760987E 09	435.05761 34.099609 60.978570 61.278571 99.932914	29476.197 0 8284149 0.8284159 0.7691898	2518,9637 -0,4598519E 09	436.76303 33.687734 62.199999 62.500000 100.40643	29736.003 0 0.2486486 0.2486496
34.676922 33.442307 100.06699	27.023126 -69.821692 101.24396 100.44677 99.623322 21.305280	1738-6151 47-941351	3017.5204 14989.109 34.415384 33.480769 100.03720	26.858745 -68.844687 101.75833 100.92789 100.10213 21.306957	1899.0598 50.168839	2789.4813 13861.069 34.864286 33.178571 99.912846	26.678615 -67.823609 102.28760 101.42482 100.59809 21.311099	2077,7069 52,850921	2560.0673 12737.379 33.750000 33.499999 100.30450	26.481131 -66.755621 102.83223 101.93813
28,353515 5,0258943 99,819732	0 -2.1293135 -0.1460391 6.5724127 575.19450	55239.174 17767.608	14861.586 5.6278546 28.403309 5.0469158 99.892114	0 0 -5.1730935 -0.1567410 7.4677532 628.42474	51289.570 18565.126	14899.305 5.5795420 28.581608 5.1225724 100.14564	0 0 -8.4309134 -0.1674430 8.4494574 684.23241	47367.854 19416.199	14753.920 5.7883953 27.879885 4.8165137 99.168440	0 0 -11.902772 -0.1781450
28,239539 4,9546787 99,871748	779988.50 0.2169115E C8 16402.101 16402.102 17788.719 128.36960	-2295.0144 128.03543	14796.961 5.6882853 28.280935 4.9717855 99.930588	790417.00 0.2170174E 08 17188.506 17188.507 18576.215 130.08591	-2150.7052 128.84702	14835.295 5.6407649 28.458844 5.0452102 100.18947	797236.00 0.2170873E 08 18032.025 18032.026 19420.381	-1979,2515 129,31180	14713.557 5.8089085 27.878825 4.795325	800472.50 0.2171216E 08 18935.344 18939.344
m 4 m	0*1 420,00000 P 2 24213,884 1.3 68,103,882 4 575,22541 5 11,117449	0 1 1148.9192 4 2 3571.9690	C 1 29667.267 E 2 11.316140 N 3 56.684243 T 4 5.0091501	0*1 44C.C0000 P 2 22855.745 1 3 £6.363759 4 628.46098 5 12.077095 6 0	0 1 1293,2283 4 2 3572,7805	C 1 29743.315 E 2 11.220307 N 3 57.046452 T 4 5.0836802 5	0*1 46C.00000 P 2 21500.581 1 3 67.459013 4 684.27466 5 13.079662 6 0	0 1 1464.6820 4 2 3573.2453	C 1 29476.157 E 2 11.597304 N 3 55.758710 T 4 4.8079029	D#1 479,99999 P 2 20145,444 1 3 6E,338411 4 742,8534C

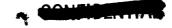


* CONSIDERATION

0 435.12869	179.59283 -178.52218	0.8000295 -1,733015 174.0333 176.9666 100.66085	0 0.9428415E 08 0 0 435.35609 -179.63604	3.4613948 -0.5.554051 173.80653 175.87585	942841 5.4741 9.3898	-178.51763 13.781395 9.945946 173.77053 175.85585	0 0.9428415E 38 0 0 435.51563	-179.37983 -178.51762 14.219980 10.379980
00	0.3626450 28.561906	436.13399 34.164610 38.126666 38.126666 100.57436	-0 0 0 1.5583141 0 -0		-0 0 0 1.5724379 0 -0	28.561035 437.52461 33.837224 38.053509 96.809924	-0 0 0 1.5730777 0	0.2994807 28.561034 437.56839 33.826612 38.052999
0.2316637 0	2622.4097 -0.4417121E 09	435.18012 34.070802 60.400002 61.333334 99.929788	29704.449 0 -0.1776857 -0.1776848 -0.1659918 0	,	29546.274 0 -0.2797709 -0.2615356 0	-0.42141895 436.49466 33.752844 61.677699 61.624499 100.24841	29540.197 0 -0.2835941 -0.2835932 -0.2651157	2749.8867 -0.4212356E 09 436.53428 33.743104 61.709998
101,11184	2277.5329 56.139754	2330.6279 11613.742 34.316665 32.699998 99.940981	26.311284 -65.874716 103.327441 102.35634 101.53165 20.978558	7,55005 153,417 0709,05 3,71360 2,60340 9,99741	6.26634 5.64690 03.3869 02.4629 01.6388 1.29995	50143272 60.243272 2107.8950 10483.178 33.393600 32.523399 100.24287	26.264411 -65.637172 103.39182 102.46755 101.64345 21.300109	2503.2530 60.282589 2105.9412 10473.644 33.380000
9.5247402 742.80448	43459.562 20327.500	14900,348 5,5791370 28,585473 5,1236371 100,15265	5458 1218 4474 •276	886.73 886.73 597118 .51975 095434	4 - 2 2 2 2 2 2 2 3 - 6 9 9 8 9 9 9 8 9 9 9 9 8 9 9 9 9 9 9 9	59565-496 21302-341 14804-618 5-7097577 28-127466 4-9262100 99-509206	0 0 -14.262739 -0.2159228 10.701602 804.37265	39532.328 21310.943 14801.456 5.7144467 28.112165
20327.956 131.74083	-1772.5277	14826.936 5.6514174 28.419384 5.0287180 100.13302	0047 • 217 9712 9712 9712 1101 31.7	129,48975 14808,994 5,6737357 28,336635 4,9943522 100,01185	5.0 120 120 155 155 107	-1519,49124 129,49124 14732,936 5,7791055 27,973738 4,8404962 99,498198	800096.50 0.2171200E 08 19923.184 19923.185 21311.703 131.67895	-1517.5848 129.49112 14730.021 5.7834718 27.959632
5 14.128264 6 0	1 1671.4058 2 3573.4136	1 29736.003 2 11.230554 3 57.004858 4 5.0758721	1 495.830C0 2 19061.915 3 66.23C238 4 791.33109 5 14.953404 6 0	3573.423 29704.44 11.27085 56.85638 5.044545	495.8300 2 16790.10 3 67.69306 4 803.8923 5 15.21720 5 0	1 1923.9570 2 3573.4248 1 25546.274 2 11.488863 5 56.101204 4 4.8830944	1 499,59999 2 18778,600 3 67,672714 4 804,42896 5 15,226758 6 0	1 1926.3487 2 3573.4247 1 29540.197 2 11.497918 3 56.071796
٠, ٠	04	0 m S F	0		*	04 OMZ-		04 OMS

00	
A MALE PARTY	11.

175.85500 96.650175	0 0.9428415E 08 0 0 437.16051	-177,68398	19.454560 20.900015 173.50390 176.71454 93.930198	0 0.9428415E 38 0 0 436.14391	-173.65277 -178.51438	11.000010 6.250063 173.40250 176.60000 97.960819	0 0 0.9428415F 38 0 0 435.22380	-155.81758 -178.51197	1.0714624 -0.5713937 173.20500 176.47786 100.06708	ი 0 0.9428415E 08 0
38.052999 96.688054	-0 0 0 1.6895223 0	0.2288138 28.560772	438.40684 33.618329 37.967272 37.967272	-0 0 0 1.8414055 -0	0.1490201 28.560358	437,10818 33,935061 37,905000 37,905000 97,537932	-0 0 2.0206992 0	0.6133951E-01 28.559813	436.35026 34.115623 37.830714 37.830774 100.59421	-0 0 0 2.2232773
61.649998 100.25845	29442.569 0 -0.7322340 -0.7322330 -0.6867867	2908.1720 -0.3983087E 09	436.99421 33.628233 61.893637 61.945454 100.45056	29592.607 0 -1.1773891 -1.1773882 -1.1079035	3111.6817 -0.3722586E 09	436.24683 33.812495 61.425001 61.675000 100.15300	29722.757 0 -1.6151342 -1.6151333 -1.5246811	3382.6996 -0.3424336E 09	435.15565 34.074419 60.842858 61.371430 99.979341	29668.722 0 -2.0388184 -2.0388184 -1.9307165
32,520000 100,25197	26.026398 -64.464750 103.97021 103.01710 102.19625 21.318111	2755.9124 65.561646	1875,2943 9354,3153 33,045454 31,736363 100,35759	25.764745 -63.234517 104.56546 103.58497 102.76903 21.334806	3042,5806 72,562534	1646.3030 8229.4657 33.04999 31.65000 100.18595	25,476712 -61,941723 105,17838 104,17219 103,36293 21,350193	3369.9721 82.246013	1419,3837 7096,9266 33,335713 31,935713 99,935361	25.159122 -60.580956 105.80992 104.77985 103.97917
4.9194903 99.487952	0 0 -18.569456 -0.2126601 11.989084 869.17265	35627.743 22359.467	14738.505 5.8152665 27.803062 4.7810470 99.064830	0 0 -22.781478 -0.2064536 13.398918 937.46629	31706.003 23481.898	14833.293 5.6688766 28.266185 4.9862056 99.701945	0 0 -26.839933 -0.1973031 14.943159 1009.5742	27827.622 24611.060	14886,361 5,5987695 28,516853 5,0934144 100,05864	0 0 -30.685935 -0.1852087 16.636235
4.8344027 99.478511	796225.25 0.2170836E 08 20978.384 20978.384 22366.490 131.04182	-1201,1915 129,66849	14695.343 5.8374206 27.790812 4.7608034 99.244314	788775.00 0.2170116E 08 22124.101 22124.102 23511.493 129.81567	-795.95490 131.45117	14750.594 5.7534610 28.059034 4.8768966 99.617448	777392.50 0.2169006E 08 23374.59C 23374.591 24760.946 127.94235	-268.72702 146.25919	14827.676 5.6510869 28.42331 5.0297105 100.13802	761724.25 0.2167469E 08 24746.209 24746.209 26131.194
T 4 4.8766911 5	0*1 519.59959 P 2 17426.564 I 3 67.349561 4 865.23708 5 16.379065	0 1 2242.742C 4 2 3573.6020	C 1 29442.569 E 2 11.652687 N 3 55.593874 T 4 4.7709060	0*1 535.95999 P 2 16070.663 1 3 67.85C555 4 937.53963 5 17.589557	0 1 2647.5786 4 2 3575.3847	C 1 29592.607 E 2 11.42238 N 3 56.325219 T 4 4.9311463	0*1 559.59999 P 2 14709.145 1 3 6E.253040 4 1009.6573 5 18.863563	0 1 3175.2065 4 2 3590.1927	C 1 29722.757 E 2 11.249856 N 3 56.940185 T 4 5.0614144	0*1 575,99999 p 2 1334,585 l 3 62,109258 d 1085,9588 5 20,207223



SONEIDENTIAL

435.60483	-35.179876 -178.50926	4.8750105 2.1250124 173.01000 176.36125 99.165977	0 0.9428415E 08 0 437.15527	-15.314361 -178.50643	19.285742 20.142894 172.85286 176.26000 93.865561	0 0.9428415E 08 0 0 436.42253	-14.638713 -178.50615	11.857143 10.428571 172.81857 175.24000 96.536115	0 0 0.9428415E 08 0 436.51953	-10.871477 -178.50346	16.636340 8.1817918 172.61003 176.11363
0-	0.6144752E-01 28.559167	436,67553 34,038030 37,758749 37,758749 99,37901	-0 0 2.4559071 -0	0.1795506 28.558450	438,40538 33,615531 37,704285 37,704285 95,190545	-0 0 0 2,4932443 -0	0.1927928 28.558374	437,58309 33,820287 37,692857 37,692857 97,246378	-0 0 2.7791141 -0	0.3242100 28.557648	437.34991 33.875483 37.619091 37.619091
0	3760.5555 -0.3080263E 09	435,59606 33,968229 61,075000 61,475000 100,05387	29440.428 0 0 -2.4367752 -2.4367752 -2.3147478	4320,3754 -0,2681133E 09	436.98526 33.626943 61.900001 62.357144 100.45022	29551.305 0 -2.4746456 -2.4746456 -2.3514442	4391.4923 -0.2637714E 09	436,33317 33,789317 61,499999 61,871428 100,26182	29535.101 0 -2.7868996 -2.7868996 -2.6555262	5244.5231 -0.2208685E 09	436.76036 33.681953 61.772726 61.772726
21,364273	3746,3564 96,404590	1193.8270 5959.9872 32.812500 31.412499 100.03650	24.808285 -59.146031 106.46079 105.40924 104.61902 21.377044	4181.0934 118.71399	965.15644 4833.7274 32.228570 30.828570 100.35554	24.771214 -58.998200 106.52700 105.47342 104.68435 21.378250	4228.2647 121.65722	942.01572 4722.0269 32.485714 31.085714 100.20578	24.419793 -57.629494 107.13173 106.06111 105.28387 21.388509	4693.2602 158.77375	737.80684 3703.0624 32.036364 30.636364
1085.8653	26395.440 23339.360	14863.575 5.6284015 28.409628 5.0475482 99.905483	0 0 -34.260614 -0.1701704 18.495308 1166.7646	27765.568 19312.647	14737.230 5.8180936 27.797438 4.777570 99.056257	0 0 -34.508231 -0.1583216 18.691105 1175.1261	27920.220 18894.651	14799.186 5.7189838 28.101303 4.9136881 99.472692	0 0 -37.062461 -0.1216920 20.541307 1252.7853	29420.800 15014.448	14815,439 5,6952342 28,180248 4,9480403
125,36369	85,545197 547,69882	14796.427 5.69C7785 28.277450 4.9689950 99.926978	741445.25 0.2165474E 08 26254.774 26254.774 27638.052 122.02619	100.71600 1652.1677	14694.478 5.8384901 27.788452 4.7555272 99.238474	739153.75 0.2165248E 08 26414.055 26414.055 27797.144	100.91077 1794.2068	14743,400 5.7638142 28.025502 4.8623189 99.568861	716329,50 0,2162999E 08 27941,756 27941,757 29323,017	100.26276 3500.9164	14710.942 5.8121836 27.869770 4.7950602
0 9	1 3529,4787 2 3991,6324	1 29668-722 2 11.315180 3 56.687078 4 5.0080552	*1 599,9999999999999999999999999999999999	1 3544.6495 2 5096.1012	1 29440.428 2 11.656584 3 55.588890 4 4.7686262	11 6C2.00000 2 11852.551 3 67.712603 4 1175.2321 5 21.774182 6 0	1 3544.8443 2 5238.1403	1 25551,305 2 11,482798 3 56,126805 4 4,8879032	11 615,99998 2 10627,524 2 0620435 4 1252,9021 5 23,133294	1 3544.1963 2 6944.8500	1 29535.101 2 11.507418 3 56.050018 4 4.87C7728
	0 4	Ç Ψ Z ►	Ö a. –	04	O W Z F	* a -	04	J w Z ⊢	* a =	04	ÇΨZ⊢



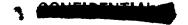
COMPLETE	

97.211009	0 0.9428415E 38 0 0 435.25783	-8.7494856 -178.50024 3.4615197 -2.3846353 172.41000 175.98923 100.52891	0 0.9428415E 08 0 0 435.10618	-7.2127596 -178.49537 1.6666768 -3.2222154 172.21555 175.87222	0 0.9428415E 08 0 633.51466	-178.49135 -29.000000 -50.000000 172.02683 1175.75455
95.901203	-0 0 0 3.2038988 -0	0.4983289 28.556728 436.15796 34.158276 37.542307 37.542307	-0 0 0 3.7568781 0	0.7144836 28.555544 436.07259 34.178157 37.473332 37.473332	0 0 0 4.6032297 0 -0	28.553900 430.81429 35.307656 37.402277 109.77990
100,20839	29714.908 0 -3.0419083 -3.0419073 -2.9074574	7058.8658 -0.1640986E 09 435.41556 34.008394 61.038459 61.238460 99.935279	29735.535 0 -3.1341743 -3.1341743 -3.0050306	12390.766 -0.9348494E 08 435.19619 34.059714 60.188889 99.915718	30290,964 0 -2,9663315 -2,9663315 -2,8530121 0	-5162808.0 431.23122 34.949234 59.00000 59.00000
100,30389	23.988184 -56.021728 107.82370 106.73693 105.97555 21.398667	5305.9255 247.92601 507.28770 2582.7264 32.107692 30.707693	23.506378 -54.309585 108.53751 107.43803 106.69654 21.407517	6065.4431 576.58980 279.80687 1452.6172 31.95555 30.55555	22.984429 -52.539395 109.24898 108.14109 107.42419 21.414823	44427.321 44427.321 67.067810 332.75916 30.811387 26.753021 99.034100
99.581940	0 0 -38.977847 -0.6553493E-01 22.800321 1344.5833	31308.446 10482.706 14898.404 5.5842267 28.574049 5.1169214 100.13959	0 0.4893145E-02 25.305869 1443.0439	33507.113 5580.0061 14904.157 5.5773327 28.600824 5.1280469 100.17826	0 0 -38.689235 0 28.001511 1545.6260	286.33525 286.33525 15211.043 5.2418955 30.065761 5.7356657 102.24099
99,349662	686463.50 0.2160052E 08 29848.450 29848.450 31227.470 112.97736	97,295258 7132,5692 14807,784 5,6758510 28,332543 4,9917700 100,00368	652510.25 0.2156700E 32065.882 32065.883 33442.604 107.3893.8	93.833099 17799.833 14822.658 5.6569269 28.402787 5.026864 100.10413	617530.50 0.2153248E 08 34641.183 34641.182 36015.892 101.63245	91.00808 / 441749.58 15071.201 5.3859240 29.563309 5.4889948 101.78265
ĸ	0*1 639,59998 P 2 9274,6086 1 3 6£,269669 4 1344,7128 5 24,735166	0 1 3541.2288 4 2 10576.503 C 1 29714.908 E 2 11.260078 N 3 56.906591 T 4 5.0538365	0*1 659.99998 P 2 7914.9586 1 3 68.34C871 4 1443.1865 5 26.447972 6 0	D 1 3537.7666 4 2 21243.766 C 1 29735.535 E 2 11.234260 N 3 57.003612 T 4 5.0740871	# 0 W 4 N 0 -	U 1 3534,9416 4 2 445153.52 C 1 30290.564 E 2 10.627820 N 3 55.629070 T 4 5.6106588

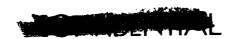


REFERENCES

- 1. Hofeller, G. W.: Centaur Unified Test Plan. AC-6/SD-2 Flight Test Plan Sec. 8.6., Rev. B. Rep. No. AY 62-0047, General Dynamics/Convair, Aug. 11, 1965.
- Anon: Centaur Test Report (AC-6), Propellant Tanking (CTP-INT-1003A), Conducted July 13, 1965. Test Summary, NASA, Goddard Launch Operations, July 1965.
- 3. Anon: Centaur Test Report (AC-6), Flight Acceptance Composite Test (CTP-INT-1000), Conducted July 28, 1965. Test Summary, NASA, Goddard Launch Operations, July 1965.
- 4. Anon: Centaur Test Report (AC-6), Composite Readiness Test, Conducted July 31, 1965. Test Summary, NASA, Goddard Launch Operations, Aug. 1965.
- 5. Anon: Atlas-Centaur Flight Evaluation Report. Vehicle AC-6. Rep. No. GD/C BNZ65-037, General Dynamics/Convair, Oct. 22, 1965.
- 6. Staff of Lewis Research Center: Postflight Evaluation of Atlas-Centaur AC-4 (Launched Dec. 11, 1964). NASA TM X-1108, 1965.
- 7. Anon: Centaur Monthly Configuration, Performance, and Weight Status Report. Rep. No. GDC63-0495-26, General Dynamics/Convair, July 21, 1965.
- 8. O'Connor, H. T.: A Comparison of Six- and Twelve-Variable Engine Models for the MA-5 Booster Engine. Rep. No. GD/C-CHA65-016, General Dynamics/Convair, Apr. 15, 1965.
- 9. Tulino, J. N.; and Staley, C. F.: Investigation of Effect of Hydrogen Snow Accumulation of the Centaur Retromaneuver and the Surveyor Payload. Rep. No. PWA FR-1595, Pratt and Whitney Aircraft Corp., Sept. 30, 1965.
- 10. Foushee, B. R.: Liquid Hydrogen and Liquid Oxygen Density Data for use in Centaur Propellant Loading Analysis. Rep. No. AE62-0471, General Dynamics/Astronautics, May 1, 1962.
- 11. Galleher, V. R.; Giberson, W. E.; Margraf, H. J.; and Gautschi, T. F.:
 Surveyor Spacecraft/Launch Vehicle. Interface Requirements. Surveyor
 Project Control Document. Project Document No. 1 (Rev. 1), Calif. Inst.
 of Tech., Jet Propulsion Lab., Dec. 19, 1963.
- 12. Staff of Lewis Research Center: Postflight Evaluation of Atlas-Centaur AC-3 (Launched June 30, 1964) NASA TM X-1094, 1965.
- 13. McGowan, P. R.: Flight Dynamics and Control Analyses of the LV-3C Launch Vehicle (Atlas/Centaur AC-6 and AC-7). Rep. No. GD/C-DDE65-O21, General Dynamics/Convair, Apr. 1965.
- 14. Stubblefield, W. O.: Flight Dynamics and Control Analysis of the Centaur Vehicle (Atlas/Centaur AC-6). Rep. No. GD/C-DDE65-033, General Dynamics/Convair, May 1965.



- 15. Zobal, S. A.: AC-6 Firing Tables. Rep. No. GD/C-BTD65-042, Rev. I, General Dynamics/Convair, July 6, 1965.
- 16. Roberts, R. E.: Final Guidance Equations and Performance Analysis for Centaur AC-6. Rep. No. GD/C-BTD65-059, General Dynamics/Convair, Apr. 15, 1965.
- 17. Rung, R. B.; and Renzetti, N. A.: Summary of Deep Space Network Operations Support of Atlas/Centaur AC-6 Mission. Rep. No. EPD 314, Calif. Inst. of Tech., Jet Propulsion Lab., Aug. 26, 1965.
- 18. Anon: Centaur Monthly Configuration, Performance, and Weight Status Report. Rep. No. GDC63-0495-29, General Dynamics/Convair, Oct. 21, 1965.



"The aeronautical and space activities of the United States shall be conducted so as to contribute... to the expansion of human knowledge of phenomena in the atmosphere and space. The Administration shall provide for the widest practicable and appropriate dissemination of information concerning its activities and the result: thereof."

-NATIONAL AERONAUTICS AND SPACE ACT OF 1958

NASA SCIENTIFIC AND TECHNICAL PUBLICATIONS

TECHNICAL REPORTS: Scientific and technical information considered important, complete, and a lasting contribution to existing knowledge.

TECHNICAL NOTES: Information less broad in scope but nevertheless of importance as a contribution to existing knowledge.

TECHNICAL MEMORANDUMS: Information receiving limited distribution because of preliminary data, security classification, or other reasons.

CONTRACTOR REPORTS: Technical information generated in connection with a NASA contract or grant and released under NASA auspices.

TECHNICAL TRANSLATIONS: Information published in a foreign language considered to merit NASA distribution in English.

SPECIAL PUBLICATIONS: Information derived from or of value to NASA activities. Publications include conference proceedings, monographs, data compilations, handbooks, sourcebooks, and special bibliographies.

TECHNOLOGY UTILIZATION PUBLICATIONS: Information on technology used by NASA that may be of particular interest in commercial and other nonaerospace applications. Publications include Tech Briefs; Technology Utilization Reports and Notes; and Technology Surveys.

Details on the availability of these publications may be obtained from:

SCIENTIFIC AND TECHNICAL INFORMATION DIVISION

NATIONAL AERONAUTICS AND SPACE ADMINISTRATION

Washington, D.C. 20546

